JAERI 1199

JAERI 1199

JAERI Fast Reactor Group Constants Systems Part II-1

December 1970

日本原子力研究所
Japan Atomic Energy Research Institute

日本原子力研究所は，研究成果，調査結果などを JAERI レポートとして，つぎの４種に分けそれぞれの通し番号を付し，不定期に刊行しております．

1. 研究報告	まとまった研究の成果あるいはその一部における重要な結果の報告	JAERI 1001-
2. 調査報告	総説・展望・調査の結果などをまとめたもの	JAERI 4001-
3. 年　　報	研究・開発その他の活動状況などの報告	JAERI 5001-
4. 資　　料	施設の概要や手引きなど	JAERI 6001-

このうち既刊分については「JAERI レポート一覧」にタイトル・要旨をまとめて掲載し，また新刊レポートは「研究成果要旨集」(隔月刊)で逐次紹介しています．

これらのリスト・研究報告書の入手および複写・翻訳などのご要求は，日本原子力研究所技術情報部（茨城県那珂郡東海村）に申しこんでください．

Japan Atomic Energy Research Institute publishes the nonperiodical reports with the following classification numbers:

1. JAERI 1001-　Research reports
2. JAERI 4001-　Survey reports and reviews
3. JAERI 5001-　Annual reports
4. JAERI 6001-　Manuals etc.

Requests for the above publications, and reproduction and translation should be addressed to Division of Technical Information, Japan Atomic Energy Research Insitute, Tokai-mura,Naka-gun, Ibaraki-ken, Japan

---

編集兼発行　日本原子力研究所
印　　刷　三美印刷株式会社

JAERI 1199 Errata

Page	Line	As Printed	To Read
1	28	schimidt	Schmidt
3	16	utilzed	utilized
4	Eq. (2. 1. 3)	$\sigma_{cn}=\sigma_{cT}=\sum_{c'\neq n}\sigma_{cc'}$	$\sigma_{cn}=\sigma_{cT}-\sum_{c'\neq n}\sigma_{cc'}$
4	4, 5	momemtrum	momentum
7	Eq. (2. 1. 32)	$\sqrt{\Gamma_\lambda\Gamma_{\lambda'}g^I_{\lambda\lambda'}}$	$\sqrt{\Gamma_\lambda\Gamma_{\lambda'}}\,g^I_{\lambda\lambda'}$
8	21	broadend	broadened
10	23–24	Eq. (2. 2. 12)	Eq. (2. 2. 24)
11	25	varaiation	variation
12	13	$f(V\sqrt{\alpha})$	$f(v\sqrt{\alpha})$
12	14	g_t	g_J
13	30	importnat	important
14	4	calcuation	calculation
16	34	as narrow as possible in that ...	as narrow as possible so that ...
17	16	can always the narrow	can always choose the narrow
18	11	on state is $j=\frac{1}{2}$ is	on state $j=\frac{1}{2}$ is
18	20	Eqs. form	Eqs. from
22	Eq. (2. 6. 17)	$\langle\Gamma_{nlij}\rangle=\langle j\Gamma_{nljj}\rangle v_l\sqrt{E}$	$\langle\Gamma_{nljj}\rangle=\langle\Gamma^0_{nljj}\rangle v_l\sqrt{E}$
27	6	aroand	around
29	Eqs. (3. 3. 4)	$\lambda_c=\sum_\alpha b_{\alpha c}y_{\lambda\alpha}$	$\gamma_{\lambda c}=\sum_\alpha b_{\alpha c}y_{\lambda\alpha}$
29	Eqs. (3. 3. 4) and (3. 3. 5)	$P_{\alpha'}$	P'_α
29	16	$P_{\alpha'}$	P'_α
34	1	^{239}U	^{239}Pu
37	Table 4. 1-2 (b)	$E=2.73$	$E=0.273$
37	Table 4. 1-4 (b)	$=20.1$	$=201.$
37	last	erew	are
60	Table 5. 5-11	Karlsrube	Karlsruhe
68, 69	Eq. (6. 2-6)	$\sigma_{\lambda t}$	σ_{rt}

69	Eq. (6. 2-9)	$\left[1-\frac{1}{\Delta E}\sum_{\lambda'}\Gamma_{2\lambda'}J_{2\lambda'}\right.$ $\left.-\frac{1}{\Delta E}\Gamma_{\lambda'}\Gamma_{2\lambda'}J_{2\lambda'}\right]$	$\left[1-\frac{1}{\Delta E}\sum_{\lambda'}\Gamma_{2\lambda'}J_{2\lambda'}\right]$ $-\frac{1}{\Delta E}\sum_{\lambda'}\Gamma_{2\lambda'}J_{2\lambda'}$
72	2	predominate	predominant
82, 87, 90, 95		LETHERGY	LETHARGY
89	12	0. 843	1. 112
		0. 926	0. 991
	15	0. 903	0. 950
		0. 726	1. 049
	27	0. 955	0. 997
	30	0. 903	0. 974
	33	0. 939	0. 993
97	12	−0. 486	1. 021
	52	−0. 002	0. 090
	53	−0. 045	0. 074
99	12	2. 9 E-03	-2. 7 E-03
	52	3. 5 E-04	-5. 7 E-03
	53	9. 0 E-03	1. 1 E-03
106	Note 1, U-235	25	20
	Pu-240	10	15
112	C-IV-2	Tableof	Table of
112	C-IV-2	Shieldirg	Shielding

JAERI Fast Reactor Group Constants Systems Part II-1

Summary

Improvements have been made for the treatments of effective cross section of heavy nuclides in the resonance energy region, and fast reactor group constants in this energy region have been produced for nuclides ^{235}U, ^{238}U, ^{239}Pu, and ^{240}Pu.

These group constants are thought to be accurate compared with existing fast group constants in the following sense:

1) The resonance parameters (including those in the unresolved resonance energy region) are evaluated so as to fit measured cross sections.

2) Accurate cross sections are obtained by a calculating procedure, which uses a reasonable representation of cross sections, without waste of huge computing time.

3) The effective cross sections are obtained using exact spectra as weights, because conventional approximation methods yield less accurate results.

4) An investigation was made for the treatment of interference effects. And interference effects with ^{238}U is taken into account for shielding factors.

5) The energy variation of $\alpha(\sigma_c/\sigma_f)$ values and σ_f for ^{235}U and ^{239}Pu is properly reproduced, and an appropriate group structure is adopted taking this energy variation into consideration.

For analyses and design studies of fast reactor systems, the present group constants should be used together with those listed in the report JAERI 1195.

March. 1970

Satoru KATSURAGI
Yukio ISHIGURO
Hideki TAKANO
Masayuki NAKAGAWA
Division of Reactor Engineering
Takai Research Establishment
Japan Atomic Energy Research Institute

高速炉用群定数セット　JAERI-Fast Set II-1

要　旨

従来不正確に扱われていた重い核の共鳴域の炉定数の求め方を改良し，^{235}U, ^{238}U, ^{239}Pu, ^{240}Pu の高速炉用炉定数を作成した．この炉定数はつぎの点で従来のものよりすぐれている．

1) 共鳴パラメータを評価し，測定と合うようにした．

2) 上記パラメータにもとづいて合理的かつ，経済的に精度のよい断面積が求められるようにした．

3) 実効断面積を求めるのに用いられた従来の方法は不正確なので，中性子束を正しく求める方法によった．

4) 相互干渉効果を扱う方法を検討し，^{233}U との相互干渉効果を正しく扱えるようにした．

5) ^{239}Pu, ^{235}U の $\alpha(\sigma_c/\sigma_f)$ や σ_f のエネルギー変動が正しく考慮されており，それに適当な群構造が使われている．

この報告中の炉定数と JAERI 1195 に報告されている炉定数を合わせて用いることにより，高速炉の解析・設計を行なうことができる．

1970年3月

日本原子力研究所　東海研究所
原子炉工学部
桂　木　　学
石　黒　幸　雄
高　野　秀　機
中　川　正　幸

CONTENTS

目　　次

1. Introduction

For analyses and design studies of characteristic features of fast reactors, multi-group treatments are frequently used. For this treatments the multi-group cross section set is indispensable. The YOM[1], HR[2] and ABBN[3] sets have been introduced from oversea countries. The YOM set was prepared for analyses of fast reactors having a hard neutron spectrum, and hence, was not designed adequately for treatments of fast reactors having a soft neutron spectrum. By this reason the set cannot be applied to the studies aiming at commercial fast reactors. The HR set is equipped with a device treating composition dependence of effective resonance cross sections. However it is thought that the group structure is not adequate for predictions of the characteristics of a fast reactor.

The ABBN set treats composition dependence of cross sections, as the HR set, not only for heavy element cross sections but also for light and medium weight elements. Moreover in the ABBN set the composition dependence of diffusion coefficients is taken into account. The concept of this set has been thought to be constituted satisfactorily for general use.

There are, however, several draw-backs found in the ABBN set[4][5]. The first one is the treatments of elastic removal cross sections. In the ABBN set the elastic removal cross sections are calculated from those for infinite dilution and self-shielding factors for the elastic scattering cross sections. The self-shielding factors for the elastic removal cross sections behave rather differently from those for the elastic scattering cross sections. A notable examples are removal cross sections near the 2.85 kev sodium resonance energy. This problem might be to be solved mainly by treating adequately the elastic removal cross sections for light and intermediate elements.

The second draw-back is the accuracy of cross sections or nuclear data on which the group averaged cross sections are based. A large number of informations have been accumulated since that time of publication of the ABBN set. Especially the cross sections and α values of ^{239}Pu in the ABBN set are thought inaccurate in view of the recent informations. The new information about α values of ^{239}Pu suggests that fission width of the ($J=1$, $1=0$) sequence may be narrow that the self-shielding factors based on the older values of width will be in error. For the capture cross sections of ^{238}U, it is thought that the average capture width is about 20% smaller than that recommended by schmidt and some portion of p-wave resonance levels are missing in the energy range from 1 to 4 keV. An evaluation of heavy elements resonance cross sections is needed.

The self shielding factors in the ABBN set were obtained by assuming the constancy of collision density within groups. Moreover in the resolved resonance regions the isolated narrow resonance approximation was used and in the unresolved resonance regions the approximations based on the method A and B were applied.

The elastic removal cross sections of heavy elements may be usually less important for predicting characteristics of fast reactors such as critical masses, effective multiplication factors and various reaction rates etc.. However for the evaluation of the Doppler reactivity effect, which consists of differences in small positive and negative contributions, the elastic removal cross sections and their temperature dependence of heavy elements might become comparatively important. In fact some resonances, especially some of scattering resonances, exist near lower boundaries of groups where main contributions to the elastic removal cross sections come from. The group constants should be designed so as to treat this effect in detail.

The last short coming is that in the ABBN set the mutual interference effects between resonances of different nuclides and self overlapping effects are not treated accurately, whereas according to recent analyses of Doppler effects it is recognized that the mutual shielding effects, especially between ^{238}U and fissile elements are comparatively significant.

Thus the self-shielding factors obtained with these assumptions, methods and nuclear data are not expected to be accurate.

For the fast reactors, the contributions to reactivity effects from unresolved resonance energy regions become relatively important compared with thermal reactors. For the treatments of effective cross sections in the energy regions, there are studies by many authors[6-9]. The treatments, however, are based on the assumption of constancy of collision density. The program MC²[10] has made use of Hwang's method extensively. The Hwang's approximation method, however, is no more than crude approximation. Moreover it should be very important for group constants to be consistent with α values. And resonance parameters should be biased to reproduce observed values. The program MC² is not designed adequately for considering this consistency so that group constants produced by MC² cannot be applied for highly accurate analyses of fast reactors without changing some parts of group constants in the unresolved resonance regions.

If individual resonance parameters and hence high resolution cross sections in the unresolved resonance regions are obtained, it will be very easy to overcome the draw-backs mentioned above; that is, the self overlapping effects can be directly treated because cross sections already include this effects and the mutual shielding effects can also be taken into accounts. The concept of group constants, however, should be changed or improved for including the latter effects.

The system of group constants has been studied for light and medium elements as well as for heavy elements except for resonance energy regions. It has been made clear that width of groups nearly equal to 0.25 in lethargy is satisfactory for reproducing variation of flux and for taking account of competitions between absorption and slowing down process to some extents[11].

For the cross sections of heavy elements in the resonance energy, it is not assured that effective cross sections can be treated by the same basis as the ABBN set, in such circumstances mentioned already. For producing resonable and accurate group constants of heavy elements in resonance energy regions, the problems we have to solve are as follows:

(1) First of all, the average resonance parameters for the unresolved resonance region should be evaluated so as to fit to recent experimental results. At the same time resolved resonance parameters should be selected in due consideration of recent informations.

(2) It is absolutely necessary to generate, by an appropriate numerical methods, high resolution cross sections for the unresolved resonance region which reproduce temperature dependence accurately. The high resolution cross sections must agree with low resolution experiments within the limits of assigned errors.

(3) An appropriate form for treating mutual shielding effects with ^{238}U should be determined. For this purpose appropriate parameters must be introduced.

(4) Corresponding to the high resolution cross sections generated, which naturally contain self overlapping effects, it is necessary to develop a program calculating ultra fine neutron spectrum. In this case the slowing down equation should be solved with energy scale for preserving accuracies. Speeding up the program is essential, because the high resolution cross sections will be given at huge numbers of energies.

In the following we will report how to treat the problems mentioned above.

2. Cross Sections in Resonance Regions

There are many expressions proposed for the calculations of resonance cross sections. Most of the expressions are reduced to the single level formula of Breit and Wigner, when the width of the resonance is very small compared with the spacing of resonances and cross sections are produced by summing contribution from each resonance. The single level formula has always been adopted for analyses of resonance absorption due to fertile elements in nuclear reactor.

However, as pointed out by many investigators, for fissile elements the single level formula fails for reproducing shapes of cross sections, especially in a case where interference effects between levels are very significant. For reactor physics calcualations, consideration for Doppler effects due to thermal motion of nuclei are important. Most of the expressions proposed are not applicable to the reactor calculations, because devices for treating the Doppler broadening are not provided satisfactorily. The recent study of ADLER and ADLER[12] aimed at an improvement of resonance formula with respect to this inconvenience and have an advantage that multi-level cross section can be expressed by resonance parameters independent of energy and the Doppler broadening can be treated by rather simple expressions[13]. Hence their expression can be applicable for reactor physics calculation. Unfortunately, resonance parameters, which should be used for their expression, are not provided sufficiently enough to be utilzed by reactor physics calculations.

There is another expression, which is obtained by VOGT[14),15]. The expression is very useful, because parameters for the single level formula can be used in this expression and the Doppler-broadening cross section is readily given by a simple formula[16]. In this report, interpretation and reproduction of heavy element cross sections are performed using an expression based on the approximations made by VOGT.

2.1 The Multi-level Formula

The R-matrix formalism by WIGNER and EISENBUD[17] treats the formal theory of nuclear reactions, and the cross section can be formulated by energy-independent R-matrix parameters except for the neutron width. However, the theory requires a huge number of complicated unknown parameters which represent the internal structure of the compound nucleus. In fact R-matrix contains parameters for very many channels available as well as an infinite number of levels. Therefore, this formalism is too complicated for general use in nuclear reactor physics. Especially, matrix inversions needed for obtaining the collision matrix is almost impossible. Usually transformation is performed form R-matrix formalism into the form involving the inversion of a reciprocal level matrix A. In this formalism the level matrix C ($=A^{-1}$) is formally of infinite order yet. However, in some cases it can be approximated by a small finite sub-matrix relating to only a few levels.

Another exremal case is that only a small number of channels are concerned with a cross section. In this case we require only a part of elements of collision matrix which is again expressed by a reciprocal level matrix. This follows from the fact that for the slow neutron fission only a few levels are sufficient for an analysis of cross sections. Moreover we cannot separate contribution from each fission channel, and number of open channels for radiative capture is thought to be infinitely large.

In this report we will be concerned with reactions induced by neutrons of energy less than ten

kev. The predominant contribution to cross sections comes from s-wave neutrons, but p-wave neutrons contribute very little in the resonance region of interest. Therefore it is sufficient for us to consider, at first, s-wave neutron reactions. We shall consider reactions in which a neutron of orbital angular momentum l and angular momemtrum j interacts with a nucleus of spin I, and forming a compound nucleus of total angular momentrum J, which ranges from $|I-J|$ to $I+J$. If neutrons entering from c-channel exit through c′-channel, then the cross section for this reaction is given by.

$$\sigma_{cT}=\frac{2\pi}{k^2}g_J Re\ (1-U^J_{cc}), \tag{2.1.1}$$

$$\sigma_{cc'}=\frac{\pi}{k^2}g_J|U^J_{cc'}|^2, \tag{2.1.2}$$

$$\sigma_{cn}=\sigma_{cT}=\sum_{c'\neq n}\sigma_{cc'}=\frac{\pi}{k^2}g_J|1-U^J_{cn}|^2 \tag{2.1.3}$$

where $k=\sqrt{2mE/\hbar}$ is the neutron wave number, $g_J=\dfrac{2J+1}{2(2I+1)}$ the statistical spin factor. In the above expressions, the $U^J_{cc'}$ is the collision matrix which represents a complex amplitude of outgoing spherical wave through channel c′ after forming compound nucleus of the total angular momentum J. The collision matrix is given by[14]

$$U^J_{cc'}=e^{i(\phi_c+\phi_{c'})}\ [\delta_{cc'}+i\sum_{\lambda\lambda'}\sqrt{\Gamma_{\lambda c}\Gamma_{\lambda' c'}}\ A_{\lambda\lambda'}] \tag{2.1.4}$$

where λ and λ' represent levels of resonance in the J-state, δ the Kronecker's δ-function. The $\Gamma_{\lambda c}$ denotes partial width for disintegration of the state λ (J) through channel c. $\sqrt{\Gamma_{\lambda c}}$ is given by

$$\sqrt{\Gamma_{\lambda c}}=\sqrt{2P_c}\gamma_{\lambda c}\ . \tag{2.1.5}$$

Here, the phase shift ϕ and the penetration factor P_c are given as

$$\begin{aligned}&\phi_c=-ka,\quad P_c=ka \quad \text{for neutrons of } l=0\\ &\phi_c\cong\frac{1}{3}(ka)^3,\ P_c=\frac{(ka)^3}{1+(ka)^2} \quad \text{for neutrons } l=1\end{aligned} \tag{2.1.6}$$

where a is the radius of target nucleus.

Substituting Eq. (2.1.4) into Eqs. (2.1.1), (2.1.2) and (2.1.3) yields

$$\begin{aligned}\sigma_{cT}&=\frac{2\pi}{k^2}g_J Re\ \{1-e^{2i\phi_c}\ [1+i\sum_{\lambda\lambda'}\sqrt{\Gamma_{\lambda c}\Gamma_{\lambda' c}}A_{\lambda\lambda'}]\}\\ &\cong\frac{2\pi}{k^2}g_J\ \{2\phi^2_c+2\phi_c\sum_{\lambda\lambda'}\sqrt{\Gamma_{\lambda c}\Gamma_{\lambda' c}}\ Re\ (A_{\lambda\lambda'})\\ &\quad+(1-2\phi^2_c)\sum_{\lambda\lambda'}\sqrt{\Gamma_{\lambda c}\Gamma_{\lambda' c}}Im(A_{\lambda\lambda'})\},\end{aligned} \tag{2.1.7}$$

$$\sigma_{cc'}=\frac{\pi}{k^2}g_J\sum_{\lambda\lambda'}\sum_{\lambda''\lambda'''}\sqrt{\Gamma_{\lambda c}\Gamma_{\lambda' c'}\Gamma_{\lambda'' c'}\Gamma_{\lambda''' c'}}A_{\lambda\lambda'}A^*_{\lambda''\lambda'''}, \tag{2.1.8}$$

$$\sigma_{cn}=\sigma_{cT}-\sum_{c\neq n}\sigma_{cc'}\ . \tag{2.1.9}$$

We have neglected the terms of order ϕ^3_c, however the above expressions are valid for energy ranges of interest. According to LANE and THOMAS[18] and VOGT[14], the reciprocal level matrix $A_{\lambda\lambda'}$ is the inverse of the following matrix

$$(A^{-1})_{\lambda\lambda'}=(E_\lambda-E)\delta_{\lambda\lambda'}-\frac{i}{2}\sum_{c''}\sqrt{\Gamma_{\lambda c''}\Gamma_{\lambda' c''}} \tag{2.1.10}$$

where E_λ is the resonance energy.

Note that if all the off-diagonal elements of A^{-1} vanish, the expressions (2.1.7), (2.1.8) and (2.1.9) are reduced to the single level formula. Various expressions were derived by approximating the off-diagonal elements of the level matrix by this time. From measurements of cross sections, we obtain usually information on total reaction widths such as fission, capture and neutron,

instead of partial widths $\Gamma_{\lambda c}$. Each reaction width observed is defined as a summation over channels to each reaction. The last term of Eq. (2. 1. 10) is rewritten as

$$\sum_{c''}\sqrt{\Gamma_{\lambda c''}\Gamma_{\lambda' c''}}=\sum_{c''\in n}\sqrt{\Gamma_{\lambda' c''}}+\sum_{c''\in\gamma}^{N_\gamma}\sqrt{\Gamma_{\lambda c''}\Gamma_{\lambda' c''}}+\sum_{c''\in f}^{N_f}\sqrt{\Gamma_{\lambda c''}\Gamma_{\lambda' c''}} \tag{2. 1. 11}$$

For s-wave neutron the channel leading to a neutron emission is only the entrance channel, and any other with an l value differing by at least 2, because of the conservation rule of parity, may be neglected for our purpose. For neutron capture, there are very many channels open. Moreover, because the sign of $\sqrt{\Gamma_{\lambda c}}$ is assumed to be changing with level and channel, the second term $\Sigma\sqrt{\Gamma_{\lambda c''}\Gamma_{\lambda' c''}}$ in Eq. (2. 1. 11) can be neglected if $\lambda\neq\lambda'$. On the other hand in the last term $\sqrt{\Gamma_{\lambda c'}}$ is thought as a component of vectors whose length is $(\Gamma_{\lambda f})^{1/2}$, then $\Sigma\sqrt{\Gamma_{\lambda c''}\Gamma_{\lambda' c''}}$ can be written as

$$\sum_{c''\in f}\sqrt{\Gamma_{\lambda c''}\Gamma_{\lambda' c''}}=(\Gamma_{\lambda f}\Gamma_{\lambda' f})^{1/2}\cos\theta_{\lambda\lambda'}\ , \tag{2. 1. 12}$$

where $\theta_{\lambda\lambda'}$ is an angle between two vectors $\Gamma_{\lambda c}$ and $\Gamma_{\lambda' c}$. By this notation, Eq. (2. 1. 10) is rewritten as

$$(A^{-1})_{\lambda\lambda'}=\begin{cases}E_\lambda-E-\dfrac{i}{2}\Gamma_\lambda & \text{for } \lambda=\lambda'\\ -\dfrac{i}{2}[(\Gamma_{\lambda c}\Gamma_{\lambda' c})^{1/2}+(\Gamma_{\lambda f}\Gamma_{\lambda' f})^{1/2}\cos\theta_{\lambda\lambda'}] & \text{for } \lambda\neq\lambda'\ .\end{cases} \tag{2. 1. 13}$$

Generally $|E_\lambda-E|$ is larger than any off-diagonal elements of the level matrix. If A^{-1} is rewritten as

$$A^{-1}=D+B,$$

where D is the diagonal matrix, then we have

$$A=(D+B)^{-1}=D^{-1}(1+BD^{-1})^{-1}\cong D^{-1}-D^{-1}BD^{-1}\ . \tag{2. 1. 14}$$

Using this approximate expression for the reciprocal level matrix, we have

$$\begin{aligned}A_{\lambda\lambda'}&\cong\frac{\delta_{\lambda\lambda'}}{(E_\lambda-E)-\frac{i}{2}\Gamma_\lambda}+\frac{i}{2}\frac{(1-\delta_{\lambda\lambda'})[(\Gamma_{\lambda c}\Gamma_{\lambda' c})^{1/2}+(\Gamma_{\lambda f}\Gamma_{\lambda' f})^{1/2}\cos\theta_{\lambda\lambda'}]}{[(E_\lambda-E)-\frac{i}{2}\Gamma_\lambda][(E_{\lambda'}-E)-\frac{i}{2}\Gamma_{\lambda'}]}\\ &\cong\frac{(E_\lambda-E)+\frac{i}{2}\Gamma_\lambda}{(E_\lambda-E)^2+\left(\frac{\Gamma_\lambda}{2}\right)^2}\delta_{\lambda\lambda'}+\frac{i}{2}G_{\lambda\lambda'}\end{aligned} \tag{2. 1. 15}$$

where

$$\begin{aligned}G_{\lambda\lambda'}=&\frac{(1-\delta_{\lambda\lambda'})[(\Gamma_{\lambda c}\Gamma_{\lambda' c})^{1/2}+(\Gamma_{\lambda f}\Gamma_{\lambda' f})^{1/2}\cos\theta_{\lambda\lambda'}]}{(E_{\lambda'}-E_\lambda)^2+\left(\frac{\Gamma_{\lambda'}-\Gamma_\lambda}{2}\right)^2}[(E_{\lambda'}-E_\lambda)+\frac{i}{2}(\Gamma_{\lambda'}-\Gamma_\lambda)]\\ &\times\left\{\frac{E_\lambda-E+\frac{i}{2}\Gamma_\lambda}{(E_\lambda-E)^2+\left(\frac{\Gamma_\lambda}{2}\right)^2}-\frac{E_{\lambda'}-E+\frac{i}{2}\Gamma_{\lambda'}}{(E_{\lambda'}-E)^2+\left(\frac{\Gamma_{\lambda'}}{2}\right)^2}\right\}.\end{aligned} \tag{2. 1. 16}$$

Hence real and imarginary parts of the matrix $A_{\lambda\lambda'}$ are given by

$$Re(A_{\lambda\lambda'})=\frac{(E_\lambda-E)\delta_{\lambda\lambda'}}{(E_\lambda-E)^2+\left(\frac{\Gamma_\lambda}{2}\right)^2}+\frac{1-\delta_{\lambda\lambda'}}{2}[(\Gamma_{\lambda c}\Gamma_{\lambda' c})^{1/2}+(\Gamma_{\lambda f}\Gamma_{\lambda' f})^{1/2}\cos\theta_{\lambda\lambda'}]g^R{}_{\lambda\lambda'} \tag{2. 1. 17}$$

$$Im(A_{\lambda\lambda'})=\frac{\frac{\Gamma_\lambda}{2}}{(E_\lambda-E)^2+\left(\frac{\Gamma_\lambda}{2}\right)^2}+\frac{1-\delta_{\lambda\lambda'}}{2}[(\Gamma_{\lambda c}\Gamma_{\lambda' c})^{1/2}+(\Gamma_{\lambda f}\Gamma_{\lambda' f})^{1/2}\cos\theta_{\lambda\lambda'}]g^I{}_{\lambda\lambda'} \tag{2. 1. 18}$$

where $g^R{}_{\lambda\lambda'}$ and $g^I{}_{\lambda\lambda'}$ are defined as

$$g^{R}{}_{\lambda\lambda'}=h_{\lambda\lambda'}\left(\frac{\Gamma_\lambda(E_\lambda-E_{\lambda'})+(\Gamma_\lambda-\Gamma_{\lambda'})(E_\lambda-E)}{(E_\lambda-E)^2+\left(\frac{\Gamma_\lambda}{2}\right)^2}\frac{\Gamma_{\lambda'}(E_\lambda-E_{\lambda'})+(\Gamma_\lambda-\Gamma_{\lambda'})(E_{\lambda'}-E)}{(E_{\lambda'}-E)^2+\left(\frac{\Gamma_{\lambda'}}{2}\right)^2}\right) \tag{2.1.19}$$

$$g^{I}{}_{\lambda\lambda'}=h_{\lambda\lambda'}\left(\frac{\frac{\Gamma_\lambda}{2}(\Gamma_\lambda-\Gamma_{\lambda'})-2(E_\lambda-E_{\lambda'})(E_\lambda-E)}{(E_\lambda-E)^2+\left(\frac{\Gamma_\lambda}{2}\right)^2}\frac{\frac{\Gamma_{\lambda'}}{2}(\Gamma_\lambda-\Gamma_{\lambda'})-2(E_\lambda-E_{\lambda'})(E_{\lambda'}-E)}{(E_{\lambda'}-E)^2+\left(\frac{\Gamma_{\lambda'}}{2}\right)^2}\right) \tag{2.1.20}$$

$$h_{\lambda\lambda'}=\frac{1}{2}\frac{1}{(E_{\lambda'}-E_\lambda)^2+\left(\frac{\Gamma_{\lambda'}-\Gamma_\lambda}{2}\right)^2}\,.$$

By this approximation, we have, for the total cross section

$$\sigma_{cT}\cong\frac{2\pi}{k^2}g_J\left\{2\phi^2{}_c+\sum_\lambda\left(\frac{\frac{1}{2}\Gamma_{\lambda c}\Gamma_\lambda}{(E_\lambda-E)^2+\left(\frac{\Gamma_\lambda}{2}\right)^2}+2\phi_c\frac{\Gamma_{\lambda c}(E_\lambda-E)}{(E_\lambda-E)^2+\left(\frac{\Gamma_\lambda}{2}\right)^2}\right)\right.$$
$$\left.+\sum_\lambda\sum_{\lambda<\lambda'}\sqrt{\Gamma_{\lambda c}\Gamma_{\lambda' c}}\left(\sqrt{\Gamma_{\lambda c}\Gamma_{\lambda' c}}+\sqrt{\Gamma_{\lambda f}\Gamma_{\lambda' f}}\cos\theta_{\lambda\lambda'}\right)\left(g^{I}{}_{\lambda\lambda'}+2\phi_c g^{R}{}_{\lambda\lambda'}\right)\right\}, \tag{2.1.21}$$

In the above equation, the first term is the so called potential scattering, the second term corresponds to the sigle level formula and the third term is the correction term due to interference between levels. Usually the second term in the last bracket can be neglected.

It should be noted from Eqs (2.1.15) and (2.1.16) that $A_{\lambda\lambda'}$ $(\lambda\neq\lambda')$ is smaller than $A_{\lambda\lambda}$, because of a factor $(\Gamma_{\lambda c}\Gamma_{\lambda' c})^{1/2}$. Retaining terms up to second order power of Γ_λ, the cross section for excit channel c′ can be rewritten as

$$\sigma_{cc'}\cong\frac{\pi}{k^2}g_J\sum_\lambda\sum_{\lambda'}\sqrt{\Gamma_{\lambda c}\Gamma_{\lambda' c}\Gamma_{\lambda c'}\Gamma_{\lambda' c'}}A_{\lambda\lambda}A^*{}_{\lambda'\lambda'}$$
$$=\frac{\pi}{k^2}g_J\sum_\lambda\left[\Gamma_{\lambda c}\Gamma_{\lambda c'}|A_{\lambda\lambda}|^2+2\sum_{\lambda'>\lambda}\sqrt{\Gamma_{\lambda c}\Gamma_{\lambda' c}\Gamma_{\lambda c'}\Gamma_{\lambda' c'}}Re(A_{\lambda\lambda'}A^*{}_{\lambda'\lambda})\right]$$
$$=\frac{\pi}{k^2}g_J\sum_\lambda\left(\frac{\Gamma_{\lambda c}\Gamma_{\lambda c'}}{(E_\lambda-E)^2+\left(\frac{\Gamma_\lambda}{2}\right)^2}+2\sum_{\lambda'>\lambda}\sqrt{\Gamma_{\lambda c}\Gamma_{\lambda' c}\Gamma_{\lambda c'}\Gamma_{\lambda' c'}}g^{I}{}_{\lambda\lambda'}\right). \tag{2.1.22}$$

By applying the same procedure as done for Eq. (2.1.11), the following expressions will be obtained for the capture and fission cross sections.

$$\sigma^{s}{}_{cT}\cong\frac{\pi}{k^2}g_J\sum_\lambda\frac{\Gamma_{\lambda c}\Gamma_{\lambda\gamma}}{(E_\lambda-E)^2+\left(\frac{\Gamma_\lambda}{2}\right)^2}\,, \tag{2.1.23}$$

$$\sigma^{s}{}_{cf}\cong\frac{\pi}{k^2}g_J\sum_\lambda\left(\frac{\Gamma_{\lambda c}\Gamma_{\lambda f}}{(E_\lambda-E)^2+\left(\frac{\Gamma_\lambda}{2}\right)^2}+2\sum_{\lambda'>\lambda}(\Gamma_{\lambda c}\Gamma_{\lambda' c})^{1/2}(\Gamma_{\lambda f}\Gamma_{\lambda' f})^{1/2}\cos\theta_{\lambda\lambda'}g^{I}{}_{\lambda\lambda'}\right). \tag{2.1.24}$$

The contribution from p-wave neutron to the cross section is rather small compared with that of s-wave nuetron in the energy range of interest. And interference effects for p-wave cross section can be neglected definitely. Therefore single level expression is sufficient for use.

$$\sigma^{p}{}_{cT}=\frac{\pi}{k^2}g_J\sum_{\lambda J}\frac{\Gamma_{\lambda c}\Gamma_\lambda}{(E_\lambda-E)^2+\left(\frac{\Gamma_\lambda}{2}\right)^2} \tag{2.2.25}$$

$$\sigma^{p}_{c\gamma}=\frac{\pi}{k^2}g_J\sum_{\lambda\in J}\frac{\Gamma_{\lambda c}\Gamma_{\lambda\gamma}}{(E_\lambda-E)^2+\left(\frac{\Gamma_\lambda}{2}\right)^2} \tag{2.1.26}$$

$$\sigma_{cf}=\frac{\pi}{k^2}g_J\sum_{\lambda\in J}\frac{\Gamma_{\lambda c}\Gamma_{\lambda f}}{(E_\lambda-E)^2+\left(\frac{\Gamma_\lambda}{2}\right)^2}\,. \tag{2.1.27}$$

Summalizing the above arguments, the following expressions will be obtained:

$$\begin{aligned}\sigma_t(E)\cong 4\pi a^2+\sum_{J\in S}g_J\sum_{\lambda\in J}\Bigg(&\frac{\pi}{k^2}\frac{\Gamma_{\lambda nJ}\Gamma_\lambda}{(E-E_\lambda)^2+\left(\frac{\Gamma_\lambda}{2}\right)^2}\\&+\frac{4\pi a}{k}\frac{\Gamma_{\lambda nJ}(E-E_\lambda)}{(E-E_\lambda)^2+\left(\frac{\Gamma_\lambda}{2}\right)^2}+\frac{\pi}{k^2}\sum_{\lambda'>\lambda}\sqrt{\Gamma_{\lambda nJ}\Gamma_{\lambda' nJ}}\left(\sqrt{\Gamma_{\lambda nJ}\Gamma_{\lambda' nJ}}\right.\\&\left.+\sqrt{\Gamma_{\lambda f}\Gamma_{\lambda' f}}\cos\theta_{\lambda\lambda'}\right)g^{I}_{\lambda\lambda'}\Bigg)+\frac{\pi}{k^2}\sum_{\lambda\in p}g_J\sum_{\lambda\in J}\frac{\Gamma_{\lambda nJ}\Gamma_\lambda}{(E-E_\lambda)^2+\left(\frac{\Gamma_\lambda}{2}\right)^2}\end{aligned} \tag{2.1.28}$$

$$\sigma_\gamma(E)\cong\frac{\pi}{k^2}\left(\sum_{J\in a}g_J\sum_{\lambda\in J}\frac{\Gamma_{\lambda nJ}\Gamma_{\lambda\gamma}}{(E-E_\lambda)^2+\left(\frac{\Gamma_\lambda}{2}\right)^2}+\sum_{J\in p}g_J\sum_{\lambda\in J}\frac{\Gamma_{\lambda nJ}\Gamma_\gamma}{(E-E_\lambda)^2+\left(\frac{\Gamma_\lambda}{2}\right)^2}\right) \tag{2.1.29}$$

$$\begin{aligned}\sigma_f(E)\cong\frac{\pi}{k^2}\Bigg(&\sum_{J\in a}g_J\sum_{\lambda\in J}\Bigg\{\frac{\Gamma_{\lambda nJ}\Gamma_{\lambda f}}{(E-E_\lambda)^2+\left(\frac{\Gamma_\lambda}{2}\right)^2}\\&+2\sum_{\lambda'>\lambda}\sqrt{\Gamma_{\lambda nJ}\Gamma_{\lambda' nJ}}\sqrt{\Gamma_{\lambda f}\Gamma_{\lambda' f}}\cos\theta_{\lambda\lambda'}g^{I}_{\lambda\lambda'}\Bigg\}\\&+\sum_{J\in p}g_J\sum_{\lambda\in J}\frac{\pi}{k^2}\left\{\frac{(\Gamma_{\lambda nJ})^2}{(E-E_\lambda)^2+\left(\frac{\Gamma_\lambda}{2}\right)^2}\right\},\end{aligned} \tag{2.1.30}$$

$$\begin{aligned}\sigma_n(E)\cong 4\pi a^2+\sum_{J\in a}g_J\sum_{\lambda\in J}\frac{\pi}{k^2}\Bigg(&\frac{(\Gamma_{\lambda nJ})^2}{(E-E_\lambda)^2+\left(\frac{\Gamma_\lambda}{2}\right)^2}\\&+\frac{4\pi a}{k}\frac{\Gamma_{\lambda nJ}(E-E_\lambda)}{(E-E_\lambda)^2+\left(\frac{\Gamma_\lambda}{2}\right)^2}+\frac{\pi}{k^2}\sum_{\lambda'>\lambda}\Gamma_{\lambda nJ}\Gamma_{\lambda' nJ}g^{I}_{\lambda\lambda'}\Bigg)\\&+\frac{\pi}{k^2}\sum_{J\in p}g_J\sum_{\lambda\in J}\frac{(\Gamma_{\lambda nJ})^2}{(E-E_\lambda)^2\left(\frac{\Gamma_\lambda}{2}\right)^2}\end{aligned} \tag{2.1.31}$$

If we use auxiliary symbols σ_o and σ_p for the peak cross section and the potential scattering respectively, the above expressions are rewritten

$$\begin{aligned}\sigma_t(E)=\sigma_p+\sum_{J\in a}\sum_{\lambda\in J}\Bigg[&\sigma_{o\lambda}\sqrt{\frac{E_\lambda}{E}}\frac{1}{q^2{}_\lambda+1}+\sigma_{op\lambda}\frac{2q_\lambda}{q^2{}_\lambda+1}\\&+\frac{1}{\sqrt{E}}\sum_{\lambda'>\lambda}\sqrt{\sigma_{o\lambda}\sqrt{E_\lambda}\sigma_{o\lambda'}\sqrt{E_{\lambda'}}}\left(\sqrt{\Gamma_{\lambda nJ}\Gamma_{\lambda' nJ}}+\sqrt{\Gamma_{\lambda f}\Gamma_{\lambda' f}}\cos\theta_{\lambda\lambda'}\right)\\&\sqrt{\Gamma_\lambda\Gamma_{\lambda'}}g^{I}_{\lambda\lambda'}\Bigg]+\sum_{J\in p}\sum_{\lambda\in J}\sigma_{o\lambda}\sqrt{\frac{E_\lambda}{E}}\frac{p(E)}{q^2{}_\lambda+1}\end{aligned} \tag{2.1.32}$$

$$\begin{aligned}\sigma_n(E)=\sigma_p+\sum_{J\in a}\sum_{\lambda\in J}\Bigg[&\sigma_{o\lambda}\frac{\Gamma^{a}_{\lambda nJ}}{\Gamma_\lambda}\frac{1}{q^2{}_\lambda+1}+\sigma_{op\lambda}\frac{2q_\lambda}{q^2{}_\lambda+1}\\&+\sum_{\lambda'>\lambda}\sqrt{\sigma_{o\lambda}\sigma_{o\lambda'}\Gamma^{a}_{\lambda nJ}\Gamma^{a}_{\lambda' nJ}\Gamma_\lambda\Gamma_{\lambda'}}g^{I}_{\lambda\lambda'}\Bigg]+\sum_{J\in p}\sum_{\lambda\in J}\sigma_{o\lambda}\frac{\Gamma^{a}_{\lambda nJ}}{\Gamma_\lambda}\frac{(p(E))^2}{q^2{}_\lambda+1}\,,\end{aligned} \tag{2.1.33}$$

$$\sigma_\gamma(E)=\sum_{J\in a}\sum_{\lambda\in J}\left[\sigma_{o\lambda}\sqrt{\frac{E_\lambda}{E}}\frac{\Gamma_{\lambda\gamma}}{\Gamma_\lambda}\frac{1}{q^2{}_\lambda+1}\right]+\sum_{\lambda\in p}\sum_{\lambda\in J}\left[\sigma_{o\lambda}\sqrt{\frac{E_\lambda}{E}}\frac{p(E)}{q^2{}_\lambda+1}\right], \tag{2.1.34}$$

$$\sigma_f(E)=\sum_{J\in a}\sum_{\lambda\in J}\left[\sigma_{o\lambda}\sqrt{\frac{E_\lambda}{E}}\frac{\Gamma_{\lambda f}}{\Gamma_\lambda}\frac{1}{q^2{}_\lambda+1}+\sqrt{\frac{1}{E_\lambda}}\sum_{\lambda'>\lambda}\sqrt{\sqrt{\sigma_{o\lambda}}\sqrt{E_\lambda\sigma_{o\lambda'}}\sqrt{E_{\lambda'}}}\right.$$
$$\left.\times\sqrt{\Gamma_{\lambda f}\Gamma_{\lambda f}\Gamma_\lambda\Gamma_{\lambda'}}\times\cos\theta_{\lambda\lambda'}g^1{}_{\lambda\lambda'}\right]+\sum_{J\in p}\sum_{\lambda\in J}\sigma_{o\lambda}\sqrt{\frac{E_\lambda}{E}}\frac{\Gamma_{\lambda f}}{\Gamma_\lambda}\frac{1}{q^2{}_\lambda+1}, \tag{2.1.35}$$

$$g^1{}_{\lambda\lambda'}=2h_{\lambda\lambda'}\left[\frac{1}{\Gamma_\lambda}\frac{\Delta\Gamma_{\lambda\lambda'}+2\Delta E_{\lambda\lambda'}q_\lambda}{q^2{}_\lambda+1}-\frac{1}{\Gamma_{\lambda'}}\frac{\Delta\Gamma_{\lambda\lambda'}+2\Delta E_{\lambda\lambda'}q_{\lambda'}}{q^2{}_{\lambda'}+1}\right], \tag{2.1.36}$$

where

$$\sigma_{o\lambda}=\frac{4\pi}{k^2{}_\lambda}g_J\frac{\Gamma^n{}_{\lambda nJ}}{\Gamma_\lambda},\quad \sigma_p=4\pi a^2, \tag{2.1.37}$$

$$\sigma_{op\lambda}=(\sigma_{o\lambda}\sigma_p g_J\Gamma^n{}_{\lambda nJ}/\Gamma_\lambda)^{1/2},\quad q_\lambda=2(E-E_\lambda)/\Gamma_\lambda, \tag{2.1.38}$$

$$\Gamma_{\lambda nJ}=\Gamma^n{}_{\lambda nJ}(E/E_\lambda)^{1/2},\quad \Delta\Gamma_{\lambda\lambda'}=\Gamma_\lambda-\Gamma_{\lambda'},\quad \Delta E_{\lambda\lambda'}=E_\lambda-E_{\lambda'} \tag{2.1.39}$$

$$p(E)=\frac{(ka)^2}{1+(ka)^2}.$$

Here an energy dependence of the total width Γ_λ can be safely neglected in the vicinity of a resonance, because $\Gamma_{\lambda\gamma}$ and $\Gamma_{\lambda f}$ vary very slightly with energy and $\Gamma_{\lambda n}$ is very small compared with the summation of others, although it depends on enegry.

Note that derivation of the above expressions was made in the frame of center of mass system. For reactor calculation, however, we need the expressions in the frame of laboratory system. In the latter system all the expression should be multiplied by (A+1)/A, and we must use resonance parameters defined in the laboratory system. Therefore the following peak cross section

$$\sigma_{o\lambda}=\frac{4\pi}{k^2{}_\lambda}g_J\frac{A+1}{A}\frac{\Gamma^n{}_{\lambda nJ}}{\Gamma_\lambda}, \tag{2.1.40}$$

and the resonance parameters in the laboratory system will be used in the latter discussions. In the next we derive the expressions for Doppler-broadened cross sections following Buckler and Pull's derivation[16].

2.2 Doppler-broadend Cross Sections

In the previous section 2.1 reaction cross sections have been derived for the case where target nucleus is at rest. Actually, the target nuclei are in thermal motion and because of this motion the relative velocity of target nucleus to a neutron takes various values, so that the cross section of the previous section must be averaged with this velocity distribution. Let us assume that velocity $\vec{V}$ of target nucleus in laboratory system follows Maxwellian distribution corresponding to the temperature T of the target material. Then, an effective cross section $\sigma_{eff}(E)$ for neutrons of velocity $\vec{v}$ in the laboratory system can be defined as

$$\sigma_{eff}(E)=\int_0^\infty dV\int_{-1}^{1}d\mu\frac{|\vec{v}-\vec{V}|}{v}\sigma(E')N(V) \tag{2.2.1}$$

where

$$E'=\frac{1}{2}m|\vec{v}-\vec{V}|^2=\frac{1}{2}m(v^2+v^2-2vV\mu) \tag{2.2.2}$$

μ is the direction cosine between the direction of $\vec{V}$ and that of $\vec{v}$, and

$$N(V)dVd\mu=2\pi\left(\frac{\alpha}{\pi}\right)^{3/2}\exp(-\alpha V^2)V^2dVd\mu, \tag{2.2.3}$$

$$\alpha=M/2kT, \tag{2.2.4}$$

M=the mass of the target nucleus,

m=the mass of the neutron,
k=Boltzmann's constant,

$$E=\frac{1}{2}mv^2. \tag{2.2.5}$$

In Eq. (2.2.1), $\sigma(E)$ is the expressions of Eqs. (2.1.28), (2.1.29), (2.1.30) and (2.1.31) which have already been derived for a stationary target nucleus.
Let

$$E_1(V)=\frac{1}{2}m(V-v)^2 \tag{2.2.6}$$

and

$$E_2(V)=\frac{1}{2}m(V+v)^2 . \tag{2.2.7}$$

From Eq. (2.2.2), for all values of μ,

$$E_1(V)\leq E'\leq E_2(V),\quad E_1(0)=E'=E_2(0), \tag{2.2.8}$$

$$\frac{\partial\mu}{\partial E'}=-\frac{1}{mvV}=-\frac{1}{V\sqrt{2mE}}, \tag{2.2.9}$$

so that Eq. (2.2.1) can be rewritten as

$$\begin{aligned}\sigma_{\text{eff}}(E)&=\frac{1}{E}\sqrt{\frac{\alpha}{2m\pi}}\int_0^\infty 2\alpha V\exp(-\alpha V^2)\left[\int_{E_1(V)}^{E_2(V)}\sqrt{E'}\sigma(E')dE'\right]dV\\&=\frac{1}{E}\sqrt{\frac{\alpha}{2m\pi}}\int_0^\infty \exp(-\alpha V^2)\cdot S(V)dV ,\end{aligned} \tag{2.2.10}$$

where

$$S(V)=\sqrt{E_2(V)}\sigma(E_2)\frac{\partial E_2}{\partial V}-\sqrt{E_1(V)}\sigma(E_1)\frac{\partial E_1}{\partial V} . \tag{2.2.11}$$

It should be noted that the cross sections of Eqs. (2.1.28)~(2.1.31) consist of the summation of the following two forms of cross section.

$$\sigma^{(1)}(E)=C^1\frac{1}{\sqrt{E}}\frac{\frac{\Gamma_\lambda}{2}}{(E-E_\lambda)^2+\left(\frac{\Gamma_\lambda}{2}\right)^2} \tag{2.2.12}$$

and

$$\sigma^{(2)}(E)=C^2\frac{1}{\sqrt{E}}\frac{E-E_\lambda}{(E-E_\lambda)^2+\left(\frac{\Gamma_\lambda}{2}\right)^2} . \tag{2.2.13}$$

If the complex function $\Omega(V)$ is defined by

$$\Omega(V)=\frac{i}{E_2(V)-E_\lambda+i\frac{\Gamma_\lambda}{2}}\frac{\partial E_2}{\partial V}-\frac{i}{E_1(V)-E+i\frac{\Gamma_\lambda}{2}}\frac{\partial E_1}{\partial V} , \tag{2.2.14}$$

then, real and imaginary parts of $\Omega(V)$ are

$$Re(\Omega)=\frac{\frac{\Gamma_\lambda}{2}}{(E_2-E_\lambda)^2+\left(\frac{\Gamma_\lambda}{2}\right)^2}\frac{\partial E_2}{\partial V}-\frac{\frac{\Gamma_\lambda}{2}}{(E_1-E_\lambda)^2+\left(\frac{\Gamma_\lambda}{2}\right)^2}\frac{\partial E_1}{\partial V} \tag{2.2.15}$$

and

$$Im(\Omega)=\frac{E_2-E_\lambda}{(E_2-E_\lambda)^2+\left(\frac{\Gamma_\lambda}{2}\right)^2}\frac{\partial E_2}{\partial V}-\frac{E_1-E_\lambda}{(E_1-E_\lambda)^2+\left(\frac{\Gamma_\lambda}{2}\right)^2}\frac{\partial E_1}{\partial V} . \tag{2.2.16}$$

Let

$$P-iQ=\sqrt{\frac{2}{m}\left(E_\lambda-i\frac{\Gamma_\lambda}{2}\right)} ,$$

then Eq. (2. 2. 14) becomes

$$\Omega(V)=2\left[\frac{Q+i(P-v)}{V^2+(Q+i(P-v))^2}-\frac{Q+i(P+v)}{V^2+(Q+i(P+v))^2}\right]$$

$$=2\sqrt{\alpha}\left[\frac{\omega_1}{\alpha V^2+\omega_1^2}-\frac{\omega_2}{\alpha V^2+\omega_2^2}\right], \qquad (2.2.17)$$

where

$$\omega_1=\sqrt{\alpha}(Q+i(P-v)) , \qquad (2.2.18)$$

$$\omega_2=\sqrt{\alpha}(Q+i(P+v)) . \qquad (2.2.19)$$

Hence, using the complex probability integral $F(\omega)$:

$$F(\omega)=\int_0^\infty e^{-z^2}\frac{\omega}{z^2+\omega^2}dz , \qquad (2.2.20)$$

Eq. (2. 2. 10) is rewritten by the function $F(\omega)$, because

$$\int_0^\infty e^{-\alpha V^2}\Omega(V)dv=2[F(\omega_1)-F(\omega_2)] . \qquad (2.2.21)$$

In fact, from the above relation the effective values of two typical cross sections of Eqs. (2. 2. 12) and (2. 2. 13) become

$$\sigma^{(1)}{}_{\mathrm{eff}}(E)=\frac{2C^1}{E}\sqrt{\frac{\alpha}{2m\pi}}Re[F(\omega_1)-F(\omega_2)] \qquad (2.2.22)$$

and

$$\sigma^{(2)}{}_{\mathrm{eff}}(E)=\frac{2C^2}{E}\sqrt{\frac{\alpha}{2m\pi}}Im[F(\omega_1)-F(\omega_2)] . \qquad (2.2.23)$$

Using the above results, we can readily derive the expressions for the effective cross sections corresponding to Eqs. (2. 1. 28)~(2. 1. 31). At first, the second term of Eq. (2. 1. 28) becomes

$$\frac{\pi}{k^2}\sum_{\lambda\in s}g_J\left(\sum_{\lambda\in J}\frac{\Gamma_{\lambda nJ}\Gamma_\lambda}{(E-E_\lambda)^2+\left(\frac{\Gamma_\lambda}{2}\right)^2}\right)$$

$$=2\pi\frac{E}{k^2}\sum_{J\in s}g_J\left(\sum_{\lambda\in J}\Gamma^\circ{}_{\lambda nJ}\frac{1}{\sqrt{E}}\frac{\frac{\Gamma_\lambda}{2}}{(E-E_\lambda)^2+\left(\frac{\Gamma_\lambda}{2}\right)^2}\right) . \qquad (2.2.24)$$

Here, $\frac{E}{k^2}$ and $\Gamma^\circ{}_{\lambda nJ}$ $(=\Gamma_{\lambda nJ}/\sqrt{E})$ are taken to be constnat. Also, by neglecting the energy dependence of the partial widths $\Gamma_\lambda\gamma$ and $\Gamma_{\lambda f}$, it can be assumed that Γ_λ is a constant in the vicinity of energy E_λ of the level, as mentioned already at the end of the previous section. Thus, noting that the Eq. (2. 2. 24) is the from of Eq. (2. 2. 12), we can write the effective value for Eq. (2. 2. 12) as

$$4\pi\frac{E}{k^2}\sum_{J\in s}g_J\left\{\sum_{\lambda\in J}\Gamma^0{}_{\lambda nJ}\frac{1}{E}\sqrt{\frac{\alpha}{2m\pi}}Re[F(\omega_1)-F(\omega_2)]\right\} . \qquad (2.2.25)$$

On the other hand, the third term of Eq. (2. 1. 28), that is, the interference term between resonance and potential scattering, is written as follows,

$$\frac{4\pi a}{k}\sum_{J\in s}g_J\left(\sum_{\lambda\in J}\Gamma_{\lambda nJ}\frac{E-E_\lambda}{(E-E_\lambda)^2+\left(\frac{\Gamma_\lambda}{2}\right)^2}\right)$$

$$=4\pi a\left(\frac{\sqrt{E}}{k}\right)\sum_{J\in S}g_J\left(\sum_{\lambda\in J}\Gamma^\circ{}_{\lambda nJ}\frac{E-E_\lambda}{(E-E_\lambda)^2+\left(\frac{\Gamma_\lambda}{2}\right)^2}\right) . \qquad (2.2.26)$$

This form differs from that of Eq. (2. 2. 13) by the extra factor $\sqrt{E}$. The effective contribution therefore can not be expressed by the terms of $F(\omega)$. However, it is possible to take the factor $\sqrt{E}$ outside the integration in Eq. (2. 2. 10), under the following considerations. In the

enegry regions of our interest, $\sqrt{E}$ will be slowly varying compared with the resonance line shape. Moreover, the contribution from the interference scattering term will be small compared with that from the pure resonance scattering. Thus we obtain the effective cross section for Eq. (2. 2. 26)

$$8\pi a\left(\frac{\sqrt{E}}{k}\right)\sqrt{\frac{\alpha}{2m\pi}}\sum_{J\in s}g_J\left\{\sum_{\lambda\in J}\Gamma^{\circ}{}_{\lambda nJ}\frac{1}{\sqrt{E}}Im[F(\omega_1)-F(\omega_2)]\right\}. \tag{2. 2. 27}$$

The fourth term of Eq. (2. 1. 28) is the interference between pairs of s-wave resonance levels and

$$\frac{\pi}{k^2}\sum_{J\in s}g_J\sum_{\lambda'>\lambda}\sqrt{\Gamma_{\lambda nJ}\Gamma_{\lambda' nJ}}(\sqrt{\Gamma_{\lambda nJ}\Gamma_{\lambda' nJ}}+\sqrt{\Gamma_{\lambda f}\Gamma_{\lambda' f}}\cos\theta_{\lambda\lambda'})g^1{}_{\lambda\lambda'}$$
$$=\pi\left(\frac{E}{k^2}\right)\sum_{J\in s}g_J\left[\sum_{\lambda\in J}\sum_{\lambda'>\lambda}\sqrt{\Gamma^{\circ}{}_{\lambda nJ}\Gamma^{\circ}{}_{\lambda' nJ}}(\sqrt{\Gamma_{\lambda nJ}\Gamma_{\lambda' nJ}}+\sqrt{\Gamma_{\lambda f}\Gamma_{\lambda' f}}\cos\theta_{\lambda\lambda'})\frac{1}{\sqrt{E}}g^1{}_{\lambda\lambda'}\right], \tag{2. 2. 28}$$

where

$$g^1{}_{\lambda\lambda'}=h_{\lambda\lambda'}\left\{(\Gamma_\lambda-\Gamma_{\lambda'})\frac{\frac{\Gamma_\lambda}{2}}{(E-E_\lambda)^2+\left(\frac{\Gamma_\lambda}{2}\right)^2}+2(E_\lambda-E_{\lambda'})\frac{E-E_\lambda}{(E-E_\lambda)^2+\left(\frac{\Gamma_\lambda}{2}\right)^2}\right.$$
$$\left.-(\Gamma_\lambda-\Gamma_{\lambda'})\frac{\frac{\Gamma_{\lambda'}}{2}}{(E-E_{\lambda'})^2+\left(\frac{\Gamma_{\lambda'}}{2}\right)^2}-2(E_\lambda-E_{\lambda'})\frac{E-E_{\lambda'}}{(E-E_{\lambda'})+\left(\frac{\Gamma_{\lambda'}}{2}\right)^2}\right\} \tag{2. 2. 29}$$

and $g^1{}_{\lambda\lambda'}$ equals to Eq. (2. 1. 20). We now make the approximation that $\sqrt{\Gamma_{\lambda nJ}\Gamma_{\lambda' nJ}}$ is a constant because the interference is significant only for fissile nuclei and $\Gamma_n\ll\Gamma_f$ for these nuclei. Then, the effective contribution corresponding to Eq. (2. 2. 28) is, by uisng Eqs. (2. 2. 22) and (2. 2. 21),

$$2\pi\left(\frac{E}{k^2}\right)\sqrt{\frac{\alpha}{2m\pi}}\sum_{J\in s}g_J\sum_{\lambda\in J}\sum_{\lambda'>\lambda}\sqrt{\Gamma^{\circ}{}_{\lambda nJ}\Gamma^{\circ}{}_{\lambda' nJ}}(\sqrt{\Gamma_{\lambda nJ}\Gamma_{\lambda' nJ}}+\sqrt{\Gamma_{\lambda fJ}\Gamma_{\lambda' fJ}}\cos\theta_{\lambda\lambda'})$$
$$\times\frac{h_{\lambda\lambda'}}{E}\{(\Gamma_\lambda-\Gamma_{\lambda'})\cdot Re[F(\omega_1)-F(\omega_2)-F(\omega'_1)+F(\omega'_2)]$$
$$+2(E_\lambda-E_{\lambda'})Im[F(\omega_1)-F(\omega_2)-F(\omega'_1)+F(\omega'_2)]\}. \tag{2. 2. 30}$$

In this equation, ω'_1 and ω'_2 denote that the values are obtained for the λ'-level.

Let us consider the effetive contribution of the p-wave cross sections having the form

$$\frac{\pi}{k^2}\sum_{J\in p}g_J\sum_{\lambda\in J}\frac{\Gamma_{\lambda nJ}\Gamma_\lambda}{(E-E_\lambda)^2+\left(\frac{\Gamma_\lambda}{2}\right)^2}$$
$$=2\pi\left(\frac{E}{k^2}\right)\left(\frac{P_c}{E^{3/2}}\right)\sum_{\lambda\in p}g_J\sum_{\lambda\in J}\Gamma^{\circ}{}_{\lambda nJ}\sqrt{E}\frac{\frac{\Gamma_\lambda}{2}}{(E-E_\lambda)^2+\left(\frac{1}{2}\Gamma_\lambda\right)^2} \tag{2. 2. 31}$$

where P_c is the penetration factor of p-wave neutron and given by Eq. (2. 1. 6). In the energy range under consideration as $ka\ll1$, the energy varaiation of $1+(ka)^2$ can be neglected. Then, the effective p-wave cross sections for Eq. (2. 2. 31) becomes

$$2\pi\left(\frac{E}{k^2}\right)\left(\frac{P_c}{E^{3/2}}\right)\sum_{J\in p}g_J\left\{\sum_{\lambda\in J}\left(\Gamma^{\circ}{}_{\lambda nJ}\frac{E_\lambda}{\sqrt{E}}\frac{\frac{\Gamma_\lambda}{2}}{(E-E_\lambda)^2+\left(\frac{\Gamma_\lambda}{2}\right)^2}+\frac{\Gamma_\lambda}{2\sqrt{E}}\frac{E-E_\lambda}{(E-E_\lambda)^2+\left(\frac{\Gamma_\lambda}{2}\right)^2}\right)\right\}$$
$$=4\pi\left(\frac{E}{k^2}\right)\left(\frac{P_c}{E^{3/2}}\right)\sqrt{\frac{\alpha}{2m\pi}}\sum_{J\in p}g_J\sum_{\lambda\in J}\frac{\Gamma^{\circ}{}_{\lambda nJ}}{E}[E_\lambda Re(F(\omega_1)-F(\omega_2))$$
$$+\frac{1}{2}\Gamma_\lambda Im(F(\omega_1)-F(\omega_2))]. \tag{2. 2. 32}$$

Finally, from Eqs. (2. 2. 6)~(2. 2. 11), the effective contribution of the potential scattering cross sections is

$$\frac{4\pi a^2}{E}\sqrt{\frac{\alpha}{2m\pi}}\int_0^\infty e^{-\alpha V^2}m\sqrt{\frac{m}{2}}[(V+v)^2-(V+v)|V-v|]dV$$
$$=4\pi a^2\sqrt{\frac{\alpha}{\pi}}\left[2\int_0^V e^{-\alpha V^2}(1+V^2)dV+4\int_V^\infty e^{-\alpha V^2}\frac{V}{v}dV\right]$$
$$=4\pi a^2 f(v\sqrt{a}) \qquad (2.2.33)$$

where

$$f(X)=1+\frac{1}{2X^2}+\frac{1}{\sqrt{\pi}X}e^{-X^2}-\frac{1}{\sqrt{\pi}}\left(2+\frac{1}{X^2}\right)\int_X^\infty e^{-z^2}dz$$
$$X=V\sqrt{\alpha}=\sqrt{\frac{ME}{mkT}} \qquad (2.2.34)$$

In the resonance energy regions where $X\gg 1$, the effective potential scattering cross section can be taken to be equal to $4\pi a^2$.

Combining the above results, the final form of the Doppler-broadened total cross section can be written as

$$\sigma_t(E)\cong 4\pi a^2 f(V\sqrt{\alpha})+\frac{4\pi}{k^2}\sqrt{\frac{\alpha}{2m\pi}}\left\{\sum_{J\in s}g_J\sum_{\lambda\in J}\Gamma^\circ{}_{\lambda nJ}Re[F(\omega_1)-F(\omega_2)]\right\}$$
$$+\frac{8\pi a}{k}\sqrt{\frac{\alpha}{2m\pi}}\sum_{J\in s}g_t\left\{\sum_{\lambda\in J}\Gamma^\circ{}_{\lambda nJ}Im[F(\omega_1)-F(\omega_2)]\right\}$$
$$+\frac{2\pi}{k^2}\sqrt{\frac{\alpha}{2m\pi}}\sum_{J\in s}g_J\sum_{\lambda\in J}\sum_{\lambda'>\lambda}\sqrt{\Gamma^\circ{}_{\lambda nJ}\Gamma^\circ{}_{\lambda' nJ}}(\sqrt{\Gamma_{\lambda nJ}\Gamma_{\lambda' nJ}}+\sqrt{\Gamma_{\lambda tJ}\Gamma_{\lambda' tJ}}\cos\theta_{\lambda\lambda'})$$
$$\times h_{\lambda\lambda'}\{(\Gamma_\lambda-\Gamma_{\lambda'})Re[F(\omega_1)-F(\omega_2)-F(\omega_1')+F(\omega_2')]$$
$$+2(E_\lambda-E_{\lambda'})Im[F(\omega_1)-F(\omega_2)-F(\omega_1')+F(\omega_2')]\}$$
$$+\frac{4\pi}{k^2}\sqrt{\frac{\alpha}{2m\pi}}\left(\frac{P_c}{E^{3/2}}\right)\left\{\sum_{J\in p}g_J\sum_{J\in\lambda}\Gamma^\circ{}_{\lambda nJ}[E_\lambda Re(F(\omega_1)-F(\omega_2)\right.$$
$$\left.+\frac{1}{2}\Gamma_\lambda Im(F(\omega_1)-F(\omega_2))]\right\}. \qquad (2.2.36)$$

In Eq. (2. 2. 24), the fission, capture and scattering cross sections differ only by the factors $\Gamma_{\lambda\gamma}/\Gamma_\lambda$, $\Gamma_{\lambda t}/\Gamma_\lambda$ and $\Gamma_{\lambda nJ}/\Gamma_\lambda$, respectively. Hence, each effective cross section is given as follows:

$$\sigma_\gamma(E)\cong\frac{4\pi}{k^2}\sqrt{\frac{\alpha}{2m\pi}}\sum_{J\in s}g_J\sum_{\lambda\in J}\Gamma^\circ{}_{\lambda nJ}\frac{\Gamma_{\lambda\gamma}}{\Gamma_\lambda}Re[F(\omega_1)-F(\omega_2)]$$
$$+\frac{4\pi}{k^2}\sqrt{\frac{\alpha}{2m\pi}}\left(\frac{P_c}{E^{3/2}}\right)\sum_{J\in p}g_J\sum_{\lambda\in J}\Gamma^\circ{}_{\lambda nJ}\frac{\Gamma_{\lambda\gamma}}{\Gamma_\lambda}\left[E_\lambda Re[F(\omega_1)-F(\omega_2)]\right.$$
$$\left.+\frac{\Gamma_\lambda}{2}Im[F(\omega_1)-F(\omega_2)]\right], \qquad (2.2.37)$$

$$\sigma_t(E)\cong\frac{4\pi}{k^2}\sqrt{\frac{\alpha}{2m\pi}}\sum_{J\in s}g_J\sum_{\lambda\in J}\Gamma^\circ{}_{\lambda nJ}\frac{\Gamma_{\lambda t}}{\Gamma_\lambda}Re[F(\omega_1)-F(\omega_2)]$$
$$+\frac{4\pi}{k^2}\sqrt{\frac{\alpha}{2m\pi}}\left(\frac{P_c}{E^{3/2}}\right)\sum_{J\in p}g_J\sum_{\lambda\in J}\Gamma^\circ{}_{\lambda nJ}\frac{\Gamma_{\lambda t}}{\Gamma_\lambda}\left[E_\lambda Re[F(\omega_1)-F(\omega_2)]\right.$$
$$\left.+\frac{\Gamma_\lambda}{2}Im[F(\omega_1)-F(\omega_2)]\right]$$
$$+\frac{2\pi}{k^2}\sqrt{\frac{\alpha}{2m\pi}}\sum_{J\in s}g_J\sum_{\lambda\in J}\sum_{\lambda'>\lambda}\sqrt{\Gamma^\circ{}_{\lambda nJ}\Gamma^\circ{}_{\lambda' nJ}}\sqrt{\Gamma_{\lambda tJ}\Gamma_{\lambda' tJ}}\cos\theta_{\lambda\lambda'}$$
$$\times h_{\lambda\lambda'}\{(\Gamma_\lambda-\Gamma_{\lambda'})Re[F(\omega_1)-F(\omega_2)-F(\omega_1')+F(\omega_2')]$$
$$+2(E_\lambda-E_{\lambda'})Im[F(\omega_1)-F(\omega_2)-F(\omega_1')+F(\omega_2')]\}, \qquad (2.2.38)$$

$$\sigma_n(E)\cong 4\pi a^2 f(V\sqrt{\alpha})+\frac{4\pi}{k^2}\sqrt{\frac{\alpha}{2m\pi}}\sum_{J\in s}g_J\sum_{\lambda\in J}\Gamma^\circ{}_{\lambda nJ}\frac{\Gamma_{\lambda nJ}}{\Gamma_\lambda}Re[F(\omega_1)-F(\omega_2)]$$

$$+\frac{8\pi a}{k^2}\sqrt{\frac{\alpha}{2m\pi}}\sum_{J\in s}g_J\sum_{\lambda\in J}\Gamma^{\circ}_{\lambda nJ}\,Im[F(\omega_1)-F(\omega_2)]$$
$$+\frac{2\pi}{k^2}\sqrt{\frac{\alpha}{2m\pi}}\sum_{J\in s}g_J\sum_{\lambda\in J}\sum_{\lambda'>\lambda}\sqrt{\Gamma^{\circ}_{\lambda nJ}\Gamma_{\lambda' nJ}}\sqrt{\Gamma_{\lambda nJ}\Gamma_{\lambda' nJ}}h_{\lambda\lambda'}\{(\Gamma_\lambda-\Gamma_{\lambda'})$$
$$\times Re[F(\omega_1)-F(\omega_2)-F(\omega_1')+F(\omega_2')]$$
$$+2(E_\lambda-E_{\lambda'})Im[F(\omega_1)-F(\omega_2)-F(\omega_1')+F(\omega_2')]\}$$
$$+\frac{4\pi}{k_2}\sqrt{\frac{\alpha}{2m\pi}}\left(\frac{P_c}{E^{3/2}}\right)\sum_{J\in p}g_J\sum_{\lambda\in J}\Gamma^{\circ}_{\lambda nJ}\frac{\Gamma_{\lambda nJ}}{\Gamma_\lambda}\Big[E_\lambda Re[F(\omega_1)-F(\omega_2)]$$
$$+\frac{\Gamma_\lambda}{2}Im[F(\omega_1)-F(\omega_2)]\Big]\ . \qquad (2.2.39)$$

In the derivation of these expressions, we have made various approximations to the energy variation of various quantities. Especially, in the derivation of Eq. (2.2.27) for the interference scattering cross section, we neglected the $\sqrt{E}$ variation of the cross section with energy, therefore, Eq. (2.2.27) becomes a constant, when $E\to 0$. On the other hand, all the other terms appearing in the cross sections can be shown to have a predominantly $E^{-1/2}$ variation with energy, when the neutron energy is very low. However, in the energy region of interest, the errors by this approximation will be very small.

Finally, we will describe briefly the numerical method for obtaining values of Doppler-broadened function $F(\omega)$. The usual Doppler functions $\psi(\theta, x)$ and $\chi(\theta, x)$ are difined by

$$\psi(\theta,x)=\frac{\theta}{2\sqrt{\pi}}\int_{-\infty}^{+\infty}\frac{e^{-\frac{\theta^2(x-y)^2}{4}}}{1+y^2}dy\ , \qquad (2.2.40)$$

$$\chi(\theta,x)=\frac{\theta}{2\sqrt{\pi}}\int_{-\infty}^{+\infty}\frac{ye^{-\frac{\theta^2(x-y)^2}{4}}}{1+y^2}dy\ , \qquad (2.2.41)$$

where

$$x=\frac{2}{\Gamma_\lambda}(E-E_\lambda)\ , \qquad (2.2.42)$$

$$\theta=\frac{\Gamma_\lambda}{\Delta},\quad \Delta=\sqrt{\frac{4mkTE}{M}}\ . \qquad (2.2.43)$$

Let

$$z=\frac{\theta}{2}(y-x),\quad \omega_0=\frac{\theta}{2}(1-ix)$$

then

$$\psi(\theta,x)+i\chi(\theta,x)=\frac{\theta}{2\sqrt{\pi}}\int_{-\infty}^{\infty}e^{-z^2}\frac{i}{z+i\omega_0}dz$$
$$=\frac{\theta}{\sqrt{\pi}}\int_0^{\infty}e^{-z^2}\frac{\omega_0}{z+\omega_0^2}dz\ . \qquad (2.2.44)$$

Therefore,

$$\psi(\theta,x)=\frac{\theta}{\sqrt{\pi}}Re[F(\omega_0)] \qquad (2.2.45)$$

and

$$\chi(\theta,x)=\frac{\theta}{\sqrt{\pi}}Im[F(\omega_0)]\ . \qquad (2.2.46)$$

For the importnat energy region near resonance levels, $\sqrt{\frac{E_\lambda}{E}}$ in Eqs. (2.1.32)$\sim$(2.1.35) is nearly equel to unity, and also $\frac{1}{2}\ \Gamma_\lambda/E_\lambda\ll 1$. In this case, ω_0 is nearly equal to ω_1 of Eq. (2.2.18), and the imaginary part of ω_2 of Eq. (2.2.19) becomes very large, then $F(\omega_1)\cong F(\omega_0)$ and $F(\omega_2)\cong 0$. Therefore, $\psi(\theta, x)$ and $\chi(\theta, x)$ are a very good approximation of Doppler-broadening function $F(\omega)$, in the relatively higher energy regions.

Actually, in numerical calculation of the cross sections expressed by Eqs. (2. 2. 36)～(2. 2. 39), the accuracy of results depends naturally on the number of resonances in the summation, λ, and the accuracy of $F(\omega)$. Moreover, in calculating cross sections, the frequency of calculation $F(\omega)$ is extremely high, so that a high speed numerical technique for the calcuation of $F(\omega)$ is desired. We have used such a numerical method[19] for our calcualations of cross sections. The function $F(\omega)$ satisfies the following differential equation

$$-\frac{dF(\omega)}{d\omega}+2\omega F(\omega)=\sqrt{\pi}\ . \tag{2. 2. 47}$$

Differentiating Eq. (2. 2. 47) n-times, we obtain

$$F^{n+1}=2[\omega F^n+nF^{n-1}]: n=1, 2, 3\cdots\cdots\ . \tag{2. 2. 48}$$

If a numerical table of $F(\omega)$ is given, we can obtain the values in the immediate neighborhood of some ω_k by the use of Eqs. (2. 2. 47), (2. 2. 48) and the following Taylor expansions

$$F(\omega)=F(\omega_k)+(\omega-\omega_k)F'(\omega_k)+\frac{(\omega-\omega_k)^2}{2!}F''(\omega_k)+\cdots\cdots\ . \tag{2. 2. 49}$$

Now, noting that

$$F(\omega)=-F(-\omega)\ ;\ F(\bar{\omega})=\overline{F(\omega)}\ , \tag{2. 2. 50}$$

it is sufficient to provide a numerical table of $F(\omega)$ for a quadrant in the complex ω-plane. The square with corners $0, 5i$, $5i+5, 5$ was chosen and divided into 2500 equal squares by a 50×50 uniform mesh parallel to the axes. The values of $F(\omega)$ for these 2500 points were computed by using the code of BROAD.[16]

In the case that $|\omega|\geqq5$, $F(\omega)$ is written in the form

$$\begin{aligned}F(\omega)&=\int_0^\infty\frac{\omega e^{-z^2}}{z^2+\omega^2}dz\\&=\omega e^{\omega^2}\int_0^\infty\left[\frac{1}{z^2+\omega^2}-2\int_0^1 xe^{-(z^2-\omega^2)x^2}dx\right]dz\\&=\sqrt{\pi}\,e^{\omega^2}\left[\frac{\sqrt{\pi}}{2}-\omega\int_0^1 e^{-\omega^2x^2}dx\right]\\&=\sqrt{\pi}\,e^{\omega^2}\int_\omega^\infty e^{-z^2}dz\end{aligned} \tag{2. 2. 51}$$

and integrating by parts gives

$$\begin{aligned}F(\omega)&=\sqrt{\pi}\int_\omega^\infty ze^{-(z^2-\omega^2)}\frac{dz}{z^2}\\&=\sqrt{\pi}\left[\frac{1}{2\omega}-\frac{1}{2}\int_\omega^\infty e^{-(z^2-\omega^2)}\frac{dz}{z^2}\right]\\&\cong\frac{\sqrt{\pi}}{2\omega}\left[\sum_{n=0}^{N}(-1)^n\frac{1\cdot3\cdot5\cdots\cdots(2n-1)}{(2\omega^2)^n}\right],\end{aligned} \tag{2. 2 52}$$

where, in practical calculation, N is determined as the smallest integer for which either $N-\frac{1}{2}>|\omega|^2$ or $\frac{1\cdot3\cdot5\cdots(2N-1)}{(2|\omega|^2)^{N-1}}<0.5\times10^{-7}$.

2. 3 The Statistical Distribution of Resonance Parameters

In the sections 2. 1 and 2. 2 expressions for various cross sections were derived. For fast reactors, main contributions to the Doppler coefficient of reactivity come from the energy range where resonance parameters for individual resonances are not known, especially for fissile nuclei, because by the Deppler broabening it is impossible to separate a contribution of each resonance from experimental results. Therefore for treatments of cross sections in this energy range, statistical

methods are usually adopted. The frequency distribution laws necessary to these treatments are obtained from the studies of a set of parameters in the resolved resonance region. A number of studies of distribution laws have been made. In this section, we will describe the laws of the frequency distributions.

For the reduced neutron width $\Gamma_n^{(0)}$ for an entrance channel, the law of frequency distribution was derived by statistical arguments, which assume that expansion coefficients of the amplitude of wave function into composite states of a neutron and the traget nucleus are real and distributed normally with respect to levels. PORTER and THOMAS[20] tested this distribution law by maximum likelihood method and confirmed that the Porter-Thomas' χ^2 distribution of one degree of freedom is valid for reduced neutron width. Many other investigators reached the same conclusion as above.

The χ^2 distribution function is given by

$$P_\nu(x)dx=\frac{\nu}{2\Gamma(\nu/2)}\left[\frac{\nu x}{2\langle x\rangle}\right]^{\nu/2-1}\exp\left(-\frac{\nu x}{2\langle x\rangle}\right)\frac{dx}{\langle x\rangle} \tag{2.3.1}$$

where $\langle x\rangle$ is the mean value of x, ν is the degree of freedom and $\Gamma(x)$ is the Γ-function. We note that with the above distribution

$$\lim_{\nu\to\infty} P_\nu(x)=\delta(x-\langle x\rangle) \tag{2.3.2}$$

$$\langle x^2\rangle/\langle x\rangle^2=1+\frac{2}{\nu} \tag{2.3.3}$$

where

$$\langle f(x)\rangle=\int_0^\infty P_\nu(x)f(x)dx. \tag{2.3.4}$$

If there are ν channels for which the mean of reduced neutron width over levels is all equal, then we have, from the convolution law of the χ^2 distribution, the χ^2-distribution of ν degrees of freedom for total reduced neutron width. For slow neutron only one netrance and exit channel is open, therefore

$$\Gamma^\circ_{\lambda nJ}=\Gamma_{\lambda nJ}/\sqrt{E} \tag{2.3.5}$$

obeys the χ^2-distribution of 1-degree of freedom. When the spin of nucleus is not zero and neutrons having radial angular momentum l (>0) are considered, several channels are open for the reaction and ν should be carefully decided.

For radiative capture, as mention already there are a huge number of channels open. That is, it is expected that the frequency distribution of the total radiation width obeys the χ^2-distribution of large degree of freedom. For heavy elements variance of Γ_γ is very small and Γ_γ is thought to be almost constant especially in the energy region of interest. In fact experimental results show this constancy of the total radiative capture widths. This fact has been utilized in reactor physics calculation.

Generally, the channels for nuclear reaction are defined by the nature of the particles and their internal states. If this definition is valid, there should be a large number of channels available for the fission process and interference effects between levels should be neglected and fission cross sections should be reproduced by the single level Breit-Wigner expression. However this is not the case. The interpretation for this peculiarity of fission process was presented by BOHR[21]. The fission process passes at the saddle point deformation through transition states. A few transition states are reached because of conservation of energy and angular momentum, etc. For fission process, the channels should be the transition states, instead of particle channels which lead to fission product formation, because these transition states are true entrance to the fission process. In fact from analyses of slow neutron fission cross section. $\Gamma_f=\langle\Gamma_f^2\rangle/\langle\Gamma_f\rangle^2\cong 2$ is obtained for every fissionable element[22]. Moreover, more sophisticated analyses of accurate measurements gives us

informations about fission width for every J-state[23),24)]. For s-wave fission width, spin dependence of fission widths is found for ^{239}Pu. This means that we should refer to the application of collective model to the fission process and determine true number of fission channels and corresponding fission width. The fission process will be described in the next chapter.

For level spacing distribution, Wigner distribution is confirmed to be valid for every nucleus[20)]. The derivation of this law is based on statistical consideration of eigen values of Hamiltonian of interacting system. The spacing of two levels is give by $|E_1-E_2|=\sqrt{(H_{11}-H_{22})^2+4(H^{12})^2}$ where the values of matrix elements are thought to be randomly distributed. This is equivalent to the following statement: for $t=|E_1-E_2|=\sqrt{x^2+y^2}$, x and y is independent of each other and the values are distributed randomly and uniformely, then the probability for finding a level between r and $r+dr$ is given by const. r. If $P(r)\,dr$ is the probability for finding second level between r and $r+dr$, then $Q(r)=1-\int_0^r P(r')dr'$ is the probability not finding a level between 0 and r. $P(r)$ is equal to the product $Q(r)$ and const. r. This leads to a differential equation for $P(r)$ and we have the Wigner distribution, i. e.,

$$P_0(x)dx=(\pi/2)\exp(-\pi x^2/4D^2)\frac{xdx}{D^2} \tag{2. 3. 6}$$

with

$$\langle D^2\rangle/\langle D\rangle^2=\frac{4}{\pi}\cong 1.273.$$

In the above we have described statistical distribution laws of parameter based on statistical independence. The existence of correlations between these parameters has not been discovered yet.

2. 4 Average Cross Sections in the Unresolved Resonance Energy Region

As mentioned already in the previous section, the contribution to the Doppler reactivity comes from the unresolved resonance energy region, especially for fissible nuclei. In this region we must obtain cross sections by using the distribution laws for resonance parameters. The effective group cross sections are obtained from these cross sections. However it is important to confirm reliability of statistical parameters adopted. For this purpose we need average cross sections which do not mean the averages over $1/E$ spectrum but those to be compared with experimentally measured values. In this region, however, contributions from inelastic scattering process is rather significant, so the (n, n′) process should be included.

The expressions for cross sections are given by Eqs. from (2. 1. 32) to (2. 1. 35). The average cross sections is defined over a wide energy width enough to include sufficiently large number of resonances. Hence the same distribution laws of resonance parameters as found for a set of resolved resonances are seen in this energy range. However the energy range should be taken as narrow as possible in that the range is considered as a representative point of measurement. We shall define the average cross section as follows,

$$\langle\sigma_x\rangle=\frac{1}{\Delta E}\int_{\Delta E}\sigma_x(E)dE. \tag{2. 4. 1}$$

Note that the low resolution experiments at high energy give the values corresponding to the above quantities, that is, for experimental results in the energy region of interest, Eq. (2. 4. 1) is applicable. The contribution from resonances to Eq. (2. 4. 1) can be calculated as follows. That is, the contribution from the single level term is written as

$$\int_{\Delta E}f(E)\frac{dE}{q^2_\lambda+1}\cong\frac{\Gamma_\lambda}{2}f(E_\lambda)\int_{-\infty}^{\infty}\frac{dq_\lambda}{q^2_\lambda+1}=\frac{\pi}{2}\Gamma_\lambda f(E_\lambda) \tag{2. 4. 2}$$

$$\int_{\Delta E} f(E)\frac{q_\lambda dE}{q^2{}_\lambda+1}\cong 0 \tag{2.4.3}$$

where $f(E)$ is a product of slowly varying functions such as $\sqrt{\frac{E_\lambda}{E}}$ and a penetration factor $P(E)$, and its energy variation can be neglected in this energy range, because the energy rangy was chosen as narrow as possible. It was assumed that area under a resonance level is not changed with the temperature of target sample and energy range for integrations can be extended to infinity.

The interference term yields no contribution to cross sections, because contructive and destructive contribution cancels each other. Therefore in the present approximation we have

$$\langle\sigma_t\rangle=\sigma_p+\frac{\pi}{2}\frac{1}{\Delta E}\sum_{l,J}\sum_\lambda \Gamma_\lambda\sigma_{o\lambda}P_l(E_\lambda)$$

$$=\sigma_p+\frac{\pi}{2}\frac{2.60\times10^{-6}A}{\Delta E(A+1)}\sum_{l,J}g_J\sum_\lambda\frac{\Gamma_{\lambda nJ}}{E_\lambda} \tag{2.4.4}$$

$$\langle\sigma_\gamma\rangle=\frac{\pi}{2}\frac{2.60\times10^{-6}A}{\Delta E(A+1)}\sum_{l,J}g_J\sum_\lambda\frac{\Gamma_{\lambda nJ}\Gamma_{\lambda\gamma}}{E_\lambda\Gamma_\lambda} \tag{2.4.5}$$

$$\langle\sigma_f\rangle=\frac{\pi}{2}\frac{2.60\times10^{-6}A}{\Delta E(A+1)}\sum_{l,J}g_J\sum_\lambda\frac{\Gamma_{\lambda nJ}\Gamma_{\lambda f}}{E_\lambda\Gamma_\lambda} \tag{2.4.6}$$

$$\langle\sigma_n\rangle=\sigma_p+\frac{\pi}{2}\frac{2.60\times10^{-6}A}{\Delta E(A+1)}\sum_{l,J}g_J\sum_\lambda\frac{(\Gamma_{\lambda nJ})^2}{E_\lambda\Gamma_\lambda} \tag{2.4.7}$$

In the above equations E_λ is thought as almost constant, because the energy range is narrow. Hence it is substituted by a representative energy in the energy range. For heavy element we can always the narrow energy range which satisfies our requirements. By this approximation, Eqs. from (2.4.4) to (2.4.7) are rewritten as

$$\langle\sigma_t\rangle=\sigma_p+\frac{\pi}{2}\sum_{l,J}\sigma^0{}_J\cdot\frac{1}{\Delta E}\sum_\lambda\Gamma_{\lambda nJ}$$

$$\cong\sigma_p+\frac{\pi}{2}\sum_{l,J}\sigma^0{}_J\frac{\langle\Gamma_{nJ}\rangle_\lambda}{\langle D_J\rangle_\lambda} \tag{2.4.8}$$

$$\langle\sigma_x\rangle\cong\frac{\pi}{2}\sum_{l,J}\sigma_{oJ}\frac{1}{\langle D_J\rangle_\lambda}\left\langle\frac{\Gamma_{nJ}\Gamma_x}{\Gamma}\right\rangle_\lambda (x=\gamma \text{ or f}) \tag{2.4.9}$$

$$\langle\sigma_s\rangle\cong\sigma_p+\frac{\pi}{2}\sum_{l,J}\sigma^0{}_J\frac{1}{\langle D_J\rangle_\lambda}\left\langle\frac{\Gamma_n{}^2{}_J}{\Gamma}\right\rangle_\lambda \tag{2.4.10}$$

$$\sigma^0{}_J=\frac{2.60\times10^{-6}}{E}\cdot\frac{A+1}{A}g_J \tag{2.4.11}$$

where the symbol $\langle\ \rangle_\lambda$ means average over levels. If we use the cross section for formation of compound nucleus we have other forms

$$\langle\sigma_t\rangle=\sigma_p+\sum_{l,J}\langle\sigma_{clJ}\rangle \tag{2.4.12}$$

$$\langle\sigma_x\rangle=\sum_{l,J}\langle\sigma_{clJ}\rangle\left\langle\frac{\Gamma_{nJ}\Gamma_x}{\Gamma}\right\rangle_\lambda/\langle\Gamma_{nJ}\rangle_\lambda \tag{2.4.13}$$

$$\langle\sigma_s\rangle=\sigma_p+\sum_{l,J}\langle\sigma_{clJ}\rangle\left\langle\frac{\Gamma_n{}^2{}_J}{\Gamma}\right\rangle_\lambda/\langle\Gamma_{nJ}\rangle_\lambda \tag{2.4.14}$$

where

$$\langle\sigma_{clJ}\rangle=\frac{\pi}{2}\sigma_{oJ}\langle\Gamma_{nJ}\rangle_\lambda/\langle D_J\rangle_\lambda. \tag{2.4.15}$$

The average over levels is obtained by the distribution laws of resonance parameters because of large number of resonances are involved in this energy range. On the other hand, the radiative capture width Γ_γ is thought as constant so we have

$$\langle\sigma_\gamma\rangle=\sum_{l,J}\langle\sigma_{clJ}\rangle\frac{\langle\Gamma_\gamma\rangle_\lambda}{\langle\Gamma_{nJ}\rangle_\lambda}\left\langle\frac{u}{1+u+v+w}\right\rangle_\lambda, \tag{2.4.16}$$

$$\langle\sigma_f\rangle=\sum_{l,J}\langle\sigma_{clJ}\rangle\frac{\langle\Gamma_\gamma\rangle_\lambda}{\langle\Gamma_{nJ}\rangle_\lambda}\left\langle\frac{uv}{1+u+v+w}\right\rangle, \tag{2.4.17}$$

$$\langle\sigma_{in}\rangle=\sum_{l,J}\langle\sigma_{clJ}\rangle\frac{\langle\Gamma_\lambda\rangle_\lambda}{\langle\Gamma_{nJ}\rangle_\lambda}\left\langle\frac{uw}{1+u+v+w}\right\rangle_\lambda, \tag{2.4.18}$$

$$\langle\sigma_s\rangle=\langle\sigma_t\rangle-\Sigma\langle\sigma_x\rangle \tag{2.4.19}$$

where σ_{in} is the inelastic cross sections, and u, v and w are difined by.

$$u_\lambda\equiv\frac{\Gamma_{\lambda n}}{\langle\Gamma_\gamma\rangle_\lambda}=\frac{1}{\langle\Gamma_\gamma\rangle_\lambda}\sum_{j\in l,J}^{N_{nlJ}}\Gamma_{\lambda nljJ}=\sum_{j\in l,J}^{N_{nlJ}}u_{\lambda ljJ}, \tag{2.4.20}$$

$$v_\lambda\equiv\frac{\Gamma_{\lambda f}}{\langle\Gamma_\gamma\rangle_\lambda}=\frac{1}{\langle\Gamma_\gamma\rangle_\lambda}\sum_{c\in f}^{N_{flJ}}v_{\lambda c} \tag{2.4.21}$$

$$w_\lambda\equiv\frac{\Gamma_{\lambda in}}{\langle\Gamma_\gamma\rangle_\lambda}=\frac{1}{\langle\Gamma_\gamma\rangle_\lambda}\sum_{\nu,l}\sum_{jl,J}^{N^\nu_{inlJ}}\Gamma_{\lambda^\nu inljJ}=\sum_{\nu,l}\sum_{jl,J}^{N^\nu_{inlJ}}w^\nu{}_{\lambda inljJ}. \tag{2.4.22}$$

Here, N_{xlJ} means number of channels for the reaction process x through the states of total angular momentum J of compound nucleus, and ν means the ν-th excited level. For s-wave neutron, only one state is $j=\frac{1}{2}$ is available to reactions and only one entrance chnnel is open for neutron. We shall adopt the assumption of the j-indpendence of reduced neutron width. We can simplify the above expressions as

$$u_\lambda=\frac{N_{nlJ}\Gamma_{\lambda nljJ}}{\langle\Gamma_\gamma\rangle_\lambda},\quad \Gamma_{\lambda n}\cong N_{nlJ}\Gamma_{\lambda nljJ} \tag{2.4.23}$$

$$w_\lambda\cong\sum_{\nu,l}\frac{N^\nu_{inlJ}}{\langle\Gamma_\gamma\rangle_\lambda}\Gamma^\nu{}_{\lambda inljJ}=\sum_{\nu,l}w^\nu{}_{\lambda lJ}. \tag{2.4.24}$$

From the above assumption, for elastic and inelastic neutron reduced width we must use the χ^2 distribution of N_{xlJ} degrees of freedom for reduced width of channels specified by the quantum number (l, J). If any evidence on the j-dependence of these width is found we must use the χ^2 distribution for the channel specified by (l, j, J).

The last terms in Eqs. form (2.4.16) to (2.4.18) are given by

$$\left\langle\frac{ux}{1+u+v+w}\right\rangle=\int dx_1dx_2\cdots dx_N\frac{\langle\Gamma_\gamma\rangle^{-m_1-m_2}x_1^{m_1}x^{m_2}P_{n_1}(x_1)P_{n_2}(x_2)\cdots P_{n_N}(x_N)}{1+\frac{1}{\langle\Gamma_\gamma\rangle}(x_1+x_2+\cdots+x_N)}$$

$$=\frac{2^Na_1^{m_1}a_2^{m_2}}{\prod_{\nu=1}^{N}\Gamma\left(\frac{n_\nu}{2}\right)}\int dy_1dy_2\cdots dy_N\frac{y_1^{k_1}y_2^{k_2}\cdots y_N^{k_N}e^{-(y_1^2+y_2^2+\cdots+y_N^2)}}{1+a_1y_1+a_2y_2+\cdots+a_Ny_N^2}$$

$$=a_1^{m_1}a_2^{m_1}\int_0^\infty dse^{-s}\prod_{\rho=1}^{N}\left(\frac{2}{\Gamma\left(\frac{n_\rho}{2}\right)}\int_0^\infty dt\ t^{k_\rho}e^{-(1+a_\rho s)t^2}\right) \tag{2.4.25}$$

where $\rho=1$ is used for u, $\rho=2$ is used for x, m_1 or m_2 is an integer 0 or 1. And k_ρ is given by

$$k_\rho=\begin{cases}2m_\rho+n_\rho-1 & \text{for } \rho=1 \text{ or } 2\\ n_\nu-1 & \text{for } \rho>2.\end{cases} \tag{2.4.26}$$

Since the number n is 1 or at most 2 and

$$\frac{2}{\Gamma\left(\frac{n}{2}\right)}\int_0^\infty dt\ t^ke^{-(1+as)t^2}=\begin{cases}\dfrac{1}{2^m(1+as)^{m+1/2}} & \text{for } n=1\\ \dfrac{1}{(1+as)^{m+1}} & \text{for } n=2\end{cases} \tag{2.4.27}$$

with

$$a=\frac{2\langle x\rangle}{n\langle\Gamma_\gamma\rangle}\,, \tag{2.4.28}$$

the expressions of cross sections can be given by

$$\langle\sigma_\gamma\rangle=\sum_{l,J}\langle\sigma_{clJ}\rangle\int_0^\infty F_{lJ}(s)e^{-s}ds \tag{2.4.29}$$

$$\langle\sigma_f\rangle=\sum_{l,J}\langle\sigma_{clJ}\rangle\left[\sum_{c'}\langle v_{lJc'}\rangle\int_0^\infty\frac{F_{lJ}(s)e^{-s}}{1+2\langle v_{lJc'}\rangle s}ds\right] \tag{2.4.30}$$

$$\langle\sigma_{in}\rangle=\sum_{l,J}\langle\sigma_{clJ}\rangle\left[\sum_{\nu}\sum_{l',J'}\langle w_{l'J'}{}^{\nu}\rangle\int_0^\infty\frac{F_{lJ}(s)e^{-s}}{1+2\langle w_{l'J'}{}^{\nu}\rangle s}ds\right]. \tag{2.4.31}$$

where

$$F_{lJ}(s)=\frac{1}{[1+2\langle u_{lJ}\rangle s]^{1+N_{lJ}/2}\left[\prod_{c'=1}^{N_{lJ}}(1+2\langle v_{lJc'}\rangle s)^{1/2}\right]\left[\prod_{\nu',l',J'}^{NinlJ}(1+2\langle w^{\nu'}{}_{l'J'}\rangle s)^{1/2}\right]}.$$

2.5 Conservation Rules for Spin and Parity

For calculating cross sections it is necessary to know open channels. Otherwise we will obtain false results for the cross sections in question. In fact cross sections are composed of contributions from each channel. Especially for inelastic scattering there are usually various channels available so that we have to assign quantum number specifying these channels.

For entrance channels the total angular momentum J is given by the well known vector addition law

$$\vec{J}=\vec{j}+\vec{I},\qquad \vec{j}=\vec{l}+\vec{s} \tag{2.5.1}$$

where s $(=+\frac{1}{2})$ denotes the spin of a neutron. Using this relation, the possible total angular momentums J of conpound nucleus which can be reached from the given j are

$$J=I+j,\ I+j-1,\ \cdots\cdots,\ |I-j| \tag{2.5.2}$$

and the total anglar momentum j of a neutron are

$$j=l+s,\ |l-s| \tag{2.5.3}$$

If parities of the compound nucleus, the target nucleus and a nautron is denoted by Π_c, Π_t and Π_n $(=(-1)^l)$ respectively, then we have from the conservation rule

$$\Pi_c=\Pi_n\times\Pi_t=(-1)^l\Pi_t \tag{2.5.4}$$

For the exit channels from the compound nucleus the similar relation holds

$$\vec{J}=\vec{j}'+\vec{I}^*\,, \tag{2.5.5}$$

$$\vec{j}'=\vec{l}'+\vec{s} \tag{2.5.6}$$

$$\Pi_c=(-1)^{l'}\Pi^*{}_r \tag{2.5.7}$$

where the superscripts * and ′ means the state of residual nucleus and the state of a neutron emitted respectively. From the above we have the conservation of spin and parity

$$\vec{j}+\vec{I}=\vec{J}=\vec{j}'+\vec{I}^*\qquad(-1)^l\Pi_r=(-1)^{l'}\Pi^*{}_r\,. \tag{2.5.8}$$

For ^{235}U, ^{238}U, ^{239}Pu and ^{240}Pu, we shall asign both entrance and exit channels. The energy range under consideration is below 30 keV. The excited states, particularly low lying, of these nuclei are well known experimentally. Here we have adopted the level scheme evaluated at AWRE[25]. The low lying levels for ^{235}U and ^{239}Pu reproduced in the TABLE (2.5.1). For ^{238}U and ^{240}Pu, however the first excited state lies above 30 keV. The excited levels for these nucleus do not concern with reaction process considered. For ^{235}U and ^{239}Pu the two low lying excited levels as well as the ground level should be taken into accounts. Because of its spin and parity the first excited state cannot reach to any exit channels with accompanying s and p-wave neutrons. The possible entrance channels which lead to formation of the compound nucleus and exit channels

leading to the residual nucleus are shown in the TABLE (2. 5. 2) and (2. 5. 3). In the TABLE (2. 5. 4) possible entrance channels for formation of the compound nucleus of ^{238}U and ^{240}Pu are shown.

TABLE 2. 5. 1 Level scheme for ^{235}U and ^{239}Pu

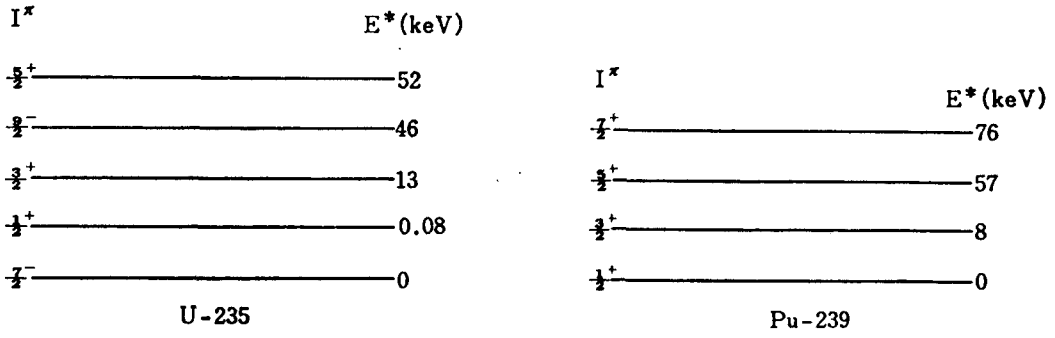

TABLE 2. 5. 2 Entrance and exit channels for compound nucleus formed by neutron and ^{235}U

$\left(I^{\pi}=\frac{7^-}{2},\ I^{\pi *}=\frac{3^+}{2}\right)$

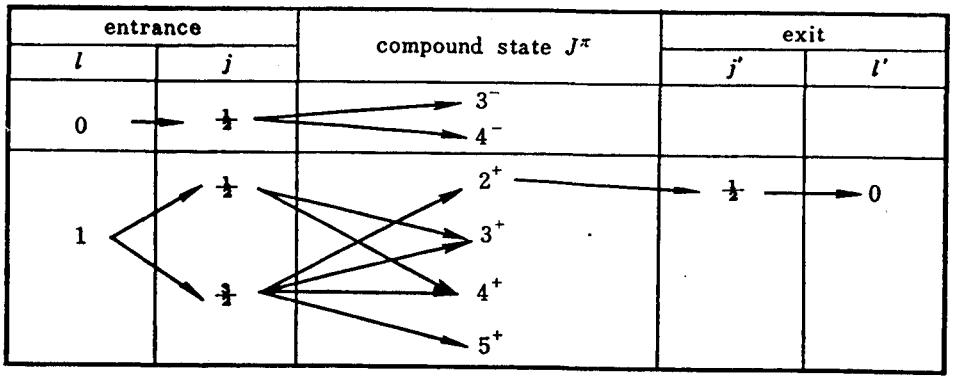

TABLE 2. 5. 3 Entrance and exit channels for compound nucleus formed by neutron and ^{239}Pu

$\left(I^{\pi}=\frac{2^+}{2},\ I^{\pi *}=\frac{3^+}{2}\right)$

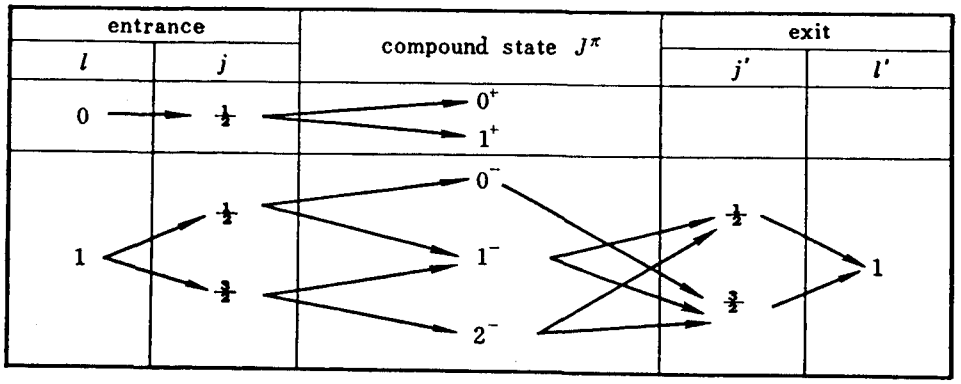

TABLE 2. 5. 4 Entrance channels for compound nucleus formed by neutron and nucleus with 0^+

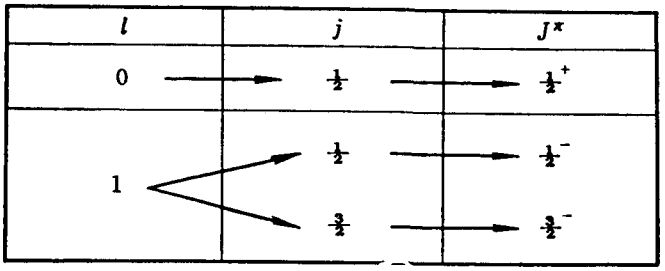

2.6 The Mean Resonance Parameters

It is necessary to have mean values of various resonance parameters including level spacings for obtaining averaged cross sections in the unresolved resonance region. For extrapolating mean resonance parameters obtained from resolved resonance paramenters into those of the unlesolved resonance energy and other channels, we should have knowledges of energy and (l, J^{π}) dependences of mean parameters. In this section we will describe the mean resonance parameters except for the fission widths.

The level spacing is proportional to the inverse of the level density. The latter quantity is obtained by the method of statistical thermodynamics. In the nuclear reactions, compound nucleus, which is composed of some number of particles, protons and neutrons, can exchange particles with its environment. Therefore it is open system in the thermodynamic sense. The probability for finding a compound nucleus specified by a number of constants of motion is given by the grand canonical ensemble

$$\exp(-\beta E_l+\sum_k \beta\mu_k C_{kl}+\Omega) \tag{2.6.1}$$

where Ω/β is the free energy, μ_k is an adjustable parameter, associated with the k-th constant of motion and C_{kl} is the value of the k-th constant of motion for the l-th level. The summation over states is given by

$$\exp(-\Omega)=\sum_l \exp(-\beta E_l+\sum_k \beta\mu_k C_{kl}). \tag{2.6.2}$$

The sum over states and probability are connected with the level density in the following manner. The sum over the level l is replaced by an integration using the level density.

$$\exp(-\Omega)=\sum_{k=1}^{K}\sum_{C_k}\int dE\rho(E,C'_1,\cdots C'_k)\exp(\beta E+\sum_{k=1}^{K}\beta\mu_k C_k) \tag{2.6.3}$$

From this we obtain the level density by the Laplace inversion and the method of steepest descent.

$$\rho(E,C'_1,\cdots C'_k)\propto|detA|^{1/2}\exp(\beta E-\sum\beta\mu_k C'_k+\Omega) \tag{2.6.4}$$

where E and C'_k are determined from the saddle point conditions

$$E=-\frac{\partial\Omega}{\partial\beta} \tag{2.6.5}$$

$$C'_k=-\frac{\partial\Omega}{\partial(\beta\mu_k)} \tag{2.6.6}$$

The matrix A is the reciprocal of a coefficient matrix a_{ij}, and a_{ij} is given by

$$\frac{\partial^2\Omega}{\partial(\beta\mu_i)\partial(\beta\mu_j)} \quad (\mu_0=1) \tag{2.6.8}$$

Using the Fermi gas consisting A particles, we have

$$\rho(E-E(\beta=\infty))\propto U^{-1}\exp\left\{\pi\left(\frac{2U\rho}{3}\right)^{1/2}\right\} \tag{2.6.9}$$

where $E(\beta=\infty)$ is the ground state energy, U is excitation energy $(E-E(\beta=\infty))$, and ρ is the density of particle states at the Fermi energy ε_0. The ρ and ε_0 are given by

$$\varepsilon_0=\left(\frac{\pi}{3}\right)\frac{9}{4}\frac{\hbar}{2Mr_0^2} \quad (M\text{: nucleon mass, } r_0 \text{ nuclear radius})$$

$$\rho=\frac{3}{2}\frac{\varepsilon_0}{A}.$$

By using these expression and setting $E(\beta=\infty)\cong-$Binding Energy

$$\rho(E)\cong\rho(0)e^{E/0.6}$$
$$D(E)\cong D(0)e^{-E/0.6} \tag{6.6.10}$$

where $E \ll$ Binding energy and unit of E is MeV.
The energy denpendence (6. 6. 10) or more accurately (2. 7. 9) is not significant for our present treament.

If a nucleon in the compound nucleus excited from its ground state to the next higher level of the single particle level, the difference in energy is proportional to $2\left(\frac{C_k}{\beta}\right)^2$ (sum of annihilation and creation). The difference is just the same as spacing of the single particle level. Hence if nucleons in the compund nucleus are exicted, and energy of the nucleus is elevated to the next higher level, the difference in energy is written as

$$\frac{1}{\rho}\sum_k \frac{C_k^2}{2\left(\frac{C_k}{\beta}\right)^2}. \tag{2. 6. 11}$$

On the other hand

$$\frac{\partial^2 \Omega}{\partial(\beta\mu_k)^2} = \sigma_k^2 = \frac{\left(\frac{C_k}{\beta}\right)^2}{\pi}\left\{6\rho(E-E(\beta=\infty))\right\}^{1/2}. \tag{2. 6. 12}$$

Now setting $E-E(\beta=\infty) = E-E_0+E_0-E(\beta=\infty)$ and assuming $E-E_0<E_0-E(\beta=\infty)$ we have

$$\rho(E,C_k) \cong \rho(E)\cdot(\sigma_1\sigma_2\cdots\cdots\sigma_k)^{-1}\exp\{C_k^2/2\sigma_k^2\} \tag{2. 6. 13}$$

From the above equation the spin dependence of the level density is obtained as

$$\rho(E/M) = \rho(E,0)\exp(-\hbar^2/M^2\beta/2\theta) \tag{2. 6. 14}$$

where θ is the moment of inertia, $\frac{\theta}{\hbar^2\beta}=\sigma_M^2$ and $\frac{\hbar^2/M}{2\theta}$ is the rotational energy. By taking difference in $\rho(E, M)$ between the total angular momentum J and $J+1$, we have

$$\rho(E, J) \propto \exp\{-J(J+1)/2\sigma_M^2\}\cdot(2J+1)\rho(E). \tag{2. 6. 15}$$

Usualey exponential factor is very close to unity for heavy nucleus under study. Hence

$$D(E, J) \propto D(E, 0)\frac{1}{2J+1}. \tag{2. 6. 16}$$

The above J dependence was confirmed to be approximately valid from comparison of measured level spacing.

For the capture width there should be energy dependence, because the width is related to matrix elements for dipole transitons. However in the energy rangy of interest the dependence can be neglected.

For the energy depedences of neutron widths the following relation is well known

$$\langle\Gamma_{nljJ}\rangle = \langle\Gamma_{nljJ}\rangle v_l\sqrt{E} \tag{2. 6. 17}$$

where $\langle\Gamma_{nljJ}\rangle$ is the reduced neutron width and v_l is the penetration factor for a neutron having an orbital angular momentum l.

There should be dependence of reduced neuron widths on total angular momentum J as well as isotopic spin τ because isotopic spin and spin-orbit coupling interactions exist between a nucleus and neutron. However there are not sufficient evidence which supports definitely this spin dependence of reduced width. The independence of the width on j has been assumed and no cross section has been found such that this assumption is seriously contradicting to experimental results.

For obtaining $\langle\Gamma^0_{nlJ}\rangle$, it is convenient to introduce the strength function S_l, which gives a measure for strength of the pole of R-matix and is directly connected with the total cross section for the l neutron.

$$S_l = \frac{1}{2l+1}\sum_J (g_J/D_J)\cdot\sum_j \langle\Gamma_{nljJ}{}^{(0)}\rangle \tag{2. 6. 18}$$

The strength function is rather not sensitive to missing of levels because it can be determined by the ratio $\langle\Gamma_{nljJ}{}^{(0)}\rangle/D_J$.

FESHBACH suggested[26] the validity of J independence of the strength function, which, however,

is by no means obvious. For the J dependence of the strength function, a few studies have been performed so far. According to analyses by JULIEN[27] the J denpendence is plausible for the nuclei of spin 3/2, but evidences for other spin have not been known. Due to lower l value neutrons J dependence is not significant. Therefore usually J-independence of strengh function is assumed. Then we have for

$$S_0=\frac{\langle\Gamma_{n1/2J}^{(0)}\rangle}{\langle D_J\rangle}=\frac{g_J\langle\Gamma_{n1/2}^{(0)}\rangle}{\langle D_s\rangle} \tag{2.6.19}$$

where $\langle D_s\rangle=\langle D_J\rangle$ g_J is the observed level spacing for s-wave neutron. And

$$\langle\Gamma_{n1/2J}\rangle=\frac{S_0\langle D_s\rangle}{g_J}\sqrt{E}\,. \tag{2.6.20}$$

Smilary for p-wave neutrons

$$S_l=\frac{1}{2l+1}\frac{\langle\Gamma_{nljJ}^0\rangle}{\langle D_J\rangle}\sum_{J,j}\sum g_J=\frac{\langle\Gamma_{nljJ}^0\rangle}{\langle D_J\rangle}\,, \tag{2.6.21}$$

$$\langle\Gamma_{nljJ}\rangle\cong S_l\langle D_J\rangle v_l\sqrt{E}\,. \tag{2.6.22}$$

For inelastic scattering we have assumed

$$\langle\Gamma^n{}_{inljJ}\rangle=\langle\Gamma_{nljJ}\rangle\frac{v_l(E^n)\sqrt{E^n}}{v_l(E)\sqrt{E}} \tag{2.6.23}$$

where $E^n=E-E_n^*$ and E_n^* is energy of the n-th excited level.

3. The Nuclear Fission and Fission Widths

Soon after the discovery of nuclear fission, BOHR and WHEELER[28] developed the liquid drop model of atomic nuclei for studies of the mechanism of nuclear fission. In the classical liquid drop model a nucleus is considered an uniformly charged incompressible liquid drop. The nuclear fission is thought as an irreversible division of the liquid drop into smaller droplets as the results of an extreme deformation caused by mutual repulsion of electric charges. Because of large ionizing power of fission fragments and penetrating power observed, it was thought to be valid in the nuclear fission that a very large amount of energy is released. Assuming that the large energy release is due to the surface energy and Coulomb energy, BOHR and WHEELER[28] have studied the properties of the liquid drop. This model was successful in qualitative interpretation of various experimental results such as the distribution of fission fragments, energy release and electric charge, etc.

The much efforts for developing the model of the nuclear fission has been made. Especially HILL and WHEELER[29], and BOHR[30] and MOTELSON[31] have studied the role of individual particle motion as well as collective motions of the nucleus. The studies have open the gate leading to the present unified model for the nuclear fission.

3.1 The Liquid Drop Model and Barrier to Fission

The liquid drop model for the fissile nucleus is based on the assumption that the uniformly charged incompressible liquid is under influence of surface tension. The idea is based on that the energy release in the fission process is caused by some part of nuclear forces and the Coulomb energy, and the former effect resembles to the energy due to surface tensions of a drop of liquid.

Because of the assumption of incompressibility, all deformations take place at constant volume. The potential energy due to nuclear forces can be split into two terms, one proportional to the volume of the nucleus and the other to the surface area of the nucleus. Therefore at stable state of nucleus the first contribution plays no role, but only the second contribution is significant. This surface term opposes to the repulsive force due to the electro-static Coulomb force. For some shapes of the deformations, however, the latter force overcome the former and fissioning begins.

For a stable nucleus the sum of the surface and Coulomb energy changes is positive for any small deformation from its equilibrium shape. The surface energy E_s and the Coulomb energy E_c are given by

$$E_s = 4\pi R^2 \rho_s \tag{3.1-1}$$

$$E_c = \frac{3Z^2e^2}{5R} \tag{3.1-2}$$

where ρ_s is the surface tension per unit area. A deformation of axially symmetric shape is given by the simple expression for the radius

$$r(\theta) = R(1+\alpha_1+\alpha_2 P_2(\cos\theta)+\alpha_3 P_3(\cos\theta)+\cdots\cdots) \tag{3.1-3}$$

where θ is measured from the axis of symmetry. Then a straightforward calculation gives the increased energy of the drop by the deformation as follows:

$$E_{s+c} = 4\pi(r_0 A^{1/3})^2 \rho_s [1+2\alpha_2^2/5+0(\alpha_3^2)]+3(Ze)/(5r_0A^{1/3})[1-\alpha_2^2/5+0(\alpha_3^2)]. \tag{3.1-4}$$

Here we used $R=r_0 A^{1/3}$. The above equation shows that changes in the energy E_{s+c} are caused by the terms proportional to α_2. If the coefficient of α_2

$$4\pi r_0^2 \rho_s A^{2/3} \frac{2}{5}\left\{1-\frac{Z^2}{A}\left[10\left(\frac{4}{3}\pi r_0^3\right)\rho_s/e^2\right]^{-1}\right\} \tag{3.1-5}$$

is negative, the nucleus is not stable for any small deformation described by $P_2(\cos\theta)$. That is, if we increase the value of (Z^2/A), we finally reach a critical value

$$(Z^2/A)_{crit}=10\left(\frac{4}{3}\pi r_0^3\right)\rho_s/e^2 \tag{3.1-6}$$

Beyond the above critical value the liquid drop is no longer stable with respect to the P_2 deformation. Hence the ratio

$$x=\frac{(Z^2/A)}{(Z^2/A)_{crit}} \tag{3.1-7}$$

defines the degree of stability of a nucleus.

Although nuclei having Z^2/A a little less than $(Z^2/A)_{crit}$ are stable with respect to small deformations, a large deformation will produce the long range repulsive force which overcomes the short range surface tension. And if the nucleus is sufficiently deformed, it will be possible for the nucleus to proceed nuclear fission. If the potential energy of deformation is plotted as a function of paramaters such as α_2, there should be a saddle point which corresponds to the critical deformation beyond which the nuclear fission sets forth. (Fig. 3.1-1) The potential energy required for this critical point, the calculation of this barrier hight was carried out by using more accurate representation to the deformation[33].

According to experimental data for fission, the threshold energy E_f is not far from 6 MeV for heavy elements. From this value, $x=0.74$ is obtained by using data of ^{238}U. Then the

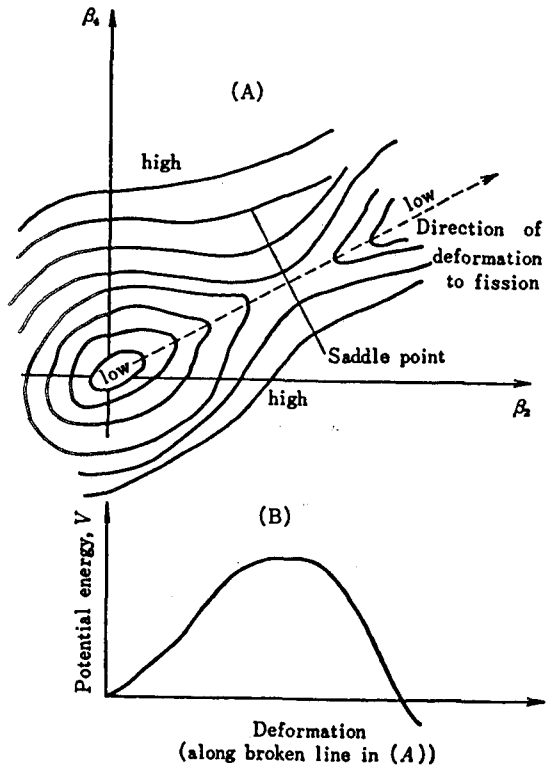

Fig. 3.1-1 Potential energy contours in the plane of the two principal deformation parameters (A), and the potential energy along the direction of fission (quoted from ref. 32).

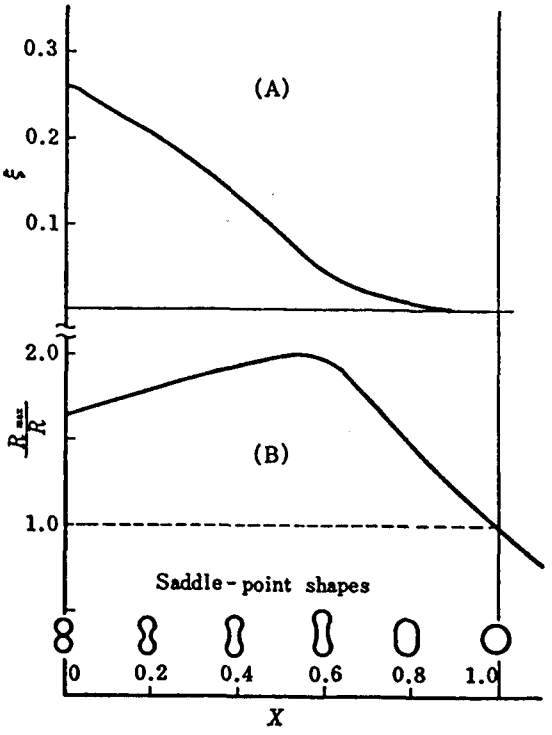

Fig. 3.1-2 The conventional picture of fission. (A) shows the threshold energy ξ, (B) the major-semi axes of the saddle-point shapes, as function of x (quoted from ref. 34).

critical value of $(Z^2/A)_{crit}$ is determined to be nearly equal to 50. A typical example of the shape of critical deformation, threshold energy and length of major semi axis are reproduced in Fig. 3. 1-2.

The fission width by the liquid drop model was derived by considering micro-canonical ensemble and given by[28]

$$\Gamma_f=\frac{D}{2\pi}N^* \tag{3.1-8}$$

where D is the level spacing and N^* is the number of levels of the transition state energetically available to the reaction. The transition state in the above means group of levels arising from excitation of all degrees of freedom other than fission. Today the transition state is applied to individual levels involved in the above definition.

In the above equation, if N^* is zero, the tunneling effect should be considered. Usually for the potential barrier the form of inverted one dimensional harmonic oscillator is assumed, and the transmission factor becomes[29]

$$P_f=\frac{1}{1+\exp\{2\pi(E_f-E)/\hbar\omega\}} \tag{3.1-9}$$

where ω is the circular frequency of the harmonic oscillator. The $\hbar\omega$ depends strongly on x, and takes the maximum 0.85 MeV at $x=0.83$ and is decreasing sharply below $x=0.7$[35]. For the compound nucleus ^{236}U and ^{230}Pu; $\hbar\omega$ is usually set euqal to 0.5 MeV. However the lowest barrier derived above corresponds to symmetrical fission. On the other hand experiments show asymmetric fission.

3.2 The Unified Model and Transition States of Even-even Compound Nucleus

In the previous section relation of the fission width to the level in transition state (older sense) was described. However the symmetric fission is contradictory to experimental results. And the observed lower value of fission width was not explained. On the other hand, the success of the shell model of nuclear structure stimulated studies of the role of individual particle motion in the nuclear fission. It was found that extra neutrons outside the closed shell play important role for nuclear deformations. Force due to these extra neutrons is strong enough to deform nucleus in permanently stable shape. The total energy of nucleons in a deformed potential well was minimized for obtaining preferred deformation of the nucleus. This model was successful for explaining ground state spin. However, there are many nuclei having a larger quadrupole moment.

Although the liquid drop model and the single particle model represent opposite approximation to the nuclear structure, each is successful for explaining specific feature of nuclear structure. Especially for explaining large quadrupole moments, which is thought due to large deformation of nucleus, and a number of fission phenomena, the combining of the two models has been studied by BOHR A. *et al.*[36),36)]. In this unified model the nucleus is described as a shell structure capable of performing oscillations in shape and size and rotations. These oscillations and rotations of nucleus as a whole induce variations of potential field and hence are strongly coupled with single particle motions.

The total energy of a nucleus is described by a Hamiltonian which consists of Hamiltonians describing nuclear surface oscillations and single particle motions and interactions between surface oscillations and single particle motions. For treating the surface oscillations nucleus is considered as incompressible irrotational fluid and the surface of nucleus is represented by the similar formula as Eq. (3.1-3). However, α 's are varying with time. Assuming harmonic oscillation for

α, equating the potential energy terms for oscillation to deformation energy E_{s+c}, and defining masses for this mode of oscillation the Hamiltonian for the surface oscillations is derived. The Hamiltonian thus derived is divided into vibrational and rotational parts. When the deformation is described by the spherical harmonics of order 2, the former consists of two modes of vibrations β and γ. The β-vibration corresponds to a collective motion about the equilibrium deformation along the axis of symmetry. The γ-vibration corresponds to periodic oscillations aroand symmetry axis. The range of γ-vibration is limitted. For the deformations of order 3, the mass asymetric and bending vibrations are expected.

The rotational band is always associated with these vibration. However at the saddle point the nucleus is much deformed and have much larger moment of inertia compared with that of equlibrium state. By this reason, the separation between rotational levels in transition states should be correspondingly smaller than that of equilibrium state.

These collective levels has been tabulated by WHEELER[37], and it was confirmed that model gives reliable assignments of low-lying levels of stable deformed nucleus. Many levels of excited states, which are predicted by this model, has been found by experiments. The TABLE 3. 2-1 shows the levels due to LYNN's prediction[38]. This table shows an outline of transition state spectrum for even-even fissionning nucleus. The projection K of angular momentum along the symmetry axis is thought as a good quantum number, when nucleus passes from the saddle point to fission. In the table this quantum number is also shown. LYNN has obtained transition state spectrum for each fissioning nucleus from the TABLE 3. 2-1 and experimental results of cross sections. The transition state spectrum calculating neutron induced fission of ^{235}U and ^{239}Pu are shown in the TABLE 3. 2-2 and 3. 2-3 respectively[38]. Our evaluation has been performed based on this table.

TABLE 3. 2-1 A summary of evidence and speculation on the transition states of a fissioning even nucleus

Approximate features on the energy scale (origin is the fission threshold)	Apporoximate energy of transition state (in MeV)	Transition state quantum numbers		Description of transition state
		K^π	I^π	
0.0 MeV (fission threshold)⟶	0. 0	0^+	0^+ 2^+ 4^+, etc.	'Ground'
	~0. 5	0^-	1^- 3^- 5^-, etc.	1 quantum of mass asymmetry vibration
	0. 7	2^+	2^+ 3^+ 4^+, etc.	1 quantum of gamma vibration
$\approx E_{th,n}$ for ^{242}Pu ⟶				
	0. 9	1^-	1^- 2^- 3^-, etc.	1 quantum of bending vibration
1. 0 MeV⟶				
$\approx E_{th,n}$ for ^{236}U⟶	1. 2	2^-	2^- 3^- 4^-, etc.	1 quantum of mass asymmetry vibration combined with 1 quantum of gamma vibration
$\approx E_{th,n}$ for ^{234}U⟶ $\approx E_{th,n}$ for ^{240}Pu ⟶	1. 4	1^+	1^+ 2^+ 3^+, etc.	1 quantum of mass asymmetry vibration combined with 1 quantum of bending vibration
	1. 6	0^+	0^+ 2^+	2 quantam of gamma vibration
		4^+	4^+ 5^+, etc.	
	1. 7	1^-	1^- 2^-, etc.	1 quantum of gamma vibration combined with 1 quantum of bending vibration
		3^-	3^- 4^-, etc.	

TABLE 3. 2-2 Alternative fission channel scheme of $^{235}U+n$

(for s-wave resonances)

Nature of transition state	Projection of angular momentum of cylindrical asymmetry axis (K)	Spin and parity relevant to compound nucleus	Energy of transition state with respect to neutron separation energy (in MeV)
Mass asymmetry vibration (+rotation)	0	3^-	−0.6
Bending vibration (+rotation)	1	3^-, 4^-	−0.3
Combination state of gamma vibration and mass asymmetry vibration (+rotation)	2	3^-, 4^-	+0.4

(for p-wave neutron resonances)

Nature of transition state	Projection of angular momentum on cylindrical symmetry axis (K)	Spin and parity relevant to compound nucleus	Energy of transition state with respect to neutron separation energy (in MeV)
"Ground" (+rotation)	0	2^+, 4^+	−0.8
Combination state of bending vibration and mass asymmetry vibration (+rotation)	1	2^+, 3^+, 4^+, 5^+	−0.1
Gamma vibration (+rotation)	2	2^+, 3^+, 4^+, 5^+	+0.2

TABLE 3. 2-3 Fission channel scheme of $^{239}Pu+n$

(for s-wave resonances)

Nature of transition state	Projection of angular momentum on cylindrical symmetry axis K	Spin and parity relevent to compound nucleus (J^π)	Energy of transition state with respect to neutron separation energy (in MeV)
"Ground"	0	0^+	−1.5
2 phenons of gamma vibration	0	0^+	0.0
Combination state of mass asymmetry vibration and bending vibration	1	1^+	+0.15

(for p-wave resonances)

Nature of transition states	Projection of angular momentum on cylindrical symmetry axis K	Spin and parity relevant to compound nucleus (J^π)	Energy of transition state with respect to neutron separation energy (in MeV)
Mass asymmetry vibration	0	1^-	−0.9
Bending vibration (+rotation)	1	1^-, 2^-	−0.45
Combination state of gamma vibration and mass asymmetry vibration	2	2^-	−0.15
Combination state of gamma vibration and bending vibration (+rotation)	1	1^-, 2^-	+0.3

3.3 The Fission Channel and Statistics

The number of fission channels becomes very large, when channels are defined by the nature of outgoing particles. If this is true, then fission width distribution becomes uniform and fission cross section should be reproduced by the Breit-Wigner's single level expression.

In the collective model, however, because of conservation of energy, momentum and angular distribution etc., a few transition states are available to fission. In this model, reduced width amplitude will consist of two factors. One factor $y_{\lambda a}$ is the amplitude of the eigen state λ in

transition state ψ_α That is to say, $y_{\lambda\alpha}=(\psi_\alpha, X_\lambda)$. The other is coefficient $b_{\alpha c}$ representing the dependence of the wave function ψ_c at the channel entrance at $r_c=a_c$, on the transition state. That is, $b_{\alpha c}\propto\int_{rc=ac}\psi_c^*\psi_\alpha dS_c$, where S_c is nuclear surface. Then amplitude of reduced width is given by

$$\lambda_c=\sum_\alpha b_{\alpha c}y_{\lambda\alpha} \quad c\in \text{ fission product channel.} \tag{3. 3-1}$$

Therefore the fission channel width $\Gamma_{\lambda c}$ is

$$\Gamma_{\lambda c}=2P_c[\sum_\alpha b_{\alpha c}^2 y_{\lambda\alpha}^2+\sum_{\alpha\neq\alpha'} b_{\alpha c}b_{\alpha' c}y_{\lambda\alpha}y_{\lambda\alpha'}]. \tag{3. 3-2}$$

The total fission width becomes

$$\Gamma_{\lambda f}=\sum_{c\in f}\Gamma_{\lambda c}=\sum_\alpha y_{\lambda\alpha}^2\sum_{c\in f}2P_c b_{\alpha c}^2+\sum_{\alpha\neq\alpha'}y_{\lambda\alpha}y_{\lambda\alpha'}\Gamma_{\lambda\alpha'}\sum_{c\in f}2P_c b_{\alpha c}b_{\alpha' c}. \tag{3. 3-3}$$

Because number of fission channel is large and sign pattern of $b_{\alpha c}$ is thought as random. $\sum_{\alpha f} P_c b_{\alpha c}b_{\alpha c}$ assume very small value. With this condition the second term in Eq. (3. 3-3) can be neglected. And if we define the following new transmission factor

$$P_{\alpha'}=\sum_{c\in f}P_c b_{\alpha c}^2, \tag{3. 3-4}$$

the corresponding width is

$$\Gamma_{\lambda\alpha}=2P_{\alpha'}y_{\lambda\alpha}^2. \tag{3. 3-5}$$

Note that the transmission factor $P_{\alpha'}$ defined above corresponds just to that of Eq. (3. 1-5). The transition state α can be thought just like true channel in the usual sense, Then the statistic properties of the total fission width are obtained from those of partial widths of saddle point channel $\Gamma_{\lambda\alpha}$. By the above argument $\Gamma_{\lambda\alpha}$ is expected to have the χ^2 distribution of one degree of freedom. If there are N transition states available to fission and the mean fission widths assume a same value, then the total fission width is distributed by the distribution of N degrees of freedom. The fission widths for same J values are therefore given by the χ^2 dsitribution with $\nu=N$, when all transmissin factors are equal to unity. If the factors is not equal to unity we must apply the χ^2 -distribution with $\nu=1$ for each channel α.

When the channels are not fully open, an effective number of open channel is introduced for obtaining information on availability of channels. The effective number due to WHEELER[37] is

$$N_{\text{eff}}=\sum_\alpha P_\alpha^{J\pi}=\frac{2\pi\langle\Gamma_{fJ^\pi}\rangle}{\langle D_J\rangle} \tag{3. 3-5}$$

where $P_\alpha^{J\pi}$ is the factor defined in (3. 1-9). It should be remain that N_{eff} is not necessarily an integer.

An another definition of the effective number is defined by the variance. If the χ^2 distribution with $\nu=1$ is assumed, for each channel we have

$$N_{\text{eff}}^2=\frac{2\langle\Gamma_f\rangle^2}{\langle\Gamma_f^2\rangle-\langle\Gamma_f\rangle^2}=\frac{\langle\sum_\alpha P_\alpha\rangle^2}{\sum_\alpha P_\alpha^2}, \tag{3. 3-6}$$

where we omitted superscript J and π. It can be easily proved that N_{eff} given by Eq. (3. 3-6) is greater than N_{eff} of Eq. (3. 3-5).

The effective number of open channel is only a measure for showing status of channels. The degree of freedom is always 1 for each channels in disregards of channel's opening. In other words, N_{eff} is not concerned with the actual total fission width distribution.

4. Resolved Resonance Parameters and Averaged Resonance Parameters in Unresolved Resonance Region

We have mentioned the theories needed for the calculations of the resonance cross sections. In this section, we will mainly concern with the data used in calculations such as resolved or averaged resonance parameters and averaged level spacing etc.

Much works have been made for evaluation and compilation of the resonance parameters and various tabulated results are available[39),40)]. After these works, many experimental results with higher accuracy have been obtained, and spin assignment of levels and cross-section fitting by the multi-level formalism have been carried out. For the unresolved resonance region, a great deal of new informations on the cross sections have also been available. Hence, the present stage is considered to be a good time for the re-evaluation of the average resonance parameters. Especially, an important problem in this field is the high α value of ^{239}Pu, and it will hence be necessary to calculate the Doppler coefficient of reactivity and the breeding ratio of a fast reactor by taking accurately the high α value into consideration.

Here, we will compile the resolved resonance parameters and evaluate the averaged resonance parameters by taking the recent experimental results into accout. These studies will mainly started with the data compiled by SCHMIDT[40)].

4.1 Resonance Parameters in Resolved Region

Here, we show briefly, in a tabulated form, the resolved resonance parameters used for the calculation of effective group cross section. There are much numbers of resonance levels for which spin is not assigned and we assumed $g_J=1/2$ for such levels. As mentioned in chapter 2, a multi-level formalism for resonance cross sections is preferable for lower energy region and we adopted an approximate representation based on VOGT[15)]. Hence, introduction of a new level parameter $\xi_{\lambda c}$ is needed for this purpose and this parameter is defined by

$$\xi_{\lambda c}=\sqrt{\Gamma_{\lambda c}}/(\Gamma_{\lambda f})^{1/2}. \tag{4.1-1}$$

Therefore, Eq. (2.1-14) can be rewritten as

TABLE 4.1-1 List of references quoted in the assignment of the resolved resonance parameters

Nuclide	Energy range (eV)	References	Remarks
^{235}U	147.33 ~ 63.13	SCHMIDT[40)]	
	62.443~ 3.608	DRAWBAUGH and GIBSON[41)]	
	3.16 ~ 0.938	SCHMIDT[40)]	The multilevel correction was made.
^{238}U	3904.4 ~−18.0	SCHMIDT[40)] GLASS *et al.*[42)]	The partial modification was made to Γ_γ, from the results of Petrel bomb experiment.
^{239}Pu	442.41 ~ 301.81	DERRIEN *et al.*[43)]	Γ_γ and g_J were assumed to be 0.0387 eV and 1/2, respectively.
	298.1 ~ −1.2	DURSTON and KATSURAGI[44)] FARRELL[23)]	The spins of levels from 14 to 90 eV were assigned from the results of the analysis by FARRELL.
^{240}Pu	5692.0 ~ 1.054	KOLER and BOCKHOFF[45)] WEIGMANN and SCHMIDT[46)]	$\Gamma_\gamma=0.0232$ eV

TABLE 4. 1-2 (a) The resonance parameters of ^{235}U in resolved region

147.330	0.500	0.002670	0.047900	0.046900
145.600	0.500	0.007240	0.047900	0.049900
143.120	0.500	0.000120	0.047900	0.045200
142.050	0.500	0.005602	0.047900	0.040900
141.800	0.500	0.000595	0.047900	0.059200
140.240	0.438	0.001303	0.047900	0.057000
139.170	0.500	0.000472	0.047900	0.064700
137.510	0.500	0.003049	0.047900	0.029200
136.290	0.500	0.003152	0.047900	0.035700
135.470	0.500	0.003957	0.047900	0.048400
135.150	0.500	0.003953	0.047900	0.092200
133.620	0.500	0.004393	0.047900	0.040200
133.040	0.500	0.001153	0.047900	0.063000
132.680	0.500	0.001152	0.047900	0.040900
132.110	0.500	0.002184	0.047900	0.078600
131.640	0.500	0.001033	0.047900	0.217500
131.230	0.500	0.002177	0.047900	0.208000
129.920	0.500	0.001710	0.047900	0.051500
128.140	0.500	0.001472	0.047900	0.051500
127.740	0.500	0.000644	0.047900	0.081200
126.450	0.500	0.003936	0.047900	0.037100
126.010	0.500	0.002021	0.047900	0.038300
125.620	0.500	0.004147	0.047900	0.035200
124.750	0.500	0.002178	0.047900	0.085500
123.960	0.500	0.000111	0.047900	0.122600
123.590	0.500	0.000400	0.047900	0.088600
122.890	0.500	0.000599	0.047900	0.066600
121.900	0.500	0.005631	0.047900	0.064700
118.620	0.500	0.003050	0.047900	0.059200
118.300	0.500	0.001523	0.047900	0.099800
115.920	0.500	0.002864	0.047900	0.067500
115.080	0.500	0.000440	0.047900	0.171000
113.540	0.500	0.001438	0.047900	0.044000
111.660	0.500	0.001131	0.067800	0.029100
111.130	0.500	0.000485	0.059100	0.043400
110.180	0.500	0.000577	0.047900	0.013400
109.820	0.500	0.002117	0.073700	0.024200
108.860	0.500	0.001762	0.064600	0.031100
108.060	0.500	0.000437	0.047900	0.009500
107.610	0.500	0.004118	0.050700	0.022200
106.720	0.500	0.000111	0.047900	0.072600
106.090	0.500	0.001164	0.047900	0.057700
105.550	0.500	0.000308	0.047900	0.038300
105.180	0.500	0.002400	0.047900	0.073700
104.160	0.500	0.000265	0.047900	0.033500
103.500	0.500	0.002065	0.047900	0.096000
102.940	0.500	0.002516	0.047900	0.037100
101.850	0.500	0.000363	0.055300	0.051300
100.980	0.500	0.000995	0.046500	0.044500
100.290	0.500	0.000661	0.046500	0.087800
99.530	0.500	0.000619	0.047900	0.106500
98.100	0.500	0.002783	0.047900	0.081200
96.410	0.500	0.001031	0.047900	0.111200
95.560	0.500	0.001584	0.047900	0.104000
94.340	0.500	0.000699	0.047900	0.007000
94.080	0.500	0.003977	0.056400	0.014600
93.240	0.500	0.000328	0.077700	0.089000
92.580	0.500	0.002531	0.054300	0.041200
92.060	0.500	0.000720	0.042100	0.092200
91.260	0.500	0.002961	0.047900	0.059900
90.340	0.500	0.004847	0.043800	0.014400
89.800	0.500	0.000663	0.039700	0.097600
89.100	0.500	0.000179	0.047900	0.092200
88.780	0.500	0.003298	0.047900	0.096700
87.600	0.500	0.000739	0.047900	0.102200
86.790	0.500	0.000717	0.047900	0.092200
86.250	0.500	0.000050	0.047900	0.111200
85.630	0.500	0.000601	0.047900	0.088600
85.000	0.500	0.001014	0.047900	0.062100
84.280	0.500	0.001900	0.047900	0.081200
84.050	0.500	0.001504	0.047900	0.065600
83.610	0.500	0.001170	0.044700	0.072100
82.640	0.500	0.002200	0.047900	0.014400
82.100	0.500	0.000050	0.047900	0.129400
81.420	0.500	0.000893	0.039000	0.070000
80.340	0.500	0.000735	0.056000	0.113000
79.670	0.500	0.000687	0.045000	0.075000
78.470	0.500	0.000133	0.047900	0.038300
78.100	0.500	0.001016	0.040000	0.099000
77.500	0.500	0.001021	0.065000	0.055000
76.770	0.500	0.000068	0.029000	0.045900
75.530	0.500	0.001234	0.047900	0.037100
75.180	0.500	0.001301	0.047900	0.066600
74.540	0.500	0.002961	0.054000	0.061000
72.910	0.500	0.000256	0.047900	0.122800
72.370	0.500	0.003199	0.052000	0.075000
71.520	0.500	0.000465	0.047900	0.171000
70.750	0.500	0.002246	0.047900	0.080000
70.430	0.500	0.002904	0.047900	0.072600
69.290	0.500	0.000741	0.047900	0.088000
68.510	0.500	0.000132	0.047900	0.046900
67.220	0.500	0.000090	0.077100	0.065800
66.400	0.500	0.000367	0.039000	0.028000
65.780	0.500	0.000308	0.030000	0.030000
64.290	0.500	0.001251	0.043000	0.016000
64.280	0.500	0.001251	0.043000	0.016000
63.630	0.500	0.001260	0.047900	0.042200
62.443	0.500	0.000601	0.124000	0.722000
61.081	0.500	0.000805	0.121000	0.281000
60.815	0.500	0.000155	0.041000	0.101000
60.205	0.500	0.001114	0.058100	0.205000
59.792	0.500	0.000098	0.047300	0.142000
58.689	0.500	0.001213	0.043900	0.089900
58.092	0.500	0.001102	0.012600	0.012300
57.869	0.500	0.000811	0.039000	0.093700
56.532	0.500	0.003510	0.004000	0.007500
56.245	0.500	0.005710	0.041500	0.935000
55.870	0.500	0.001512	0.074200	0.126000
55.112	0.500	0.002224	0.004840	0.005060
54.140	0.500	0.000278	0.074100	0.262000
53.455	0.500	0.000518	0.040300	0.082600
52.243	0.500	0.002726	0.072100	0.356000
51.653	0.500	0.000326	0.014500	0.034500
51.295	0.500	0.003442	0.056000	0.115000
50.482	0.500	0.001215	0.051900	0.075300
50.123	0.500	0.000256	0.018600	0.012200
49.448	0.500	0.000958	0.063600	0.025600
48.788	0.500	0.001068	0.104000	0.141000
48.319	0.500	0.001201	0.081700	0.266000
47.980	0.500	0.000759	0.049800	0.045300
47.020	0.500	0.001030	0.058500	0.121000
46.808	0.500	0.000646	0.041500	0.105000
45.800	0.500	0.000196	0.059000	0.092400
44.948	0.500	0.000975	0.087900	0.552000
44.619	0.500	0.000792	0.054600	0.117000
43.962	0.500	0.000682	0.063700	0.129000
43.407	0.500	0.000677	0.060200	0.035400
42.723	0.500	0.000331	0.071800	0.029900
42.240	0.500	0.000489	0.078000	0.131000
41.887	0.500	0.001229	0.049700	0.022300
41.611	0.500	0.000089	0.000800	0.000900
41.398	0.500	0.000773	0.077000	0.399000
40.562	0.500	0.000413	0.053800	0.217000
39.911	0.500	0.000311	0.022300	0.153000
39.420	0.500	0.002456	0.041300	0.061400
38.288	0.500	0.000562	0.033600	0.471000
35.205	0.500	0.004547	0.051900	0.105000
34.866	0.500	0.001246	0.040800	0.116000
34.379	0.500	0.002177	0.047800	0.047900
33.540	0.500	0.001825	0.044000	0.032800
32.088	0.500	0.001871	0.046100	0.065900
30.891	0.500	0.000494	0.036700	0.020000
30.627	0.500	0.000259	0.067200	0.131000
29.668	0.500	0.000190	0.052400	0.039500
28.756	0.500	0.000030	0.023100	0.072700
28.371	0.500	0.000292	0.081700	0.207000
27.823	0.500	0.000715	0.050600	0.087300
27.182	0.500	0.000053	0.000650	0.000530
26.822	0.500	0.000238	0.005900	0.126000
26.482	0.500	0.000524	0.048900	0.161000
25.757	0.500	0.000098	0.045500	0.131000
25.590	0.500	0.000190	0.010400	0.253000
25.473	0.500	0.000437	0.021800	0.438000
25.239	0.500	0.000097	0.007100	0.192000
25.067	0.500	0.000121	0.034300	0.252000
24.735	0.500	0.000322	0.006900	0.780000
24.350	0.500	0.000178	0.044100	0.077200
24.231	0.500	0.000200	0.030100	0.018900
23.605	0.500	0.001059	0.086200	0.210000
23.408	0.500	0.000579	0.021800	0.004400
22.933	0.500	0.000429	0.041000	0.046600
21.064	0.500	0.001550	0.040800	0.032800
20.628	0.500	0.000167	0.039600	0.041800
20.132	0.500	0.000158	0.096600	0.267000
19.293	0.500	0.003254	0.039600	0.059000
18.969	0.500	0.000086	0.012800	0.036900
18.051	0.500	0.000402	0.049500	0.134000
16.664	0.500	0.000286	0.043600	0.107900
16.088	0.500	0.000363	0.033900	0.020800
15.407	0.500	0.000235	0.038200	0.044500
14.541	0.500	0.000099	0.035100	0.017700
13.986	0.500	0.000650	0.084100	0.495000
13.695	0.500	0.000010	0.000700	0.004400
13.270	0.500	0.000030	0.043300	0.076700
12.860	0.500	0.000051	0.052200	0.060400
12.395	0.500	0.001275	0.036600	0.028800
11.660	0.500	0.000622	0.040000	0.007400
10.721	0.500	0.000049	0.000490	0.733000
10.180	0.500	0.000063	0.043100	0.060100
9.665	0.500	0.000094	0.012200	0.500000
9.287	0.500	0.000153	0.039300	0.071900
8.993	0.500	0.000081	0.040700	0.178000
8.777	0.500	0.001129	0.039300	0.085000
7.076	0.500	0.000127	0.040500	0.031900
6.381	0.500	0.000278	0.042400	0.012200
6.203	0.500	0.000032	0.026700	0.079800
6.106	0.500	0.000009	0.009230	0.207000
5.732	0.500	0.000028	0.049000	0.443000
5.435	0.500	0.000008	0.086600	0.134000
4.844	0.500	0.000059	0.039600	0.003860
3.608	0.500	0.000046	0.038200	0.054000
3.160	0.563	0.000029	0.031000	0.155000
2.820	0.438	0.000003	0.045000	0.064000

TABLE 4. 1-3 The resonance parameters of ^{238}U in resolved region

3904.400	1.000	0.224947	0.019100
3895.000	1.000	0.004993	0.019100
3871.300	1.000	0.248879	0.019100
3858.100	1.000	0.341625	0.019100
3832.000	1.000	0.006190	0.019100
3799.700	1.000	0.003082	0.019100
3783.700	1.000	0.276803	0.019100
3764.700	1.000	0.034360	0.019100
3733.300	1.000	0.152752	0.019100
3717.700	1.000	0.060973	0.019100
3693.000	1.000	0.243080	0.019100
3674.000	1.000	0.003031	0.019100
3647.000	1.000	0.003020	0.019100
3630.000	1.000	0.216898	0.019100
3625.000	1.000	0.003010	0.019100
3611.000	1.000	0.003005	0.019100
3600.000	1.000	0.003000	0.019100
3593.000	1.000	0.015585	0.019100
3574.000	1.000	0.239132	0.019100
3561.500	1.000	0.143228	0.019100
3526.000	1.000	0.010688	0.019100
3312.000	1.000	0.002963	0.019100
3492.000	1.000	0.011228	0.019100
3484.300	1.000	0.118056	0.019100
3470.000	1.000	0.001178	0.019100
3459.100	1.000	0.382292	0.019100
3436.900	1.000	0.190532	0.019100
3419.000	1.000	0.002924	0.019100
3409.000	1.000	0.105096	0.019100
3387.800	1.000	0.008149	0.019100
3371.000	1.000	0.002903	0.019100
3355.700	1.000	0.075307	0.019100
3334.000	1.000	0.057741	0.019100
3321.300	1.000	0.081836	0.019100
3310.900	1.000	0.094942	0.019100
3295.000	1.000	0.008610	0.019100
3280.000	1.000	0.103088	0.019100
3249.200	1.000	0.011400	0.019100
3226.000	1.000	0.022719	0.019100
3206.000	1.000	0.056622	0.019100
3139.000	1.000	0.043141	0.019100
3179.400	1.000	0.062025	0.019100
3160.000	1.000	0.010118	0.019100
3149.000	1.000	0.061728	0.019100
3133.200	1.000	0.005597	0.019100
3109.400	1.000	0.100372	0.019100
3081.100	1.000	0.004441	0.019100
3060.200	1.000	0.027660	0.019100
3041.000	1.000	0.002757	0.019100
3029.000	1.000	0.137591	0.019100
3015.000	1.000	0.007138	0.019100
3003.100	1.000	0.093161	0.019100
2987.400	1.000	0.005466	0.019100
2974.000	1.000	0.002727	0.019100
2967.400	1.000	0.008171	0.019100
2956.300	1.000	0.015224	0.019100
2932.300	1.000	0.024909	0.019100
2923.600	1.000	0.004326	0.019100
2906.500	1.000	0.002697	0.019100
2897.800	1.000	0.026916	0.019100
2882.900	1.000	0.526188	0.019100
2866.100	1.000	0.079253	0.019100
2845.200	1.000	0.002667	0.019100
2828.600	1.000	0.009041	0.019100
2806.200	1.000	0.006887	0.019100
2798.000	1.000	0.002645	0.019100
2787.900	1.000	0.010560	0.019100
2761.900	1.000	0.015766	0.019100
2750.100	1.000	0.039331	0.019100
2730.000	1.000	0.002612	0.019100
2716.800	1.000	0.070887	0.019100
2695.600	1.000	0.023364	0.019100
2672.800	1.000	0.175777	0.019100
2631.600	1.000	0.001026	0.019100
2620.600	1.000	0.040953	0.019100
2604.000	1.000	0.002551	0.019100
2598.700	1.000	0.360752	0.019100
2580.700	1.000	0.243843	0.019100
2559.300	1.000	0.217535	0.019100
2548.700	1.000	0.343296	0.019100
2520.700	1.000	0.010041	0.019100
2489.800	1.000	0.054888	0.019100
2454.000	1.000	0.002477	0.019100
2446.200	1.000	0.111293	0.019100
2426.500	1.000	0.081278	0.019100
2410.200	1.000	0.004418	0.019100
2392.500	1.000	0.011250	0.019100
2356.000	1.000	0.063100	0.019100
2352.000	1.000	0.063047	0.019100
2337.400	1.000	0.004835	0.019100
2315.900	1.000	0.014437	0.019100
2302.000	1.000	0.000960	0.019100
2288.700	1.000	0.002392	0.019100
2281.270	1.000	0.109854	0.019100
2266.430	1.000	0.145201	0.019100
2259.060	1.000	0.065591	0.019100
2241.530	1.000	0.001420	0.019100
2235.730	1.000	0.004728	0.019100
2229.960	1.000	0.004722	0.019100
2201.420	1.000	0.112606	0.019100
2194.000	1.000	0.002342	0.019100
2185.990	1.000	0.364686	0.019100
2172.000	1.000	0.002330	0.019100
2152.770	1.000	0.176312	0.019100
2145.950	1.000	0.034743	0.019100
2124.350	1.000	0.004609	0.019100
2096.490	1.000	0.010073	0.019100
2088.630	1.000	0.013710	0.019100
2031.060	1.000	0.049574	0.019100
2023.580	1.000	0.202429	0.019100
1974.650	1.000	0.466589	0.019100
1968.660	1.000	0.576805	0.019100
1917.100	1.000	0.021892	0.019100
1902.270	1.000	0.020935	0.012100
1845.600	1.000	0.013318	0.011800
1808.260	1.000	0.017009	0.013600
1797.700	1.000	0.002120	0.019100
1782.300	1.000	0.464390	0.031200
1755.800	1.000	0.062853	0.019400
1744.000	1.000	0.001670	0.019100
1723.000	1.000	0.013698	0.020700
1709.400	1.000	0.035816	0.023400
1700.710	1.000	0.000825	0.019100
1688.330	1.000	0.078070	0.017400
1662.080	1.000	0.163074	0.015300
1645.400	1.000	0.000811	0.019100
1638.190	1.000	0.040475	0.017100
1622.890	1.000	0.084599	0.013500
1598.160	1.000	0.319816	0.017600
1565.000	1.000	0.001978	0.019100
1550.000	1.000	0.001181	0.019100
1546.000	1.000	0.000786	0.019100
1532.000	1.000	0.001957	0.019100
1523.100	1.000	0.214648	0.016400
1473.800	1.000	0.078700	0.018800
1444.100	1.000	0.021661	0.015200
1427.730	1.000	0.030228	0.022300
1419.640	1.000	0.009420	0.019100
1417.000	1.000	0.001129	0.019100
1410.000	1.000	0.001126	0.019100
1405.110	1.000	0.076844	0.020800
1393.000	1.000	0.138095	0.020000
1335.720	1.000	0.001096	0.019100
1317.210	1.000	0.003992	0.019100
1298.440	1.000	0.002883	0.019100
1273.200	1.000	0.028546	0.033000
1267.010	1.000	0.026696	0.028300
1245.120	1.000	0.229361	0.021600
1210.930	1.000	0.009048	0.014000
1194.960	1.000	0.091606	0.019000
1177.620	1.000	0.063485	0.017700
1167.460	1.000	0.080295	0.015900
1140.380	1.000	0.219502	0.015200
1131.450	1.000	0.002186	0.019100
1108.880	1.000	0.029970	0.016900
1102.340	1.000	0.000664	0.019100
1098.350	1.000	0.014918	0.020200
1094.800	1.000	0.000662	0.019100
1081.100	1.000	0.000658	0.019100
1070.500	1.000	0.000327	0.019100
1068.100	1.000	0.000817	0.019100
1053.930	1.000	0.074668	0.016100
1033.160	1.000	0.000643	0.019100
1029.030	1.000	0.003208	0.019100
1023.000	1.000	0.006397	0.012500
1011.250	1.000	0.001908	0.019100
1000.300	1.000	0.001265	0.019100
991.780	1.000	0.346418	0.016900
958.430	1.000	0.157888	0.012300
936.870	1.000	0.146920	0.020900
932.500	1.000	0.000305	0.019100
925.180	1.000	0.008517	0.041000
909.900	1.000	0.000905	0.019100
905.110	1.000	0.045128	0.018400
891.290	1.000	0.000896	0.019100
866.520	1.000	0.004121	0.019100
856.150	1.000	0.080465	0.023100

TABLE 4. 1-3 (continued)

851.020	1.000	0.055427	0.020100
846.620	1.000	0.000582	0.019100
821.580	1.000	0.058760	0.020000
790.880	1.000	0.005062	0.046000
779.140	1.000	0.001675	0.019100
765.050	1.000	0.006638	0.011700
742.950	1.000	0.000545	0.019100
732.260	1.000	0.001353	0.019100
730.100	1.000	0.000811	0.019100
721.800	1.000	0.001343	0.019100
708.460	1.000	0.018632	0.013400
693.230	1.000	0.034228	0.016500
677.000	1.000	0.000520	0.019100
661.180	1.000	0.115710	0.018800
628.670	1.000	0.004012	0.019100
623.930	1.000	0.000424	0.019100
619.940	1.000	0.028384	0.019800
595.150	1.000	0.081726	0.020800
980.200	1.000	0.026978	0.024400
936.050	1.000	0.000472	0.019100
935.490	1.000	0.037025	0.024900
918.590	1.000	0.043268	0.022400
488.890	1.000	0.000442	0.019100
478.700	1.000	0.003063	0.019100
469.910	1.000	0.005166	0.019100
454.170	1.000	0.000426	0.019100
434.190	1.000	0.008335	0.019100
410.230	1.000	0.019241	0.014400
397.560	1.000	0.005982	0.019100
376.920	1.000	0.001126	0.019100
347.920	1.000	0.082071	0.017900
311.120	1.000	0.000988	0.019100
291.110	1.000	0.015356	0.031400
273.740	1.000	0.025149	0.026100
269.940	1.000	0.000227	0.019100
242.880	1.000	0.000156	0.019100
237.400	1.000	0.027734	0.031400
208.650	1.000	0.056334	0.023800
190.340	1.000	0.150381	0.018500
169.540	1.000	0.003474	0.016200
145.800	1.000	0.000857	0.019100
116.930	1.000	0.036009	0.023300
102.780	1.000	0.065897	0.024900
90.000	1.000	0.000076	0.019100
80.770	1.000	0.002067	0.019100
66.300	1.000	0.025160	0.017350
38.700	1.000	0.031138	0.020900
21.000	1.000	0.008707	0.025000
10.200	1.000	0.000001	0.025000
6.680	1.000	0.001525	0.025000
-18.000	1.000	0.004794	0.025000

TABLE 4. 1-4 (a) The resonance parameters of ^{239}U in resolved region

442.41	0.5	0.004204	0.0387	0.3728
438.72	0.5	0.002827	0.0387	0.01794
437.76	0.5	0.004037	0.0387	0.01926
429.64	0.5	0.003606	0.0387	0.73564
428.33	0.5	0.027567	0.0387	6.0783
417.85	0.5	0.004088	0.0387	0.09119
417.66	0.5	0.002043	0.0387	0.10841
412.31	0.5	0.009380	0.0387	0.09289
408.71	0.5	0.001940	0.0387	0.10936
406.95	0.5	0.001452	0.0387	0.290027
406.03	0.5	0.000282	0.0387	0.27857
404.24	0.5	0.020044	0.0387	0.1045
401.56	0.5	0.015510	0.0387	0.1522
397.5	0.5	0.001993	0.0387	0.2
396.	0.5	0.003143	0.0387	0.06613
394.43	0.5	0.009771	0.0387	0.020742
391.52	0.5	0.000989	0.0387	0.050705
389.51	0.5	0.002092	0.0387	0.03321
385.90	0.5	0.002003	0.0387	0.95935
384.26	0.5	0.008546	0.0387	0.030875
382.43	0.5	0.001955	0.0387	0.09067
381.0	0.5	0.001952	0.0387	0.2
378.04	0.5	0.001486	0.0387	0.091210
377.10	0.5	0.002971	0.0387	0.03
375.02	0.5	0.004004	0.0387	0.0003
371.72	0.5	0.011008	0.0387	0.5
370.31	0.5	0.003906	0.0387	0.3120
368.0	0.5	0.003049	0.0387	0.2
363.00	0.5	0.020957	0.0387	0.1
359.99	0.5	0.000531	0.0387	0.03682
357.87	0.5	0.018917	0.0387	0.5
354.89	0.5	0.000602	0.0387	0.02
352.82	0.5	0.005841	0.0387	0.02
350.30	0.5	0.032247	0.0387	0.02605
346.56	0.5	0.005193	0.0387	1.1561
343.18	0.5	0.023730	0.0387	0.01261
339.24	0.5	0.004917	0.0387	0.03738
337.95	0.5	0.012096	0.0387	0.02321
335.93	0.5	0.026612	0.0387	0.0177
333.94	0.5	0.008241	0.0387	0.02006
330.65	0.5	0.004521	0.0387	1.4598
325.3	0.5	0.011723	0.0387	0.0535
322.5	0.5	0.018317	0.0387	0.0911
320.0	0.5	0.001788	0.0387	0.2
316.66	0.5	0.007740	0.0387	0.02655
313.62	0.5	0.020312	0.0387	0.0259
311.0	0.5	0.001743	0.0387	0.2
309.01	0.5	0.021093	0.0387	0.0252
308.2	0.5	0.004406	0.0387	0.1069
307.0	0.5	0.001792	0.0387	0.2
305.0	0.5	0.001746	0.0387	0.2
301.81	0.5	0.027308	0.0387	0.042
298.100	0.750	0.010014	0.038700	0.046300
296.000	0.500	0.004645	0.038700	0.086700
291.800	0.500	0.007004	0.038700	0.030400
286.700	0.500	0.008839	0.038700	1.000000
282.500	0.750	0.024035	0.038700	0.005300
279.100	0.250	0.023723	0.038700	0.019500
275.200	0.750	0.028036	0.038700	0.299000
272.300	0.750	0.023927	0.038700	0.015300
269.200	0.500	0.008532	0.038700	0.333000
262.200	0.500	0.008145	0.038700	1.000000
261.800	0.250	0.111838	0.038700	6.320000
255.800	0.750	0.010300	0.038700	1.000000
254.200	0.500	0.007286	0.038700	1.000000
250.900	0.750	0.023918	0.038700	0.015300
248.500	0.750	0.014660	0.038700	0.034300
247.100	0.500	0.001258	0.038700	1.000000
242.600	0.250	0.017133	0.038700	0.052700
238.700	0.750	0.005098	0.038700	0.068500
234.000	0.250	0.013614	0.038700	0.019700
231.100	0.750	0.101853	0.038700	0.012100
227.500	0.500	0.007225	0.038700	1.000000
224.600	0.500	0.002248	0.038700	1.000000
222.800	0.500	0.004627	0.038700	0.051700
219.600	0.500	0.023370	0.038700	1.000000
216.300	0.750	0.006324	0.038700	0.021700
210.900	0.500	0.002765	0.038700	1.000000
207.100	0.750	0.010146	0.038700	0.011300
203.600	0.250	0.035934	0.038700	0.298000
199.200	0.750	0.008892	0.021600	0.125000
196.400	0.750	0.005043	0.058500	0.068900
195.100	0.250	0.054754	0.038700	0.337000
190.300	0.500	0.002345	0.038700	0.118900
188.400	0.500	0.001894	0.038700	1.000000
185.100	0.500	0.006939	0.038700	1.750000
183.700	0.500	0.009515	0.038700	1.000000
178.800	0.500	0.002006	0.038700	0.014600
177.100	0.750	0.003859	0.062200	0.007000
175.800	0.500	0.003182	0.032900	0.043900
170.500	0.500	0.004440	0.038700	1.260000
166.900	0.750	0.005814	0.038700	0.047700
164.400	0.750	0.025387	0.040200	0.011800
160.900	0.500	0.003044	0.038700	0.508000
157.000	0.250	0.034833	0.038700	0.704000
151.800	0.500	0.000616	0.038700	1.000000
149.400	0.500	0.002200	0.051300	0.036500
148.000	0.500	0.001946	0.038700	0.009100
146.300	0.750	0.007741	0.054200	0.014200
143.200	0.500	0.011009	0.038700	0.053200
136.800	0.250	0.009591	0.038700	0.026500
135.400	0.500	0.000582	0.038700	0.092700
133.800	0.750	0.005921	0.027600	0.011400
131.900	0.250	0.034684	0.038700	0.003740
127.600	0.500	0.001615	0.038700	0.215000
126.300	0.500	0.002810	0.050000	0.032200
123.400	0.500	0.000933	0.023200	0.051000
121.300	0.500	0.004185	0.038700	0.035300
118.900	0.750	0.014721	0.052300	0.065700
116.100	0.250	0.009913	0.027000	0.188000
110.400	0.500	0.001366	0.038700	0.003100
106.800	0.750	0.007957	0.034900	0.033100
105.400	0.750	0.005852	0.038700	0.102500
103.000	0.250	0.006749	0.038700	0.083700
101.200	0.500	0.000402	0.038700	0.311000
97.600	0.500	0.001156	0.038700	0.360000
95.500	0.250	0.010398	0.038700	0.230000
90.900	0.750	0.012394	0.038700	0.114600
85.600	0.250	0.040709	0.038700	0.216700
82.000	0.500	0.007697	0.038700	1.500000
75.210	0.750	0.050863	0.044900	0.095000
74.310	0.750	0.003276	0.036600	0.029500
66.830	0.500	0.001726	0.038700	1.000000
65.960	0.750	0.012507	0.022400	0.077000
63.400	0.500	0.006880	0.038700	0.013900
61.100	0.500	0.011178	0.038700	2.000000
59.390	0.250	0.016800	0.048600	0.133000
58.000	0.500	0.008423	0.038700	0.805000
57.600	0.500	0.008500	0.038700	0.546000
55.790	0.250	0.004332	0.026000	0.022000
52.600	0.750	0.010081	0.037300	0.007700
50.220	0.750	0.003047	0.041300	0.011200
49.850	0.500	0.000212	0.059800	0.750000
47.600	0.250	0.005381	0.038700	0.301000
44.500	0.750	0.006537	0.027800	0.004200
41.400	0.750	0.006048	0.059200	0.010700
35.300	0.500	0.000475	0.038700	0.004100
34.600	0.500	0.000018	0.038700	1.000000
32.300	0.500	0.000455	0.038700	0.189000
27.300	0.500	0.002090	0.038700	0.002800
26.200	0.750	0.001740	0.038700	0.035700
23.900	0.500	0.001467	0.038700	0.037100
22.200	0.750	0.002214	0.031300	0.075000
17.600	0.750	0.001594	0.039100	0.046300
15.500	0.750	0.000787	0.038700	0.760500
14.680	0.750	0.002184	0.038700	0.031700
14.280	0.500	0.000831	0.038700	0.052500

TABLE 4. 1-5 (a) The resonance parameters of ^{240}Pu in resolved region

5692.000	1.000	0.091000	0.023200
5681.000	1.000	0.106000	0.023200
5615.000	1.000	0.062000	0.023200
5592.000	1.000	0.207000	0.023200
5574.000	1.000	0.758000	0.023200
5544.000	1.000	0.582000	0.023200
5522.000	1.000	0.172000	0.023200
5510.000	1.000	0.355000	0.023200
5499.000	1.000	0.087000	0.023200
5489.000	1.000	0.050000	0.023200
5417.000	1.000	0.235000	0.023200
5393.000	1.000	0.084000	0.023200
5367.000	1.000	0.070000	0.023200
5350.000	1.000	0.153000	0.023200
5334.000	1.000	0.203000	0.023200
5299.000	1.000	0.270000	0.023200
5279.000	1.000	0.140000	0.023200
5249.000	1.000	0.524000	0.023200
5215.000	1.000	0.163000	0.023200
5194.000	1.000	0.313000	0.023200
5162.000	1.000	0.040000	0.023200
5148.000	1.000	0.050000	0.023200
5134.000	1.000	0.042000	0.023200
5113.000	1.000	0.093000	0.023200
5072.000	1.000	0.509000	0.023200
4993.000	1.000	0.092000	0.023200
4969.000	1.000	0.158000	0.023200
4958.000	1.000	0.291000	0.023200
4894.000	1.000	0.059000	0.023200
4823.000	1.000	0.063000	0.023200
4812.000	1.000	0.172000	0.023200
4792.000	1.000	0.133000	0.023200
4779.000	1.000	0.034000	0.023200
4771.000	1.000	0.022000	0.023200
4766.000	1.000	0.015000	0.023200
4735.000	1.000	0.056000	0.023200
4745.000	1.000	0.245000	0.023200
4721.000	1.000	0.510000	0.023200
4646.000	1.000	0.149000	0.023200
4615.000	1.000	0.262000	0.023200
4599.000	1.000	0.075000	0.023200
4588.000	1.000	0.526000	0.023200
4570.000	1.000	0.220000	0.023200
4458.000	1.000	0.102000	0.023200
4433.000	1.000	0.047000	0.023200
4422.000	1.000	0.061000	0.023200
4398.000	1.000	0.078000	0.023200
4386.000	1.000	0.032000	0.023200
4376.000	1.000	0.082000	0.023200
4329.000	1.000	0.302000	0.023200
4288.000	1.000	0.316000	0.023200
4270.000	1.000	0.159000	0.023200
4221.000	1.000	0.068000	0.023200
4203.000	1.000	0.438000	0.023200
4161.000	1.000	0.089000	0.023200
4149.000	1.000	0.265000	0.023200
4134.000	1.000	0.067000	0.023200
4122.000	1.000	0.497000	0.023200
4100.000	1.000	0.257000	0.023200
4084.000	1.000	0.120000	0.023200
4031.000	1.000	0.109000	0.023200
3990.000	1.000	0.029000	0.023200
3975.000	1.000	0.102000	0.023200
3954.000	1.000	0.092000	0.023200
3917.000	1.000	0.163000	0.023200
3900.000	1.000	0.209000	0.023200
3872.000	1.000	0.046000	0.023200
3852.000	1.000	0.098000	0.023200
3844.000	1.000	0.076000	0.023200
3800.000	1.000	0.101000	0.023200
3723.000	1.000	0.060000	0.023200
3702.000	1.000	0.051000	0.023200
3665.000	1.000	0.054500	0.023200
3657.000	1.000	0.293000	0.023200
3595.000	1.000	0.028500	0.023200
3567.500	1.000	0.162000	0.023200
3555.000	1.000	0.091000	0.023200
3493.500	1.000	0.065000	0.023200
3465.500	1.000	0.344000	0.023200
3458.000	1.000	0.068000	0.023200
3423.000	1.000	0.034500	0.023200
3332.000	1.000	0.014500	0.023200
3268.500	1.000	0.134000	0.023200
3237.500	1.000	0.072000	0.023200
3192.500	1.000	0.349000	0.023200
3172.500	1.000	0.225000	0.023200
3112.700	1.000	0.038500	0.023200
3088.000	1.000	0.035000	0.023200
3077.400	1.000	0.128000	0.023200
3054.700	1.000	0.047000	0.023200
3029.000	1.000	0.021000	0.023200
3018.000	1.000	0.117000	0.023200
3004.000	1.000	0.076500	0.023200
2994.700	1.000	0.036000	0.023200
2986.200	1.000	0.012500	0.023200
2980.500	1.000	0.108000	0.023200
2968.600	1.000	0.085000	0.023200
2938.000	1.000	0.132000	0.023200
2905.000	1.000	0.115000	0.023200
2895.600	1.000	0.060000	0.023200
2882.000	1.000	0.030000	0.023200
2859.700	1.000	0.027000	0.023200
2843.500	1.000	0.157000	0.023200
2817.600	1.000	0.041200	0.023200
2748.400	1.000	0.102000	0.023200
2739.200	1.000	0.177000	0.023200
2717.700	1.000	0.040700	0.023200
2692.800	1.000	0.345000	0.023200
2652.400	1.000	0.036300	0.023200
2639.500	1.000	0.426000	0.023200
2575.300	1.000	0.047500	0.023200
2549.200	1.000	0.079700	0.023200
2538.600	1.000	0.287500	0.023200
2521.000	1.000	0.109500	0.023200
2485.300	1.000	0.021200	0.023200
2470.800	1.000	0.045500	0.023200
2459.400	1.000	0.025600	0.023200
2434.300	1.000	0.205000	0.023200
2416.000	1.000	0.064900	0.023200
2405.000	1.000	0.025100	0.023200
2386.100	1.000	0.018700	0.023200
2365.800	1.000	0.241000	0.023200
2350.900	1.000	0.031600	0.023200
2334.400	1.000	0.036600	0.023200
2303.300	1.000	0.017200	0.023200
2290.700	1.000	0.208500	0.023200
2277.900	1.000	0.427000	0.023200
2256.600	1.000	0.134500	0.023200
2240.600	1.000	0.034100	0.023200
2198.200	1.000	0.130000	0.023200
2182.000	1.000	0.085600	0.023200
2154.000	1.000	0.014300	0.023200
2110.700	1.000	0.013700	0.023200
2082.800	1.000	0.098800	0.023200
2055.600	1.000	0.068500	0.023200
2033.400	1.000	0.101500	0.023200
2022.900	1.000	0.055500	0.023200
2016.700	1.000	0.052500	0.023200
1998.300	1.000	0.005600	0.023200
1991.500	1.000	0.114500	0.023200
1973.100	1.000	0.068100	0.023200
1956.200	1.000	0.261000	0.023200
1949.100	1.000	0.082500	0.023200
1943.300	1.000	0.008000	0.023200
1916.600	1.000	0.035900	0.023200
1901.600	1.000	0.209000	0.023200
1872.700	1.000	0.077400	0.023200
1852.700	1.000	0.034400	0.023200
1841.200	1.000	0.125800	0.023200
1779.000	1.000	0.491000	0.023200
1771.400	1.000	0.009800	0.023200
1763.700	1.000	0.051700	0.023200
1741.600	1.000	0.024900	0.023200
1724.100	1.000	0.083500	0.023200
1687.900	1.000	0.032700	0.023200
1662.600	1.000	0.063900	0.023200
1643.000	1.000	0.107100	0.023200
1621.400	1.000	0.028600	0.023200
1609.600	1.000	0.034800	0.023200
1575.300	1.000	0.126200	0.023200
1563.700	1.000	0.114700	0.023200
1549.500	1.000	0.156700	0.023200
1540.700	1.000	0.101000	0.023200
1481.200	1.000	0.009400	0.023200
1462.900	1.000	0.021000	0.023200
1450.200	1.000	0.064600	0.023200
1429.000	1.000	0.015000	0.023200
1426.100	1.000	0.036700	0.023200
1408.600	1.000	0.010900	0.023200
1401.200	1.000	0.005200	0.023200
1389.000	1.000	0.014200	0.023200
1377.000	1.000	0.064700	0.023200
1362.900	1.000	0.007400	0.023200
1350.900	1.000	0.008300	0.023200
1345.000	1.000	0.026100	0.023200
1328.100	1.000	0.369000	0.023200
1300.300	1.000	0.245000	0.023200
1281.400	1.000	0.004300	0.023200
1254.700	1.000	0.076800	0.023200

TABLE 4. 1-5 (a) (continued)

1236.500	1.000	0.011400	0.023200
1228.000	1.000	0.010000	0.023200
1208.900	1.000	0.062900	0.023200
1190.800	1.000	0.114800	0.023200
1185.500	1.000	0.157500	0.023200
1159.600	1.000	0.022100	0.023200
1142.700	1.000	0.040400	0.023200
1135.800	1.000	0.006700	0.023200
1128.800	1.000	0.050100	0.023200
1115.700	1.000	0.002600	0.023200
1099.800	1.000	0.084100	0.023200
1072.600	1.000	0.109300	0.023200
1045.700	1.000	0.004000	0.023200
1041.600	1.000	0.012700	0.023200
1024.100	1.000	0.005000	0.023200
1001.800	1.000	0.098200	0.023200
979.200	1.000	0.007300	0.023200
971.300	1.000	0.080400	0.023200
958.400	1.000	0.071500	0.023200
943.500	1.000	0.122800	0.023200
915.300	1.000	0.036100	0.023200
908.900	1.000	0.079100	0.023200
903.900	1.000	0.021800	0.023200
891.500	1.000	0.094500	0.023200
876.500	1.000	0.013900	0.023200
854.900	1.000	0.048000	0.023200
845.600	1.000	0.010300	0.023200
819.900	1.000	0.110000	0.030000
810.500	1.000	0.213000	0.045000
791.000	1.000	0.023900	0.080000
782.200	1.000	0.002800	0.023200
778.300	1.000	0.001200	0.023200
758.900	1.000	0.006000	0.023200
750.000	1.000	0.068200	0.049000
743.300	1.000	0.001000	0.023200
712.100	1.000	0.001300	0.023200
678.600	1.000	0.026000	0.026000
665.100	1.000	0.019700	0.026500
637.500	1.000	0.011700	0.022000
632.500	1.000	0.013300	0.025000
608.100	1.000	0.022800	0.021000
596.800	1.000	0.057500	0.025000
584.100	1.000	0.001140	0.023200
566.300	1.000	0.031500	0.021500
553.200	1.000	0.018500	0.024500
546.400	1.000	0.031000	0.025000
530.800	1.000	0.000700	0.023200
526.100	1.000	0.000910	0.023200
514.300	1.000	0.021500	0.025500
499.300	1.000	0.019300	0.021500
493.900	1.000	0.005800	0.023200
473.300	1.000	0.004200	0.023200
466.500	1.000	0.003100	0.023200
449.800	1.000	0.016500	0.026500
445.800	1.000	0.001400	0.023200
419.000	1.000	0.006100	0.023200
405.000	1.000	0.108500	0.026000
372.000	1.000	0.013800	0.021500
369.700	1.000	0.032500	0.025000
346.000	1.000	0.016500	0.021500
338.400	1.000	0.005700	0.023200
320.700	1.000	0.019300	0.021000
318.300	1.000	0.005200	0.023200
304.900	1.000	0.007200	0.023200
287.100	1.000	0.138700	0.026000
260.500	1.000	0.023200	0.024000
239.200	1.000	0.012200	0.021500
199.600	1.000	0.000940	0.023200
192.000	1.000	0.000200	0.023200
185.800	1.000	0.016300	0.022000
170.100	1.000	0.013700	0.022000
162.700	1.000	0.008600	0.020000
151.900	1.000	0.014200	0.021500
135.300	1.000	0.018500	0.024500
130.700	1.000	0.000150	0.023200
121.600	1.000	0.014500	0.021500
105.000	1.000	0.045500	0.026000
92.510	1.000	0.003000	0.023200
90.770	1.000	0.013500	0.019500
72.780	1.000	0.022000	0.021000
66.620	1.000	0.055900	0.023500
41.620	1.000	0.016800	0.021800
38.320	1.000	0.019200	0.020000
20.450	1.000	0.002700	0.023200
1.056	1.000	0.023000	0.031000

TABLE 4. 1-2 (b) The resonance parameters of ^{235}U at lower energies

E_λ (eV)	g_J	$\Gamma_{\lambda n}{}^0$ (meV)	$\Gamma_{\lambda\gamma}$ (meV)	$\Gamma_{\lambda f}$ (meV)	$\xi_{\lambda 1}$	$\xi_{\lambda 2}$
3.16	0.562	0.01631	31.0	155.0	−0.707	−0.707
2.82	0.438	0.00179	45.0	64.0	0	0
2.035	0.438	0.00631	35.0	12.0	0	0
1.14	0.562	0.01405	44.0	124.6	−0.240	0.971
2.73	0.562	0.00574	29.0	88.0	0.131	−0.991
−0.938	0.562	1.327	27.6	169.4	1.0	0

TABLE 4. 1-4 (b) The resonance parameters of ^{239}Pu lower energies

E_λ (eV)	g_J	$\Gamma_{\lambda n}{}^0$ (meV)	$\Gamma_{\lambda\gamma}$ (meV)	$\Gamma_{\lambda f}$ (meV)	$\xi_{\lambda 1}$	$\xi_{\lambda 2}$
15.5	0.75	0.2	37.8	760.5	−1	0
14.68	0.75	0.57	37.8	31.7	0	0
14.28	0.5	0.22	37.8	52.5	0	0
11.9	0.75	0.31	40.9	22.0	0	0
10.93	0.75	0.55	31.5	146.7	−1	0
7.82	0.75	0.31	40.6	41.5	−0.6	0.8
0.296	0.25	0.42	38.6	55.4	0	0
−1.2	0.75	0.771	39.0	20.1	0	0

$$\sum_{\alpha f}\sqrt{\Gamma_{\lambda c}\Gamma_{\lambda' c}}=(\Gamma_{\lambda f}\Gamma_{\lambda f})^{1/2}\sum_{c}\xi_{\lambda c}\xi_{\lambda' c} \qquad (4.1\text{-}2)$$

where the summation over C is extended over all open fission channels.

TABLE 4. 1-1 shows list of references quoted in the assignment of the resolved resonance parameters. TABLE from 4. 1-1 (a) to 4. 1-5 (a) show the resolved resonance parameters of ^{235}U, ^{238}U, ^{239}Pu and ^{240}Pu at higher energies, respectively, where the multi-level parameters defined by Eq. (4. 1-1) are not assigned or may not be needed. TABLE 4. 1-2 (b) and 4. 1-4 (b) show the resolved resonance paramters including $\xi_{\lambda c}$ of the fissile nuclide ^{235}U and ^{239}Pu at lower energy ranges.

4. 2 Average Resonance Parameters Used in the Construction of Cross Sections

Recently, there seem to be considerable new experimental data which have not been taken into consideration in evaluations of average resonance parameters[40),47),48)]. Hence, an attempt was made to re-evaluate basic average data of ^{235}U, ^{238}U, ^{239}Pu and ^{240}Pu in the unresolved resonance region. Starting from a set of trial values for average data, mainly based on the data compiled by SCHMIDT[40)], various average resonance parameters were obtained from empirical matching to measured cross sections. In the important region for the calculation of the Doppler coefficient of reactivity, the resonances are resolved for ^{238}U and ^{240}Pu[40),45),46)], although they may not be sufficiently accurate, due to missing levels, p-wave mixing, etc. For ^{235}U and ^{239}Pu, this energy range is unresolved, but the s-wave neutrons are thought to contribute mainly to the cross section. At high resonance energies, say $E>5$ keV, one of principal unknowns for all these nuclides is the strength function for the p-wave neutrons, which is fairly sensitive to the cross section. Hence, the strength function for the p-wave neutrons was chosen as one of main fitting parameters for the cross-section fit. In this case, the strength function was assumed to be the same for all J states of a given l, where the neutrons of $l\geq 2$ was neglected.

For fissile nuclides and ^{240}Pu, the fission widths as functions of energy were calculated from fission channel theory in the previous chapter. In our calculations, the fission widths erew

allowed to depend on J. The fission channel scheme recommended by LYNN[38] of TABLE 3. 2-2 and 3 was adopted to our calculations for ^{235}U and ^{239}Pu, while the calculation for ^{240}Pu were carried out assuming a simple model of one channel.

By changing the strength function of the p-wave and the barrier positions, a few calculations of the average cross sections were made for each nucleus, under the assumption of the one-level formula for resonance shape. In these calculation, the average radiative capture width was assumed to be independent of l and J. The computations are carried out by the use of the modified version of the PODGE code[49].

^{238}U: Most of the resolved and average resonance parameters were adopted from the data recommended by SCHMIDT[40]. Several calculations showed that lower values of Γ_γ were preferable for matching to high resolution data of the capture cross section at higher energies[42]. Hence, the value of Γ_γ was fixed to 0. 0191 eV which was obtained from the recent analysis of resolved resonance by Petrel bomb explosion[50]. The results obtained are shown by curves in Fig. 4. 2-1.

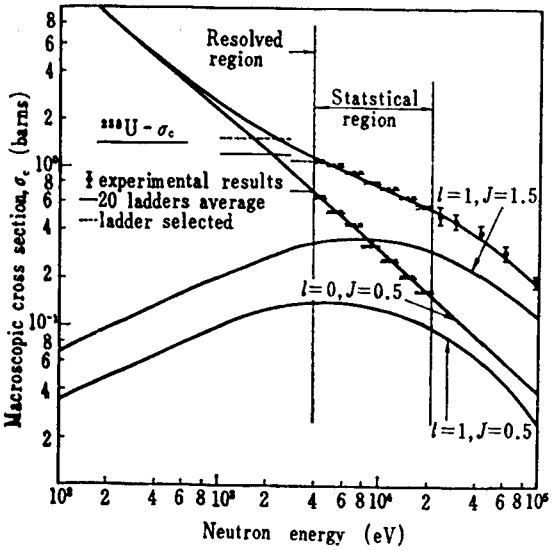

Fig. 4. 2-1 The capture cross section of ^{238}U obtained by the statistical method; the curves were obtained by the MOLDER code[49].

^{235}U: The average resonance parameters were based mainly SCHMIDT data, again. As to channel scheme for fission, it was found that LYNN's recommended data for the energy of transition states should be decreased by about 0. 2 MeV in order to make the cross sections fit measured results. The results for the fission cross section and the alpha value are shown in Figs. 4. 2-2 and 3, respectively, which also include experimental results of the fission cross section[39),50~53] and of the alpha value[39),40),51~57].

^{239}Pu: This case also started with Schmidt data except for the fission widths. For ^{239}Pu, there is some special interest, since most of recent experiments[58~61] indicate higher alpha values in the keV region, than those recommended until now[40], and seem to show abnormal dependence on energy. Of these experimental results, there are grounds to rely on the values obtained by GWIN *et al.*[61], as shown by analysis of critical experiments and of reactivity worth of ^{239}Pu, in soft spectrum core[62),63]. Hence, in our evaluation, exphasis was put on the results of GWIN *et al.* For the fission cross section, however, coincidence between various experiments seems to be fairly good[50),61),64),65]. In order to increase the alpha value in the keV region, invesfigations are made for the level scheme of fission channels, and it was found that the fit to higher alpha values can be made by changing slightly the energies of transition states recommended by LYNN. This is the same conclusion as DURSTON and KATSURAGI[44] reached. At higher resonance energy

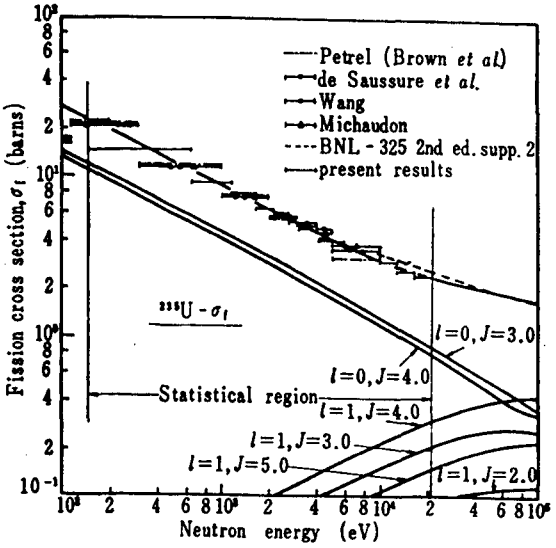

Fig. 4.2-2 The fission cross section of ^{235}U obtained by the statistical method; the curves were obtained by the MOLDER code[49].

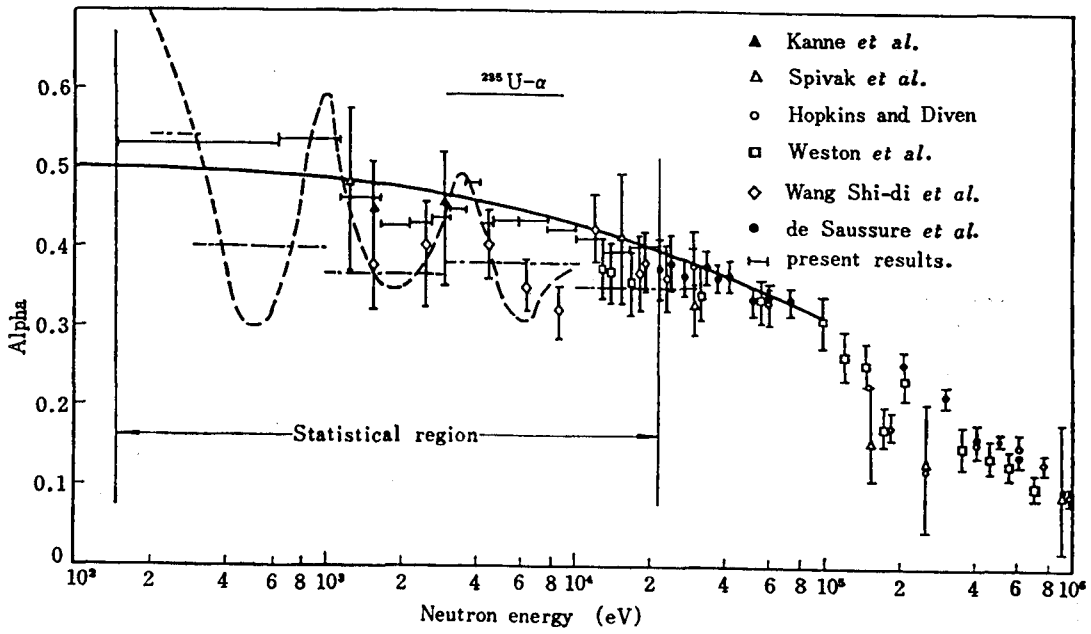

Fig. 4.2-3 The alpha value for ^{235}U in the keV region; the curve was obtained by the MOLDER code[49].

region, however, rather larger value of 3.0×10^{-4} was needed for the strength function of the p-wave neutrons. This value still lies in the uncertainty range given by SCHMIDT. The curves in Figs. 4.2-4 and 5 show the present results evaluated for the fission cross section and the alpha value.

^{240}Pu: The resolved and average resonance parameters for the s-wave neutrons were taken from those measured in Belgium[45),46)]. For the capture cross section, there are only exprerimental data of Pattenden at Harwell[47] available for our evaluation. It should be noted that this data shows good agreement with the average cross section obtained from the resolved resonance parameters[45),46),47)], as seen in Fig. 4.2-6. On the other hand, for fission cross section, we used the average cross section obtained from the measurements using the nuclear explosion PETREL[50]. The evaluated results are shown in Figs. 4.2-6 and 7. It will be seen from Fig. 4.2-7 that the values of the fission widths for the resolved levels should be asigned in future experiment.

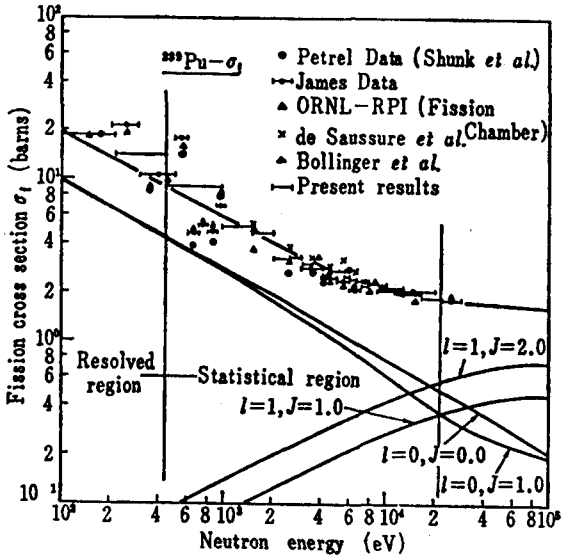

Fig. 4.2-4 The fission cross section of ^{239}Pu obtained by the statistical method; the curves were obtained by the MOLDER code[49].

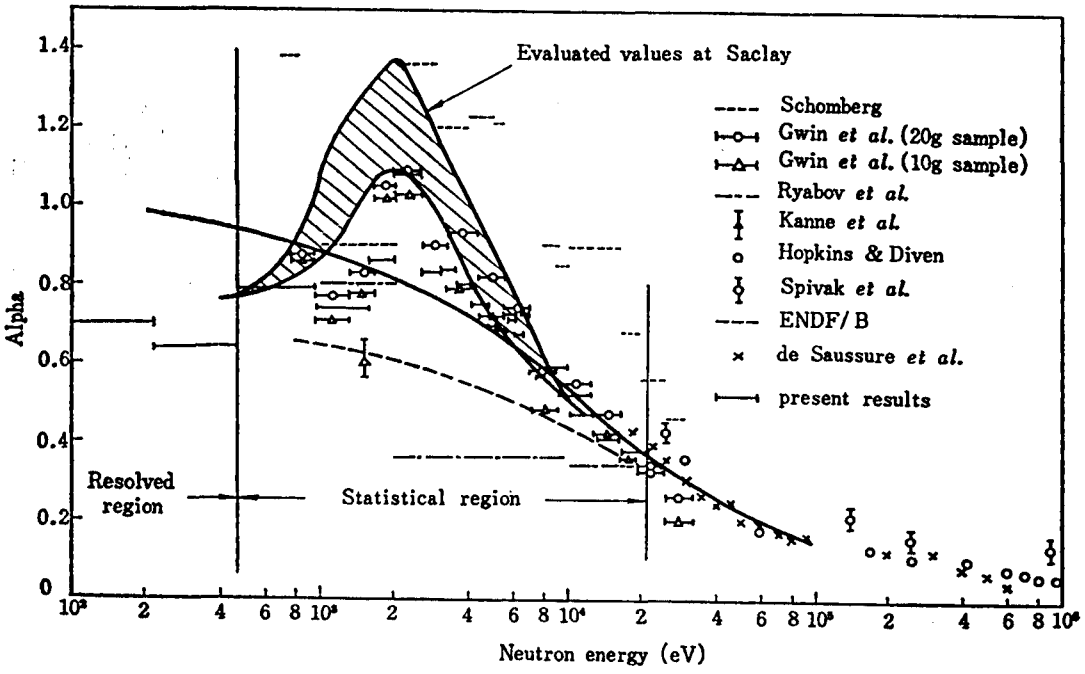

Fig. 4.2-5 The alpha value for ^{239}Pu in the keV region; the curve was obtained by the MOLDER code[49].

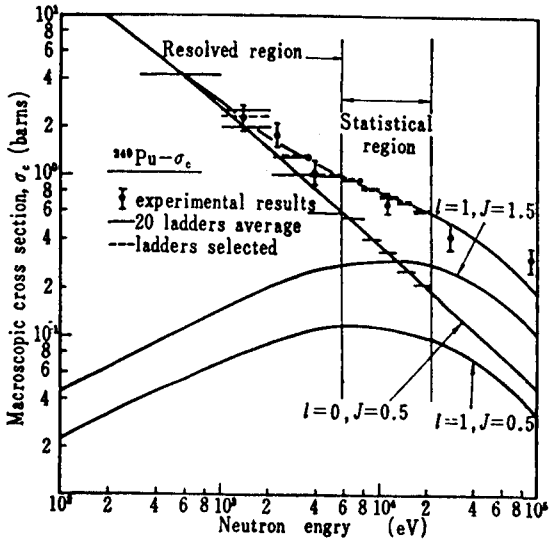

Fig. 4.2-6 The capture cross section of ^{240}Pu obtained by the statistical method; the curves were obtained by the MOLDER code[49].

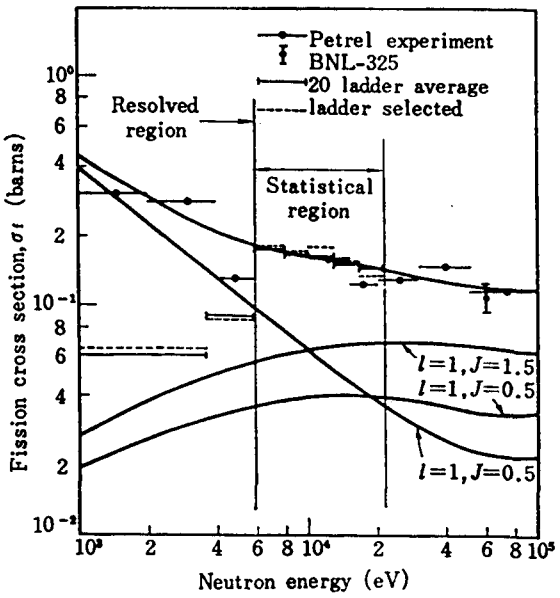

Fig. 4.2-7 The fission cross section of ^{240}Pu.

TABLE 4.2-1 summarizes the final results for the average resonance parameters obtained by the present evaluation, which were also used for the construction of ladders. TABLE 4.2-2 summarizes the barrier positions for fission widths. The calculated results for the fission widths are shown in TABLE 4.2-3. This table shows that fission widths for states (l, J) is not generally equal, so the use of effective channel number[38] will not always give good results. Therefore, for the construction of ladders, we assumed the chi-square distribution of freedom 1 for each fission channel of compound states (l, J^π). One thing to be mentioned here is the level scheme of inelastic scattering, for which the data evaluated in AWRE[25] were used and are shown in TABLE 2.5-1.

TABLE 4. 2-1 Average resonance parameters used for the construction of ladders

Isotope	(l, J)	D_J (eV)	$\Gamma_n^0 \times 10^3$ (eV)	Γ_γ (eV)
^{235}U	(0, 3)	1.143	0.118	0.048
	(0, 4)	0.889	0.092	0.048
	(1, 2)	1.600	0.282	0.028
	(1, 3)	1.143	0.402[a]	0.048
	(1, 4)	0.889	0.313[a]	0.048
	(1, 5)	0.727	0.128	0.048
^{238}U	(0, 0.5)	18.30	1.885	0.019
	(1, 0.5)	18.30	3.624	0.019
	(1, 1.5)	9.15	1.812	0.019
^{239}Pu	(0, 0)	8.78	0.939	0.039
	(0, 1)	2.93	0.313	0.039
	(1, 0)	8.78	2.634[a]	0.039
	(1, 1)	2.93	0.778	0.039
	(1, 2)	1.76	0.564	0.039
^{240}Pu	(0, 0.5)	15.50	1.628	0.021
	(1, 0.5)	15.50	2.720	0.021
	(1, 1.5)	7.75	1.360	0.021

a) The χ^2 distribution of freedom 2 was assumed.

TABLE 4. 2-2 Barrier positions for fission (MeV) barrier height $\hbar\omega = 0.5$ MeV

Isotope	(l, J^π)	1	2	3
$^{235}U+n$	$(0, 3^-)$	−0.8	−0.5	0.2
	$(0, 4^-)$	−0.5	0.2	
	$(1, 2^+)$	−1.1	−0.4	−0.1
	$(1, 3^+)$	−0.4	−0.1	
	$(1, 4^+)$	−1.1	−0.4	−0.1
	$(1, 5^+)$	−0.4	−0.1	
$^{239}Pu+n$	$(0, 0^+)$	−1.5	0.1	
	$(0, 1^+)$	0.2		
	$(1, 1^-)$	−0.9	−0.45	0.3
	$(1, 2^-)$	−0.5	−0.3	0.3
$^{240}Pu+n$	$(0, 0.5^+)$	0.52		
	$(1, 0.5^-)$	0.45		
	$(1, 1.5^-)$	0.44		

TABLE 4. 2-3 Fission widths and number of fission channels used for the construction of ladders: $E \leq 100$ keV

	(l, J)	Number of channels	Γ_{fi} (eV)			Γ_f (eV)
			1	2	3	
$^{235}U+n$	(0, 3)	3	0. 182—0. 154	0. 182—0. 154	0. 014—0. 034	0. 377—0. 342
	(0, 4)	2	0. 141—0. 120	0. 011—0. 027		0. 152—0. 146
	(1, 2)	3	0. 255—0. 216	0. 253—0. 216	0. 199	0. 706—0. 630
	(1, 3)	2	0. 181—0. 154	0. 142		0. 322—0. 296
	(1, 4)	3	0. 141—0. 120	0. 141—0. 120	0. 111	0. 392—0. 350
	(1, 5)	2	0. 115—0. 098	0. 091		0. 205—0. 188
$^{239}Pu+n$	(0, 0)	2	1. 397—1. 638	0. 310—0. 819		1. 707—2. 456
	(0, 1)	1	0, 035—0. 121			0. 035—0. 121
	(1. 0)	0				
	(1, 1)	3	0. 466—0. 546	0. 464—0. 545	0. 011—0. 041	0. 940—1. 132
	(1, 2)	3	0. 279—0. 327	0. 273—0. 325	0. 006—0. 025	0. 558—0. 667
$^{240}Pu+n$	(0, 0. 5)	1	0. 004—0. 001			0. 004—0. 011
	(1, 0. 5)	1	0. 009—0. 025			0. 009—0. 025
	(1, 1. 5)	1	0. 005—0. 014			0. 005—0. 014

5. Construction of Resonance Cross Sections by Generation of Resonance Parameters

The calculating method of resonance absorption and Doppler coefficient of reactivity in thermal reactors is considered to be fairly satisfactry, because the neutron spectrum does not deviate much from $1/E$ and the contributions to the Doppler effect and resonance absorption almost come from lower energies where accurate resonance parameters are obtained. Moreover, the ratio of fissile to fertile isotopes is generally quite small, hence the contributions to the Doppler effect from fissible isotopes are very small. Therefore, in thermal reactors the Doppler effect and resonance absorption can be estimated in sufficient accuracy even if we neglect the interference effects between different resonance isotopes which are theoretically thought to be one of the most difficult problems. To make matters better, the predominant resonance absorber in thermal reactors is usually the fertile isotope ^{238}U for which the assumption of isolated resonance[66] is considered to be sufficiently satisfied at lower energies.

In fast reactors which contain resonance absorbers in higher volume ratio than thermal assemblies, the neutron spectrum is, however, entirely different and is much depleted due to resonance absorption. Moreover, to make matters worse, the ratio of fissile to fertile isotopes will be generally much larger and the interference effects between various resonance isotopes become quite important. On the other hand, the level spacing between resonances decreases generally with energy and especially for the fissile nuclides the level spacing is much smaller. Hence, the second kind of interference effect may be important, that is, there may be the interference between neighboring resonances in the same isotope. These facts make the treatment of resonance absorption more complex and difficult than in thermal reactors.

For fast reactor analysis, the effective cross sections have often been calculated by using $1/(E\sigma_t(E))$ spectrum based on the assumption of the constant collision density. Even if we would start with this assumption, we however met to the difficulty of the calculation of the integrals appered in the expression of the effective cross sections. Espeically in the unresolved region, one has only a knowledge of the average value of a resonance parameter and the probability distribution of local to average values but he has not imformation regarding the actual value of the parameter at any energy. Hence, the various approximation methods have been proposed for the estimation of the effective cross sections[6),7),8),9)].

On the other hand, in a typical large fast reactor, the Doppler effect comes most from lower energy resonances, say $E_l<4\,\mathrm{keV}$ where the rapid energy dependence of the α value of ^{239}Pu and the sodium resonance at $E\cong 3\,\mathrm{keV}$ are considered to play an important role[5)]. Without taking this facts into account, accurate calculation of effective cross sections will be impossible. We can not expect that high accuracy for the Doppler coefficient of reactivity is obtained from the calculation based on the $1/(E\sigma_t(E))$ spectrum.

In order to avoid the shortcomings of the semi-analytical methods based on the $1/(E\sigma_t(E))$ spectrum, new methods which have recourse to the statistical ones have been prepared for the calculations of the effective cross sections[19),67)]. From the knowledge of the statistical distributions of resonance parameters and level spacing, it is possible to generate a sequence of resonances over some energy interval by random sampling technique, and we hence are driven to a statistical description of cross sections. These resonance parameters generated can then be used in such codes as SDR[49)], FIFF RAFF[68)], or RABBLE[69)], whice have veen developed for the resolved

resonance region. Fairly detailed studies of the mathematical and physical properties of resonance sequences and the corresponding quanties of interest in fast reactor physics have been made by several authors[70)-74)]. In this chapter, investigations will in more detail be made for the relation between the statistics of the various cross sections corresponding to resonance sequences generated and representative of measured cross sections by a simple resonance sequence. And we will show the procedure for constructing a single ladder of resonances that can represent poorly resolved data points both for capture and fission cross sections.

5. 1 Sampling Technique

As mentioned in chapter 2, the resonance widths and the level spacing are distributed about their mean values according to the χ^2 and Wigner distributions, respectively, i. e.,

$$P_n(x)dx=\frac{n}{2\Gamma(n/2)}[nx/2]^{(n/2)-1}\exp(-nx/2)dx \tag{5. 1-1}$$

$$P_0(x)dx=\frac{\pi}{2}\exp(-\pi x^2/4)xdx \tag{5. 1-2}$$

The χ^2 distribution of Eq. (5. 1-1) is known as the distribution that a statistical variable

$$x=X_1^2+X_2^2+\ldots X_n^2 \tag{5. 1-3}$$

follows, where the n samples $X_1, X_2, \ldots X_n$ do the normal distribution

$$P(X)dX=\frac{1}{\sqrt{2\pi}}\exp(-X^2/2)dX \tag{5. 1-4}$$

Hence, by forming a normal distribution, we can generate the statistical variables which are distributed according to the χ^2 distribution.

Let ξ_1 and ξ_2 be samples from an uniform distribution in the range (0-1), i. e.,

$$p(\xi)=1 \qquad 0\leqq\xi\leqq 1 \tag{5. 1-5}$$

which is obtained from a multiplicative type of random-number generator. Then the following quantities x_1 and x_2 defined by

$$x_1=(-2\ln\xi_1)^{1/2}\sin 2\pi\xi_2 \tag{5. 1-6}$$

$$x_2=(-2\ln\xi_1)^{1/2}\cos 2\pi\xi_2, \tag{5. 1-7}$$

give two variables on the normal distribution. That is, we find, for the Wronskian for the variable inversion,

$$\frac{\partial(\xi_1,\ \xi_2)}{\partial(x_1,\ x_1)}=\frac{1}{2\pi}\exp[-(x_1^2+x_2^2)/2] \tag{5. 1-8}$$

or

$$d\xi_1 d\xi_2=P(x_1)dx_1P(x_2)dx_2\,. \tag{5. 1-9}$$

The required χ^2-distribution is now obtained as the sum of the squares of samples from independent normal distribution.

As stated in chapter 2, we use generally the multilevel formalism for the resonance cross section, hence additional level parameter $\xi_{\lambda c}$ of Eq. (4. 1-1) is needed in the unresolved region, too. As $\sqrt{\Gamma_{\lambda c}}$ of Eq. (4. 1-1) is considered to follow a normal distribution, the parameter $\xi_{\lambda c}$ may be assumed to be distributed according to the normal distribution. In our calculation, one of the variables given by Eqs. (5. 1-6) and (5. 1-7) is used to give the values of $\xi_{\lambda c}$, where a normalization

$$\sum_c \xi_{\lambda c}^2=1 \tag{5. 1-10}$$

is made.

If x is sample obtained by the procedure stated above, from the χ^2 distribution of freedom 2

$$P_2(x)dx=e^{-x}dx, \tag{5. 1-11}$$

the variable inversion

$$y=\sqrt{4x/\pi} \tag{5.1-12}$$

gives the needed Wigner distribution, i. e.,

$$P_2(x)dx=(\pi/2)\exp(-\pi y^2/4)ydy, \tag{5.1-13}$$

Here, we showed that, starting from an uniform distribution, we can generate the samples distributed about their mean following the χ^2 or Wigner distribution. Therefore, with knowledge of the average values of the resonance parameters and level spacing, we thus can construct any number of the sequences of resonances over some energy interval. We shall discuss in the next section the statistical properties of the energy average cross sections corresponding to these sequences of resonances and the method to select the best sequence which reproduce low-resolution experimental results.

5.2 On the Statistics for Sequences of Resonances

Few computer codes have been prepared for generating the resonance sequences according to the method mentioned above[49),67),75)]. Starting with some initial energy E_0, high in the unresolved region, resonances are generated over the complete energy range of interest. Since the generated parameters can be treated in the same way as the resolved resonance parameter, the infinitely dilute cross sections can be calculated by Eqs. (2.1-32)～(2.1-35). Especially the energy average cross sections can be given by Eqs. (2.4-4)～(2.4-7).

In should be noted here that we can formally generate infinite numbers of the resonance sequences by changing random number starter for the first level at the starting energy E_0. From the mathematical view-point, the cross section for each sequence is itself a random variable and all the sequences are equally probable. As a result, the cross sections computed from the resonance sequences are distributed around the mean value following a normal distribution[72),73)]. If the number of sequences becomes infinite, the mean values and the standard deviation of the resonance parameters averaged over all resonances in each sequence will converge to the theoretical value; in other word, the average cross sections for infinite number of sequencs in a narrow energy interval can be obtained from the average over distribution function assumed for generating sequences, that is, they can be calculated by Eqs. (2.4-16)～(2.4-19).

A few investigators have adressed themselves to the question of how sensitive are the required quantities to the particular sequence of resonances in the unresolved region[72-74)]. KELBER and KIER[72)] concluded that, on the basis of statistical information only, typical group averaged quantities can be calculated only with a large probable error and that the Doppler coefficient of ^{239}Pu for large dilute fast reactors can be estimated with a relative probable error no great than 100%.

It is not assured, however that we can obtain good representation of the actual cross sections from choosing any sequence of resonances based on the equal probability of occurance. In fact, for some sequences, the cross sections in a narrow energy interval around the energy point under consideration are quite different from low-resolution experimental data. The concept of "equal probability of occurance of all sequences" should be discarded when it disagrees with existing experimental information. Hence, in the case, we can not give physical meaning to the mean value of the cross sections obtained through averaging over all sequences of resonances. On the other hand, except for some experimental uncertainties we always obtain a fixed value for a cross section from every measurement. So predictions of resonance parameters should be biased to agree with experimental data. This statement is especially true when fissile nuclides are considered; we must evaluate, at one time, both the capture and fission cross sections through the value of alpha, the fission-to-capture ratio. The low-resolution experimental data for alpha in the

keV energy region are not always smoothly varying with energy and, therefore, the value is strongly dependent on the particular sequence of resonances and cannot be represented by a mean over the sequences. Hence, it is concluded that the conventional method[76] of obtaining cross sections by averaging over distribution functions will not alway give a very predictions for the Doppler coefficient of reactivity. Moreover, to calculate accurate effective cross sections without assuming such approximations as isolated narrow-resonances overlap, etc., it is better to construct the cross sections from particular sequence of resonances.

Here, a note should be taken of the following points: When average resonance parameters were evaluated in the unresolved region, the energy width ΔE for averaging cross section was assumed to contain enough number of resonances so that the averaging process over the energy width was converted into the integration on distribution functions. The cross sections calculated thus were considered to correspond to the experimental data of low resolution. For lower energy region, however, energy resolution of experiment becomes narrower and number of resonances in each experimental point is to be smaller. Hence, measured cross sections may largely be distributed statistically around some mean value, excluding experimental errors. The abnormal behavior of the alpha value of ^{239}Pu in the keV energy region may be a result of such statistical distribution.

Therefore, an evaluated curve for cross section should represent the mean value over such statistical distribution or fluctuation of the measured cross section. The magnitude of such fluctuation may be different from one nuclide to another. For an example of ^{239}Pu, the fluctuation of cross sections is thought to be large, since the level spacing is wider and the total width is thought to be largely fluctuated due to $\Gamma_t \cong \Gamma_f$. By the convetional treatment for calculating effective cross sections[76),77], we can not take this fact into account and hence, cannot expect high accuracy to be obtained in the calculation of the Dopper coefficient of reactivity. In general, it is quite natural to suppose that a resonance cross section consists of a particular sequence of resonances.

5.3 Method of Selecting the Best Sequence of Resonance

In the previous section, it was shown that only a single sequence of resonance is necessary for obtaining a representative of the actual cross sections at every energy and [the Doppler coefficient of reactivity can be estimated accurately only through the construction of the particular sequence. Dyos[73] provided a method of selecting the sequence that reproduced measured resonance integral or pointwise data over some energy range. Recently this method was also applied[74] to the estimation of the Doppler coefficient of reactivity in a large heterogeneous fast reactor. We cannot, however, attach physical significance to the procedure of Dyos[73], which disregards available individual data values. That is, it is doubtful if the ladder that can reproduce the resonance integral over a wider energy range can always be representative of pointwise cross sections except for extremely rare accidental case. Moreover, the average resonance parameters for ^{238}U, especially for the p-wave neutrons used for the construction of ladders, were not consistent with recent high-accuracy measurement[61]. For fissile nuclides, in addition to the fission cross section, a rather complicated energy-variation of alpha should be considered. And, to make matters worse, the direct generation of sequences over complete energy ranges requires large amounts of computer time due to the narrow level spacing of fissile nuclide. Therefore this procedure is very expensive compared with the usefulness of the results obtained. Hence, because it is unfeasible to apply the method of Dyos[73] to the calculation of the cross sections for fissile nuclides over complete energy range, a new method is needed.

Only a particular small subset of sequences of resonances reproduce the energy-averaged

cross sections on all sub-intervals in the complete energy range. In this case, the cross sections may be low-resolution experimental data or may be the curves predicted for the cross sections over some energy range where no accurate experimental data have been obtained. Under some criterion, the best sequence is chosen from the small subset of sequences. If there is no particular sequence that satisfies the criterion, the generation of sequences will be continued until the particular ones are generated.

Only the cross sections of Eqs. (2. 4-4)～(2. 4-7) can be compared with experimental results, or can be given numerical values from data evaluations or theoretical considerations. Therefore, it is reasonable to assume the following criteria for the sequence selection:

A. The sequence selected should reproduce, within assigned errors, both the capture and fission cross sections on all the sub-intervals in the complete range of interest.

B. The means and standard deviations of the level spacings and widths for the special values of (l, J) of the sequence are as close as possible to those obtained theoretically, throughout the whole range.

For fertile nuclides, it is rather easy to select a sequence satisfying the above criteria from the many ladders constructed by straightforward generation, because the level spacing for the nuclides are very wide and the actual pointwise data for the capture cross section are rather smooth. However, for the case of ^{239}Pu, it is almost prohibitive, from the stand-point of computer time, to obtain a ladder that can reproduce the recent results for alpha, for example that of GWIN *et al*[6-1], from the straightforward generation of many sequences in the complete energy range. This special behavior of alpha for fissile nuclides seems, however, to be restricted to the lower energy regions, say $E \leq 10$ keV.

In this lower energy region contributions from the inelastic scattering are neglected. We divide this energy range into a few sub-ranges so that in each the energy dependence of the fission width can be neglected. As will be seen in the previous section, two or three sub-ranges will be sufficient to this end. Next, each of the sub-ranges is again divided into equal energy intervals. It is desirable that this energy interval be so narrow that its width corresponds to the width of the low-resolution measurements. On the other hand, the width is wide enough to include a sufficient number of resonances. Usually it is not possible to generate a resonance ladder so that the first and last resonances in each (l, J) sequence are located just on an energy boundary. If a sub-interval is wide enough it contains a sequence with a sufficient number of resonances so that removal or inclusion of a few of them does not significantly affect the statistical property of the sequence. Therefore, neglect or inclusion of a few resonances at the lower boundary does not affect characteristic features of the cross sections. First we generate many sequences in one of the sub-intervals by putting the first resonance in each (l, J) sequence at the upper energy boundary of this interval. We stop generating a sequence in each (l, J) sequence when the next resonance would fall into the next lower energy sub-interval. Then the energy averaged cross-section for each sequence are calculated for both capture and fission. When the same sequences are generated in another sub-interval, the corresponding cross sections in this sub-interval are related to those in the previous one in a quite simple manner. It is expected from analytical procedure that the cross sections vary as $(E_k)^{1/2}$. It was confirmed numerically, that, in every sub-interval, the relative magnitude of an averaged cross section for each sequence is scarcely varied even though sequences are removed from one sub-interval into another one. An example of this fact for the case of ^{239}Pu is shown in TABLE 5. 3. 1. That is, if we generate the same sequences in one sub-interval as those generated in the other sub-interval, we can expect nearly equal frequency distributions on relative values of cross sections.

The measured cross sections are scattered around its mean value over the whole energy

TABLE 5. 3-1 Relative magnitude of averaged cross sections of ^{239}Pu ($J=1$); obtained by the same ladders

Energy interval (eV)	σ_c	σ_f	σ_n
7730. —7239.	1. 0181	1. 2965	1. 0774
	0. 9722	1. 0664	0. 8571
	0. 9304	0. 8203	0. 9147
	0. 9643	0. 9304	0. 9111
	1. 1549	0. 9875	1. 2979
	1. 0508	0. 9862	1. 0819
	1. 0088	0. 9824	1. 0630
	1. 0171	0. 9190	0. 9101
	0. 9048	0. 8270	0. 8005
	0. 9786	1. 1843	1. 0863
3600. —3100.	1. 0225	1. 2827	1. 0875
	0. 9733	1. 0723	0. 8205
	0. 9363	0. 8049	0. 9137
	0. 9681	0. 9200	0. 8976
	1. 1900	0. 9955	1. 3805
	1. 0496	0. 9848	1. 0862
	1. 0217	1. 0188	1. 1001
	1. 0055	0. 8928	0. 8745
	0. 8680	0. 8273	0. 7557
	0. 9651	1. 2009	1. 0837
1000. —500.	1. 0147	1. 2965	1. 0762
	0. 9662	1. 0628	0. 8433
	0. 9340	0. 8157	0. 9164
	0. 9651	0. 9245	0. 9070
	1. 1685	0. 9876	1. 3245
	1. 0539	0. 9873	1. 0853
	1. 0107	0. 9922	1. 0725
	1. 0146	0. 9120	0. 8994
	0. 8948	0. 8305	0. 7878
	0. 9774	1. 1911	1. 0875

range, hence we have to select appropriate statistical resonance parameters so that mean value of cross sections for an infinite number of ladders are obtained by the conventional methods.[76),77)] Then we can know about relative maximum deviations of experiments from the theoretical mean values. These maximum deviations give information on the number of sequences need for reproducing experiments over the whole energy range. That is, if we generate N ladders in one sub-interval and assume that each of the sequences consists of approximately n resonances, then standard deviation of the mean corss section for each sequence is given by $\Delta\sigma/\sqrt{n}$, where $\Delta\sigma$ is the standard deviation of the cross section obtained by assuming that at every energy, frequency distributions for resonance parameters are definitely given. The quantity $\Delta\sigma$ was obtained by numerical calculation of $(\langle\sigma_x\rangle^2-\langle\sigma_x^2\rangle)^{1/2}$ for the χ^2-distributions and was shown to have a value of $\sim 1.4\,\sigma_x$ for both the capture and fission cross sections of all the nuclei under consideration. Now if the actual maximum deviation of the experimental value from the theoretical value is ϵ, the total number of sequences N is determind so that a narrow interval $d\epsilon$ around ϵ would contain a few, say M, ladders given by

$$N=10\sqrt{\pi}\,Mx^{-1}\exp(x^2) \tag{5. 3-1}$$

with

$$x=\sqrt{n}\,\epsilon/\Delta\sigma \quad \text{and} \quad \epsilon/d\epsilon=10. \tag{5. 3-2}$$

Here, we assume a normal distribution with a standard deviation of $\Delta\sigma/\sqrt{n}$ for the N sequences generated.

With this background, many sequences of resonances are generated in certain sub-intervals. Here we denote the capture and fission cross sections which are obtained from the n-th sequence by σ_{cn} and σ_{fn}, respectively. If N sequences have been generated, their mean values are

$$\langle\sigma_{xN}\rangle=\frac{1}{N}\sum_{n=1}^{N}\bar{\sigma}_{xn}. \tag{5. 3-3}$$

Futhermore, the ratio U_{xn} of each cross section to the mean is calculated by

$$U_{xn}=\bar{\sigma}_{xn}/\langle\sigma_{xn}\rangle,\ n=1\ldots N. \tag{5. 3-4}$$

As mentioned above, it was shown that this artio varied only slightly from one sub-interval to another.

If N was a large enough number, the mean value $\langle\sigma_{xN}\rangle$ would be very close to the energy average of the theoretical value in the interval, i. e.,

$$\langle\sigma_{xN}\rangle\cong\langle\sigma_x\rangle\cong\int_{\Delta E_s}\sigma_x(E)dE/\Delta E_s. \tag{5. 3-5}$$

Here, ΔE_s is the energy width of the sub-interval and $\sigma_x(E)$ is the mean for an infinite number of sequences which was obtained by the conventional method. On the other hand, we can prepare another ratio of cross sections in each sub-interval, defined by

$$U_x^e=\sigma_x^e/\langle\sigma_x\rangle \tag{5. 3-6}$$

where σ_x^e is the experimental pointwise data. Hence, we can, in general, obtain a few sequences in each sub-interval such that for both capture and fission

$$|U_x^e-U_{xn}|\leq e_x \tag{5. 3-7}$$

where e_x is the value of the assigned error. Linking these shorter sequences, without duplication, over the complete energy range, we can obtain a few long sequences from which the best sequence can be selected following Criterion B.

As seen from the procedure mentioned above, generation of as many ladders as possible in the subinterval will lead to the selection of the best sequence.

For this purpose, one of the authors (Y. ISHIGURO) has prepared the computer code BABEL[75] based on RESP code by BRISSENDEN *et al.*[49] which takes into consideration the statistics for inelastic neutron scattering as well as other reactions.

5. 4 Construction of Resonance Cross Sections

The sets of parameters in the statistical resonance regions were generated using the computer code BABEL mentioned in sec. 5. 3. Starting with some random number, this code can construct as many sequences of resonances as desired over some energy sub-interval in the unresolved region and can calculate the average cross sections for each sequence. Letting the last random number for the next, the computations are continued until the required number of sequences is constructed. This code calculates the mean values and the standard deviations of resonance parameter and level spacings for each sequence. and also investigates the statistics of various quantities over all the sequences in each energy sub-interval.

For the fertile nuclides, ^{238}U and ^{240}Pu, calculations were carried out by straightforward generation of resonances in the whole energy range starting with $E=21.5$ keV. In this case, the resonances of the p-wave neutrons were taken into consideration up to 1 keV, where they still contribute to the capture cross section as seen from Figs. 4. 2-1 and 4. 2-6. However most of p-wave resonance are thought to be missing from the resolved resonance parameters. Criteria A and B of sec. 5. 3 for the selection of a single sequence were set up only for capture cross sections. Here the cross section curves assigned by the MOLDER code[49] (the modified PODGE) were selected as the standard, and the error assigned from the standard was assumed to be 4%, as inferred from the experimental errors and the conditions of the curve fitting by the MOLDER code.[49] It was found that the single sequence desired could be selected from twenty or thirty sequences under our variable conditions. The results for sequence selection are given by the

dashed bars in Figs. 4.2-1 and 4.2-6. The dashed bars in Fig. 4.2-7 give the result for the fission cross section of ^{240}Pu which is obtained from the sequence selected for capture cross sections. TABLE 5.4-1 shows the information related to the statistics of resonance parameters and the level spacing of the selected sequence.

On the other hand, for the fissile nuclides, ^{235}U and ^{239}Pu, the selection of the single sequence was done by the method mentioned in the previons section. For this purpose, the energy between 4.65, or 7.73 keV, and the upper energy of resolved resonance was divided into sub-intervals of 500 and 520 eV for ^{235}U and ^{239}Pu, respectively. In each sub-interval, the quantity U_x^e, defined by Eq. (4.3-5), was prepared both for the fission and the capture cross sections from experimental data. In this case, alpha obtained by GWIN *et al.*[61] was adopted for ^{239}Pu, and that for ^{235}U was the one evaluated by SCHMIDT[40]. In these energy ranges, the *s*-wave components are the main contributors to the cross sections. Hence, in one of these sub-intervals 100 sequences were constructed for the *s*-wave resonances and the ratio U_{xn} defined by Eq. (4.3-4) was calculated for each sequence. The number 100 was chosen by considering deviations of experimental data from the values obtained from the MOLDER code. Here, the random number beginning each sequence has been the final number of the preceding one in order to link these shorter sequences for obtaining the long sequence covering the whole range. At each sub-interval, a sequence was selected following Criterion A without duplication and the single long sequence required was obtained from linking them sequentially. For higher energy ranges, the cross-section curves are quite smooth and, in addition, the average level spacing for these nuclides are very narrow. Hence, construction of a few sequences over the range was sufficient to fit the cross sections in this energy range. This is reasonable because the effective cross sections in this range are not highly shielded and the contribution to the Doppler coefficient of reactivity is fairly small.

The bars in Figs. 4.2-2 and 4.2-3 show the present results of the sequence selection for ^{235}U. It will be seen that the sequence selected is a good representative of the fission cross sections

TABLE 5.4-1 Statistical characteristics of D, $\Gamma_n^{(0)}$ and Γ_f of ^{235}U, ^{238}U, ^{239}Pu, and ^{240}Pu*

Isotope	(l, J)	Energy range	Average value over the selected ladder for		
			D (eV)	$\Gamma_n^{(0)}[\times 10^3$ (eV)]	Γ_f (eV)
^{235}U	(0, 3)	10 keV—147.33 eV	1.141 (1.27)	0.115 (2.90)	0.386 (1.94)
	(0, 4)		0.894 (1.27)	0.092 (3.01)	0.154 (2.69)
	(1, 2)	10—1 keV	1.569 (1.28)	0.273 (3.18)	0.698 (1.67)
	(1, 3)		1.125 (1.27)	0.398 (2.01)[a]	0.321 (2.02)
	(1, 4)		0.873 (1.27)	0.305 (2.02)[a]	0.384 (1.69)
	(1, 5)		0.727 (1.27)	0.124 (2.99)	0.204 (2.02)
^{238}U	(0, 0.5)	21.5—3.9 keV	17.88 (1.27)	1.961 (2.76)	
	(1, 0.5)	21.5—1 keV	17.95 (1.29)	3.409 (3.13)	
	(1, 1.5)		8.99 (1.28)	1.700 (3.05)	
^{239}Pu	(0, 0)	10 keV—442.41 eV	8.91 (1.28)	0.928 (3.11)	1.668 (2.07)
	(0, 1)		2.92 (1.26)	0.326 (2.92)	0.037 (2.83)
	(1, 0)	10—1 keV	8.62 (1.27)	2.912 (2.92)	
	(1, 2)		2.90 (1.28)	0.751 (1.99)	0.933 (2.00)
	(1, 3)		1.73 (1.27)	0.560 (3.02)	0.573 (2.04)
^{240}Pu	(0, 0.5)	21.5—5.9 keV	15.46 (1.29)	1.529 (2.90)	0.004 (2.78)
	(1, 0.5)	21.5—1 keV	14.59 (1.25)	2.615 (2.95)	0.010 (2.99)
	(1, 1.5)		7.53 (1.27)	1.355 (2.88)	0.006 (2.81)

* The values in parentheses show the variance $\langle x^2\rangle/\langle x\rangle^2$, which is $(1+2/n)$ for the χ^2-distribution in n degrees-of-freedom and is $4/\pi \cong 1.27$ for the WIGNER distribution.

[a] The χ^2-distribution in two degrees-of-freedom was assumed.

obtained from experiment. As alpha, the presults represent quantatively the same variation with respect to energy as that of SCHMIDT[40], but are a little higher in value because of our evaluation by the MOLDER code. To obtain the sequence that gives the same alpha as Schmidt, more ladders would be needed. However, this was not done since there are some ambiguities in the Schmidt evaluation.

For ^{239}Pu the results are shown in Figs. 4.2-4 and 4.2-5. It is astonishing that the sequence which is selected from only 100 generated in a narrower energy interval can be a quite good representative of alpha obtained by GWIN *et al.*[61]. Also, the fission cross section obtained is satisfactory. Due to wider level spacing, the present method of ladder selection should be able to reproduce the alpha-energy curve obtained by experiments if more sequences are generated. In this case, the statistics of such a sequence may be inconsistent with the distribution functions assumed. TABLE 5.4-1 removes such a question and indicates that the statistics of the particular sequence also obeys the distribution functions assumed. Fig. 5.4-1 shows the infinite-dilution capture cross sections of ^{239}Pu obtained and compares them with those given in the cross-section libraries prepared for fast reactor calculations[3),78]. It should be noted that the present results reflect very well the aspect expected from the recent high values of alpha in the keV region. Moreover, it will be almost impossible to obtain a sequence such as those selected here, from the straightforward generation of ladders as described.

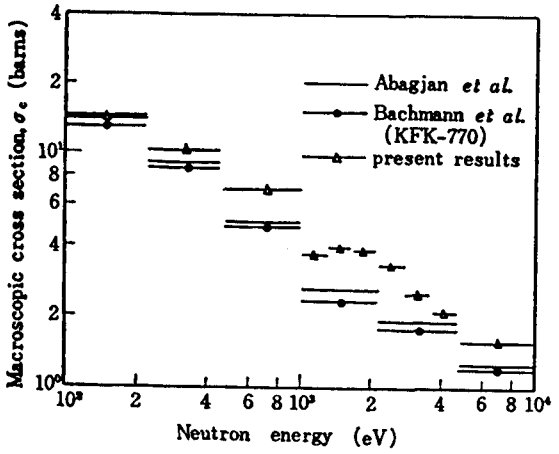

Fig. 5.4-1 Comparison of group capture cross section of ^{239}Pu.

5.5 Calculations of the Doppler-broadened Cross Sections and Discussions of the Results

The Doppler-broadened cross sections derived in the section 2.2 were calculated by using the resonance level parameters that were generated by the statistical method in the previous sections. This calculation of the cross sections was performed by the code MCROSS[79], and the capture, fission and total cross sections were tabulated over energy ranges from 21.5 keV to 0.1 eV for the fertile materials ^{238}U and ^{240}Pu and from 10 keV to 0.1 eV for the fissionable materials ^{235}U and ^{239}Pu, respectively. Temperatures selected for these calculations are 300°K, 900°K and 2100°K and the results for all the materials were tabulated in accordance with the energy boundaries and mesh widths shown in TABLE 5.5-1. Here, we will discuss the various problems arising in the calculations of the cross sections and also show the results, for the infinitely dilute resonance integrals and for the energy-average cross sections with those obtained previously by experiments or evaluations.

It is necessary that the number of resonances for the summation over λ in Eqs. (2.2-36)~(2.3-39) are taken sufficiently large for the accurate calculation of the cross sections. As the

TABLE 5.5-1 Energy boundaries and mesh used to tabulate cross sections

Mesh (eV)	Upper energy (eV)	Lower energy (eV)	No. of mesh points
↑	21500.0	20240.0	2320
	20240.0	18960.0	2560
	18960.0	17680.0	2560
	17680.0	16400.0	2560
0.5	16400.0	15120.0	2560
	15120.0	13840.0	2560
	13840.0	12560.0	2560
	12560.0	11280.0	2560
↓	11280.0	10000.0	2560
↑	10000.0	9770.0	921
	9770.0	9130.0	2560
	9130.0	8490.0	2560
	8480.0	7850.0	2560
0.25	7850.0	7210.0	2560
	7210.0	6570.0	2560
	6570.0	5930.0	2560
	5930.0	5290.0	2560
↓	5290.0	4650.0	2560
↑	4650.0	4390.0	2080
	4390.0	4070.0	2560
	4070.0	3750.0	2560
0.125	3750.0	3430.0	2560
	3430.0	3110.0	2560
	3110.0	2790.0	2560
	2790.0	2470.0	2560
↓	2470.0	2150.0	2560
↑	2150.0	2120.0	480
	2120.0	1960.0	2560
	1960.0	1800.0	2560
0.0625	1800.0	1640.0	2560
	1640.0	1480.0	2560
	1480.0	1320.0	2560
	1320.0	1160.0	2560
↓	1160.0	1000.0	2560
↑	1000.0	920.0	2560
	920.0	840.0	2560
	840.0	760.0	2560
0.03125	760.0	680.0	2560
	680.0	600.0	2560
	600.0	520.0	2560
	520.0	440.0	2560
↓	440.0	460.0	2560
↑	476.0	436.0	2560
	436.0	396.0	2560
	396.0	356.0	2560
	356.0	316.0	2560
	316.0	276.0	2560
0.015625	276.0	236.0	2560
	236.0	196.0	2560
	196.0	156.0	2560
	156.0	116.0	2560
	116.0	76.0	2560
↓	76.0	36.0	2560
↑ 0.01 ↓	54.8	29.2	2560
	59.2	3.6	2560
↑ 0.002 ↓	10.0	5.0	2500
	5.0	0.1	2450

computing time for these calculations are mainly governed by the frequency of the calculation of Doppler broadened function $F(\omega)$, it is impossible and wasteful, generally, to take a very large number of resonances into account. Therefore, the determination of this number of resonances, λ, for each absorber nucleus is the most important in the tabulation of cross section. In this determination of λ, we should note that the number λ depends on the level spacing, the effect of Doppler broadening and interference scattering, which vary with each absorber nucleus. For example, the interference scattering of fertile material ^{238}U is very large, so that the tails of a resonance affect the cross sections far from the resonance level. Considering these resonance characteristics, investigations were made for the number λ for which the curves of cross sections are sufficiently continuous and also energy average cross sections take satisfactorily same values for various temperatures. The final results for ^{235}U, ^{238}U, ^{239}Pu and ^{240}Pu are shown in TABLE 5.5-2. In Fig. 5.5-1, the variations in the cross section curves of ^{235}U caused by the number λ is shown for the temperature of 300°K. This figures shows that the cross section curves are sufficiently continuous for $\lambda=16$. Fig. 5.5-2 shows the variation of the energy average cross section in the same energy interval as Fig. 5.5-1. From Figs. 5.5-1 and 5.5-2 we can expect that the

TABLE 5.5-2 The number of resonances in the summations: λ
(l is the orbital angular momentum of the incident neutron)

Absorber / T (°K)	^{235}U		^{238}U		^{239}Pu		^{240}Pu	
	$l=0$	$l=1$	$l=0$	$l=1$	$l=0$	$l=1$	$l=0$	$l=1$
300	16	6	9	10	10	14	9	10
900	26	6	9	11	10	14	9	11
2100	36	8	10	12	12	16	10	12

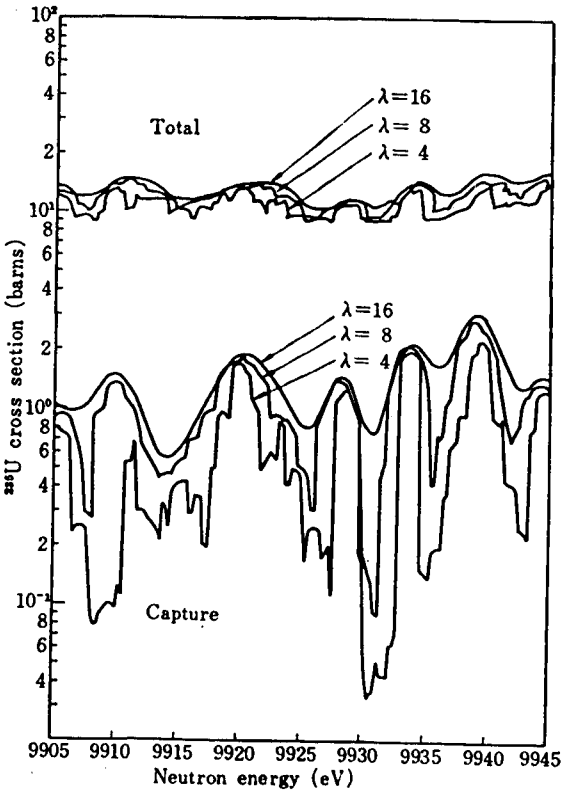

Fig. 5.5-1 Effect of the number of resonance in the summations of λ: $T=300°K$.

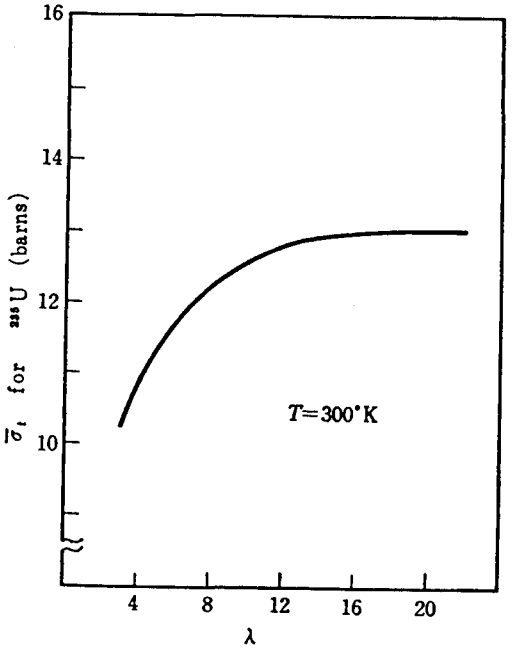

Fig. 5.5-2 Variation in simple average total cross sections for λ values.

^{235}U cross sections are obtained in the good accuracy for 300°K by using $\lambda=16$. When temperature rises from 300°K to 900°K and to 2100°K, the tails of resonance are broadened by Doppler effect and, as shown in **Fig. 5. 5-3**, the cross section curves obtained by using $\lambda=16$ become unsatisfactory. Also this tendency is obvious from **TABLE 5. 5-3** which shows the comparison of the energy average of cross sections of **Fig. 5. 5-3** for 300°K, 900°K and 2100°K. The level spacing of ^{235}U is narrower than other nuclei as shown in **TABLE 4. 3-1**. Therefore the effect of Doppler broadened tails is very large and we have to take a sufficiently large number of λ with increasing temperatures.

The above problems caused mainly by the narrower level spacing is less important for ^{238}U, ^{239}Pu and ^{240}Pu, but important is the problem related to the large interference between potential and resonance secattering of ^{238}U and ^{240}Pu. **Fig. 5. 5-4** shows the total cross section curve of ^{238}U for $\lambda=6$ and $\lambda=9$ near 1 keV. In the case of $\lambda=6$, the two discontinuous points appear near 983. 5 eV and 948. 5 eV. The λ nearest resonance levels are taken, not necessarily $\lambda/2$ on either side of an energy E, into account in the practical computer code. Therefore, the discontinous point near 983. 5 eV shows that the positive effect of interference scattering for the 936. 9 eV resonance level is neglected, and in the vicinity of 948. 5 eV the negative interference effect of the 991. 8 eV level seems to be neglected. The interference scattering of the 991. 8 eV resonance affects the cross sections over wider energy interval of about 80 eV. When $\lambda=9$, these discontinuities do not appear and the curve becomes continuous. **TABLE 5. 5-4** shows the comparison of the effective cross sections of ^{238}U for $\lambda=6$ and $\lambda=9$ from 1 keV to 773 eV obtained by ERSE

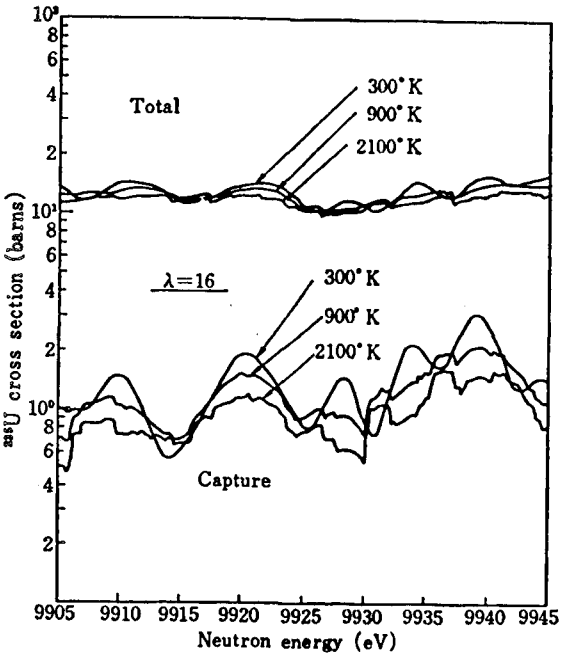

Fig. 5. 5-3 Effect of Doppler broadened resonace tails.

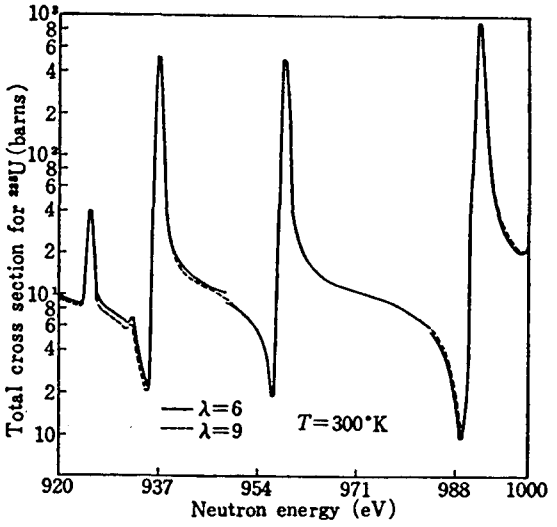

Fig. 5. 5-4 Effect of interference scattering cross sections.

TABLE 5. 5-3 Effect of Doppler broadened resonance tails for ^{235}U: $\lambda=16$

$\bar{\sigma}_x$(b) \ T (°K)	300	900	2100
$\bar{\sigma}_t$	12. 96	12. 60	11. 88
$\bar{\sigma}_c$	1. 18	1. 05	0. 84
$\bar{\sigma}_f$	2. 40	2. 22	1. 84

TABLE 5. 5-4 Interference scattering cross section and λ value for ^{238}U: $T=300$°K

λ \ $\bar{\sigma}_x$	$\bar{\sigma}_n$	$\bar{\sigma}_c$
6	14. 07	1. 075
9	13. 94	1. 075

TABLE 5.5-5 Energy dependence of potential scattering cross sections for $T=300°K$

Absorber	Atomic radius $\times 10^{12}$cm	$4\pi R^2$ (b)	$4\pi R^2 f(v\sqrt{\alpha})$(b)				
			0.1 eV	1.0 eV	10 eV	10^2 eV	10^3 eV
^{235}U	8.3300	8.7196	8.7212	8.7202	8.7198	8.7196	8.7196
^{238}U	9.2000	10.6362	10.6380	10.6368	10.6364	10.6362	10.6362
^{239}Pu	8.3008	8.8200	8.8216	8.8205	8.8202	8.8201	8.8200
^{240}Pu	9.2000	10.6362	10.6380	10.6368	10.6364	10.6362	10.6362

code[80], which calculates numerically the neutron spectrum and the effective cross sections. It is seen from TABLE 5.5-4 and Fig. 5.5-4 that the interference scattering of ^{238}U is important also for the calculation of the effective cross sections.

The energy dependence in the potential scattering cross sections is shown in TABLE 5.5-5, which shows that the energy variation in the potential scattering cross section is very small and can be neglected. We therefore may use the usual approximate expression for potential secattering cross section $\sigma_p=4\pi R^2$.

Figs. 5.5-5~5.5-8 show some portion of the cross section curves for ^{235}U, ^{238}U and ^{239}Pu that were obtained by a code MCROSS[79] under the same conditions as in TABLE 5.5-1 and 5.5-2. From these figures, the reasonable temperature variations for cross sections will be expected.

Interesting will be magnitude of the fluctuation of the tatal cross section in some typical energy region, because magnitude of this fluctuation determine the adequacy of applicability of analytical methods such as Method A and B[77] for the calculation of the effective cross section in resonance region. For example, Fig. 5.5-7 shows that the fluctuation of the total cross section

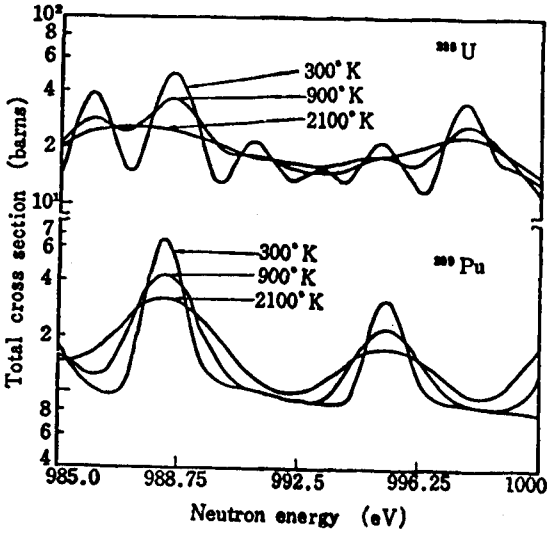

Fig. 5.5-5 Temperature variation in the cross section reproduced by the code MCROSS.

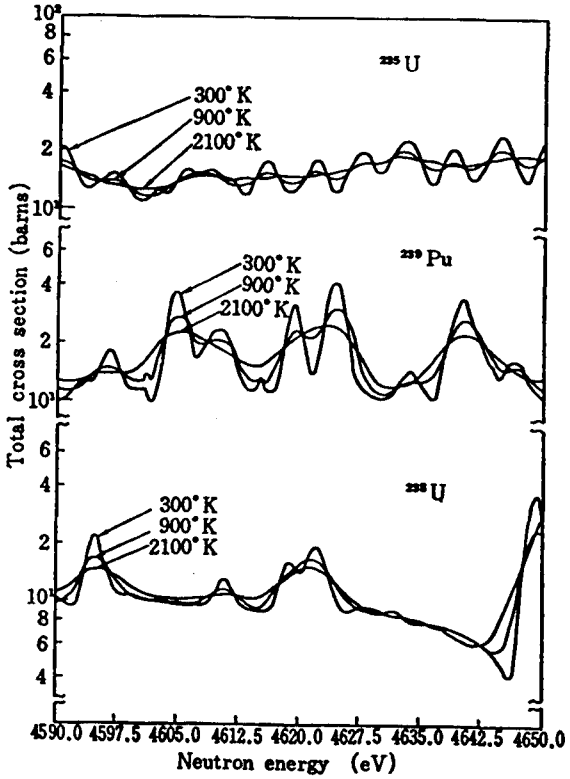

Fig. 5.5-6 Temperature variation in the cross section reproduced by the code MCROSS.

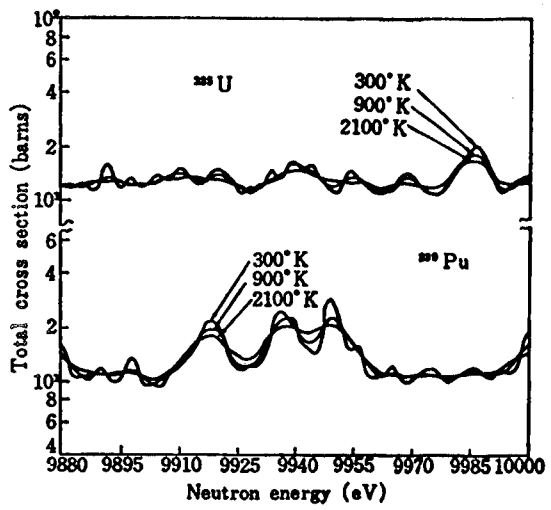

Fig. 5.5-7 Temperature variation in the cross section reproduced by the code MCROSS.

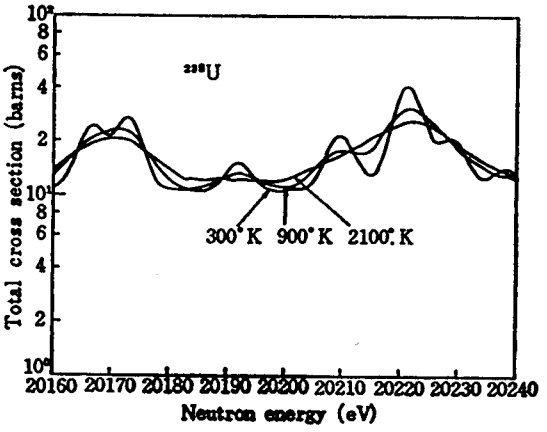

Fig. 5.5-8 Temperature variation in the cross section reproduced by the code MCROSS.

of ^{235}U is not so large in the neighborhood of 10 keV, that is, the following equation assumed for Method A

$$\frac{\sigma_t - \langle\sigma_t\rangle}{\langle\sigma_t\rangle} \ll 1 \qquad (5.5\text{-}1)$$

is sufficiently satisfied, and this is also true in Fig. 5.5-6 except for the case of 300°K. On the other hand, we can see from Fig. 5.5-8 that Eq. (5.5-1) is not satisfied for ^{238}U even at higher energies of 20 keV. In order to examine, in detail, the adequacy of the analytical treatments of

TABLE 5.5-6 $\int_{E_1}^{E_2}\sigma_t(E)dE$ for ^{235}U

E_1 (eV)	E_2 (eV)	Petrel (50)	Bowman (82)	Brooks (87)	ORNL (51)	Wang (52)	Michaudon (53)	JAERI
1.3	1.8		8.16	7.85	8.29		8.87	7.73
1.8	4.5		43.28	42.66	46.53		46.51	46.60
4.5	5.0		3.87	3.55	4.09		3.80	3.03
5.0	10.0		292.1	257.0	281.7		275.0	283.95
10.0	15.0		220.0	197.5	216.5		213.0	213.85
15.0	20.5		332.6	278.85	315.8		287.0	312.4
20.5	33.0	416± 4	457.7	417.5	447.0		427.2	472.25
33.0	41.0	466± 9	517.5	415.2	496.3		445.3	463.30
41.0	60.0	924± 12	968.6	834.1	916.9		841.3	933.85
60.0	73.0	318± 9	302.6	245.7	301.8		299.5	282.10
73.0	100.0	681± 8		580.5	665.8		632.0	538.40
100	113	227± 4		185.9	216.6		228.2	168.35
113	200	1931± 14		1600.8	1877.2		1809.3	1747.30
200	300	2175± 34			2081.8	1980	2052.5	1532.00
300	1000	8155± 65			8124.8	7975	8122.4	8261.2
1000	2000	7660±110			7566	7546	7545	7451.0
2000	3000	5460±110			5674	5560	5761	5751.0
3000	4000	4680±110			5167	4880	4887	4426.0
4000	5000	4010±110			4656	4470	4502	3868.0
5000	10000	15920±280			17700	17460	18537	15730.0
20.5	10000	53023			55890.9		56089.1	52482.31

resonance absorptions proposed for the calculation of the Doppler coefficient of reactivity in fast reactor, we compared the results obtained from the analytical methods with those from an exact numerical method in addition to above examinations of the total cross section. The results will be published in another paper[81].

Shown in TABLE 5.5-6 is the integrated fission cross sections for ^{235}U over some energy intervals. It will be seen from this TABLE that present result (JAERI) is in quite good agreement with Petrel data[50] for the total fission cross sections from 10 keV to 20.5 eV. TABLES 5.5-7 and 5.5-8 show the comparison of the present results for the capture and fission resonance integrals with those which were computed from recommended or published cross section data. The experimental data by FEINER and ESCH[88] gave for total fission resonance integral, the total capture resonance integral and the capture-to-fission ratio α_{RI} 280 ± 11 b, 140 ± 8 b and 0.50 ± 0.02, respectively ($E<0.5$ eV). Now, assume the following partial resonance integrals[89];

$RI_f=9.4$ b, $RI_c=1.46$ b for $0.45\text{ eV}\leqq E\leqq 0.5$

and $RI_f=10.74$ b, $RI_c=2.68$ b for $10\text{ keV}\leqq E\leqq\infty$

then, the resonance integrals of Hanna, Walker and JAERI are in resonable agreement with Feiner and Esch's results. As for the values of α_{RI} evaluated values seem to be fairly higher,

TABLE 5.5-7 Fission resonance integrals for ^{235}U

Energy range (eV)	BNL 325 (39)	General Atomic (84)	HANNA-WALKER (85)	Karlsurhe (86)	Winfrith (87)	JAERI
0.45—1.8	77.06	77.06	78.0	77.07	76.40	75.03
1.8—1	16.46	16.46	18.1	16.57	17.00	16.47
5—10	35.24	35.24	30.9	35.86	32.50	34.53
10—20.5	31.00	30.84	30.3	32.53	25.30	33.90
20.5—41	29.22	26.94	29.2	28.92	24.10	31.42
41—60	16.50	14.49	15.5	16.47	6.8	18.24
60—100	12.06	9.75	11.7	11.85	11.3	10.46
100—300		22.59	21.9	22.59	22.1	19.06
300—1000		14.86	12.8	14.86	14.1	13.68
1000—3000		7.67	6.8	7.67	7.6	7.64
3000—10000		5.02	5.0	5.02	4.9	4.35
0.45—10000		260.92	260.2	269.41	242.1	264.78

TABLE 5.5-8 Capture resonance integrals for ^{235}U

Energy range (eV)	Karlsruhe (87)	HANNA-WALKER (86)	Winfrith (88)	JAERI
0.45—1.8	15.12	15.0	13.6	14.48
1.8—5	12.73	13.3	14.1	12.54
5—10	24.03	31.4	27.3	25.57
10—20.5	39.88	34.6	28.0	30.88
20.5—41	34.26	14.8	33.0	20.82
41—60	13.61	5.5	6.9	9.12
60—100	6.35	3.1	7.6	9.20
100—300	11.45	10.4	10.2	12.70
300—1000	7.13	6.4	6.3	7.36
1000—3000	3.45	3.1	3.5	3.35
3000—10000	2.12	2.0	2.1	1.97
0.45—10000	170.13	139.60	152.6	147.99

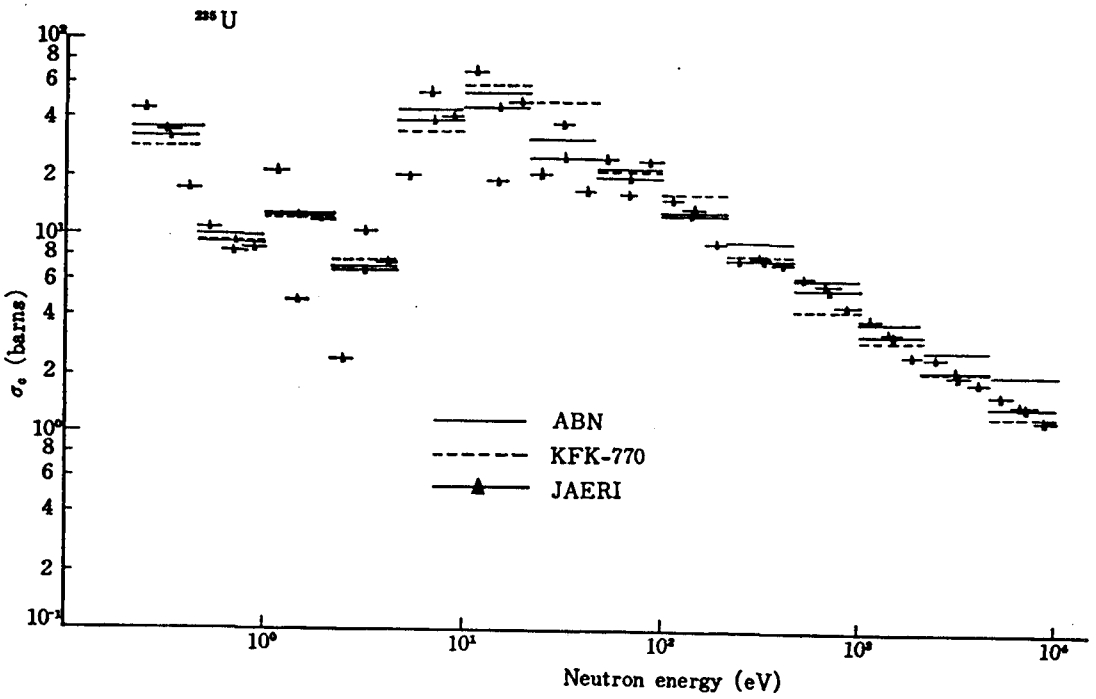

Fig. 5.5-9 Comparison of cross section for infinite dilution.

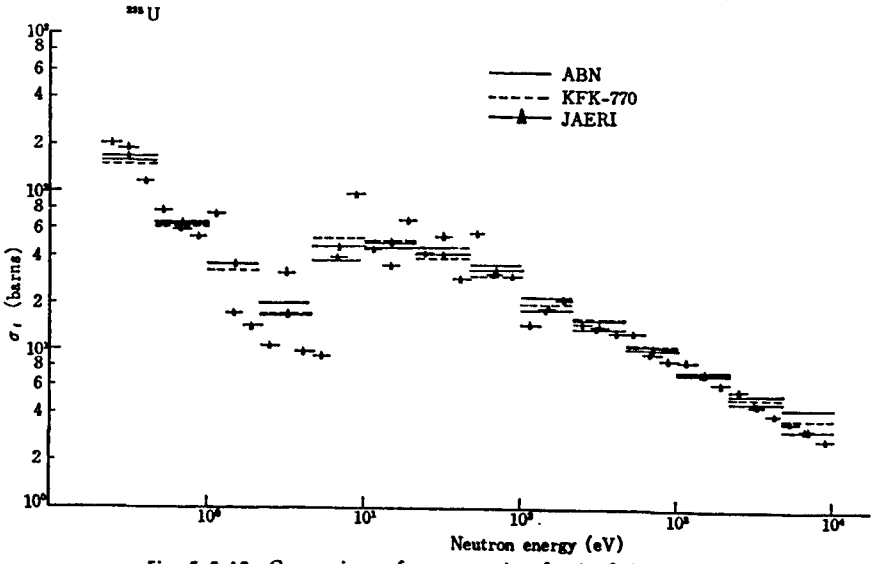

Fig. 5.5-10 Comparison of cross section for in finite dilution.

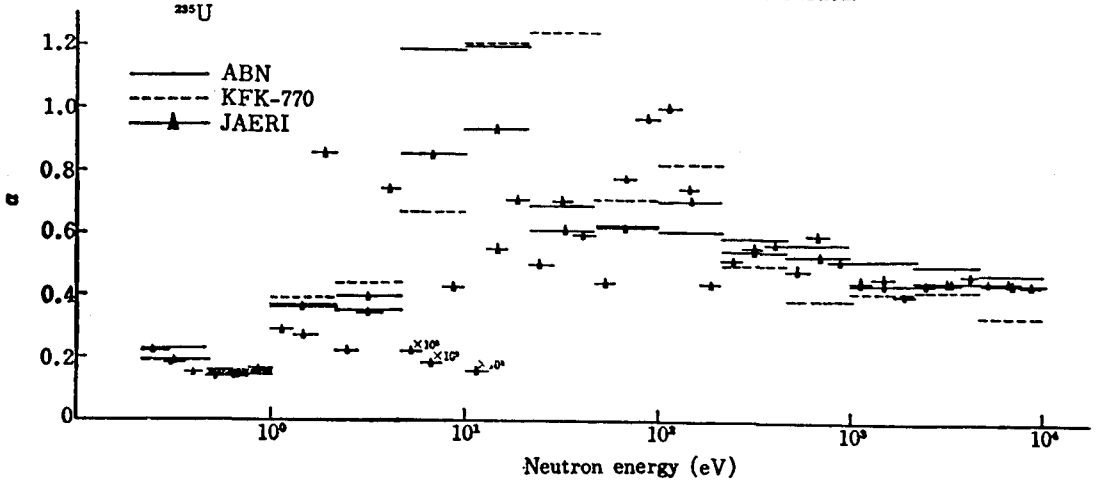

Fig. 5.5-11 Comparison of ^{235}U α-values.

TABLE 5. 5-9 $\int_{E_1}^{E_2}\sigma_f dE \Big/ \int_{E_1}^{E_2} dE$ for ^{239}Pu

E_1 (eV)	E_2 (eV)	Petrel (50)	JAERI
20. 0	30. 0	42. 2	37. 9
30. 0	40. 0	2. 16	2. 84
40. 0	24. 0	25. 9	25. 3
54. 0	70. 0	72. 2	99. 0
70. 0	92. 0	57. 9	86. 6
92. 0	112. 0	18. 6	19. 6
112. 0	140. 0	22. 2	14. 9
140	173	14. 8	16. 6
173	210	20. 9	23. 3
210	300	17. 2	20. 7
300	500	8. 75	12. 7
500	1000	7. 29	8. 37
1000	2000	3. 82	4. 52
2000	3000	2. 64	3. 06
3000	4000	2. 75	2. 96
4000	5000	2. 31	2. 51
5000	6000	2. 71	2. 62
6000	8000	2. 21	2. 22
8000	10000	2. 30	2. 18
20. 0	10000	3. 58	3. 96

TABLE 5. 5-10 Capture resonance integrals for ^{239}Pu

Energy range (eV)	Karlsruhe (86)	JAERI
4. 65—10	22. 90	21. 71
10—21. 5	53. 40	50. 32
21. 5—46. 5	23. 80	31. 70
46. 5—100	40. 40	26. 68
100—215	10. 40	10. 49
215—465	6. 92	7. 87
465—1000	3. 78	5. 29
1000—2150	1. 84	2. 89
2150—4650	1. 36	2. 02
4650—10000	0. 92	1. 18
4. 65—10000	165. 72	160. 15

TABLE 5. 5-11 Fission resonance integrals for ^{239}Pu

Energy range (eV)	Karlsruhe (86)	BNL 325 (40)	LASL (90)	JAERI
4. 65—10	26. 9	22. 3		27. 36
10—21. 5	76. 4	81. 7		79. 91
21. 5—46. 5	16. 5	19. 8	20. 9	19. 40
46. 5—100	40. 8	31. 8	42. 1	55. 97
100—215	14. 1	14. 8	13. 9	14. 02
215—465	10. 0	10. 0	9. 66	11. 48
465—1000	5. 8	6. 0	5. 94	6. 77
1000—2150	3. 11	3. 5	2. 90	3. 39
2150—4650	2. 51	2. 22	2. 04	2. 28
4650—10000	1. 88	1. 83	1. 76	1. 78
4. 65—10000	198. 0	193. 95		222. 36

that is, Winfrith[83] = 0. 597, Karlsruhe[86] = 0. 601, HANNA-WALKER[85] = 0. 513 and JAERI = 0. 534. **Figs. 5. 5-9～5. 5-11** show the comparisons of capture and fission cross sections and α-values for ^{235}U. The values of α are lower than that of ABBN[3] in keV regions.

In TABLE 5. 5-9, our fission cross section of ^{239}Pu are compared with that of Petrel experimental data. In TABLES 5. 5-10 and 11, the capture and fission resonance integrals are given. Resonance integral data are usually available only fission, and the capture cross section can not always be measured directly, but estimated from the total, elastic cross sections and the values of α or η and ν measurements. Therefore, in general, the capture cross section have very large uncertainties. FEINER and ESCH'S[88] evaluation gave $RI_f = 310 \pm 20$ b for $E > 0.5$ eV. Now, if we assume 89. 7 b for 0. 5—4. 65 eV and 9 b for $E > 10$ keV[89], total fission resonance integral give

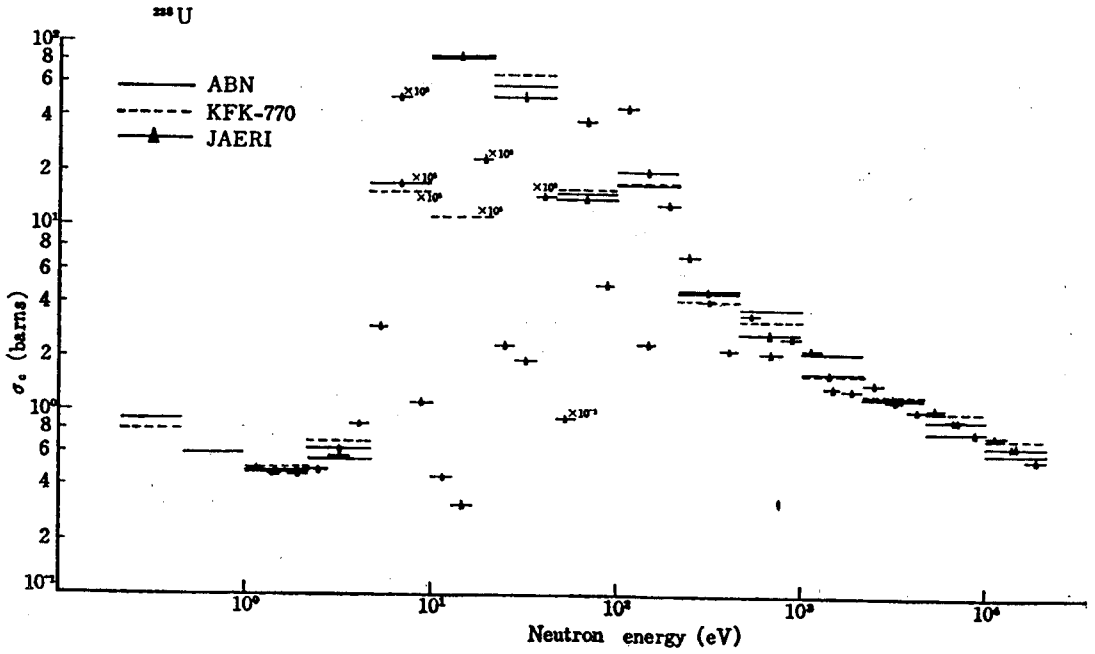

Fig. 5.5-12 Comparison of cross section for inifinite dilution.

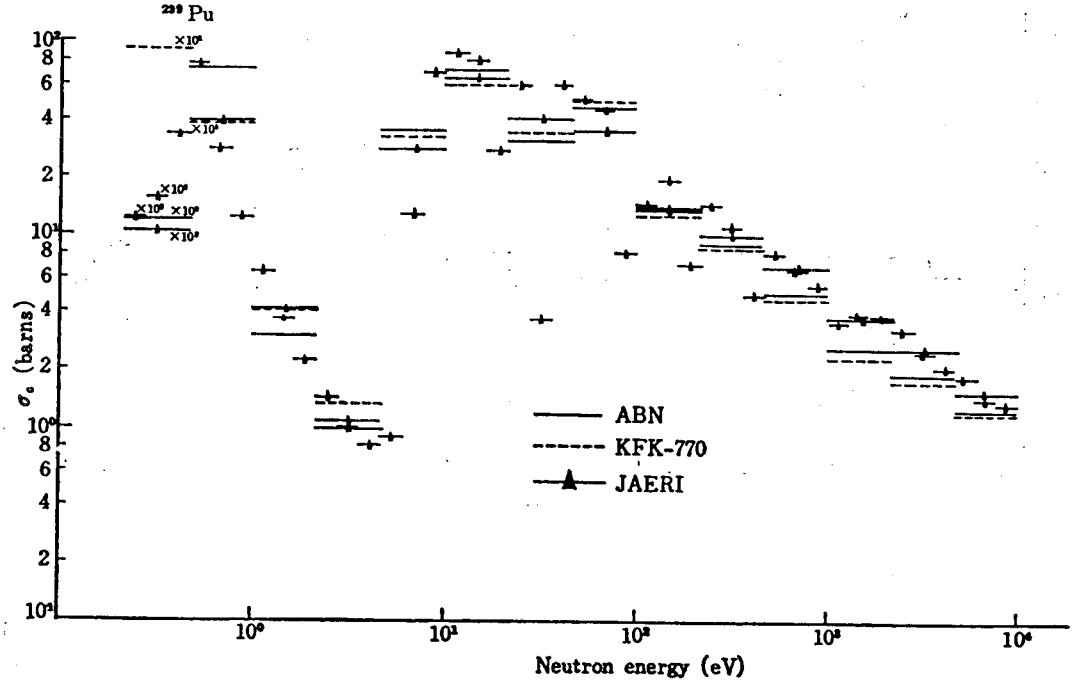

Fig. 5.5-13 Comparison of cross section for infinite dilution.

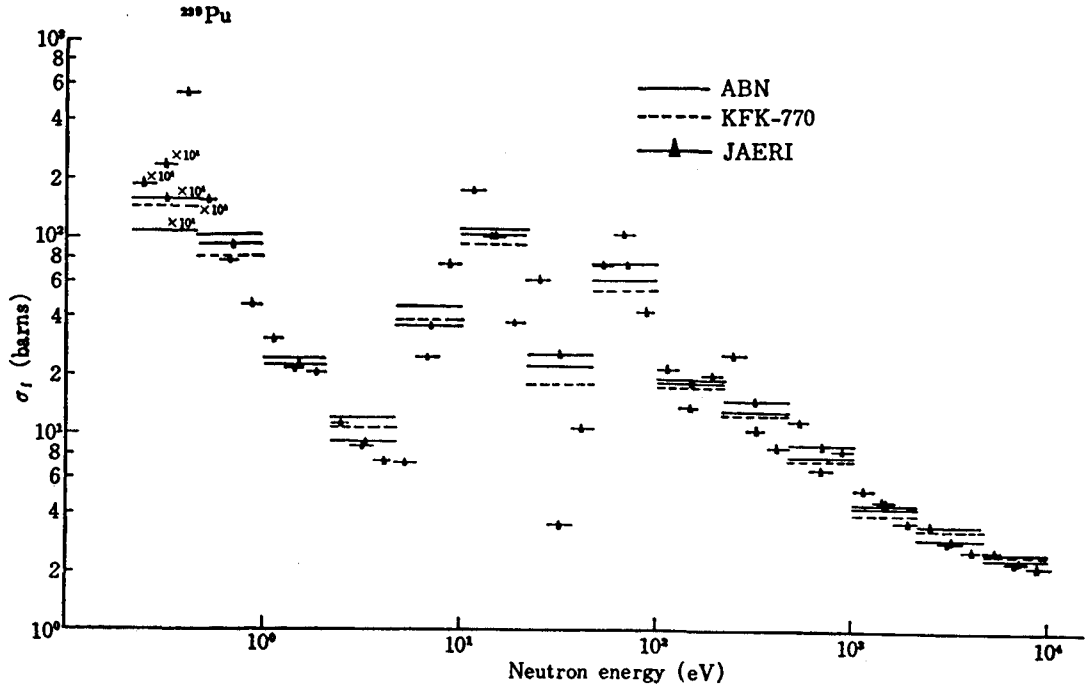

Fig. 5.5-14 Comparison of cross section for infinite dilution.

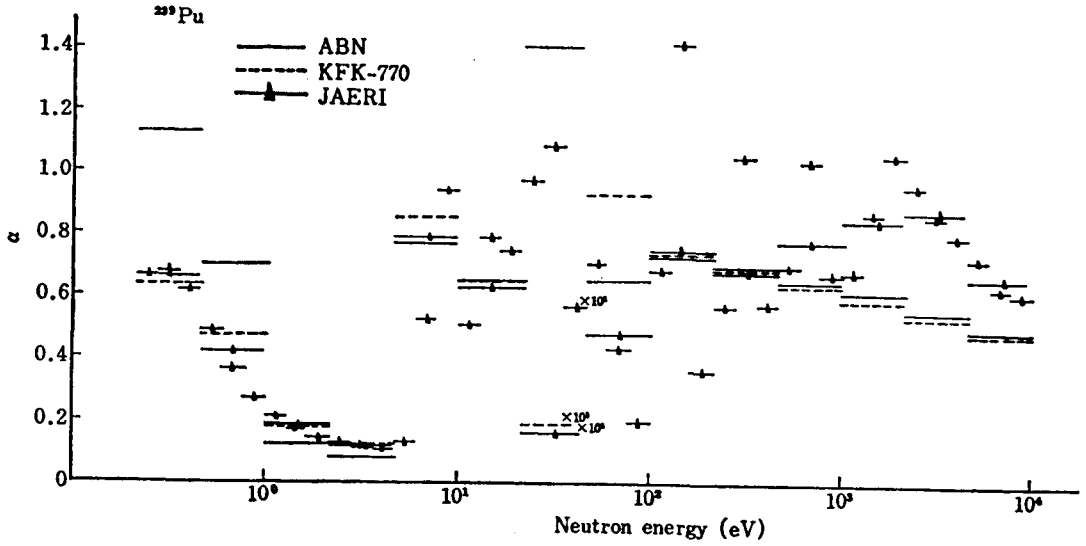

Fig. 5.5-15 Comparison of ^{239}Pu α-values.

Karlsruhe[86] = 296.7 b, BNL 325[40] = 292.65 b and JAERI = 321.06 b. As seen from TABLE 5.5-10, the capture resonance integrals of JAERI are larger in high energy regions than those of Karlsruhe. This fact may also be seen from Figs. 5.5-13, 14 and 15 which show comparison of the capture and fission cross sections and the values of α for ^{239}Pu, respectively. The present result shows obviously higher α value than that of ABBN[3] and KFK-770[78]. As mentioned in the previous chapter, our cross sections were constructed after deep consideration of the values given by GWIN *et al.*[61] and Fig. 5.5-15 reflects well this consideration in the keV region.

Fig. 5.5-12 shows the comparison of capture cross sections for ^{238}U. Fig. 5.5-16 compares the present results of the capture cross sections for ^{240}Pu with those of ABBN.

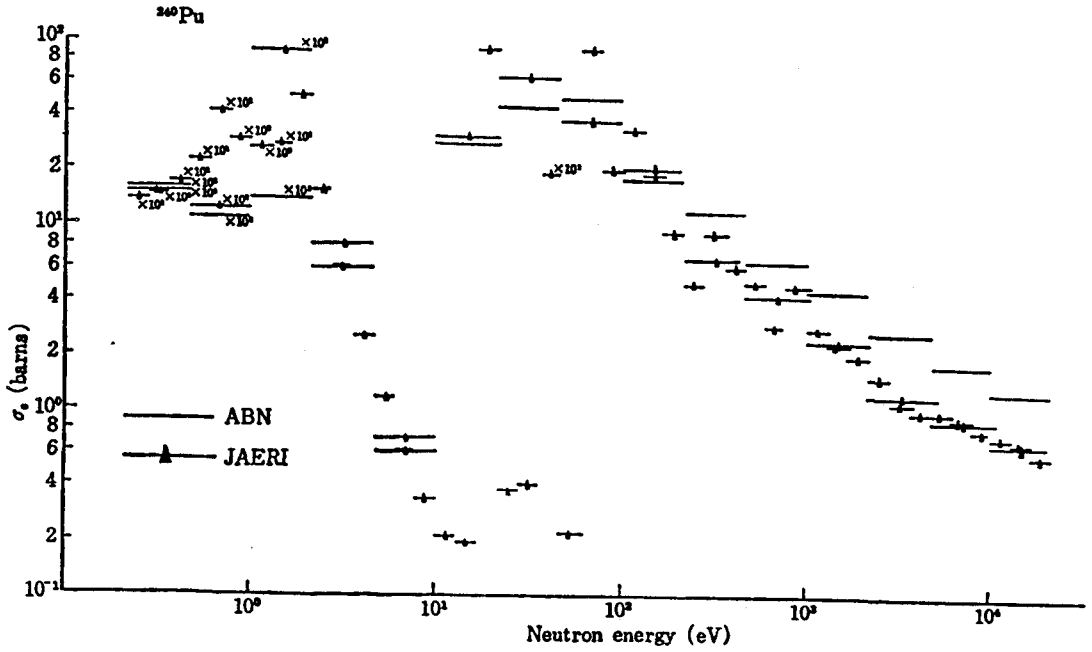

Fig. 5.5-16 Comparison of cross section for infinite dilution.

6. Method of Calculating Group Constants in Homogeneous Systems

In the previous chapters, discussions have been made on the calculating method of the microscopic resonance cross-sections and also on the various quantities needed for these calculations. Over the whole energy range of our interest, a sequence of resonances was prepared for each resonance nuclide using a statistical method. And resonance cross sections were calculated for three temperatures of 300, 900 and 2100°K for each nuclide with a suitable selection of energy mesh. Here, we will describe treatments for various group constants needed for such calculations as criticality of reactor, the Doppler coefficient of reactivity, breeding ratio, the sodium void effect, etc. The treatment here, however, will be restricted to the homogeneous system, and it is assumed that heterogeneities can be handled adequately by the equivalence relations[77].

6.1 Selection of Group Structure

Rigorously speaking, there is no set of group constant for general use, since the group effective cross sections should be obtained from averaging microscopic cross sections with weight of neutron spectrum in a reactor which depends on compositions and geometries. The group width therefore should be made as narrow as possible in order to reduce the dependence of effective group cross sections on reactor compositions and geometries, etc. The consumption of much computation time in a reactor analysis with huge number of groups is one of the drawbacks due to such group constants, from economical viewpoint. The selection of narrower group width, however, is not always the best way unless the neutron spectrum and nuclear data used are highly accurate. Hence usually appropriate devices are provided for a set of group constants and tables of constants to be used in these devices are included in the set. Devices should be represented as simply and adequately as possible.

Some criteria have been settled for selecting the group structures in such sets of group constants as the ABBN[3]. One is that the deviation in group effective cross sections due to assumed gross neutron spectra (for example, $1/(E\ \sigma_t\ (E))$ or fission spectrum) should not exceed the experimental errors of cross section used, and other various circumstances such as the maximum energy loss by a collision, threshold reaction, etc. should also be taken into consideration. Usually, the group structures with widths of about 0.7 lethargy and about 25 groups have often been used for the purpose of fast reactor analysis. There remains a doubt that these group structures are good enough for general use.

In the published set[3] of multi-group constants, only the energy dependence of the cross sections of the nuclide in question has been taken into account for preparing effective cross sections, and all other cross sections are assumed constant through out the energy interval envisaged. On the other hand, it has been known that the scattering resonance of sodium at 2.85 keV influences significantly on both the sodium void effect and the Doppler reactivity effect in a sodium cooled reactor[4),5]. That is, the interference effects between resonances of sodium and of heavy nuclide are fairly important. Hence, the group widths should be made so narrow that effective cross sections of heavy nuclide reproduce properly the interference effects even if cross sections of all other nuclide are assumed constant within each group. In addition to the energy variation of flux due to the sodium resonance, for the calculation, of the sodium void effect, the energy variation of adjoint flux near the sodium resonance which is governed largely

by that of the alpha of ^{239}Pu is quite important, thereby, again, the narrower group width is desirable in order to reflect the energy dependence of the alpha of ^{239}Pu. The group widths of the published set, however, seem to be too wide to take these facts into account. Moreover, it was found out that there were some essential defects in the treatment of removal cross sections by the ABBN set which is most important quantity for the calculation of the sodium void effect[91]. In order to avoid these defects, several computer codes have been prepared, such as ELMOE[92], ESELEM[93] and MC^2 [10]. The calculation of accurate removal cross sections of light element is one problem remained to be solved on the standpoint of reactor analysis using a set of group constants.

If discussions are limited to the group constants of heavy nuclide, the interference effects between resonances of sodium and heavy isotopes can be estimated fairly accurately by dividing each resonance energy group of the ABBN set into few more groups, since the resonance shape of sodium is represneted fairly in detail by this structure. By this division, the fluctuating energy dependence of the alpha of ^{239}Pu can also be taken into account to some extent. Hence, at least for the heavy isotopes, the effective cross sections in the resonance energy region will be treated by the concept of group constants with a group structure having more groups than the sets prepared previously.

The effective cross sections of ^{238}U were studied for the following three cases in the energy region from 4 to 2.15 keV (with lethargy width of 0.6), where most part of the sodium resonance is covered.

(1) Scattering resonance cross section of sodium, σ_m, is assumed constant throughout the group width.

(2) The energy width is divided into three equal lethargy intervals where σ_m is assumed constant, respecitvely.

(3) The resonance cross section σ_m is given by ultra fine group meshes[80].

The calculation results are shown in TABLE 6.1-1 where "EXACT" corresponds to the case (3), This table shows that the interference effect of sodium resonance on the effective cross sections of heavy nuclide can be treated satisfactorily by the division of the ABBN group width into three equal lethargy widths.

In conclusion we adopted new group structure with lethargy widths of about one third of the ABBN set. This group structure has a similar one to the GAM type library which is shown in TABLE 6.1-2.

TABLE 6.1-1 Capture and elastic scattering cross sections of ^{238}U in the compositions including sodium:
Ratio of atomic density ^{238}U : Na : O = 1 : 2 : 2, Temperature 300°K, resonance cross sections of Na was taken from SCHMIDT's data[40].

Energy (lethargy)	No. of groups	σ_m of sodium (b)	σ_a (b)	σ_s (b)
4 ~ 2.15 keV (0.6)	1	28.65	0.712	13.51
	3	40.37 166.30 10.77	0.679	13.15
	EXACT		0.675	13.08
2.15 ~ 1.0keV (0.77)	1	4.23	0.614	11.67
	EXACT		0.612	11.36

TABLE 6. 1-2 Group structure

ABBN group No.	ΔU	Fine group No.	Δu	Lower energy	Upper energy
1	0. 48	1	0. 24	8. 3	10. 5 (MeV)
		2	0. 24	6. 5	8. 3 (MeV)
2	0. 48	3	0. 24	5. 1	6. 5 (MeV)
		4	0. 24	4. 0	5. 1 (MeV)
3	0. 48	5	0. 24	3. 1	4. 0 (MeV)
		6	0. 24	2. 5	3. 1 (MeV)
4	0. 57	7	0. 285	1. 9	2. 5 (MeV)
		8	0. 285	1. 4	1. 9 (MeV)
5	0. 57	9	0. 285	1. 1	1. 4 (MeV)
		10	0. 285	0. 8	1. 1 (MeV)
6	0. 69	11	0. 23	0. 63	0. 8 (MeV)
		12	0. 23	0. 50	0. 63 (MeV)
		13	0. 23	0. 4	0. 50 (MeV)
7	0. 69	14	0. 23	0. 31	0. 4 (MeV)
		15	0. 23	0. 25	0. 31 (MeV)
		16	0. 23	0. 2	0. 25 (MeV)
8	0. 69	17	0. 23	0. 15	0. 2 (MeV)
		18	0. 23	0. 12	0. 15 (MeV)
		19	0. 23	0. 1	0. 12 (MeV)
9	0. 776	20	0. 257	77. 3	100 (KeV)
		21	0. 257	59. 8	77. 3 (KeV)
		22	0. 252	46. 5	59. 8 (KeV)
10	0. 771	23	0. 256	36. 0	46. 5 (KeV)
		24	0. 258	27. 8	36. 0 (KeV)
		25	0. 257	21. 5	27. 8 (KeV)
11	0. 761	26	0. 254	16. 6	21. 5 (KeV)
		27	0. 252	12. 9	16. 6 (KeV)
		28	0. 255	10. 0	12. 9 (KeV)
12	0. 766	29	0. 257	7. 73	10. 0 (KeV)
		30	0. 257	5. 98	7. 73 (KeV)
		31	0. 252	4. 65	5. 98 (KeV)
13	0. 771	32	0. 256	3. 60	4. 65 (KeV)
		33	0. 258	2. 78	3. 60 (KeV)
		34	0. 257	2. 15	2. 78 (KeV)
14	0. 765	35	0. 259	1. 66	2. 15 (KeV)
		36	0. 252	1. 29	1. 66 (KeV)
		37	0. 255	1. 0	1. 29 (KeV)
15	0. 766	38	0. 257	773	1000 (eV)
		39	0. 257	598	773 (eV)
		40	0. 252	465	598 (eV)
16	0. 771	41	0. 256	360	465 (eV)
		42	0. 258	278	360 〃
		43	0. 257	215	278 〃
17	0. 765	44	0. 259	166	215 〃
		45	0. 252	129	166 〃
		46	0. 255	100	129 〃
18	0. 766	47	0. 257	77. 3	100 〃
		48	0. 257	59. 8	77. 3 〃
		49	0. 252	46. 5	59. 8 〃
19	0. 771	50	0. 256	36. 0	46. 5 〃
		51	0. 258	27. 8	36. 0 〃
		52	0. 257	21. 5	27. 8 〃
20	0. 765	53	0. 259	16. 6	21. 5 〃
		54	0. 252	12. 9	16. 6 〃
		55	0. 255	10. 0	12. 9 〃
21	0. 776	56	0. 257	7. 73	10. 0 〃
		57	0. 257	5. 98	7. 73 〃
		58	0. 252	4. 65	5. 98 〃
22	0. 771	59	0. 256	3. 60	4. 65 〃
		60	0. 258	2. 78	3. 60 〃
		61	0. 257	2. 15	2. 78 〃

TABLE 6. 1-2 (continued)

ABBN group No.	ΔU	fine group No.	Δu	lower energy	upper energy
23	0. 765	62	0. 259	1. 66	2. 15 〃
		63	0. 252	1. 29	1. 66 〃
		64	0. 255	1. 0	1. 29 〃
24	0. 766	65	0. 257	0. 773	1. 0 〃
		66	0. 257	0. 598	0. 773 〃
		67	0. 252	0. 465	0. 598 〃
25	0. 771	68	0, 256	0. 360	0. 465 〃
		69	0. 258	0. 278	0. 360 〃
		70	0. 257	0. 215	0. 278 〃

6. 2 On the Accuracy of Conventional Analytical Methods

The effective cross sections can be accurately obtained by solving numerically neutron solwing down equation if the resonances are resolved experimentally. However, the numerical method spend much computing time than conventional analytical methods[77]. In particular, we will be aware of waste of time and money in calculating effective cross sections for a large number of similar compositions. Then, we are inclined to use the conventional analytical method, if it does not introduces errors, because of its simplicity. For example, the well-known group constant set ABBN[3] was produced with this method. On the other hand, another reason why they use the conventional analytical method is that the experimentally resolved resonance region is very narrow compared to important Doppler resonance region for a large fast reactor. But by the statistical method mentioned in the chapter 5, the individual resonance parameters for unresolved region have been already generated successfully and microscopic cross sections have been tabulated by using these parameters. Therefore, the accurate effective cross sections can be easily calculated by using the computer code[80]. (This is mentioned in next section.). However, before adopting this procedure the errors introduced by conventional approximation should be investigated and estimated.

The effective cross section is defined by

$$\tilde{\sigma}_x=\frac{\int_{\Delta E}\sigma_x(E)\phi(E)dE}{\int_{\Delta E}\phi(E)dE} \quad . \tag{6. 2-1}$$

In order to investigate the error introduced by the analytical methods, the effective cross sections have been accurately calculated by using the code ERSE[80]. Then, the fluctuation of collision density may be seen. For example, Fig. 6. 2-1 shows the collision density of ^{238}U in the energy range from 1. 0 keV to 800 eV. This shows certainly that the assumption of constancy of collision density is not satisfactory generally. Being well-known, all analytical methods are based on this assumption, that is, the neutron flux of Eq. (6. 2-1) varies as the inverse of total cross section:

$$\phi(E)=\frac{1}{E\Sigma_t(E)} \quad . \tag{6. 2-2}$$

Therefore, the analytical methods obtained by the approximation of this assumption will introduce errors in natural.

At first, the results obtained by calculating accurately the flux of Eq. (6. 2-2) were investigated in full detail over very wide energy range for important Doppler region in homogeneous medium. This investigation was done for cases including the self interaction effect or both the self and mutual interaction effects. By the detailed survey of the accuracy of the results obtained

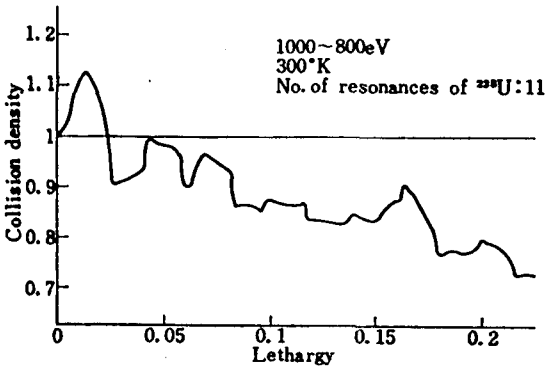

Fig. 6.2-1 Lethargy dependence of collision density for ^{238}U resonances.

by Eq. (6.2-2), the limit of accuracy for the conventional analytical methods will be estimated.

By neglecting both effects of self and mutual interactions under the assumption of Eq. (6.2-2), two typical cases of analytical method are derived. First case, the individual resonance parameters are well separated. In this case, the well-known approximations are the first order solutions such as the narrow resonance (NR) and wide-resonance (WR) approximations. Also the intermediate resonance (IR) approximation developed by GOLDSTEIN and CHOEN[94] is very useful. However, these approximations are no more than the isolated resonance approximation which assumes the constancy of asymptotic collision density within an energy group. In these approximations the effective cross section for Eq. (6.2-1) is given by the well-known expression

$$\tilde{\sigma}_x = \frac{\sum_{\lambda \in \Delta E} \sigma_{0\lambda} \frac{\Gamma_{x\lambda}}{E_\lambda} \beta_\lambda J(\theta_\lambda, \beta_\lambda)}{\Delta u - \sum_{\lambda \in \Delta E} \frac{\Gamma_\lambda}{E_\lambda} J(\theta_\lambda, \beta_\lambda)} \tag{6.2-3}$$

where the second term of denominator shows the effect of flux depression due to resonance absorption. This depression term is often neglected from a reason that the term is much smaller than lethargy width Δu. Then, the rough approximate expression is obtained as follows

$$\tilde{\sigma}_x = \frac{\sum_{\lambda \in \Delta E} \sigma_{0\lambda} \frac{\Gamma_{x\lambda}}{E_\lambda} \beta_\lambda J(\theta_\lambda, \beta_\lambda)}{\Delta u} \ . \tag{6.2-4}$$

However, the difference of results between Eqs. (6.2-3) and (6.2-4) is very large in highly enriched system of fissile than fertile materials. In the present work, Eqs. (6.2-3) and (6.2-4) for the NR-approximation are examined especially over typical energy ranges.

In high energy region, the individual resonances are largely washed out by the Doppler effect and overlapping. Then the total cross section do not fluctuate too strongly around average values, that is everywhere Eq. (5.5-1) is satisfied. Then by using Eq. (5.5-1), flux is expressed in a series expansion[95]

$$\phi(E) = \frac{1}{E\sigma_t(E)} = \frac{1}{E} \cdot \frac{1}{\langle \sigma_t \rangle + (\sigma_t - \langle \sigma_t \rangle)} = \frac{1}{E} \cdot \frac{1}{\langle \sigma_t \rangle} \left[1 - \frac{\sigma_t - \langle \sigma_t \rangle}{\langle \sigma_t \rangle} + \cdots\cdots \right] \ . \tag{6.2-5}$$

Therefore, the effective cross section is obtained by

$$\tilde{\sigma}_x = \langle \sigma_x / E\sigma_t \rangle / \langle \frac{1}{E\sigma_t} \rangle \simeq \langle \sigma_x \rangle - \frac{\langle \sigma_x \sigma_{\lambda t} \rangle - \langle \sigma_x \rangle \langle \sigma_{\lambda t} \rangle}{\langle \sigma_t \rangle} \ , \tag{6.2-6}$$

$$\langle\sigma_x\rangle=\frac{1}{\Delta E}\int_{\Delta E}\sigma_x(E)dE=\frac{1}{\Delta E}\frac{\pi}{2}\sum_{\lambda\in\Delta E}\sigma_{00\lambda}\frac{\Gamma_{n\lambda}\Gamma_{\lambda x}}{\Gamma_\lambda}\ ,$$

$$\langle\sigma_x\sigma_{\lambda t}\rangle\cong\frac{1}{\Delta E}\left(\frac{\pi}{2}\right)^{3/2}\frac{1}{2\Delta}\left[\sum_{\lambda\in\Delta E}\sigma_{00\lambda}{}^2\frac{\Gamma^2{}_{n\lambda}\Gamma_{x\lambda}}{\Gamma_\lambda}\exp\left(-\frac{\Gamma^2}{2\Delta^2}\right)\right.$$

$$\left.+\sum_\lambda\sum_{\lambda\neq\lambda'}\sigma_{00\lambda}\sigma_{00\lambda'}\frac{\Gamma_{n\lambda}\Gamma_{x\lambda}\Gamma_{x\lambda'}}{\Gamma_\lambda}\exp\left(-\frac{(E_\lambda-E_{\lambda'})^2}{2\Delta^2}\right)\right]\ , \tag{6.2-7}$$

$$\sigma_{00\lambda}=2.6\times10^6 g_\lambda/E_\lambda\ . \tag{6.2-8}$$

It is expected that equation (6.2-6) may give very good results for small fluctuation region of cross section of ^{235}U such as shown in Fig. 5.5-7. This analytical method for small fluctuation region was founded by NICHOLSON[76], and it is called as method A. On the other hand, the method for well separated region is called as method B.

Originally the method A and method B neglected interaction effects. However, by taking the interaction effects into account of, various methods[6)~9)] were also developed. In the present work, Fischer's method is examined with respects to mutual interaction effects. By the assumption of NR-approximation and series expansion in powers of term as proposed by ROWLANDS[96], Fischer's method gives effective cross sections as follows[9]

$$\tilde{\sigma}_{x1}=P_m\cdot\frac{\sum_\lambda\Gamma_{n1\lambda}J_{1\lambda}\left[1-\frac{1}{\Delta E}\sum_{\lambda'}\Gamma_{2\lambda'}J_{2\lambda'}\right]+\sum_\lambda\Gamma_{1\lambda}J^*_{1\lambda}\left[\frac{1}{\Delta E}\sum_{\lambda'}\Gamma_{2\lambda'}(J_{2\lambda'}-J^*_{2\lambda'})\right]}{\Delta E-\sum_\lambda\Gamma_{1\lambda}J_{1\lambda}\left[1-\frac{1}{\Delta E}\sum_{\lambda'}\Gamma_{2\lambda'}J_{2\lambda'}-\frac{1}{\Delta E}\Gamma_{\lambda'}\Gamma_{2\lambda'}J_{2\lambda'}\right]\left[\Delta E-\sum_\lambda\Gamma_{2\lambda}J_{2\lambda}\right]}\ , \tag{6.2-9}$$

$$P_m=\sigma_{P1}+\frac{N_2}{N_1}\sigma_{P2}+\frac{1}{N_1}\Sigma_m\ , \tag{6.2-10}$$

$$J_\lambda=J(g_\lambda,\beta_\lambda)\ , \tag{6.2-11}$$

$$J_\lambda{}^*=\int_0^\infty\frac{\phi_\lambda{}^2}{(\phi_\lambda+\beta_\lambda)^2}dx \tag{6.2-12}$$

and indices 1 and 2 show isotopes 1 and 2 respectively. The $J_\lambda{}^*$ function is accurately calculated similarly to usual J_λ function[97]. In Eq. (6.2-9), the interference scattering term was neglected. If the interaction between the resonance of isotopes 1 and 2 is neglected, Eq. (6.2-9) is equivalent to Eq. (6.2-3).

TABLE 6.2-1 The relative errors for self-shielding factor calculated by several approximate methods in energy range from 1.0 keV to 773 eV; $\sigma_m=100$(b)

Material	Reaction	T(°K)	E_x for Eq. (6.2-6)	E_x for Eq. (6.2-3)	E_x for Eq. (6.2-4)	E_x for $\phi=1/E\Sigma_t$
^{235}U	Capture	300	2.185	−1.010	12.46	1.732
		900	5.233	−0.502	13.54	
		2100	6.588	−0.284	14.05	
	Fission	300	1.613	−1.366	12.05	0.5303
		900	3.848	−1.746	12.11	
		2100	9.749	−2.505	17.22	
	Scattering	300	0.142	−0.578	0.456	0.1731
		900	0.363	−0.646	0.474	
		2100	0.595	−0.504	0.666	
^{239}Pu	Capture	300	−11.27	−6.115	7.062	2.433
		900	0.0935	−5.984	8.855	2.593
		2100	4.305	−5.384	10.13	2.633
	Fission	300	−3.953	−5.749	7.485	−0.6932
		900	4.351	−5.841	8.644	−0.5630
		2100	5.991	−6.104	9.285	−0.6195
	Scattering	300	−10.05	−1.252	2.267	0.4339
		900	4.023	−1.711	2.506	0.5229
		2100	−0.6588	−1.913	2.731	0.5442

TABLE 6. 2-2 The relative errors for self-shielding factor calculated by several approximate methods in energy range from 5. 98 keV to 4. 65 keV; $\sigma_m=100$(b)

Material	Reaction	T(°K)	E_x for Eq. (6. 2-6)	E_x for Eq. (6. 2-3)	E_x for Eq. (6. 2-4)	E_x for $\phi=1/E\Sigma_t$
^{238}U	Capture	300	1. 191	−2. 948	−0. 9936	−0. 2466
		900	1. 609	−3. 438	−1. 220	−0. 2799
		2100	1. 743	−3. 341	−0. 8869	−0. 3369
	Scattering	300	0. 1372	−0. 8311	0. 3643	−0. 2721
		900	1. 479	−1. 545	−0. 1205	−0. 3552
		2100	2. 400	−1. 543	0. 0643	−0. 4298
^{239}Pu	Capture	300	0. 602	−2. 784	2. 503	−0. 0715
		900	1. 889			−0. 0746
		2100	2. 418	−1. 984	3. 583	−0. 0804
	Fission	300	1. 267	−2. 049	2. 575	−0. 2351
		900	2. 007			−0. 2235
		2100	1. 985	−3. 548	2. 822	−0. 2223
	Scattering	300	−0. 112	−0. 904	0. 335	−0. 2397
		900	0. 413			−0. 2434
		2100	0. 502	−0. 983	0. 592	−0. 2410

TABLE 6. 2-3 The relative errors for ^{239}Pu shielding factor calculated by $\phi=1/E\Sigma_t$; $\sigma_m=100$(b), $N^8/N^9=5$.

Reaction	T(°K)	10. 0∼7. 73 keV	5. 98∼4. 65 keV	1. 0∼0. 773 keV
Capture	300	0. 4035	−0. 0796	3. 830
	900	0. 3643	−0. 1318	4. 232
	2100	0. 3482	−0. 2440	5. 063
Fission	300	−0. 0740	−0. 2190	1. 394
	900	−0. 1067	−0. 1785	2. 147
	2100	−0. 1343	−0. 1695	2. 574
Scattering	300	−0. 0139	−0. 4715	1. 078
	900	−0. 0371	−0. 5250	1. 364
	2100	−0. 0491	−0. 6022	1. 652

TABLE 6. 2-4 The relative errors for shielding factor calculated by Fischer's method; $\sigma_m=406$(b), $N^8/N^9=7$, $T=300$°K.

Reaction	1. 0∼0. 8 keV		6. 5∼5. 5 keV	
	^{238}U	^{239}Pu	^{238}U	^{239}Pu
Capture	−3. 61	−21. 4	0. 06	0. 36
Fission		−18. 1		0. 93
Scattering	3. 36	− 7. 23	6. 96	2. 5

In TABLE 6. 2-1 and 2, the relative errors of the shielding factors calculated by some approximation methods

$$E_x=\frac{f_x(\text{appr.})-f_x(\text{exact})}{f_x(\text{exact})}\times 100\ (\%) \tag{6. 2-13}$$

are shown for ^{235}U, ^{238}U and ^{239}Pu respectively. TABLE 6. 2-3 and 4 show the relative errors of mutual shielding factor (^{239}Pu and ^{238}U). In Ref. (81), the investigation for the cases mentioned above was made in full detail for Doppler energy region of interest in typical large fast reactors. From the above tables and Ref. (81), it may be seen that the errors by analytical methods are not so small to be neglected. In particular, for the temperature coefficient of shielding factor analytical methods gives large errors and that obtained by Eq. (6. 2-2) is not always satisfactory. These errors due to various approximations will give large effect for Doppler coefficient. By this

reason, the numerical calculation of effective cross section is performed over the important Doppler resonance region as mentioned in next section.

6.3 Numerical Method of Calculating Neutron Spectra and Definition of Effective Cross Sections

It was shown in the last section that the calculation based on the assumption of the constant collission density does not give high accuracy to the effective cross sections in the important energy regions for the calculation of the Doppler effect. Moreover it will be quite difficult for the calculation method to estimate the interference effect between heavy resonant isotopes accurately. Hence, it is desirable that the effective cross sections in these energy regions are calculated precisely by a direct numerical method, taking advantage of the increase in memory and speed of computer. For this purpose, we prepared a computer code ERSE[80] and, here we will simply mention the methods used in the calculations of neutron spectrum and effective cross sections.

The neutron slowing-down equation in an infinitely homogeneous mixture is

$$\Sigma_t(E)\phi(E)=\sum_j K_j(\Sigma_{s,j}\phi) \tag{6.3-1}$$

where the integral kernel K is defined by

$$K(\Psi)=\int_E^{E/\alpha}\frac{\Psi(E')dE'}{(1-\alpha)E'} \tag{6.3-2}$$

and the suffix (j) stands for the nuclear species, and other notations have the customary meanings, explanation of which will be omitted for brevity. An energy range of interest will be divided into many narrow groups of equal energy width, which must be narrow enough to describe the rapid variation of the neutron spectrum near resonance levels accurately. We also assume that one collision of neutron in a group always results in its being absorbed or scattered into a lower group. By applying a simple rectangular formula for integration we have

$$\phi_j=S_i/\Sigma_{ti} \tag{6.3-3}$$

with

$$S_i=\sum_j\frac{\Delta E}{1-\alpha_j}\sum_{l=1}^{L_j}\frac{\Sigma^j_{s,i-l}\phi_{i-l}}{E_{i-l}}, \tag{6.3-4}$$

where L_j maxmum number of groups that a neutron can reach by slowing down in a collision with the nuclear species (j). Then, assuming asymptotic flux above the energy range under consideration, we now obtain the neutron spectrum and related quantities for the first group, and can repeat this procedure for the subsequant groups. Actually Eq. (6.3-4) can be converted into a recurrence formula using the sources S_i. We obtained the neutron spectrum using the recurrence formula.

For the group structure, as selected from the standopoint of the last section, the scattering cross sections of moderator can be assumed constant within a group. Moreover, through examinations of effective cross sections obtained by the method mentioned above show that in Eq. (6.3-1) or (6.3-4) the source terms due to scattering materials can be substituted by those due to an imaginary scattering material without destroying accuracy. That is to say,

$$\sum_{j'}K_{j'}(\Sigma_{s,j'}\phi)\simeq\Sigma_{s,m}K_m(\phi) \tag{6.3-5}$$

where the summation concerning (j') is extended only over moderator species and the subscript (m) corresponds to the representative fictitious moderator. This approximation was confirmed to be quite accurate except for lower energy ranges below few eV. Moreover, it was also confirmed that the accuracy can be raised by taking the moderator mass in Eq. (6.3-5) corresponding to the average logarithmic energy loss $\bar{\xi}$ of the whole moderators. Hence our equation used in the

calculation of effective cross sections can be written as

$$[\sigma_t(E)+\sum_j R_j\sigma_{t,j}(E)+\sigma_m]\phi(E)=K(\sigma_s\phi)+\sum_j R_jK_j(\sigma_{s,j}\phi)+\sigma_mK_m(\phi) \quad (6.3\text{-}6)$$

$$R_j=N_j/N \text{ and } \sigma_m=\Sigma_{sm}/N, \quad (6.3\text{-}7)$$

where the suffix (j) corresponds to other resonant nuclear species than one species in question, σ_m to the macroscopic total cross section of moderator per the resonance species in question, and N and N_j are densities of resonant absorbers.

The group effective cross sections in the energy interval from E_{k-1} to E_k can be calculated by the use of the flux obtained from Eq. (6.3-3) and are defined by the following equations:

1) Effective capture, fission and scattering cross sections

$$\tilde{\sigma}_{xK}=\frac{\sum_{i\in K}\sigma_{xi}\phi_i}{\sum_{i\in K}\phi_i} \quad (6.3\text{-}8)$$

where the subscript x stands for capture, fission or scattering.

2) Effective total cross section

2-a) The case where interference between different resonant isotopes is absent.

$$\tilde{\sigma}_{tK}\cong\frac{\sum_i\phi_i}{\sum_i\frac{\phi_i}{(\sigma_{ti}+\sigma_0)}}-\sigma_0 \quad (6.3\text{-}9)$$

2-b) The case where the interference is present.

$$\tilde{\sigma}_{tK}\cong\frac{\sum_i\phi_i}{\sum_i\frac{\phi_i}{(\sigma^1{}_{ti}+R_1\sigma_{ti}{}^2+\sigma_0)}}-\frac{\sum_i\phi_i}{\sum_i\frac{\phi_i}{(R_1\sigma_{ti}{}^2+\sigma_0)}} \quad (6.3\text{-}9)'$$

3) Effective elastic removal cross section

$$\tilde{\sigma}_{eK}=\frac{\sum_{i'}\sigma_{si'}\phi_{i'}\frac{E_k-\alpha E_{i'}}{(1-\alpha)E_{i'}}}{\sum_i\phi_i} \quad (6.3\text{-}10)$$

where the summation concerning (i') in the numerator is extended only over the fine group numbers in the range from E_k to E_k/α.

6.4 Interference Effect between Different Resonance Isotopes

In the cross section sets developed for fast reactor analysis, the effective cross sections in the resonance energy region are usually obtained from the resonance shielding factors and cross sections for infinite dilution, originally tabulated in the ABBN set. The resonance shielding factors in the ABBN set are functions of temperature, and σ_0 which is the effective cross section of admixture per absorber atom under consideration. Some approximations, however, are assumed in obtaining the f-table. One is to neglect the resonance interfence effect comprising the self overlapping effect of the same isotope and the mutual shielding effect from different isotopes. The mutual shielding effects are dependent on the compositions and temperature of systems. Therefore it is not simple to take account of these effects in group constant calculations. Many methods have been proposed for the consideration of these effects[6),7),8),9)]. None, however, appears as yet to have provided complete answer. Here, investigation will be made for the mutual shielding effects by using the exact numerical method shown in the last section.

Fortunately, the fertile ^{238}U is the predominate resonance absorber in practical situations of fast reactor studies, too, hence we may take account of only the interference effect between one

isotope in question and ^{238}U, as the first order approximation. As an illustrated example, the resonance cross sections of ^{238}U and ^{239}Pu in the energy range from 150~230 eV are shown in Fig. 6.4-1. This figure shows that the fertile ^{238}U has high and sharp resonances with which few resonances of ^{239}Pu overlap.

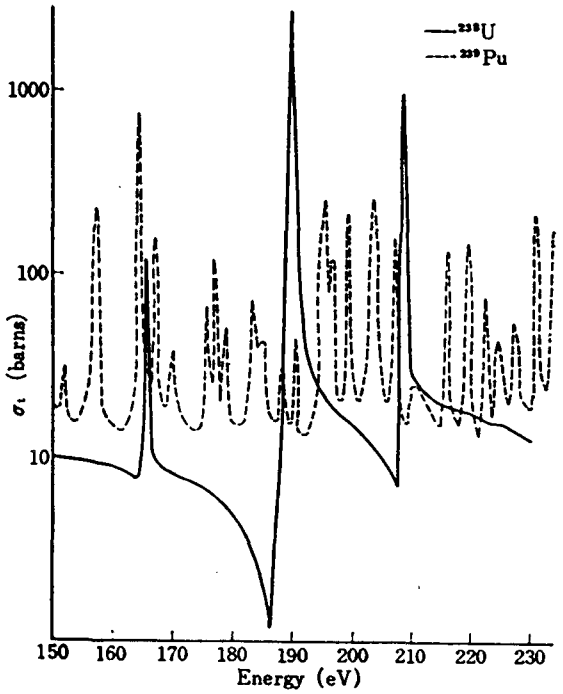

Fig. 6.4-1 Total cross sections of ^{238}U and ^{239}Pu.

Fig. 6.4-2 shows the neutron flux for a typical fast reactor composition of ^{239}Pu, ^{238}U and moderators. In this figure, the solid line corresponds to the case where the resonance of ^{238}U is smoothed out. It will be seen from this figure that the neutron flux is largely perturbed by the resonances of ^{238}U and the mutual shielding effects should be considered in the calculation of effective cross sections of ^{239}Pu.

Now, let us consider homogeneous systems composed of ^{238}U, ^{239}Pu and moderator atoms, the latter being Fe, Na and O. In this case, the neutron slowing down equation (6.3-6) is rewritten as

$$(\sigma_t^1+R^1\sigma_t^2+\sigma_m^1)\phi=K_1(\sigma_s^1\phi)+R^1K_2(\sigma^2{}_s\phi)+\sigma_m^1K_m(\phi) \quad (6.4\text{-}1)$$

$$\sigma_m^1=\Sigma_m/N^1, \quad R^1=N^2/N^1, \quad (6.4\text{-}2)$$

Where the supperscripts 1 and 2 correspond to ^{239}Pu and ^{238}U, respectively, and the capture by moderator atoms were neglected. The shielding factor is defined by

$$f_x=\sigma_x/\sigma_{x\infty} \quad (6.4\text{-}3)$$

where $\sigma_{x\infty}$ is the infinitely dilute cross section.

By introducing one more parameter R^1 we can express the resonance shielding factor of ^{239}Pu by

$$f_x=F(T,\sigma_m^1;R^1) \quad (6.4\text{-}4)$$

That is, we can express the shielding factor including the mutual interference effects by these three parameters. Though we considered only the systems which are composed of one resonance isotope besides ^{238}U, the effects of more isotopes can be treated without significant error by putting them into σ_m^1. Examinations have been made for the dependence of f_x on R^1 for typical fast reactor compositions. In these calculations we have chosen three typical regions: 155~215 eV,

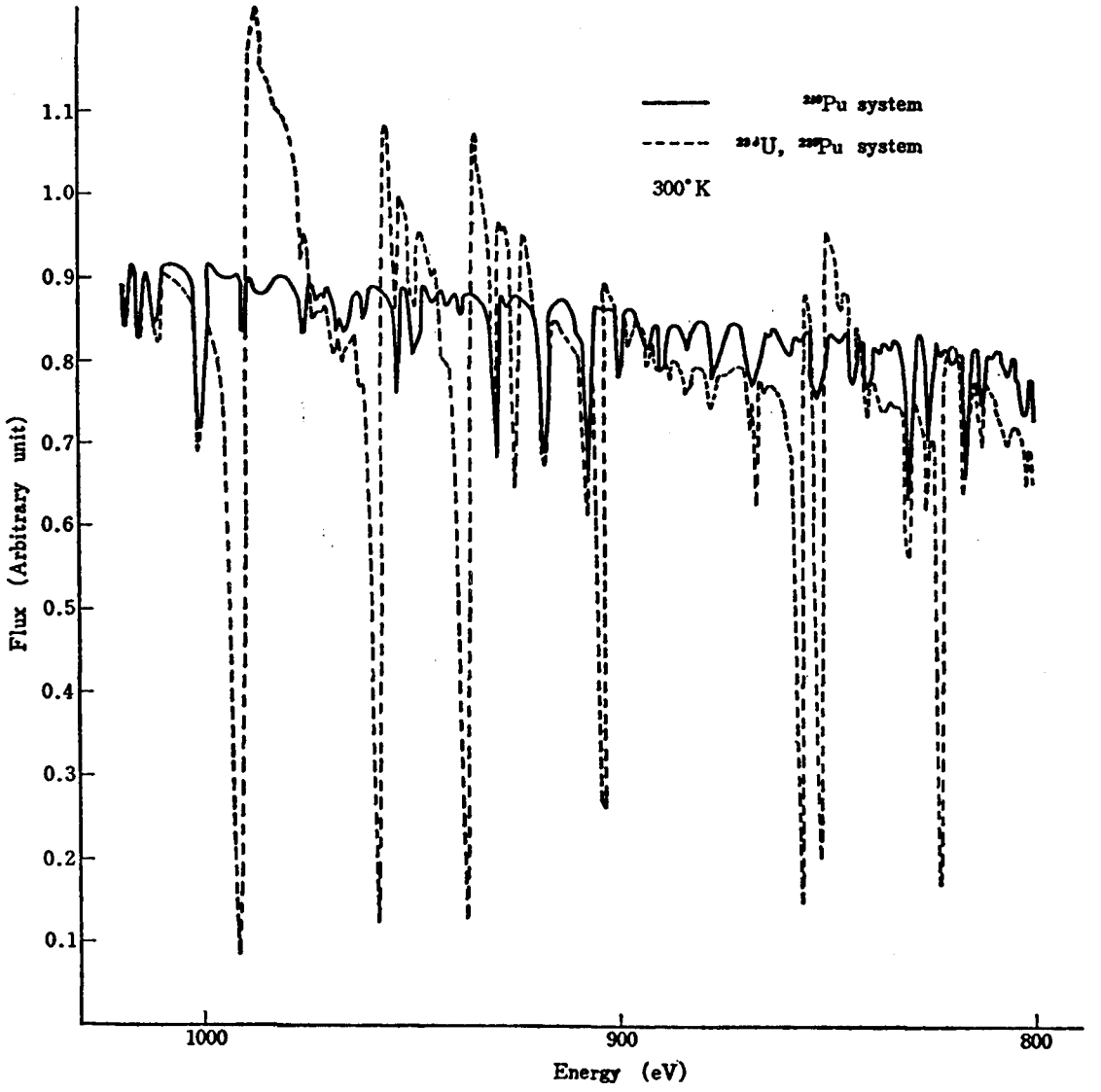

Fig. 6.4-2 Neutron spectrum in ^{239}Pu system and ^{239}Pu-^{238}U system.

800~1000 eV and 5.5~6.5 keV. In the second and third regions, the resonances of ^{239}Pu are unresolved, as are those of ^{238}U in the third region.

From Figs. 6.4-3, 4 and 5, it is seen that shielding factors vary linearly with the ratio $^{238}N/^{239}N$, and even in the lower energy region of 155~215 eV, the linearity is fairly good. Thus, shielding factors can be calculated for any $^{238}N/^{239}N$ ratio by linear interpolation or extrapolation, based on values and gradients for the ratio $^{238}N/^{239}N$ with overlapping effects taken into account. On the other hand, the shielding factors of ^{238}U are seen to be hardly affected by the resonance overlapping of ^{239}Pu.

Also included in these figures are the shielding factors for the case devoid of mutual interaction. As seen from Figs. 6.4-4 and 5, mutual shielding effects contribute considerably to the calculation of resonance shielding factors. In the energy region of 155~215 eV, f_c is changed little when the temperature was varied from 900° to 2,100°K, while in the region of 215~280 eV, the temperature increase of the same magnitude results in lowering of f_t at $^{238}N/^{239}N=10$. These results can be interpreted to prove that the shielding factors do not always increase monotonously with temperature when mutual shielding effects are taken into account. Thus, when group constants are produced, it is desirable to give consideration to these effects when dealing with important

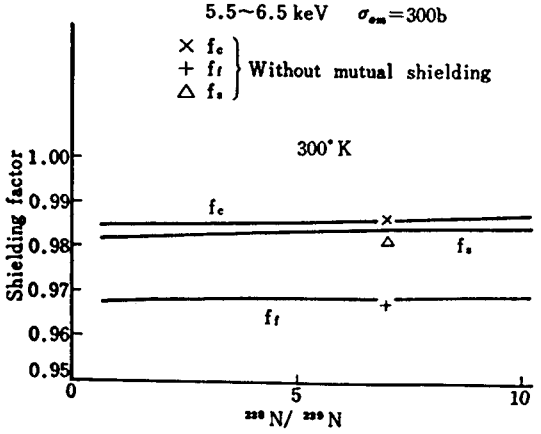

Fig. 6.4-3 Shielding factor of ^{239}Pu.

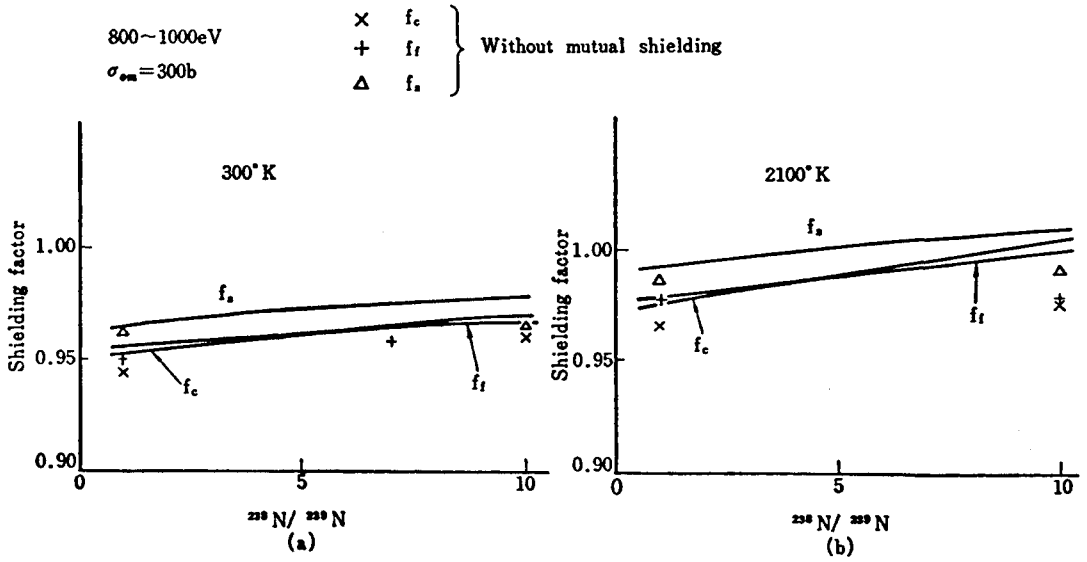

Fig. 6.4-4 Shielding factor of ^{239}Pu.

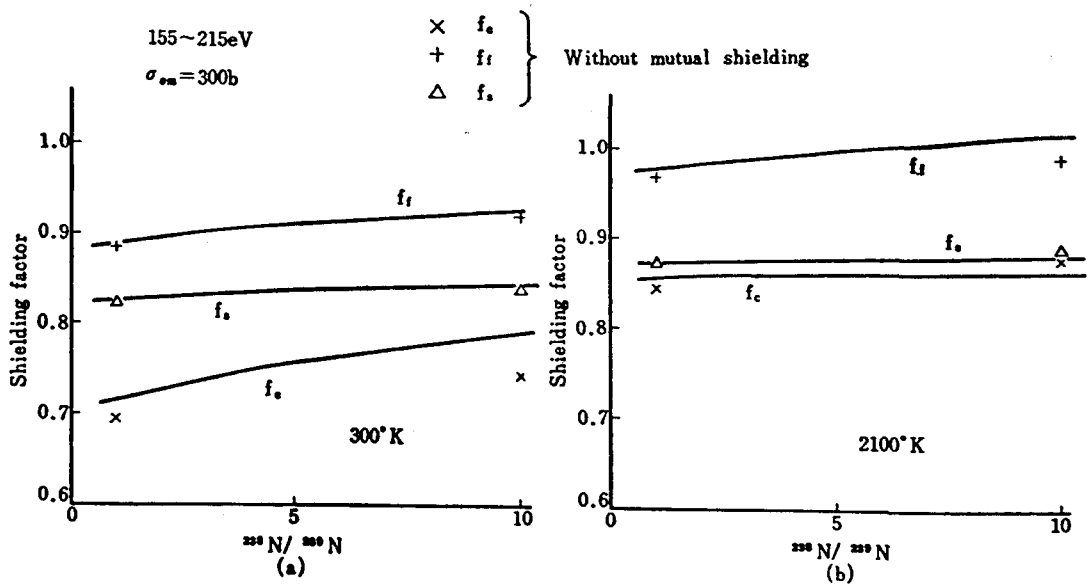

Fig. 6.4-5 Shielding factor of ^{239}Pu.

ranges of resonance energy.

From the results shown above, we have decided to produce and tabulate the shielding factor by the three parameters, temperature, σ_0 and R. Tabulated tables have been prepared for the isotopes ^{235}U, ^{239}Pu and ^{240}Pu taking account of the mutual shielding effects with ^{238}U.

6.5 A Note on the Calculation of Elastic Removal Cross Section

Elastic removal cross section has been obtained by using the self-shielding-factor for elastic scattering in the ABBN set. That is, effective elastic removal cross section was obtained from

$$\tilde{\sigma}_e = \frac{\xi}{\Delta u}\tilde{\sigma}_s = \frac{\xi}{\Delta u}\sigma_{s\infty} \cdot f_s \qquad (6.5\text{-}1)$$

where $\tilde{\sigma}_s$ is effective elastic scattering cross section, f_s, the shielding factor for elastic scattering and ξ is the average logarithmic energy loss.

On the other hand, exact effective removal cross section was defined by Eq. (6.3-10). The elastic removal cross section depends mainly on the local spectrum in the lower energy boundary of a group and is hence affected by the resonance structure of cross sections there. For an example of ^{238}U, the maximum lethargy increase by one neutron collision is 0.0167, while the present group width in the resonance region is about 0.257 ($\gg$0.0167). Moreover, the neutron spectrum decreases gradually in a group due to strong resonance absorption and the relative ratio of integrated flux over a group width to that over lower part of the width, say, 0.0167 is also necessary to be estimated accurately.

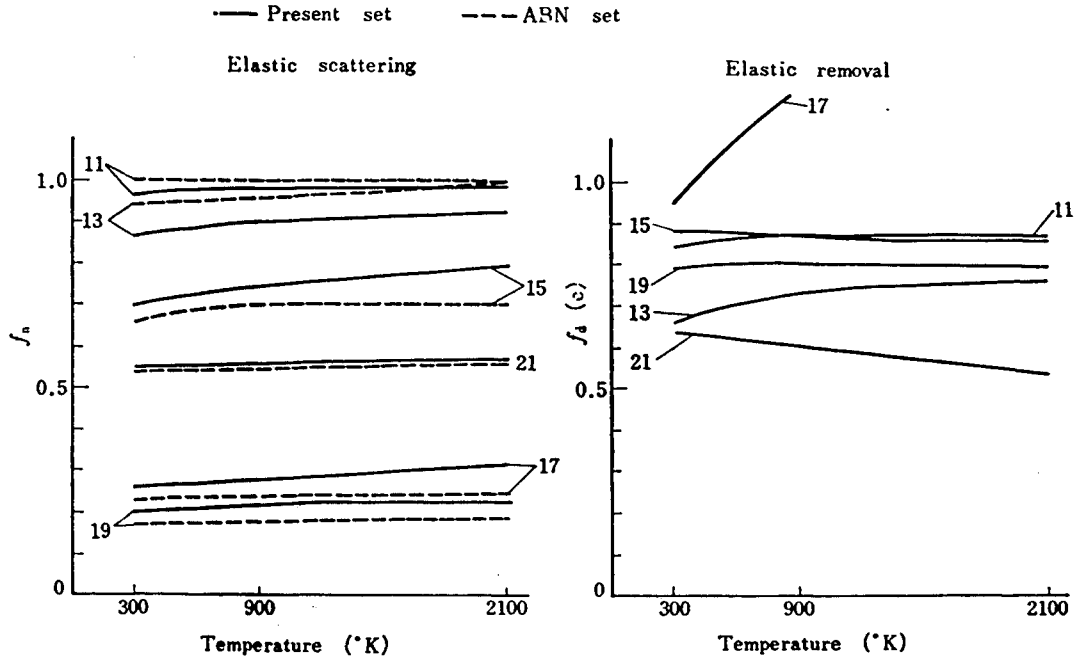

Fig. 6.5-1 Shielding factors of elastic removal and elastic scattering.

In Fig. 6.5-1, we show the shielding factors of elastic scattering and removal cross sections and also these of the ABBN set for elastic scattering. The numbers in this figure corresponds to the group numbers of the ABBN set. From this figure we can see that their shielding factors are considerably different in values and separate shielding factors should be prepared for them. Hence, in our group constant set, the shielding factors of removal cross section are also calculated by Eq. (6.3-10) and tabulated by using the three parameters in the last section.

7. Concluding Remarks

As mentioned already in the Introduction, there were many difficult problems to be solved for producing accurate group constants based on reasonable concept of set of group constants. Especially the problem for generating high resolution cross sections so as to reproduce low resolution experiments, within the limits of resonable amounts of money, time and man powers, was thought as extremely difficult. We have established the technique for the generation as explained in this report. In the course of study for this technique, we have developed several useful programs which will be used for producing group constants for other unclei treated in this report and for revising group constants.

For the α values of ^{239}Pu, we have confirmed that they are consistent with the conclusion of the specialist meeting[88] held at Winfrith last year. Moreover fission cross sections agree with measurements. For ^{238}U, the cross sections in the keV region coincide with experimental values. For ^{235}U and ^{240}Pu, cross sections seem reasonable compared with recent experimental results. Infinite dilution resonance integrals obtained for the isotopes are also very close to the previous recommendations. We have obtained high resolution cross section tapes as by-products of this study which will be used for studies of heterogeneity effects and group constants for heterogeneous systems in near future.

As for the group constants, the program solving the slowing down equation with energy meshes is very useful. By this program we have established quite effectively the present concept of group constants, especially for obtaining that of shielding factors. The group constants themselves will be used for analyses of Doppler and/or sodium void effects, because mutual interference and self overlapping effects are taken into considerations. Moreover since the constants reproduce the fluctuation in α values of ^{239}Pu which are sensitive to fission width, we can expect reasonable values for these reactivity effects, and also for the breeding ratio.

The presently derived group constants together with those reported in another report[11], which contains group constants for the following elements ^{10}B, ^{11}B, C, O, Na, Al, Cr, Fe, Ni, Cu and ^{241}Pu and those for ^{235}U, ^{238}U, ^{239}Pu and ^{240}Pu except for the resonance groups treated here, constitute so called JAERI-FAST SET. However the task for producing accurate group constants has not been finished yet. We should examine applicabilities of the JAERI-FAST SET by analysing the bench mark experiments and other measured reactivity effects. For this purpose the program EXPANDA-4[99] have been developed.

Finaly it should be noted here the group constants obtained here can be also applied for thermal reactors, if we add a few group constants for low energy neutrons. The shielding factors for higher isotopes of ^{241}Pu and ^{242}Pu will be further prepared, in the near future, by the same procedures as described in this report.

Acknowledgements

The authors are indebted to Mr. Suzuki for his arranging few computer codes for IBM 360 before this work started. They are also grateful to Miss S. Ogawa for her excellent typing of this manuscript, and to Misses M. Yamazaki and E. Tsuchida for their sincere helps in the present work.

This work was performed under the auspices of the P. N. C.

References

1) YIFTAH S., OKRENT D. and MOLDAUER P. A.: "Fast Neutron Cross Sections", Pergamon Press, London (1960).
2) HANSEN G. E. and ROACH W. H.: "Six and Sixteen Group Cross Sections for Fast and Intermediate Critical Assemblies" LAMS-2543, Los Alamos Scientific Laboratory (1961).
3) ABAGJAN L. P. *et al.*: "Group Constants for Nuclear Reactor Calculations", Consultant Bureau, New York (1964).
4) TONE T., ISHIGURO Y. and TAKANO H.: *J. Nucl. Sci Technol. (Tokyo)*, **4**, 601 (1967).
5) TONE T. and KATSURAGI S.: *J. Nucl. Sci. Technol. (Tokyo)*, **5**, 201 (1968).
6) HWANG R. N.: *Nucl. Sci. and Eng.*, **21**, 523 (1965).
7) FROELICH R., OTT K. and SCHMIDT J. J.: "Calculation of Doppler Coefficients of Dilute Fast Reactor", ANL-6972, pp. 777, Argonne National Laboratory (1963).
8) CODD J. and COLLINS P. J.: "Some Calculations Concerning the Influence of Resonance Overlapping on the Doppler Effect in a Dilute Fast Reactor", ANL-6792, 711 (1963).
9) FISCHER E. A.: *Nuckleonik*, 8. Bd., Heft 3, 146 (1966).
10) TOPPEL B. J., RAGO A. L. and OSHEA D. M.: "MC², A Code to Calculate Multigroup Cross Sections", ANL-7318, Argonne National Laboratory (1967).
11) KATSURAGI S., TONE T. and HASEGAWA H.: "JAERI Fast Reactor Group Constants Systems Part I", JAERI 1195.
12) ADLER D. B. and ADLER F. T.: *Trans. Am. Nucl. Soc.*, **5**, 53 (1963).
13) ADLER D. B. and ADLER F. T.: "Reactor Physics in the Resonance and Thermal Regions", Vol. II, pp. 37, The M. I. T. Press, London (1966).
14) VOGT E.: *Phys. Rev.*, **112**, 203 (1958).
15) VOGT E.: *Phys. Rev.*, **118**, 29 (1960).
16) MRS. BUCKLER P. A. C. and PULL I. C.: "Doppler Broadening of Cross Sections", AEEW-R 226 (1962).
17) WIGNER E. P. and EISENBUD L.: *Phys. Rev.*, **72**, 29 (1947).
18) LANE A. M. and THOMAS R. G.: *Rev. Mod. Phys.*, **30**, 257 (1958).
19) BRISSENDEN R. J. and DURSTON C.: "The Calculation of Neutron Spectra in the Doppler Region", Proc. Intern. Conf. Application of Computing Methods to Reactor Problem, May 17~19, 1965; ANL-7050, Argonne National Laboratory (1965).
20) For example, PORTER C. E.: "Statistical Theories of Spectra: Fluctuations", Academic Press, New York (1965).
21) BOHR A.: Proc. int. conf. peaceful uses atom. energy, Geneva, 1965, Vol. 2, p. 220, United Nations, New York.
22) GARRISON J. D.: "A Statistical Analysis of Resonance Parameters", Symposium on Statistical Properties of Atomic and Nuclear Spectra, State University of New York (1963).
23) FARREL J. A.: *Phys. Rev.*, **165**, 1371 (1968).
24) MICHAUDON A.: "Determination du Spin des Resonances de Noyaux Fissles", Conf. Proc., Nuclear Data for Reactors, Int. At. Energy Agency, Vienna, Vol. II, 161 (1966).
25) PARKER K.: "Neutron Cross Sections of ^{235}U and ^{238}U in the Energy Range 1 keV to 15 MeV", AWRE #0-79/63, (1963).
26) FESHBACH H.: *Ann. Rev. Nucl. Sci.* (1960).
27) JULIEN J.: Proc. int. conf. study nucl. structure neutrons, Antwerp, 156 (1965)
28) BOHR N. and WHEELER J. A.: *Phys. Rev.*, **56**, 426 (1939).
29) HILL D. L. and WHEELER J. A.: *Phys. Rev.*, **89**, 1102 (1953).
30) BOHR A.: P/911, Pro. Int. Conf. Peaceful Uses At. Energy, Geneva, **2**, 151 (1955).
31) MOTTELSON B. R.: Proc. int. conf. on nuclear structure, Kingston, 525, (1960). University of Toronto Press Toronto.
32) LYNN J. E. "The Theory of Neutron Resonance Reactions", Clarendon Press, Oxford (1968).
33) COHEN S. and SWIATECKI W. J.: *Ann. Phys.* **19**, 67 (1962); **22** 406 (1963).
34) FRASER S. and MILTON J. C. D.: "Nuclear Fission", *Ann. Rev. Nucl. Sci.*, **16**, 379 (1966).
35) WILETS L.: "Theries of Nuclear Fission", Clarendon Press, Oxford (1964).
36) BOHR A.: *Dan. Mat.-Fys. Medd.* 26, No. 14 (1952).
WILETS L.: *Phys. Rev.* **115**, 372 (1959).
37) WHEELER J. A.: "Fast Neutron Physics", (eds. FOWLER J. L. and MARON J. B.), Vol. 2, pp. 2051, Interscience, New York (1963).
38) LYNN J. E.: "Interpretation of Neutron-Induced Fission Cross Sections and Related Data", Conf. Proc., Nuclear Data for Fast Reactors Paris, Oct. 17-21, IX 1966, Int. At. Energy Agency, Vienna, Vol. II, 59 (1967).

39) STEHN J. R. *et. al.*: "Neutron Cross Sections", BNL-325, 2nd. ed. suppl. No. 2 (1964).
40) SCHMIDT J. J.: "KFK-120", Part I, Karlsruhe (1967).
OTTER J. M.: "Calculations of ^{239}Pu Resonance Cross Section Using Fission Widths from Channel Fission Theory" NAA-SR-12512, Atomic International (1967).
41) DRAWBAUGH D. W. and GIBSON G.: "A Single Level Analysis of ^{235}U Based on Recent σ_t, σ_f and σ_c Measurements" Conf. Proc., Nuclear Data for Fast Reactor Paris, Oct. 17-21, IX, 1966, Int. At. Energy Agency, Vienna, Vol. II, 251 (1967).
42) GLASS N. W. *et al.*: "^{238}U Neutron Capture Results from Bomb Source Neutron", the Neutron Cross-Section Technolo. Conf., Washington, D. C., March (1968).
43) DERRIEN H. *et al.*: "Sections Efficaces Total et de Fission du ^{239}Pu. Etude Statistique des Parameters de Resonance", Conf. Proc., Nuclear Data for Fast Reactor, Paris, Oct. 17-21, IX, 1966, Int. At. Energy Agency, Vinna, Vol. II, 195 (1967).
44) DURETON C. and KATSURAGI S.: "On the Evaluation of ^{239}Pu Data in the keV and Resolved Resonance Region", JAERI 1162 (1968).
45) KOLER W. and BOCKHOFF K. H,: *J. Nucl. Energy*, 22, 299 (1968).
46) WEIGMANN H. and SCHMIDT H.: *J. Nucl. Energy*, 22, 317 (1968).
47) PATTENDEN J. H.: private communication (1967).
48) GREEBLER P., ALINE P. and HUTCHINGS B.: "Evaluation and Complication of ^{239}Pu Cross Section Data for the ENDF-B Files", GEAP-5272, General Electric Company (1966).
49) BRISSENDEN R. J. and DURSTON C.: "A User's Guide to GENEX, SDR and Related Computor Codes", AEER-R 622, Winfrith (1968).
50) P-3 and W-8 Staff: "Fission Cross Sections from Petrel", LA-3586, Los Alamos Scientific Laboratory of University of California (1966).
51) de SAUSURE G. *et al.*: "Measurement of the Neutron Capture and Fission Cross Sections and Their Ratio Alpha for ^{233}U, ^{235}U and ^{239}Pu", Conf. Proc., Nuclear Data for Fast Reactor, Oct. 17-21, (1966), Inter. At. Energy Agency, Vienna, Vol. II, 233 (1967).
52) WANG Shih-Di *et al.*: "Proc. the Saltburg Symposium on Phys. and Chem", 1965, Int. At. Energy Agency, Vienna, Vol. I, 287 (1965).
53) MICHADON A.: "Contribution a L'etude par des Methode du Temps de L'integration des Neutrons lents avec L'^{235}U", CEA-R 2552, Saclay (1964).
54) KANNE W. R., STEWART H. B. and WHITE F. A.: Proc. of the 1st. United Nations Inter. Conf. Peaceful Uses At. Energy, Geneva, 4, 315 (1955).
55) SPIVAK P. E. *et al.*: *J. Nucl. Energy*, Part II, 79 (1957).
56) HOPKINS J. C, and DIVEN, D. C.: *Nucl. Sci. Eng.*, 12, 169 (1962).
57) WESTON L. W., de SAUSSURE, G. and GWIN, R.: *Nucl. Sci. Eng.*, 20, 80 (1964).
58) PATRICK B. H. *et al.*: "Average Value of the Fission Cross Section and Alpha for ^{239}Pu in the Energy Range 100 eV to 3 keV", EANDC (UK), 961 (1968).
59) SCHOMBERG M. G. *et al.*: "A New Method of Measuring Alph (E) for ^{239}Pu", IAEA Sump., Fast Reactor Phys. Related Safety., Karlsruhe, 1967, MS-101/41.
60) BARRE J. Y., L'Heriteau, J. P. and RIBON, P.: "Examine Critique des Values de α pur le ^{239}Pu Au-Da la de 1 keV", Reactor DRP-SMNF 623-68, Saclay (1968).
61) GWIN R. *et al.*: "Measurements of the Neutron Fission and Absorption Cross Sections of ^{239}Pu over the Energy Range 0.01 to 30 keV", ORNL-4280, UC-34-Physics, pp. 13 (1968).
62) KIEFHABER E. *et al.*: "Evaluation of Fast Reactor Critical Experiments by Use of Recent Method and Data", BNES Inter. Conf. on the Fast Reactor Physics and Design, 1. 9 (1969).
63) KUROI H. *et al.*: "Correlation of Integral Data and Cross Sections in Intermediate Core", BNES Inter. Conf. on the Fast Reactor Physics Design, 1.7 (1969).
64) JAMES G. D.: "Fission Cross-Section Measurement of ^{233}U, ^{235}U, ^{239}Pu and ^{240}Pu in the Energy Range from 1 to 25 keV", Proc. Inter. Conf. on Fast Reactor Critical Experiments and Their Analysis, Oct. 10-13, 1966, ANL-7320 (1966).
65) BOLLINGER L. M., COTO R. E. and THOMAS G. E.: Pro. of the 2nd United Nations Inter. Conf. on the Peaceful Uses of At. Energy, 15, 127 (Geneva (1968)).
66) DRESNER L. "Resonance Absorption in Nuclear Reactor", *Pergamon Press*, N. Y. (1960).
70) DYOS M. W. and STEVENS C. A.: *Nucl. Sci. Eng.*, 25, 294 (1966).
71) KELBER C. N. and KIER P. H.: *Nucl. Sci. Eng.*, 24, 383 (1966).
72) KELBER C. N. and KIER P. H.: *Nucl. Sci. Eng.*, 25, 67 (1966).
73) DYOS M. W.: *Nucl. Sci. Eng.*, 34, 181 (1968).
74) ADKINS C. R., MURLEY T. E. and DYOS M. W.: *Nucl. Sci. Eng.*, 36, 376 (1969).
75) ISHIGURO Y. and KASTURAGI, S.: "BABEL, A Program of Construction of Statistical Resonance Parameters in Unresolved Resonance Region", to be published in JAERI-memo.
76) NICHOLSON R. B.: "The Doppler Effect in Fast Neutron Reactors", APDA-139, Atomic Power Dovelop-

ment Associates (1960).
77) NORDHEIM L. W.: "The Doppler Coefficient", Technology of Nuclear Reactor Safety, 4, 22 (1964).
78) HUSCHKE H. *et al.*: "Gruppen Konstanten fur dampf- und natriumgeknhlte Schnelle Reaktoren in einer 26-Gruppendarstellung", KFK-770, (1968).
79) TAKANO H. *et al.*: "MCROSS, A Program for Culculation of Doppler Broadened Microscopic Cross Section by Multilevel Formula", to be published in JAERI-memo.
80) NAKAGAWA M. and KASTURAGI S.: "ERSE, Code to Calculate Fine Spectrum and Effective Cross Sections", to be published in JAERI-memo.
81) TAKANO H. *et al.*: "On the Accuracy of Analytical Methods for Calculation of Resonance Absorption in Doppler Resonance Region", *J. Nucl. Sci. Technol. (Tokyo)*, 7 [10], 500 (1970).
82) BOWMAN C. D. *et al.*: Rep. CONF-660303, p. 1004 (1966).
83) BROOKS F. D. *et al.*: "Eta and Neutron Cross Sections of ^{235}U from 0.04 to 200 eV" UKAEA Rep. AERE-M-1670 (1966).
84) JAONOU G. D. and DRAKE M. K.: "Neutron Cross Sections for ^{235}U" Rep. GA-5944 (1964).
85) HANNA G. C. and WALKER W. H.: "The capture and Fission Resonance Integrals of U-235", Rep. EANDC (can)-20 (1963).
86) SCHMIDT J. J.: "KFK 120", Parts II and III (1965).
87) FREEMANTLE R. G.: "The Reactions of Neutrons with U-235", Rep. AEEW-M-502 (1965).
88) FEINER F. and ESCH L. J.: "Survey of Capture and Fission Integrals of Fission Materials", ANS-meeting on Reactor Physics in the Resonance and Thermal Regions, San Diego (1966).
89) HENNIES H. H.: "Cross Sections and Resonance Parameters for ^{235}U, ^{233}U, ^{239}Pu and ^{241}Pu between Cadmium Cutoff and 10 keV", Conf. Proc., Nuclear Data for Fast Reactor, Oct. 17-21, (1966), Inter. At. Energy, Vienna, Vol. II, 333 (1967).
90) HEMMENDINGER A.: *Phys. Today*, 18, 17 (1965).
91) TONE T.: *J. Nucl. Sci. Technol. (Tokyo)*, 5, 538 (1968).
92) RAGO A. L. and HUMMEL H. H.: ANL-6805 (1965).
93) KATSURAGI S., ISHIGURO Y. and KATO O.: JAERI 1109 (1966).
94) GOLDSTEIN R. and COHEN E. R.: *Nucl. Sci. Eng.*, 13, 132 (1962).
95) FESHBACK H., GOETZEL G. and YAMAUCHI H.: *Nucl. Sci. Eng.*, 1, 4 (1956).
96) ROWLANDS J. L.: AEEW, M 398, (1963).
97) TAKANO H.: *J. Nucl. Sci. Technol. (Tokyo)*, 4, 3, 155 (1967).
98) "Meeting of Specialist on the value of Plutonium Alpha", Inter. Working Group on Fast Reactors, IAEA, June (1969).
99) SUZUKI T. "EXPANDA-4, The One-Dimentional Diffusion Equation Code for Fast Reactors Using the JAERI-FAST-SET", JAERI-memo 3660 (1969).
100) TONE T. and KATSURAGI S.: "PROF GROUCH-G, A Processing Code for Group Constants for a Fast Reactor", JAERI 1192 (1970).

Appendix Table of Group Constants

The effective cross sections for heavy isotopes ^{235}U, ^{238}U, ^{239}Pu and ^{240}Pu were calculated following the procedures shown in the last chapter. The calculations were made for the total, capture, fission, elastic scattering and removal cross sections. The results obtained were arranged in two quantities of the resonance shielding factors and infinitely dilute cross sections which were obtained from averaging microscopic cross sections at 300°K with weight of the $1/E$ spectrum. Two set of tables were prepared for the resonance shielding factors: One corresponds to the table of the ABBN type which is function of temperature and σ_0. This preparation was made for the purpose of comparison of the various results obtained from old type sets of constants with those from the following more accurate table. Another is function of temperature, σ_0 and R defined in the last chapter, which was given to only the isotopes except for ^{238}U. In this case, the shielding factors are assumed to be obtained by a linear interpolation or extrapolation of a variable R, i. e.,

$$f_x = f_x^1 R + f_x^0 \qquad \text{(A 1)}$$
$$R = {}^{238}N/{}^{235}N,\ {}^{238}N/{}^{239}N \text{ or } {}^{238}N/{}^{240}N.$$

The resonance shielding factors are to be given by these two quantities f_x^1 and f_x^0 which is shown in a tabulated form. The table of old fashion for the self-shielding factors f_x is also given later.

From these tables prepared, we can calculate the effective cross sections of heavy isotopes in the resonance region. Preparations were also made for tables of light and intermediate elements over the full energy range needed for fast reactor studies[11,100]. A couple of these tables will make it possible to carry out the necessary calculations for studies of fast reactors. For this purpose, a computer code[99] has already been prepared.

A-I-1 Table of infinite dilution cross section for U-235

GROUP	UPPER E	LOWER E	LETHARGY	TOTAL	CAPTURE	ELASTIC	REMOVAL	FISSION
29	10000.000	7730.000	0.257	13.3570	1.2506	9.2699	0.3058	2.8454
30	7730.000	5980.000	0.257	14.0890	1.4820	9.3254	0.3161	3.2912
31	5980.000	4650.000	0.252	14.7280	1.6599	9.3849	0.3084	3.6929
32	4650.000	3600.000	0.256	15.3510	1.9243	9.3582	0.3087	4.0874
33	3600.000	2780.000	0.258	16.1070	2.0783	9.3705	0.3012	4.6771
34	2780.000	2150.000	0.257	17.8370	2.5721	9.4306	0.3202	5.8344
35	2150.000	1660.000	0.259	18.3360	2.6319	9.3047	0.3008	6.3997
36	1660.000	1290.000	0.252	20.1660	3.3736	9.4909	0.3159	7.3107
37	1290.000	1000.000	0.255	22.2200	3.9243	9.4856	0.3005	8.8197
38	1000.000	773.000	0.257	23.0850	4.6151	9.5474	0.3222	8.9220
39	773.000	598.000	0.257	25.5730	5.9605	9.7156	0.2909	9.9640
40	598.000	465.000	0.252	29.3520	6.4307	9.6639	0.3392	13.3630
41	465.000	360.000	0.256	30.4970	7.6122	9.6535	0.3337	13.3380
42	360.000	278.000	0.258	31.8860	8.0265	9.4037	0.2878	14.4700
43	278.000	215.00	0.257	32.6280	7.8329	9.5164	0.3408	15.6030
44	215.000	166.000	0.259	40.3200	9.4443	9.4169	0.3010	21.4590
45	166.000	129.000	0.252	42.9950	14.1650	9.6283	0.2608	19.6210
46	129.000	100.000	0.255	39.8240	15.5710	9.4497	0.2892	14.8030
47	100.000	77.300	0.257	49.2680	19.4780	9.7300	0.3019	20.0600
48	77.300	59.800	0.257	46.8290	16.3750	9.5877	0.3125	20.9430
49	59.800	46.500	0.252	94.5580	25.1240	12.6240	0.2703	56.8090
50	46.500	36.000	0.256	55.5760	17.2600	9.4859	0.3692	29.0610
51	36.000	27.800	0.258	100.8400	37.6100	10.0540	0.3378	53.1770
52	27.800	21.500	0.257	71.7250	20.8640	9.3085	0.3199	41.5530
53	21.500	16.600	0.259	126.7900	48.1840	10.9890	0.3045	67.6130
54	16.600	12.900	0.252	62.6500	19.0820	9.0356	0.3433	34.5520
55	12.900	10.000	0.255	123.5800	69.5370	10.1480	0.2936	43.8970
56	10.000	7.730	0.257	149.7600	42.2450	9.3761	0.2525	98.1420
57	7.730	5.980	0.257	92.1530	34.2350	8.6229	0.2406	29.2950
58	5.980	4.650	0.252	37.8490	20.4470	8.1794	0.2578	9.2228
59	4.650	3.600	0.256	26.0240	7.3173	8.9011	0.3207	9.8053
60	3.600	2.780	0.258	50.3520	10.5930	9.1420	0.3023	30.6160
61	2.780	2.150	0.257	22.5560	2.3988	9.4467	0.3187	10.7110
62	2.150	1.660	0.259	36.3740	12.2900	9.7524	0.2769	14.3320
63	1.660	1.290	0.252	32.2270	4.7196	10.1380	0.2773	17.3700
64	1.290	1.000	0.255	105.2000	21.4810	10.3110	0.2556	73.4090
65	1.000	0.773	0.257	71.4710	8.6685	10.4060	0.2941	52.3960
66	0.773	0.598	0.257	77.4460	8.3335	10.8950	0.3502	58.2100
67	0.598	0.465	0.252	98.6590	10.9200	11.0820	0.2393	76.6570
68	0.465	0.360	0.256	142.9900	17.2210	11.6050	0.1932	114.1700
69	0.360	0.278	0.258	23.0380	34.1360	11.7800	0.1593	184.4600
70	0.278	0.215	0.257	255.1300	44.0810	11.5840	0.3796	199.4600

A-I-2 Shielding Factor f_x for U-235

		TOTAL			CAPTURE			ELASTIC			REMOVAL			FISSION		
		1000.	100.	10.	1000.	100.	10.	1000.	100.	10.	1000.	100.	10.	1000.	100.	10.
29	300.0	1.004	0.997	0.980	1.001	0.995	0.969	1.000	0.999	0.998	0.927	0.886	0.514	0.999	0.993	0.967
	900.0	1.002	0.998	0.986	1.000	0.996	0.977	1.000	1.000	0.999	0.924	0.888	0.529	0.999	0.995	0.974
	2100.0	1.001	0.998	0.992	1.000	0.997	0.983	1.000	1.000	0.999	0.922	0.887	0.523	0.999	0.996	0.981
30	300.0	1.002	0.994	0.970	0.998	0.990	0.951	1.000	0.999	0.996	0.935	0.875	0.409	0.999	0.992	0.963
	900.0	1.002	0.996	0.979	0.998	0.992	0.961	1.000	0.999	0.997	0.934	0.877	0.423	0.999	0.994	0.972
	2100.0	1.001	0.996	0.985	0.998	0.994	0.969	1.005	1.005	1.004	0.927	0.873	0.417	0.999	0.995	0.981
31	300.0	1.000	0.988	0.953	0.993	0.981	0.926	0.999	0.997	0.992	0.881	0.831	0.467	0.993	0.983	0.937
	900.0	0.998	0.990	0.964	0.991	0.984	0.942	0.999	0.998	0.994	0.871	0.830	0.469	0.992	0.986	0.951
	2100.0	0.996	0.991	0.974	0.991	0.987	0.952	0.999	0.998	0.996	0.867	0.829	0.465	0.993	0.989	0.961
32	300.0	1.005	0.990	0.951	1.000	0.984	0.916	0.999	0.998	0.990	0.970	0.882	0.427	1.000	0.987	0.936
	900.0	1.007	0.995	0.966	1.002	0.990	0.934	1.000	0.999	0.992	0.971	0.884	0.424	1.001	0.991	0.951
	2100.0	1.006	0.995	0.974	1.005	0.995	0.945	1.000	0.999	0.993	0.970	0.883	0.417	1.001	0.993	0.959
33	300.0	0.997	0.980	0.927	0.995	0.978	0.919	0.998	0.996	0.991	0.962	0.868	0.362	0.996	0.977	0.905
	900.0	0.997	0.985	0.945	0.996	0.985	0.942	0.998	0.998	0.995	0.961	0.869	0.358	0.997	0.983	0.925
	2100.0	0.997	0.988	0.958	0.997	0.989	0.955	0.999	0.998	0.997	0.958	0.866	0.348	0.998	0.987	0.937
34	300.0	1.005	0.978	0.902	1.002	0.973	0.885	1.001	0.997	0.985	0.947	0.816	0.309	0.993	0.968	0.878
	900.0	1.008	0.988	0.933	1.002	0.982	0.914	1.001	0.998	0.990	0.949	0.821	0.304	0.994	0.978	0.912
	2100.0	1.008	0.991	0.949	1.002	0.986	0.930	1.001	0.999	0.992	0.957	0.826	0.298	0.996	0.983	0.928
35	300.0	0.996	0.972	0.896	0.989	0.973	0.921	1.000	0.998	0.993	0.885	0.803	0.290	0.993	0.969	0.880
	900.0	1.003	0.989	0.944	0.993	0.985	0.963	1.000	0.999	0.999	0.872	0.797	0.282	0.999	0.984	0.922
	2100.0	1.008	0.999	0.967	0.996	0.992	0.984	1.000	1.000	1.002	0.870	0.800	0.282	1.003	0.994	0.954
36	300.0	0.993	0.954	0.855	0.992	0.955	0.847	0.998	0.992	0.976	0.961	0.830	0.293	0.989	0.961	0.871
	900.0	0.996	0.969	0.893	0.994	0.969	0.888	0.999	0.995	0.983	0.962	0.831	0.282	0.989	0.971	0.905
	2100.0	0.998	0.979	0.925	0.997	0.979	0.914	0.999	0.997	0.988	0.964	0.840	0.284	0.989	0.979	0.934
37	300.0	0.975	0.927	0.825	0.974	0.935	0.829	0.991	0.988	0.975	0.946	0.817	0.276	0.970	0.938	0.848
	900.0	0.983	0.948	0.868	0.979	0.953	0.875	0.993	0.991	0.982	0.947	0.817	0.260	0.978	0.958	0.891
	2100.0	0.992	0.966	0.903	0.986	0.967	0.902	0.995	0.994	0.986	0.949	0.822	0.253	0.985	0.974	0.923
38	300.0	0.998	0.921	0.767	0.972	0.900	0.709	0.997	0.986	0.962	0.936	0.748	0.201	1.001	0.938	0.781
	900.0	1.011	0.952	0.824	0.980	0.927	0.760	0.998	0.990	0.970	0.936	0.749	0.185	1.004	0.958	0.833
	2100.0	1.016	0.970	0.855	0.984	0.941	0.789	0.998	0.992	0.973	0.936	0.754	0.180	0.997	0.966	0.863
39	300.0	0.987	0.913	0.782	0.988	0.923	0.793	0.999	0.989	0.972	0.907	0.718	0.205	0.978	0.921	0.786
	900.0	0.994	0.944	0.845	0.994	0.955	0.865	1.000	0.994	0.985	0.905	0.721	0.186	0.983	0.942	0.836
	2100.0	1.000	0.965	0.893	1.000	0.972	0.905	1.001	0.998	0.993	0.901	0.703	0.172	0.987	0.960	0.883
40	300.0	0.996	0.908	0.758	0.992	0.915	0.760	0.998	0.986	0.967	0.887	0.581	0.190	0.989	0.939	0.840
	900.0	1.006	0.947	0.840	0.997	0.947	0.835	0.999	0.991	0.977	0.887	0.573	0.168	0.994	0.964	0.907
	2100.0	1.009	0.974	0.905	0.994	0.962	0.877	0.999	0.994	0.981	0.886	0.574	0.153	0.995	0.985	0.966
41	300.0	0.990	0.881	0.713	0.986	0.900	0.744	0.996	0.982	0.957	0.920	0.611	0.093	0.985	0.905	0.761
	900.0	1.002	0.925	0.793	0.997	0.945	0.838	0.999	0.989	0.970	0.927	0.611	0.080	0.992	0.933	0.821
	2100.0	1.007	0.952	0.855	1.003	0.973	0.905	1.000	0.994	0.980	0.934	0.616	0.074	0.999	0.954	0.867
42	300.0	0.982	0.847	0.657	0.987	0.863	0.676	1.001	0.987	0.969	0.923	0.629	0.121	0.985	0.882	0.708
	900.0	0.994	0.886	0.720	0.992	0.896	0.739	1.002	0.990	0.973	0.913	0.615	0.107	0.992	0.911	0.763
	2100.0	1.002	0.914	0.762	0.998	0.915	0.788	1.000	0.990	0.971	0.896	0.598	0.097	0.997	0.930	0.800
43	300.0	0.955	0.805	0.580	0.955	0.808	0.572	0.994	0.977	0.951	0.905	0.490	0.148	0.946	0.856	0.645
	900.0	0.981	0.871	0.662	0.971	0.871	0.667	0.996	0.985	0.962	0.877	0.454	0.123	0.965	0.912	0.737
	2100.0	1.015	0.935	0.742	0.989	0.919	0.746	0.999	0.993	0.971	0.867	0.428	0.108	1.000	0.971	0.828
44	300.0	0.943	0.762	0.541	0.972	0.859	0.668	0.993	0.981	0.960	0.958	0.632	0.087	0.930	0.800	0.585
	900.0	0.957	0.814	0.623	0.977	0.910	0.782	0.996	0.988	0.975	0.922	0.615	0.078	0.935	0.832	0.660
	2100.0	0.977	0.860	0.708	0.980	0.939	0.873	1.003	0.998	0.991	0.891	0.604	0.072	0.932	0.850	0.731
45	300.0	0.944	0.760	0.561	0.963	0.806	0.609	0.992	0.972	0.948	0.952	0.643	0.140	0.941	0.819	0.662
	900.0	0.971	0.841	0.684	0.980	0.875	0.733	0.997	0.982	0.959	0.951	0.619	0.102	0.966	0.883	0.763
	2100.0	1.000	0.907	0.804	0.992	0.916	0.815	0.999	0.986	0.961	0.954	0.605	0.078	1.001	0.949	0.894
46	300.0	0.961	0.735	0.470	0.960	0.786	0.505	1.001	0.983	0.965	1.061	0.776	0.170	0.970	0.824	0.585
	900.0	0.982	0.823	0.557	0.979	0.860	0.615	0.999	0.987	0.969	1.141	0.814	0.148	0.983	0.897	0.715
	2100.0	0.995	0.885	0.659	0.984	0.904	0.714	0.997	0.988	0.971	1.316	0.915	0.121	0.978	0.935	0.830
47	300.0	0.957	0.720	0.484	0.965	0.763	0.509	0.996	0.972	0.953	0.962	0.711	0.237	0.983	0.839	0.616
	900.0	0.988	0.818	0.596	0.987	0.852	0.632	1.000	0.985	0.970	0.961	0.719	0.234	0.995	0.908	0.744
	2100.0	1.008	0.883	0.700	0.999	0.908	0.730	0.999	0.991	0.983	0.957	0.728	0.239	1.001	0.946	0.835
48	300.0	0.966	0.658	0.412	0.959	0.722	0.464	0.988	0.967	0.952	0.953	0.677	0.140	0.975	0.757	0.475
	900.0	1.007	0.740	0.462	0.989	0.805	0.556	0.994	0.977	0.959	0.960	0.686	0.112	1.002	0.827	0.553
	2100.0	1.062	0.845	0.538	1.034	0.890	0.659	1.006	0.992	0.970	0.983	0.712	0.090	1.038	0.900	0.643
49	300.0	0.903	0.628	0.405	0.944	0.724	0.472	0.963	0.883	0.834	0.920	0.521	0.135	0.951	0.775	0.566
	900.0	0.936	0.702	0.467	0.967	0.798	0.561	0.982	0.931	0.882	0.938	0.529	0.136	0.969	0.828	0.634
	2100.0	0.957	0.767	0.551	0.978	0.849	0.645	0.992	0.970	0.932	0.916	0.525	0.140	0.981	0.871	0.706

50	300.0	1.091	0.825	0.603	1.044	0.812	0.581	0.983	0.965	0.936	0.763	0.824	0.354	1.046	0.883	0.720
	900.0	1.128	0.894	0.670	1.089	0.890	0.651	0.983	0.964	0.928	0.527	0.613	0.247	1.086	0.945	0.792
	2100.0	1.164	0.973	0.747	1.139	0.973	0.717	0.974	0.957	0.924	0.197	0.282	0.317	1.135	1.018	0.871
51	300.0	0.810	0.431	0.264	0.899	0.621	0.413	0.994	0.961	0.925	0.925	0.591	0.136	0.896	0.616	0.391
	900.0	0.874	0.506	0.295	0.941	0.719	0.485	1.005	0.989	0.934	0.898	0.548	0.137	0.937	0.706	0.466
	2100.0	0.953	0.637	0.378	0.994	0.847	0.613	1.019	1.022	0.975	0.855	0.508	0.134	0.999	0.837	0.575
52	300.0	0.985	0.759	0.550	0.950	0.682	0.526	0.995	0.987	0.980	0.846	0.645	0.573	1.012	0.932	0.796
	900.0	1.005	0.815	0.618	0.967	0.716	0.589	1.008	1.001	0.995	0.834	0.511	0.559	1.019	0.979	0.863
	2100.0	1.024	0.874	0.699	0.985	0.757	0.650	1.004	0.994	0.988	0.787	0.440	0.525	1.030	1.016	0.930
53	300.0	0.602	0.347	0.263	0.626	0.405	0.323	0.921	0.859	0.872	0.945	0.638	0.210	0.728	0.462	0.338
	900.0	0.669	0.373	0.285	0.680	0.447	0.367	0.934	0.863	0.872	0.922	0.622	0.187	0.791	0.513	0.383
	2100.0	0.767	0.435	0.341	0.754	0.527	0.483	0.957	0.883	0.891	0.914	0.628	0.174	0.877	0.601	0.479
54	300.0	0.975	0.777	0.558	0.996	0.882	0.738	0.994	0.985	0.967	0.963	0.765	0.255	1.002	0.872	0.683
	900.0	0.997	0.862	0.672	1.020	0.977	0.899	0.986	0.980	0.965	0.926	0.713	0.232	1.013	0.922	0.794
	2100.0	1.012	0.942	0.823	1.036	1.054	1.049	0.978	0.974	0.965	0.913	0.677	0.215	1.022	0.964	0.880
55	300.0	0.668	0.344	0.260	0.798	0.434	0.294	0.970	0.907	0.895	0.917	0.739	0.175	0.821	0.529	0.416
	900.0	0.754	0.345	0.272	0.868	0.528	0.345	0.982	0.945	0.902	0.923	0.216	0.195	0.879	0.611	0.464
	2100.0	0.835	0.464	0.295	0.928	0.654	0.435	0.965	0.924	0.899	0.895	0.699	0.214	0.932	0.710	0.546
56	300.0	0.681	0.368	0.279	0.789	0.457	0.296	0.965	0.961	0.964	0.977	0.892	0.492	0.809	0.511	0.373
	900.0	0.720	0.385	0.293	0.823	0.489	0.324	0.984	0.961	0.964	0.976	0.890	0.486	0.841	0.540	0.396
	2100.0	0.769	0.413	0.311	0.863	0.535	0.357	0.993	0.964	0.955	1.010	0.912	0.484	0.878	0.581	0.425
57	300.0	0.657	0.372	0.216	0.762	0.443	0.175	0.982	0.977	0.967	0.859	0.595	0.143	0.875	0.591	0.312
	900.0	0.635	0.384	0.217	0.745	0.475	0.181	0.959	0.956	0.944	0.844	0.562	0.109	0.867	0.620	0.322
	2100.0	0.567	0.395	0.244	0.639	0.470	0.220	0.991	0.989	0.980	0.862	0.533	0.114	0.805	0.632	0.380
58	300.0	0.949	0.717	0.417	0.910	0.607	0.320	0.993	0.993	0.985	0.884	0.675	0.107	1.130	1.085	1.166
	900.0	0.982	0.769	0.453	0.914	0.651	0.343	1.023	1.021	1.003	0.952	0.662	0.094	1.184	1.147	1.248
	2100.0	1.003	0.826	0.721	0.899	0.686	0.390	1.025	1.026	1.015	0.929	0.647	0.105	1.272	1.232	1.353
59	300.0	0.847	0.659	0.515	0.814	0.624	0.379	0.996	0.988	0.967	0.895	0.465	0.084	0.793	0.585	0.309
	900.0	0.894	0.653	0.561	0.864	0.603	0.423	1.026	1.014	1.011	0.889	0.681	0.091	0.868	0.403	0.352
	2100.0	0.929	0.752	0.579	0.955	0.784	0.507	0.995	0.991	0.982	0.870	0.504	0.094	0.892	0.699	0.389
60	300.0	1.024	0.903	0.725	1.044	1.060	1.118	1.000	1.001	1.001	0.971	0.777	0.092	1.031	0.952	0.777
	900.0	1.027	0.906	0.798	1.090	0.995	1.064	0.997	0.997	0.998	0.968	0.794	0.244	1.032	0.938	0.867
	2100.0	1.030	0.982	0.934	1.094	1.135	1.195	0.971	0.972	0.970	0.942	0.758	0.216	1.036	1.006	0.939
61	300.0	1.009	1.013	1.015	1.006	1.011	1.016	0.998	0.997	0.994	0.980	0.822	0.428	1.020	1.033	1.057
	900.0	1.019	1.013	1.027	1.036	1.041	1.048	0.994	0.995	0.990	0.976	0.815	0.421	1.037	1.026	1.082
	2100.0	1.034	1.038	1.037	1.144	1.140	1.116	0.968	0.967	0.964	0.949	0.770	0.375	1.069	1.083	1.107
62	300.0	0.987	0.906	0.811	1.001	0.925	0.804	0.999	0.999	0.998	0.984	0.867	0.388	0.993	0.968	0.918
	900.0	0.995	0.938	0.851	1.006	0.959	0.885	0.995	0.996	0.993	0.981	0.864	0.384	1.002	0.994	0.948
	2100.0	0.999	0.965	0.917	1.016	1.001	1.002	0.972	0.972	0.971	0.958	0.842	0.364	1.013	1.010	0.996
63	300.0	0.959	0.938	0.876	0.921	0.888	0.776	0.997	0.996	0.991	0.966	0.748	0.245	0.949	0.927	0.853
	900.0	0.966	0.978	0.876	0.933	0.969	0.774	0.994	0.995	0.987	0.963	0.718	0.245	0.961	0.985	0.855
	2100.0	0.960	0.953	0.886	0.935	0.933	0.811	0.973	0.972	0.967	0.942	0.717	0.226	0.960	0.959	0.878
64	300.0	0.950	0.796	0.605	0.977	0.882	0.718	1.001	1.005	1.007	0.915	0.486	0.112	0.948	0.824	0.642
	900.0	0.947	0.872	0.690	0.972	0.938	0.706	0.998	1.001	1.004	0.911	0.501	0.107	0.945	0.894	0.633
	2100.0	0.925	0.813	0.639	0.954	0.885	0.743	0.979	0.982	0.984	0.888	0.460	0.106	0.919	0.831	0.670
65	300.0	1.028	1.036	1.078	1.067	1.095	1.214	1.000	0.999	0.993	0.944	0.631	0.084	1.028	1.038	1.088
	900.0	1.036	1.014	1.099	1.082	1.032	1.266	0.998	1.000	0.989	0.941	0.628	0.080	1.037	1.016	1.112
	2100.0	1.039	1.060	1.107	1.089	1.156	1.292	1.008	0.977	0.971	0.951	0.614	0.078	1.038	1.047	1.123
66	300.0	0.969	0.953	0.930	0.970	0.956	0.936	0.990	0.988	0.983	0.923	0.466	0.061	0.965	0.947	0.920
	900.0	0.971	0.977	0.928	0.973	0.979	0.937	0.987	0.989	0.980	0.920	0.463	0.061	0.968	0.977	0.919
	2100.0	0.958	0.959	0.936	0.952	0.976	0.957	0.998	0.967	0.963	0.930	0.448	0.058	0.952	0.957	0.930
67	300.0	0.960	0.941	0.868	0.953	0.934	0.919	1.003	1.001	1.003	0.888	0.514	0.182	0.955	0.937	0.923
	900.0	0.962	0.941	0.860	0.955	0.973	0.916	1.000	0.997	0.994	0.886	0.522	0.198	0.958	0.972	0.919
	2100.0	0.962	0.912	0.731	0.955	0.936	0.918	1.000	0.998	0.997	0.886	0.500	0.141	0.958	0.939	0.926

A-I-3 Gradient f_x^1 of f_x for U-235

		TOTAL			CAPTURE			ELASTIC			REMOVAL			FISSION		
		10C0.	100.	10.	1000.	100.	10.	1000.	100.	10.	1000.	100.	10.	1000.	100.	10.
29	300.0	5.0E-04	5.6F-03	4.3E-02	8.3E-05	1.2E-03	1.5E-02	1.1E-05	1.5E-04	1.5E-03	1.6E-03	1.7E-02	4.7E-02	4.1E-05	8.1E-04	1.3E-02
	900.0	4.6E-04	5.0E-03	3.9E-02	4.8E-05	7.0E-04	9.8E-03	7.9E-06	9.7E-05	1.0E-03	2.0E-03	2.1E-02	6.0E-02	2.1E-05	5.0E-04	8.8E-03
	2100.0	4.1E-04	4.2E-03	3.7E-02	1.4E-05	3.0E-04	6.7E-03	4.3E-06	5.7E-05	6.5E-04	2.2E-03	2.3E-02	4.7E-02	4.9E-06	2.5E-04	5.2E-03
30	300.0	4.8E-04	5.2E-03	4.1E-02	2.9E-05	1.5E-04	1.1E-02	3.9E-06	8.3E-05	1.6E-03	2.0E-03	1.8E-02	2.4E-02	3.0E-06	4.2E-04	1.2E-02
	900.0	4.3E-04	4.8E-03	3.7E-02	5.2E-05	1.9E-04	6.9E-03	1.4E-06	4.6E-05	1.1E-03	2.1E-03	1.9E-02	2.7E-02	2.7E-05	4.8E-05	7.6E-03
	2100.0	4.0E-04	4.2E-03	3.7E-02	6.7E-05	4.5E-04	4.4E-03	1.1E-06	7.9E-06	6.7E-04	2.1E-03	2.0E-02	2.3E-02	3.4E-05	1.4E-04	4.6E-03
31	300.0	4.5E-04	5.1E-03	4.3E-02	4.2E-05	4.5E-05	1.2E-02	1.1E-05	1.8E-04	2.6E-03	2.6E-03	2.6E-02	8.2E-02	1.2E-04	8.5E-04	6.4E-03
	900.0	3.8E-04	4.3E-03	3.9E-02	1.5E-04	1.4E-03	1.4E-03	3.2E-06	2.1E-05	1.0E-03	3.0E-03	3.1E-02	9.3E-02	1.8E-04	1.7E-03	4.9E-04
	2100.0	3.9E-04	4.1E-03	3.8E-02	2.1E-04	2.2E-03	6.1E-04	1.3E-05	1.4E-04	8.5E-04	3.1E-03	3.2E-02	7.8E-02	1.9E-04	1.8E-03	9.6E-04
32	300.0	3.8E-04	4.8E-03	4.2E-02	5.9E-05	1.6E-04	8.8E-03	5.3E-06	1.1E-04	1.7E-03	7.2E-04	5.8E-03	5.1E-02	1.2E-05	6.1E-04	1.5E-02
	900.0	4.4E-04	5.4E-03	4.3E-02	5.3E-06	5.8E-04	1.6E-03	9.6E-06	1.4E-04	1.5E-03	7.4E-04	5.9E-03	5.0E-02	1.1E-05	6.5E-04	1.1E-02
	2100.0	5.0E-04	6.0E-03	3.7E-02	2.5E-05	7.6E-04	2.5E-03	1.2E-05	1.3E-04	7.5E-04	9.0E-04	7.3E-03	4.7E-02	1.4E-05	5.5E-04	7.4E-03
33	300.0	2.6E-04	3.6E-03	3.2E-02	1.1E-04	4.2E-04	6.4E-03	2.7E-05	2.6E-04	2.5E-03	1.5E-03	1.3E-02	3.0E-01	3.1E-05	5.3E-04	5.5E-03
	900.0	2.6E-04	3.4E-03	3.0E-02	1.2E-04	7.9E-04	2.7E-03	2.8E-05	3.1E-04	1.9E-03	1.5E-03	1.3E-02	3.1E-01	5.4E-05	1.1E-05	1.6E-03
	2100.0	3.0E-04	3.6E-03	2.7E-02	1.1E-04	8.1E-04	8.5E-04	2.3E-05	2.7E-04	2.4E-03	1.5E-03	1.3E-02	3.1E-01	4.3E-05	4.3E-05	4.9E-03
34	300.0	2.3E-04	4.0E-03	4.3E-02	1.2E-05	1.8E-03	3.2E-02	1.8E-06	2.6E-04	3.7E-03	1.7E-03	1.4E-02	1.6E-02	1.5E-04	2.6E-04	1.7E-02
	900.0	3.2E-04	4.7E-03	4.4E-02	1.3E-05	1.3E-03	2.5E-02	3.9E-06	2.6E-04	3.2E-03	2.1E-03	1.7E-02	1.7E-02	2.2E-04	5.4E-04	9.5E-03
	2100.0	4.2E-04	5.5E-03	3.4E-02	6.5E-06	8.7E-04	1.8E-02	2.5E-06	2.2E-04	2.2E-03	2.1E-03	1.8E-02	1.0E-02	4.2E-04	7.2E-04	5.0E-03
35	300.0	2.8E-04	3.9E-03	4.4E-02	1.3E-04	2.1E-04	2.0E-02	9.3E-06	9.7E-05	2.8E-03	2.4E-03	3.1E-02	4.0E-02	1.8E-04	4.3E-04	2.3E-02
	900.0	4.2E-04	4.8E-03	4.4E-02	6.9E-05	1.9E-05	1.5E-02	2.9E-06	7.2E-05	2.0E-03	2.8E-03	3.5E-02	4.8E-02	8.7E-05	1.0E-04	1.9E-02
	2100.0	5.0E-04	5.6E-03	3.5E-02	1.9E-05	3.3E-04	6.9E-03	3.6E-06	1.2E-04	1.2E-03	3.1E-03	3.8E-02	3.5E-02	3.3E-06	7.8E-04	1.0E-02
36	300.0	1.4E-04	3.0E-03	3.8E-02	1.2E-04	9.6E-05	2.0E-02	9.8E-06	2.1E-04	3.2E-03	1.5E-03	2.6E-02	1.6E-02	9.0E-05	3.8E-04	2.2E-02
	900.0	1.7E-04	2.9E-03	3.5E-02	1.3E-04	8.4E-04	8.5E-03	1.4E-06	1.7E-04	2.2E-03	1.6E-03	2.9E-02	1.5E-02	1.1E-04	3.5E-04	1.4E-02
	2100.0	2.1E-04	2.9E-03	3.0E-02	9.8E-05	7.2E-04	6.7E-03	7.0E-07	1.1E-04	1.8E-03	1.7E-03	3.1E-02	1.1E-02	1.7E-04	1.6E-03	9.0E-03
37	300.0	4.4E-04	7.7E-03	7.5E-02	1.7E-04	1.1E-03	4.5E-02	7.6E-05	6.7E-04	1.6E-03	2.5E-03	5.1E-02	4.4E-02	2.4E-05	2.7E-03	4.3E-02
	900.0	4.0E-04	7.3E-03	7.8E-02	1.6E-04	1.9E-05	3.8E-02	5.2E-05	5.0E-04	1.7E-03	2.6E-03	5.6E-02	3.5E-02	4.3E-05	2.1E-03	3.9E-02
	2100.0	4.1E-04	7.4E-03	6.8E-02	1.6E-04	1.0E-04	3.3E-02	3.3E-05	3.3E-04	2.7E-03	2.6E-03	5.9E-02	3.4E-02	2.3E-05	1.6E-03	3.0E-02
38	300.0	3.6E-04	6.4E-03	5.2E-02	2.4E-04	8.1E-05	8.6E-03	6.2E-06	3.8E-04	3.0E-03	1.0E-03	6.7E-03	9.6E-03	2.2E-04	4.9E-03	4.6E-02
	900.0	2.9E-04	5.7E-03	4.9E-02	1.7E-04	1.7E-04	2.8E-03	3.5E-07	3.0E-04	2.0E-03	1.2E-03	8.1E-03	7.6E-03	1.8E-04	3.9E-03	3.8E-02
	2100.0	1.3E-04	4.0E-03	3.9E-02	1.4E-04	3.7E-04	4.3E-04	1.2E-05	6.6E-05	1.1E-03	1.4E-03	9.6E-03	1.2E-03	5.8E-06	1.0E-03	1.9E-02
39	300.0	4.8E-04	8.0E-03	5.8E-02	9.8E-05	5.0E-03	5.1E-02	3.8E-05	1.1E-03	1.0E-02	1.4E-03	1.1E-02	1.1E-02	8.4E-05	3.4E-03	3.8E-02
	900.0	4.0E-04	6.5E-03	4.8E-02	1.1E-04	3.9E-03	3.8E-02	3.5E-05	8.2E-04	7.8E-03	1.5E-03	1.2E-02	7.8E-03	2.1E-05	1.7E-03	2.5E-02
	2100.0	3.2E-04	5.2E-03	3.6E-02	1.1E-04	3.3E-03	2.6E-02	3.9E-05	7.5E-04	5.6E-03	1.8E-03	1.3E-02	3.6E-03	9.7E-05	5.9E-04	1.8E-02
40	300.0	2.8E-04	8.1E-03	7.1E-02	8.2E-05	4.5E-03	3.6E-02	1.8E-05	7.2E-04	4.6E-03	1.0E-03	1.1E-02	1.0E-02	2.1E-04	5.9E-03	5.9E-02
	900.0	2.2E-04	7.4E-03	7.5E-02	2.2E-05	3.2E-03	2.9E-02	1.2E-05	4.3E-04	3.0E-03	1.4E-03	1.6E-02	4.7E-03	2.1E-04	5.3E-03	5.4E-02
	2100.0	2.5E-04	7.6E-03	5.8E-02	8.6E-05	1.5E-03	1.9E-02	1.2E-05	1.4E-04	3.9E-03	1.9E-03	2.2E-02	6.0E-04	2.4E-04	5.1E-03	4.1E-02
41	300.0	1.7E-04	6.7E-03	5.4E-02	2.0E-04	6.1E-03	4.9E-02	4.8E-05	1.2E-03	9.3E-03	3.0E-04	2.2E-03	6.7E-03	5.5E-05	4.1E-03	3.9E-02
	900.0	2.1E-04	6.0E-03	5.2E-02	2.3E-04	4.9E-03	4.1E-02	5.1E-05	1.0E-03	7.8E-03	5.0E-04	1.0E-03	6.8E-03	2.2E-05	2.7E-03	2.8E-02
	2100.0	2.2E-04	5.1E-03	3.9E-02	2.1E-04	3.7E-03	2.8E-02	4.8E-05	8.0E-04	5.4E-03	7.1E-04	3.7E-04	9.9E-03	6.0E-05	1.2E-03	2.0E-02
42	300.0	-3.2E-05	5.0E-03	5.4E-02	8.3E-07	5.2E-03	7.2E-02	3.0E-05	1.1E-03	9.8E-03	3.6E-04	7.6E-04	1.0E-03	1.2E-05	4.3E-03	4.9E-02
	900.0	-7.3E-05	3.7E-03	4.5E-02	5.9E-05	3.2E-03	5.5E-02	2.8E-05	1.1E-03	9.9E-03	5.1E-04	1.8E-03	4.3E-04	2.3E-05	2.9E-03	3.4E-02
	2100.0	-5.5E-05	3.2E-03	4.3E-02	1.5E-04	8.4E-04	4.7E-02	2.1E-05	9.0E-04	8.1E-03	6.5E-04	3.1E-03	1.6E-03	1.6E-05	2.5E-03	3.0E-02
43	300.0	1.9E-04	8.0E-03	5.3E-02	2.0E-04	5.3E-03	1.6E-02	5.2E-05	1.1E-03	4.6E-03	6.1E-04	6.4E-03	5.1E-03	6.4E-06	5.3E-03	4.1E-02
	900.0	2.0E-04	7.9E-03	5.8E-02	1.9E-04	3.7E-03	6.9E-03	5.2E-05	1.1E-03	3.5E-03	8.1E-04	1.3E-02	1.9E-03	3.6E-05	5.1E-03	3.9E-02
	2100.0	2.8E-04	9.5E-03	3.3E-02	2.0E-04	3.5E-03	4.5E-03	6.8E-05	1.2E-03	2.9E-03	1.1E-03	2.1E-02	8.9E-04	1.4E-04	6.4E-03	2.0E-02
44	300.0	1.2E-04	5.1E-03	4.4E-02	2.5E-04	2.1E-03	5.2E-02	5.0E-06	6.0E-04	6.9E-03	8.3E-04	6.1E-04	4.8E-03	4.7E-04	1.6E-03	1.2E-02
	900.0	1.3E-04	3.9E-03	3.7E-02	2.8E-04	6.0E-04	3.4E-02	3.0E-05	7.2E-04	7.6E-03	1.6E-03	6.6E-03	1.9E-03	4.8E-04	3.0E-03	5.8E-03
	2100.0	7.1E-04	9.8E-03	3.2E-02	9.1E-05	1.5E-03	2.1E-02	1.4E-04	2.0E-03	7.5E-03	2.2E-03	1.4E-02	5.6E-03	3.6E-04	2.9E-03	6.5E-03
45	300.0	5.9E-05	9.3E-03	7.1E-02	1.6E-05	6.9E-03	5.9E-02	5.7E-05	6.4E-04	7.9E-03	5.9E-04	4.8E-03	3.7E-02	4.1E-05	6.4E-03	6.5E-02
	900.0	-3.1E-06	6.8E-03	6.4E-02	6.1E-05	4.2E-03	3.6E-02	6.1E-05	3.5E-04	5.9E-03	7.0E-04	4.3E-03	2.4E-02	1.7E-06	3.9E-03	3.6E-02
	2100.0	1.2E-04	6.3E-03	4.6E-02	1.9E-05	3.0E-03	1.7E-02	6.0E-05	1.9E-04	4.4E-03	7.2E-04	5.2E-03	1.3E-02	8.3E-05	3.6E-03	2.1E-02
46	300.0	1.1E-03	2.0E-02	1.0E-01	7.0E-04	1.5E-02	1.1E-01	1.4E-04	2.6E-03	2.2E-02	1.1E-03	1.7E-03	3.6E-03	7.4E-04	1.6E-02	1.2E-01
	900.0	3.4E-04	1.2E-02	1.0E-01	4.3E-04	1.1E-02	9.8E-02	8.4E-05	1.8E-03	2.0E-02	1.0E-03	3.2E-03	1.7E-02	4.2E-04	1.0E-02	1.0E-01
	2100.0	-1.8E-05	3.4E-03	1.1E-01	3.0E-04	5.7E-03	8.1E-02	6.5E-05	1.2E-03	1.7E-02	2.0E-03	5.1E-03	1.3E-02	2.6E-04	4.0E-03	8.1E-02
47	300.0	9.2E-05	5.6E-03	2.0E-02	2.7E-04	6.7E-03	1.8E-02	8.2E-05	1.5E-03	5.3E-03	6.0E-04	2.1E-03	1.8E-02	1.3E-04	5.1E-03	2.3E-02
	900.0	-2.4E-05	4.1E-03	1.4E-02	2.3E-04	5.0E-03	5.8E-03	6.7E-05	1.2E-03	3.6E-03	7.2E-04	8.0E-04	1.7E-02	1.1E-04	3.2E-03	9.0E-03
	2100.0	1.4E-04	4.8E-03	1.4E-03	3.3E-04	4.5E-03	9.2E-03	9.4E-05	1.3E-03	1.8E-03	8.9E-04	8.0E-04	1.7E-02	1.6E-04	2.5E-03	4.5E-03
48	300.0	1.3E-03	1.9E-02	7.9E-02	6.9E-04	1.4E-02	8.0E-02	8.2E-05	2.1E-03	1.5E-02	4.2E-04	7.0E-04	2.6E-03	9.1E-04	1.5E-02	8.1E-02
	900.0	1.2E-03	2.0E-02	9.5E-02	6.2E-04	1.3E-02	8.6E-02	8.7E-05	2.1E-03	1.6E-02	4.4E-04	6.2E-04	1.9E-03	8.6E-04	1.4E-02	8.5E-02
	2100.0	1.2E-03	2.2E-02	1.2E-01	8.3E-04	1.5E-02	8.0E-02	7.0E-05	1.8E-03	1.2E-02	4.7E-04	4.5E-04	2.2E-03	9.5E-04	1.5E-02	7.8E-02
49	300.0	4.6E-04	8.2E-03	1.2E-02	2.0E-04	5.9E-03	4.6E-03	2.9E-04	4.1E-03	9.1E-03	1.7E-04	3.8E-03	8.2E-03	2.2E-04	5.3E-03	4.4E-05
	900.0	3.3E-04	7.0E-03	9.5E-03	8.8E-05	3.8E-03	4.9E-03	2.0E-04	3.2E-03	4.4E-03	2.0E-04	3.3E-03	7.2E-03	1.4E-04	3.8E-03	7.1E-03
	2100.0	2.5E-04	5.7E-03	3.6E-03	2.9E-05	2.2E-03	1.5E-02	1.6E-04	2.2E-03	9.9E-04	2.3E-04	2.1E-03	4.7E-03	8.7E-05	2.4E-03	1.4E-02

```
50  300.0 7.9E-04 2.0E-02 6.4E-02 1.4E-03 2.1E-02 6.1E-02-4.2E-05 1.1E-04 7.9E-04-8.1E-03-9.7E-02-3.0E-01 1.0E-03 1.7E-02 6.3E-02
    900.0 4.8E-04 1.7E-02 5.8E-02 1.1E-03 1.8E-02 5.3E-02-3.1E-05 2.3E-04 1.3E-03-6.1E-03-8.1E-02-2.4E-01 7.9E-04 1.4E-02 5.3E-02
   2100.0 2.7E-04 1.3E-02 4.1E-02 8.9E-04 1.5E-02 4.9E-02 3.2E-06 4.6E-04-9.5E-04-2.6E-03-4.3E-02-2.7E-01 5.5E-04 1.1E-02 5.0E-02

51  300.0 2.4E-03 1.7E-02 3.4E-02 8.5E-04 1.4E-02 4.2E-02 2.7E-05 2.9E-03 7.5E-05-1.5E-04 9.5E-04 8.1E-02 7.5E-04 1.4E-02 4.7E-02
    900.0 2.3E-03 2.2E-02 3.1E-02 8.1E-04 1.6E-02 2.4E-02-1.3E-05 2.9E-03 1.4E-02-1.2E-04 2.2E-03 1.8E-02 7.3E-04 1.7E-02 2.6E-02
   2100.0 1.8E-03 2.4E-02 3.8E-02 8.5E-04 2.0E-02 3.4E-02-9.0E-05 1.9E-03 7.2E-04-6.9E-05 3.7E-03 8.2E-03 7.9E-04 2.1E-02 7.1E-02

52  300.0 1.2E-03 1.6E-02 1.0E-01 4.3E-04 4.2E-03 5.1E-02 9.0E-06 3.1E-04 0.0    -5.6E-03-5.6E-02-2.4E-01 8.1E-04 1.1E-02 6.1E-02
    900.0 1.0E-03 1.5E-02 1.2E-01 3.1E-04 1.0E-02 4.8E-02 1.2E-05 5.8E-04 1.3E-04-5.7E-03-7.8E-05-2.4E-01 7.6E-04 1.9E-03 5.6E-02
   2100.0 9.1E-04 9.7E-03 1.2E-01 2.4E-04-7.8E-04 4.0E-02-1.0E-05-2.4E-04-1.2E-03-5.9E-03-4.6E-02-2.0E-01 7.3E-04 6.1E-03 4.3E-02

53  300.0 1.8E-03 6.8E-03 3.9E-02 9.2E-04 5.0E-04-2.4E-02 2.2E-04-1.0E-03-2.0E-02 6.6E-05 8.4E-03 3.7E-02 1.3E-03 6.5E-03 9.5E-03
    900.0 1.9E-03 7.4E-03 3.1E-02 8.9E-04 6.3E-04-4.4E-02 2.1E-04-5.4E-04-2.2E-02 5.4E-05 8.1E-03 3.4E-02 1.3E-03 7.2E-03 1.7E-03
   2100.0 1.5E-03 7.3E-03 2.3E-02 7.7E-04 4.9E-04-3.9E-02 1.5E-04-3.0E-04-8.5E-03-9.9E-06 6.7E-03 2.7E-02 1.2E-03 8.5E-03-3.0E-03

54  300.0 2.2E-04 6.7E-03 4.0E-02 1.6E-04 6.0E-03 4.6E-02-3.3E-06 2.5E-04 1.4E-03-5.2E-04-5.8E-03-1.0E-02 5.2E-05 3.2E-03 4.4E-02
    900.0 1.3E-04 5.1E-03 2.0E-02 5.8E-05 3.2E-03-1.1E-02-3.7E-06 1.5E-04 2.7E-03-4.9E-04-5.2E-03-1.3E-02 1.3E-05 1.8E-03-2.7E-02
   2100.0 6.4E-05 2.6E-03 3.4E-02 5.2E-06 8.3E-04 1.2E-02-5.2E-06-2.6E-06 4.1E-04-5.1E-04-6.1E-03-2.9E-03-1.3E-05 4.3E-04 2.3E-02

55  300.0 1.4E-03 1.1E-02 1.7E-02 9.7E-04 1.7E-02 5.2E-03 2.8E-04 8.3E-03 1.7E-02-1.8E-03-8.1E-02 3.1E-03 7.9E-04 1.5E-02 1.4E-02
    900.0 1.3E-03 8.1E-02 2.0E-02 7.5E-04 6.6E-02 5.8E-03 2.2E-04 6.3E-03 1.4E-02-1.7E-03 1.5E-01-5.3E-03 6.3E-04 5.2E-02 1.4E-02
   2100.0 1.2E-03 8.9E-03 2.5E-02 5.9E-04 4.2E-03-3.4E-03 1.7E-04 6.7E-04 1.6E-02-1.6E-03 7.7E-04-9.3E-03 5.1E-04 4.4E-03 1.0E-02

56  300.0 1.2E-03 6.2E-03 1.2E-02 5.4E-04 2.2E-03-5.5E-03 2.2E-04 1.7E-03 3.7E-03-2.0E-03-1.6E-02-6.1E-02 5.5E-04 2.4E-03-5.4E-03
    900.0 1.2E-03 6.8E-03 7.5E-03 4.7E-04 2.1E-03-1.1E-02 2.0E-04 1.6E-03 2.1E-03-2.0E-03-1.6E-02-4.7E-02 4.8E-04 2.4E-03-8.8E-03
   2100.0 1.1E-03 7.1E-03 1.3E-02 3.7E-04 1.9E-03-6.6E-03 1.5E-04 1.2E-03 1.4E-03-2.1E-03-1.7E-02-5.9E-02 3.9E-04 2.1E-03-7.2E-03

57  300.0-4.5E-03-1.3E-02-1.0E-02-4.3E-03-1.3E-02-1.5E-02-1.3E-04-1.2E-03-5.8E-03-4.6E-03-2.7E-02-3.1E-02-3.7E-03-1.2E-02-8.7E-03
    900.0-4.3E-03-1.5E-02 3.2E-03-4.5E-03-1.8E-02 1.9E-02-1.1E-04-9.8E-04 7.9E-03-4.6E-03-2.5E-02 8.5E-02-3.9E-03-1.7E-02 2.8E-02
   2100.0-3.5E-03-1.6E-02-1.2E-02-4.0E-03-2.4E-02-2.8E-02-1.1E-04-1.3E-03-4.6E-03-4.8E-03-2.4E-02-2.0E-02-3.7E-03-2.2E-02-2.2E-02

58  300.0 1.1E-03 4.5E-03 9.0E-03 1.0E-03 2.6E-03 1.4E-02 1.6E-05 4.9E-05-1.0E-03 1.4E-04-1.1E-02-4.3E-03-4.7E-05 1.1E-03 1.9E-02
    900.0 1.0E-03 4.9E-03 4.1E-03 9.1E-04 1.9E-03 1.7E-02 4.1E-05 4.6E-05 1.6E-03 3.9E-04-6.9E-03 2.8E-02-1.2E-04 8.1E-04-2.1E-02
   2100.0 8.3E-04 4.1E-03 1.3E-02 8.1E-04 1.3E-03 1.9E-02 2.5E-05 2.9E-06-1.1E-03 5.2E-04-4.6E-03 4.8E-04-2.5E-04 8.1E-04 2.8E-02

59  300.0-4.5E-05 3.0E-03 6.1E-03-2.1E-04 1.0E-03 1.9E-03-2.2E-05-7.6E-05 9.3E-04-3.1E-04 3.3E-03 4.4E-03-2.5E-04 9.9E-04 4.3E-03
    900.0-6.7E-05 1.4E-02 2.1E-03-2.3E-04 1.6E-02-9.2E-03-1.0E-05 1.4E-03 2.1E-03-3.8E-04-3.8E-02-1.6E-02-2.7E-04 4.9E-02 2.0E-02
   2100.0-9.5E-05 2.7E-03 7.3E-03-2.3E-04 7.9E-05-1.0E-04-1.0E-05-1.4E-05 5.1E-04-4.4E-04 6.7E-04 1.5E-03-2.9E-04 1.3E-04 3.6E-03

60  300.0 1.7E-04 3.9E-03 2.0E-02 2.5E-04 1.5E-03-4.5E-03 0.0      3.6E-05 4.4E-04-4.8E-04-1.2E-03 2.1E-02 6.3E-05 1.4E-03 1.0E-02
    900.0 1.4E-04 9.7E-03 3.6E-02 2.2E-04 2.0E-02 9.0E-02 3.7E-07 8.7E-05 4.1E-04-4.9E-04-4.6E-03 1.2E-02 5.0E-05 8.6E-03 4.0E-02
   2100.0 1.0E-04 2.3E-03 3.3E-02 2.1E-04 6.8E-04 1.2E-01 7.3E-07 1.4E-05 5.9E-03-4.9E-04-1.6E-03 7.5E-02 3.7E-05 6.8E-04 4.1E-02

61  300.0 2.5E-05 1.4E-04 1.2E-02 1.9E-05-1.7E-04 3.0E-02-4.2E-06-5.3E-06-5.6E-04-5.1E-04-1.3E-03-1.1E-02 4.4E-05 0.0      1.6E-02
    900.0 2.5E-05 2.2E-03-4.0E-03 1.5E-05-8.3E-05-1.0E-02-4.6E-06-3.8E-04 1.1E-03-5.1E-04-2.0E-03-3.0E-02 4.4E-05 5.1E-03-1.8E-02
   2100.0 2.2E-05 1.7E-04 1.1E-02-8.3E-06-1.3E-04 2.5E-02-4.6E-06-7.9E-06-5.8E-04-5.0E-04-6.9E-04-6.0E-03 4.7E-05 4.6E-05 1.6E-02

62  300.0 1.0E-04 2.8E-03 6.7E-03 1.0E-04 1.5E-03-1.1E-02-6.9E-07 7.7E-06 1.5E-04-3.5E-04-1.6E-03 2.3E-02 1.6E-05 3.1E-04-4.7E-03
    900.0 8.2E-05 2.3E-03 2.6E-02 9.2E-05 2.4E-03 2.5E-02-1.0E-06-2.3E-04 1.5E-03-3.5E-04-1.7E-03 2.0E-02 1.4E-05-1.2E-03 1.6E-02
   2100.0-5.7E-05 1.7E-03 7.1E-03-3.6E-04 6.1E-04-1.3E-02 2.6E-05-1.0E-05-5.1E-05-2.9E-04-1.7E-03 2.5E-02 5.8E-05 3.5E-05-5.2E-03

63  300.0-2.9E-05 2.7E-04-7.8E-05-5.9E-05 1.2E-04-2.3E-03-3.3E-06 0.0     -2.5E-04-3.3E-04 1.3E-03 1.1E-02-3.8E-05 7.2E-05-2.0E-03
    900.0-3.1E-05-6.5E-03 2.2E-02-6.1E-05-1.4E-02 4.3E-02-3.3E-06-4.9E-04 2.2E-03-3.3E-04 6.0E-03-1.4E-02-4.0E-05-9.3E-03 3.0E-02
   2100.0 8.8E-04 3.1E-04-7.7E-05 1.7E-03 1.3E-04-2.4E-03 5.3E-05 2.4E-06-2.7E-04-3.3E-04 1.4E-03 1.0E-02 1.1E-03 8.6E-05-2.2E-03

64  300.0 1.7E-05 3.5E-03-1.1E-02-1.7E-05 1.3E-03-2.5E-02 0.0     -4.8E-05-2.4E-04-2.7E-04 8.5E-03-1.1E-02-3.4E-05 1.7E-03-2.3E-02
    900.0 1.1E-05-1.0E-02 7.5E-02-1.7E-05-9.8E-03 7.6E-02 0.0      9.7E-05 4.9E-04-2.7E-04 4.2E-03 2.9E-03-3.5E-05-1.2E-02 7.4E-02
   2100.0 7.3E-04 2.8E-03-1.3E-02 4.0E-04 1.0E-03-2.5E-02-1.9E-05-2.4E-05 0.0     -4.6E-05 8.2E-03-1.1E-02 8.5E-04 1.5E-03-2.3E-02

65  300.0 3.9E-05 7.9E-04 2.0E-02 8.2E-05 1.5E-03 4.6E-02-3.2E-06-7.2E-05-1.7E-03-3.9E-04-3.0E-03-1.0E-01 3.4E-05 6.7E-04 2.0E-02
    900.0 4.2E-05 6.9E-03-3.4E-02 8.6E-05 1.8E-02-9.5E-02-3.2E-06-8.4E-04 2.6E-03-3.9E-04-3.0E-03-9.2E-02 3.6E-05 7.1E-03-4.1E-02
   2100.0-1.1E-04 9.8E-04 2.3E-02-2.3E-04 2.0E-03 5.4E-02-5.5E-04-7.2E-05-1.7E-03-9.1E-04-3.5E-03-1.1E-01-1.7E-05 8.2E-04 2.3E-02

66  300.0-1.1E-05 1.4E-04-4.8E-03-9.6E-06 9.3E-05-3.9E-03 0.0      0.0     -1.1E-03-3.0E-04 4.6E-03-5.5E-02-1.2E-05 1.2E-04-6.0E-03
    900.0-1.0E-05-4.3E-03 1.4E-02-9.6E-06-4.0E-03 9.9E-03-3.1E-06-8.0E-04 3.2E-03-2.9E-04 4.4E-03-5.8E-02-1.1E-05-5.1E-03 1.6E-02
   2100.0 6.2E-04 8.7E-05-4.8E-03 1.0E-03 5.7E-05-3.7E-03-5.1E-04 0.0     -1.1E-03-8.0E-04 3.3E-03-5.5E-02 7.8E-04 6.4E-05-6.0E-03

67  300.0-9.5E-06 2.8E-05 6.1E-03-1.2E-05 0.0     -2.7E-03-3.0E-06 0.0     -1.1E-02-1.8E-04 1.1E-03-2.9E-01-1.1E-05 0.0     -3.5E-03
    900.0-9.1E-06-5.1E-03 1.9E-02-9.2E-06-7.4E-03 6.9E-03 0.0      2.9E-04 1.4E-02-1.8E-04-1.7E-03-3.0E-01-1.1E-05-6.6E-03 9.4E-03
   2100.0-9.1E-06 2.5E-04-7.7E-03-9.2E-06 2.5E-04-2.7E-03 0.0      0.0     -4.5E-04-1.8E-04 1.3E-02-1.5E-01-1.1E-05 3.8E-04-2.5E-02
```

A-II-1 Table of infinite dilution cross section for U-238

GROUP	UPPER E	LOWER E	LETHERGY	TOTAL	CAPTURE	ELASTIC	REMOVAL	FISSION
26	21500.000	16600.000	0.259	15.0850	0.5679	14.5170	0.4357	
27	16600.000	12900.000	0.252	15.2220	0.6605	14.5610	0.4653	
28	12900.000	10000.000	0.255	16.0190	0.7538	15.3240	0.5064	
29	10000.000	7730.000	0.257	16.1740	0.7825	15.3920	0.7061	
30	7730.000	5980.000	0.257	16.8100	0.9285	15.8810	0.6422	
31	5980.000	4650.000	0.252	18.0670	1.0405	17.0270	0.9394	
32	4650.000	3600.000	0.256	17.3510	1.0370	16.3140	0.4608	
33	3600.000	2780.000	0.258	15.7070	1.1611	14.5460	0.3578	
34	2780.000	2150.000	0.257	19.5380	1.4391	18.0990	0.8427	
35	2150.000	1660.000	0.259	21.0310	1.3361	19.6950	1.1871	
36	1660.000	1290.000	0.252	17.8870	1.3669	16.5200	0.3837	
37	1290.000	1000.000	0.255	21.6990	2.1608	19.5380	0.5333	
38	1000.000	773.000	0.257	26.6120	2.5144	24.0960	0.3414	
39	773.000	598.000	0.257	18.5840	2.0895	16.4950	0.4517	
40	598.000	465.000	0.252	20.1060	3.3508	16.7550	0.3593	
41	465.000	360.000	0.256	14.3160	2.1882	12.1280	0.3505	
42	360.000	278.000	0.258	24.3680	3.9980	20.3700	0.3468	
43	278.000	215.000	0.257	23.9540	6.9742	16.9798	0.3567	
44	215.000	166.000	0.259	94.3290	13.2600	81.0690	0.3118	
45	166.000	129.000	0.252	13.9150	2.3132	11.6020	0.4449	
46	129.000	100.000	0.255	154.4400	43.9020	110.5400	0.0260	
47	100.000	77.300	0.257	13.8220	4.8460	8.9759	0.3547	
48	77.300	59.800	0.257	101.6000	37.1830	64.4120	0.2755	
49	59.800	46.500	0.252	10.8380	0.0913	10.7470	0.4109	
50	46.500	36.000	0.256	381.5500	146.3400	235.2200	10.6780	
51	36.000	27.800	0.258	7.6306	1.8829	5.7477	0.2864	
52	27.800	21.500	0.257	15.3390	2.2467	13.0920	0.8421	
53	21.500	16.600	0.259	313.8800	229.1100	84.7710	0.2203	
54	16.600	12.900	0.252	8.4866	0.3073	8.1793	0.2621	
55	12.900	10.000	0.255	9.5775	0.4367	9.1408	0.2761	
56	10.000	7.730	0.257	11.5000	1.1151	10.3850	0.3735	
57	7.730	5.980	0.257	548.4600	508.1800	40.2810	0.1562	
58	5.980	4.650	0.252	9.9528	2.8831	7.0697	0.2585	
59	4.650	3.600	0.256	8.9976	0.8501	8.1475	0.2736	
60	3.600	2.780	0.258	9.0693	0.5612	8.5041	0.2789	
61	2.780	2.150	0.257	9.1640	0.4742	8.6897	0.2848	
62	2.150	1.660	0.259	9.2539	0.4495	8.8045	0.2426	
63	1.660	1.290	0.252	9.3348	0.4534	8.8815	0.2413	
64	1.290	1.000	0.255	9.4106	0.4745	8.9361	0.2196	
65	1.000	0.773	0.257	9.4378	0.5061	8.9316	0.2442	
66	0.773	0.598	0.257	9.6102	0.5573	9.0529	0.2829	
67	0.598	0.465	0.252	9.6443	0.5795	9.0648	0.2245	
68	0.465	0.360	0.256	9.6950	0.6106	9.0844	0.2981	
69	0.360	0.278	0.258	9.8481	0.7258	9.1223	0.2970	
70	0.278	0.215	0.257	9.9567	0.7838	9.1729	0.2998	

A-II-2 Shielding factor f_x^0 for U-238

		1000.	100.	10.	1.	1000.	100.	10.	1.	1000.	100.	10.	1.	1000.	100.	10.	1.
26	300.0	0.994	0.954	0.874	0.836	0.998	0.977	0.912	0.793	0.997	0.976	0.922	0.891	1.000	0.994	0.998	0.669
	900.0	0.996	0.969	0.902	0.864	0.999	0.987	0.946	0.834	0.998	0.984	0.949	0.913	1.000	1.000	1.031	0.672
	2100.0	0.998	0.977	0.924	0.887	1.000	0.992	0.962	0.859	1.000	0.989	0.957	0.931	1.000	0.995	1.008	0.679
27	300.0	0.993	0.946	0.860	0.831	0.997	0.970	0.888	0.837	0.997	0.972	0.919	0.891	0.979	0.949	0.879	0.589
	900.0	0.992	0.958	0.877	0.847	0.998	0.982	0.931	0.897	0.994	0.976	0.926	0.908	0.978	0.954	0.887	0.578
	2100.0	0.998	0.974	0.918	0.893	0.999	0.989	0.954	0.930	1.000	0.988	0.954	0.941	0.981	0.958	0.893	0.601
28	300.0	0.982	0.905	0.778	0.719	0.995	0.963	0.872	0.809	0.986	0.941	0.850	0.811	0.963	0.908	0.766	0.484
	900.0	0.991	0.935	0.821	0.770	0.997	0.979	0.921	0.874	0.992	0.961	0.885	0.850	0.963	0.923	0.800	0.500
	2100.0	1.000	0.965	0.889	0.857	0.998	0.986	0.946	0.912	1.000	0.981	0.932	0.910	0.970	0.931	0.805	0.533
29	300.0	0.982	0.888	0.743	0.674	0.994	0.948	0.832	0.765	0.991	0.936	0.828	0.777	0.951	0.796	0.556	0.345
	900.0	0.990	0.925	0.797	0.741	0.997	0.971	0.890	0.840	0.995	0.959	0.872	0.827	0.959	0.829	0.581	0.357
	2100.0	0.997	0.949	0.842	0.797	0.999	0.983	0.928	0.889	0.996	0.972	0.905	0.866	0.960	0.852	0.602	0.367
30	300.0	0.914	0.860	0.705	0.633	0.991	0.929	0.784	0.720	0.986	0.917	0.797	0.743	0.959	0.862	0.627	0.314
	900.0	0.984	0.899	0.756	0.698	0.995	0.957	0.852	0.805	0.992	0.943	0.840	0.791	0.993	0.904	0.657	0.318
	2100.0	0.993	0.928	0.802	0.750	0.998	0.974	0.901	0.866	0.998	0.962	0.875	0.830	1.038	0.947	0.684	0.322
31	300.0	0.958	0.805	0.646	0.562	0.987	0.916	0.774	0.708	0.979	0.878	0.740	0.679	0.926	0.713	0.441	0.244
	900.0	0.973	0.853	0.699	0.635	0.994	0.951	0.847	0.796	0.986	0.913	0.789	0.737	0.942	0.764	0.467	0.250
	2100.0	0.978	0.884	0.739	0.681	0.997	0.970	0.893	0.849	0.987	0.933	0.826	0.778	0.933	0.782	0.483	0.255
32	300.0	0.936	0.798	0.644	0.560	0.978	0.865	0.676	0.600	0.980	0.876	0.742	0.685	0.976	0.890	0.711	0.509
	900.0	0.972	0.845	0.689	0.630	0.986	0.910	0.755	0.695	0.986	0.911	0.784	0.733	0.983	0.917	0.737	0.521
	2100.0	0.979	0.881	0.727	0.672	0.992	0.939	0.816	0.769	0.989	0.953	0.819	0.768	1.005	0.953	0.769	0.531
33	300.0	0.963	0.847	0.729	0.677	0.982	0.885	0.692	0.602	0.981	0.905	0.811	0.776	0.988	0.970	0.780	0.519
	900.0	0.976	0.882	0.768	0.728	0.989	0.925	0.772	0.691	0.988	0.930	0.844	0.815	0.988	0.971	0.782	0.503
	2100.0	0.981	0.908	0.801	0.765	0.993	0.950	0.833	0.763	0.990	0.946	0.871	0.847	0.967	0.948	0.768	0.486
34	300.0	0.919	0.713	0.567	0.480	0.959	0.740	0.563	0.476	0.957	0.810	0.664	0.610	0.932	0.697	0.373	0.236
	900.0	0.946	0.766	0.604	0.548	0.976	0.854	0.642	0.554	0.972	0.855	0.705	0.655	0.958	0.773	0.409	0.243
	2100.0	0.966	0.816	0.643	0.588	0.984	0.896	0.707	0.617	0.985	0.894	0.749	0.694	0.944	0.806	0.439	0.250
35	300.0	0.855	0.626	0.481	0.303	0.929	0.715	0.483	0.393	0.920	0.729	0.586	0.504	0.908	0.612	0.339	0.172
	900.0	0.893	0.662	0.501	0.351	0.952	0.778	0.553	0.457	0.943	0.769	0.611	0.531	0.926	0.672	0.359	0.170
	2100.0	0.918	0.696	0.527	0.417	0.963	0.822	0.611	0.516	0.958	0.803	0.638	0.562	0.901	0.693	0.373	0.169
36	300.0	0.898	0.699	0.581	0.479	0.933	0.705	0.464	0.376	0.946	0.795	0.674	0.621	0.993	0.952	0.827	0.492
	900.0	0.932	0.742	0.609	0.544	0.960	0.782	0.540	0.442	0.966	0.837	0.706	0.660	0.993	0.951	0.816	0.458
	2100.0	0.956	0.787	0.638	0.586	0.979	0.842	0.619	0.515	0.980	0.875	0.740	0.698	0.990	0.947	0.807	0.426
37	300.0	0.865	0.636	0.508	0.414	0.917	0.659	0.399	0.314	0.926	0.747	0.616	0.564	0.990	0.923	0.712	0.400
	900.0	0.907	0.684	0.539	0.477	0.947	0.743	0.485	0.395	0.951	0.794	0.652	0.606	0.990	0.919	0.702	0.380
	2100.0	0.936	0.734	0.573	0.521	0.963	0.807	0.566	0.480	0.969	0.837	0.691	0.647	0.996	0.924	0.701	0.367
38	300.0	0.760	0.472	0.356	0.250	0.854	0.499	0.250	0.184	0.863	0.604	0.457	0.395	0.980	0.971	0.879	0.583
	900.0	0.823	0.517	0.398	0.300	0.906	0.600	0.316	0.228	0.904	0.658	0.488	0.432	0.980	0.969	0.864	0.552
	2100.0	0.869	0.566	0.401	0.344	0.939	0.686	0.385	0.283	0.932	0.710	0.522	0.472	0.978	0.965	0.850	0.520
39	300.0	0.862	0.677	0.594	0.554	0.868	0.539	0.280	0.219	0.927	0.785	0.697	0.669	0.967	0.954	0.839	0.483
	900.0	0.901	0.713	0.613	0.585	0.913	0.635	0.352	0.276	0.950	0.818	0.718	0.689	0.972	0.956	0.833	0.433
	2100.0	0.930	0.749	0.634	0.607	0.941	0.712	0.422	0.335	0.967	0.851	0.741	0.707	1.001	0.979	0.833	0.380
40	300.0	0.836	0.587	0.504	0.472	0.845	0.435	0.186	0.139	0.924	0.744	0.639	0.611	0.965	0.967	0.901	0.705
	900.0	0.891	0.633	0.520	0.495	0.906	0.549	0.249	0.183	0.955	0.791	0.667	0.638	0.966	0.965	0.883	0.663
	2100.0	0.925	0.682	0.539	0.513	0.943	0.650	0.323	0.245	0.970	0.831	0.695	0.666	0.973	0.967	0.859	0.612
41	300.0	0.957	0.840	0.772	0.763	0.925	0.626	0.307	0.239	0.988	0.942	0.904	0.897	0.989	0.980	0.943	0.758
	900.0	0.974	0.873	0.789	0.775	0.956	0.734	0.414	0.345	0.993	0.957	0.915	0.907	0.989	0.977	0.925	0.687
	2100.0	0.983	0.901	0.807	0.790	0.970	0.806	0.511	0.450	0.996	0.968	0.926	0.917	0.989	0.974	0.908	0.623
42	300.0	0.894	0.497	0.458	0.453	0.731	0.320	0.125	0.088	0.826	0.628	0.561	0.552	0.985	0.980	0.945	0.694
	900.0	0.761	0.519	0.461	0.456	0.811	0.408	0.161	0.110	0.875	0.662	0.571	0.558	0.985	0.977	0.930	0.606
	2100.0	0.817	0.548	0.466	0.457	0.867	0.494	0.202	0.135	0.912	0.702	0.585	0.568	0.986	0.976	0.917	0.515
43	300.0	0.739	0.508	0.468	0.464	0.727	0.282	0.106	0.083	0.898	0.791	0.664	0.656	0.980	0.970	0.926	0.781
	900.0	0.812	0.537	0.471	0.465	0.818	0.378	0.138	0.108	0.932	0.767	0.676	0.664	0.979	0.964	0.910	0.749
	2100.0	0.864	0.577	0.478	0.469	0.878	0.477	0.182	0.142	0.954	0.804	0.692	0.677	0.979	0.957	0.890	0.709
44	300.0	0.280	0.134	0.092	0.083	0.457	0.160	0.077	0.068	0.470	0.224	0.146	0.130	1.004	1.003	0.909	0.588
	900.0	0.338	0.138	0.092	0.083	0.561	0.202	0.087	0.073	0.549	0.248	0.151	0.132	1.074	1.039	0.855	0.542
	2100.0	0.439	0.194	0.140	0.133	0.663	0.254	0.094	0.070	0.661	0.316	0.198	0.177	1.289	1.199	0.934	0.816
45	300.0	0.972	0.880	0.816	0.789	0.934	0.813	0.276	0.231	0.997	0.985	0.968	0.948	0.999	0.995	0.911	0.748
	900.0	0.979	0.900	0.825	0.792	0.925	0.693	0.349	0.318	0.997	0.988	0.970	0.946	1.000	0.995	0.902	0.707
	2100.0	0.992	0.933	0.859	0.798	0.992	0.814	0.457	0.400	0.999	0.993	0.982	0.936	0.996	0.996	0.919	0.615
46	300.0	0.237	0.117	0.088	0.083	0.381	0.126	0.054	0.034	0.431	0.208	0.147	0.139	1.023	1.039	0.808	0.365
	900.0	0.293	0.120	0.089	0.084	0.480	0.154	0.056	0.034	0.516	0.232	0.152	0.142	1.254	1.346	1.054	0.536
	2100.0	0.358	0.115	0.078	0.072	0.579	0.190	0.057	0.030	0.595	0.247	0.135	0.114	3.346	3.885	2.371	1.009
47	300.0	0.891	0.693	0.602	0.491	0.855	0.444	0.187	0.142	0.987	0.957	0.921	0.817	0.999	0.991	0.920	0.454
	900.0	0.927	0.727	0.603	0.486	0.909	0.552	0.231	0.162	0.990	0.962	0.918	0.805	0.999	0.990	0.906	0.370
	2100.0	0.951	0.772	0.618	0.512	0.939	0.641	0.277	0.181	0.993	0.968	0.918	0.856	1.054	0.990	0.887	0.329

48	300.0	0.240	0.134	0.111	0.113	0.359	0.109	0.045	0.028	0.458	0.246	0.196	0.201	0.998	0.996	0.955	0.615
	900.0	0.302	0.137	0.111	0.113	0.472	0.139	0.048	0.029	0.553	0.273	0.201	0.203	0.998	0.989	0.954	0.611
	2100.0	0.391	0.155	0.121	0.126	0.586	0.184	0.055	0.031	0.655	0.324	0.224	0.228	1.079	0.989	0.951	0.656
49	300.0	0.998	0.997	0.992	0.984	1.001	1.001	1.003	0.997	0.998	0.998	0.996	0.992	0.998	0.993	0.973	0.880
	900.0	0.998	0.997	0.992	0.984	1.001	1.002	1.004	0.997	0.998	0.998	0.996	0.992	0.998	0.993	0.973	0.873
	2100.0	0.999	0.998	0.993	1.045	1.001	1.002	1.005	1.023	0.999	0.998	0.996	1.052	1.046	0.992	0.968	0.907
50	300.0	0.125	0.064	0.047	0.042	0.229	0.068	0.020	0.008	0.282	0.134	0.090	0.075	0.464	0.159	0.033	0.007
	900.0	0.143	0.063	0.047	0.042	0.297	0.076	0.021	0.008	0.347	0.144	0.091	0.075	0.876	0.237	0.041	0.008
	2100.0	0.171	0.059	0.045	0.041	0.380	0.083	0.022	0.008	0.421	0.154	0.089	0.072	1.439	0.337	0.046	0.009
51	300.0	1.033	1.022	0.940	0.916	1.164	1.229	1.073	0.787	0.994	0.984	0.973	1.047	0.995	0.989	0.963	1.063
	900.0	1.078	1.058	0.948	0.919	1.289	1.369	1.135	0.808	1.015	1.003	0.983	1.055	0.993	0.986	0.961	1.072
	2100.0	1.178	0.843	0.981	0.659	1.429	1.388	1.167	0.812	1.132	1.073	0.990	1.001	0.926	0.987	0.968	1.017
52	300.0	0.950	0.911	0.810	0.754	0.865	0.795	0.608	0.435	0.972	0.960	0.912	0.864	0.981	0.848	0.435	0.179
	900.0	0.957	0.915	0.811	0.754	0.875	0.818	0.618	0.440	0.975	0.963	0.913	0.864	1.005	0.860	0.430	0.176
	2100.0	0.903	0.884	0.733	0.712	0.726	0.920	0.681	0.450	0.955	0.934	0.884	0.815	1.102	0.870	0.366	0.150
53	300.0	0.123	0.045	0.028	0.026	0.280	0.087	0.035	0.030	0.321	0.138	0.091	0.104	1.009	1.009	1.011	1.052
	900.0	0.158	0.044	0.027	0.026	0.370	0.104	0.037	0.031	0.405	0.153	0.091	0.102	1.002	1.008	1.015	1.063
	2100.0	0.213	0.043	0.025	0.025	0.473	0.135	0.037	0.033	0.499	0.175	0.085	0.092	1.015	1.014	1.020	0.981
54	300.0	0.998	0.998	0.998	0.993	1.013	1.013	1.010	1.035	0.997	0.997	0.998	0.993	0.997	0.993	0.976	0.873
	900.0	0.998	0.998	0.998	0.993	1.014	1.013	1.010	1.036	0.997	0.997	0.998	0.992	0.997	0.992	0.975	0.866
	2100.0	0.998	0.998	0.999	0.996	1.012	1.012	1.009	1.058	0.998	0.997	0.999	0.932	1.035	0.990	0.936	0.765
55	300.0	0.997	0.996	0.992	0.981	0.983	0.974	0.933	0.808	0.998	0.998	0.997	0.992	0.995	0.973	0.845	0.533
	900.0	0.996	0.995	0.992	0.981	0.959	0.953	0.924	0.800	0.998	0.998	0.997	0.992	0.994	0.973	0.849	0.530
	2100.0	0.996	0.995	0.994	0.976	0.960	0.947	0.946	0.767	0.998	0.998	0.998	0.936	1.066	0.972	0.832	0.393
56	300.0	0.984	0.982	0.972	0.944	0.911	0.905	0.873	0.739	0.992	0.991	0.988	0.973	0.997	0.974	0.809	0.417
	900.0	0.985	0.983	0.973	0.946	0.923	0.918	0.885	0.755	0.992	0.992	0.988	0.974	0.998	0.974	0.808	0.414
	2100.0	0.986	0.983	0.978	0.904	0.931	0.918	0.920	0.780	0.993	0.991	0.992	0.924	0.955	0.973	0.788	0.383
57	300.0	0.144	0.059	0.039	0.034	0.287	0.088	0.033	0.020	0.478	0.344	0.323	0.313	0.979	0.881	0.544	0.374
	900.0	0.174	0.058	0.039	0.034	0.356	0.099	0.035	0.020	0.535	0.356	0.325	0.315	0.972	0.871	0.535	0.362
	2100.0	0.227	0.059	0.038	0.032	0.440	0.120	0.040	0.021	0.596	0.369	0.319	0.303	0.903	0.865	0.570	0.314
58	300.0	1.034	1.038	1.019	0.981	1.180	1.208	1.150	0.957	0.974	0.971	0.979	1.006	0.995	0.978	1.052	1.391
	900.0	1.038	1.042	1.021	0.982	1.197	1.229	1.161	0.963	0.973	0.970	0.979	1.006	0.994	0.976	1.057	1.392
	2100.0	1.033	1.045	0.997	0.943	1.144	1.213	1.021	0.974	0.975	0.967	0.993	0.948	0.939	0.972	1.058	1.322

A-III-1 Table of infinite dilution cross section for Pu-239

GROUP	UPPER E	LOWER E	LETHERGY	TOTAL	CAPTURE	ELASTIC	REMOVAL	FISSION
29	10000.000	7730.000	0.257	14.3150	1.3390	10.8050	0.3472	2.1706
30	7730.000	5980.000	0.257	14.5430	1.4334	10.8610	0.3602	2.2501
31	5980.000	4650.000	0.252	15.9520	1.8894	11.4890	0.4171	2.5918
32	4650.000	3600.000	0.256	15.8700	2.0707	11.2350	0.3656	2.5878
33	3600.000	2780.000	0.258	17.2210	2.4856	11.8650	0.3283	2.8790
34	2780.000	2150.000	0.257	18.9660	3.2882	12.2560	0.3612	3.4286
35	2150.000	1660.000	0.259	19.2820	3.8134	11.8650	0.4918	3.5999
36	1660.000	1290.000	0.252	21.0410	3.9388	12.5900	0.3711	4.5164
37	1290.000	1000.000	0.255	19.7300	3.5775	10.9420	0.3568	5.2899
38	1000.000	773.000	0.257	27.2820	5.6348	13.3350	0.3824	8.3120
39	773.000	598.000	0.257	26.8790	6.9404	13.2840	0.3622	6.6543
40	598.000	465.000	0.252	33.2610	8.1922	13.4420	0.3023	11.6270
41	465.000	360.000	0.256	23.7720	4.9540	10.2040	0.3714	8.7170
42	360.000	278.000	0.258	35.9290	11.0060	14.5150	0.6168	10.4080
43	278.000	215.000	0.257	68.4340	14.6250	28.1860	0.3909	25.6230
44	215.000	166.000	0.259	38.3620	7.1746	11.3290	0.4008	19.8580
45	166.000	129.000	0.252	51.2510	19.4630	18.0750	0.3073	13.7130
46	129.000	100.000	0.255	47.6470	14.6420	11.6880	0.2880	21.3160
47	100.000	77.300	0.257	64.6250	8.2582	14.6170	0.6051	41.7500
48	77.300	59.800	0.257	191.3100	45.2080	41.1710	0.4152	104.9300
49	59.800	46.500	0.252	144.5100	51.4960	20.3210	0.3276	72.6890
50	46.500	36.000	0.256	88.5590	60.6880	17.2360	0.2601	10.6340
51	36.000	27.800	0.258	16.3420	3.6903	9.2511	0.3735	3.4007
52	27.800	21.500	0.257	133.9700	60.0080	12.4940	0.1792	61.4640
53	21.500	16.600	0.259	75.5950	27.8490	10.4760	0.2901	37.2700
54	16.600	12.900	0.252	196.9600	81.3330	12.8310	0.2794	102.8000
55	12.900	10.000	0.255	274.0098	88.7980	11.0750	0.1920	174.1400
56	10.000	7.730	0.257	155.1500	70.5320	9.8806	0.8568	74.7370
57	7.730	5.980	0.257	44.1200	12.9250	6.5921	0.2426	24.6020
58	5.980	4.650	0.252	15.9970	0.9379	7.8841	0.2673	7.1750
59	4.650	3.600	0.256	16.3670	0.8222	8.2613	0.2739	7.2833
60	3.600	2.780	0.258	18.3030	1.0093	8.5536	0.2560	8.7400
61	2.780	2.150	0.257	21.6240	1.4457	8.8238	0.2897	11.3540
62	2.150	1.660	0.259	26.7800	2.2568	9.1039	0.2516	15.4190
63	1.660	1.290	0.252	34.6140	3.7243	9.4134	0.2582	21.4770
64	1.290	1.000	0.255	46.9860	6.5249	9.7796	0.2432	30.6820
65	1.000	0.773	0.257	68.4770	12.4850	10.2070	0.2820	45.7850
66	0.773	0.598	0.257	115.9300	28.0570	11.0320	0.3527	76.8390
67	0.598	0.465	0.252	245.8600	77.0640	12.1940	0.3118	156.6000
68	0.465	0.360	0.256	894.7400	336.7500	15.9470	0.2693	542.0498
69	0.360	0.278	0.258	3934.5000	1577.0000	21.9370	0.2806	2335.5999
70	0.278	0.215	0.257	3093.2000	1229.7998	11.8560	0.3270	1851.5999

A-III-2 Shielding factor f_x^0 for Pu-239

		TOTAL			CAPTURE			ELASTIC			REMOVAL			FISSION		
		1000.	100.	10.	1000.	100.	10.	1000.	100.	10.	1000.	100.	10.	1000.	100.	10.
29	300.0	1.010	0.993	0.944	0.996	0.980	0.913	1.001	0.995	0.974	0.896	0.851	0.539	0.997	0.991	0.944
	900.0	1.008	0.997	0.964	0.994	0.985	0.937	1.001	0.997	0.982	0.882	0.840	0.532	1.000	0.995	0.959
	2100.0	1.006	0.998	0.974	0.995	0.988	0.950	1.001	0.998	0.987	0.871	0.831	0.526	1.001	0.995	0.971
30	300.0	1.010	0.986	0.919	0.999	0.974	0.882	1.002	0.993	0.962	0.896	0.845	0.496	0.996	0.978	0.911
	900.0	1.011	0.994	0.944	0.997	0.981	0.912	1.001	0.995	0.972	0.889	0.842	0.493	1.002	0.988	0.932
	2100.0	1.011	0.999	0.959	0.998	0.986	0.930	1.001	0.997	0.978	0.880	0.835	0.488	1.002	0.993	0.952
31	300.0	1.005	0.974	0.904	0.993	0.966	0.887	0.996	0.985	0.962	0.808	0.751	0.282	1.001	0.980	0.922
	900.0	1.012	0.993	0.950	1.000	0.984	0.939	0.999	0.993	0.982	0.797	0.745	0.257	1.002	1.005	0.954
	2100.0	1.017	1.005	0.982	1.005	0.994	0.968	1.002	0.998	0.996	0.795	0.745	0.270	1.007	0.999	0.978
32	300.0	0.995	0.956	0.864	0.979	0.942	0.820	0.992	0.977	0.934	0.980	0.901	0.486	1.000	0.972	0.891
	900.0	1.000	0.975	0.911	0.984	0.959	0.872	0.993	0.983	0.955	0.974	0.900	0.480	0.999	0.991	0.925
	2100.0	1.001	0.985	0.941	0.986	0.970	0.902	0.996	0.990	0.971	0.964	0.895	0.476	0.992	0.979	0.938
33	300.0	0.984	0.926	0.815	0.985	0.933	0.806	0.993	0.967	0.906	0.943	0.876	0.404	0.984	0.950	0.856
	900.0	0.984	0.951	0.874	0.983	0.955	0.878	0.992	0.978	0.936	0.944	0.879	0.387	0.985	0.969	0.903
	2100.0	0.984	0.963	0.911	0.982	0.966	0.918	0.992	0.984	0.955	0.942	0.878	0.375	0.990	0.977	0.935
34	300.0	0.999	0.921	0.762	1.007	0.930	0.722	0.996	0.961	0.881	0.969	0.851	0.399	0.994	0.948	0.835
	900.0	1.011	0.959	0.831	1.011	0.959	0.795	0.999	0.975	0.912	0.971	0.860	0.391	0.995	0.986	0.890
	2100.0	1.017	0.977	0.874	1.010	0.971	0.834	0.999	0.982	0.931	0.986	0.875	0.391	1.001	0.979	0.926
35	300.0	0.976	0.895	0.732	0.985	0.907	0.721	0.997	0.965	0.895	0.859	0.669	0.285	0.987	0.930	0.767
	900.0	0.980	0.930	0.796	0.987	0.941	0.804	0.996	0.976	0.922	0.728	0.612	0.272	0.982	0.951	0.823
	2100.0	0.988	0.950	0.838	0.992	0.957	0.846	0.998	0.983	0.937	0.706	0.602	0.266	0.980	0.958	0.857
36	300.0	0.990	0.865	0.682	0.991	0.895	0.701	0.996	0.949	0.875	0.975	0.763	0.199	1.008	0.917	0.739
	900.0	1.007	0.926	0.773	0.997	0.944	0.819	0.999	0.975	0.930	0.974	0.760	0.167	1.019	1.033	0.833
	2100.0	1.015	0.961	0.843	0.997	0.966	0.890	1.001	0.990	0.971	0.971	0.758	0.129	1.023	0.966	0.896
37	300.0	0.994	0.862	0.669	0.994	0.855	0.621	0.992	0.961	0.901	0.936	0.717	0.358	0.997	0.851	0.587
	900.0	1.018	0.919	0.743	0.992	0.908	0.730	0.994	0.973	0.924	0.938	0.697	0.331	1.037	0.939	0.684
	2100.0	1.026	0.951	0.799	0.995	0.932	0.797	0.994	0.979	0.940	0.927	0.679	0.314	1.047	0.945	0.741
38	300.0	0.954	0.767	0.541	0.982	0.819	0.522	0.985	0.902	0.786	0.925	0.745	0.268	0.973	0.831	0.574
	900.0	0.980	0.840	0.618	0.985	0.883	0.642	0.989	0.931	0.825	0.919	0.749	0.241	0.978	0.910	0.640
	2100.0	1.007	0.899	0.695	0.983	0.914	0.721	0.996	0.954	0.861	0.896	0.738	0.221	0.983	0.902	0.701
39	300.0	0.938	0.705	0.491	0.941	0.743	0.452	0.966	0.868	0.757	0.889	0.774	0.379	0.974	0.780	0.501
	900.0	0.975	0.785	0.558	0.975	0.831	0.568	0.981	0.903	0.790	0.936	0.790	0.338	1.003	0.933	0.588
	2100.0	0.999	0.848	0.629	1.001	0.892	0.664	0.992	0.930	0.822	0.975	0.795	0.304	1.021	0.905	1.567
40	300.0	0.877	0.621	0.410	0.900	0.658	0.379	0.960	0.850	0.738	0.892	0.684	0.341	0.925	0.723	0.430
	900.0	0.894	0.686	0.452	0.919	0.738	0.471	0.962	0.880	0.768	0.887	0.669	0.300	0.915	0.798	0.482
	2100.0	0.909	0.734	0.491	0.927	0.782	0.534	0.960	0.896	0.792	0.869	0.629	0.265	0.908	0.789	0.526
41	300.0	0.994	0.811	0.612	1.002	0.830	0.586	0.999	0.966	0.926	0.931	0.737	0.320	0.986	0.833	0.593
	900.0	1.021	0.877	0.677	1.024	0.909	0.720	1.002	0.978	0.943	0.930	0.736	0.277	1.002	0.979	0.663
	2100.0	1.050	0.937	0.759	1.035	0.964	0.845	1.009	0.992	0.969	0.929	0.737	0.247	1.036	0.948	0.763
42	300.0	0.930	0.626	0.423	0.946	0.647	0.352	0.976	0.843	0.725	0.899	0.595	0.189	0.973	0.777	0.538
	900.0	0.978	0.741	0.504	0.983	0.770	0.487	0.994	0.895	0.774	0.927	0.622	0.158	0.994	0.953	0.677
	2100.0	1.011	0.843	0.609	1.000	0.856	0.611	1.013	0.943	0.831	0.949	0.644	0.136	1.007	0.937	0.806
43	300.0	0.751	0.497	0.355	0.797	0.444	0.240	0.759	0.498	0.400	0.869	0.484	0.139	0.975	0.849	0.709
	900.0	0.801	0.552	0.398	0.855	0.532	0.309	0.819	0.537	0.421	0.863	0.443	0.107	0.987	1.014	0.810
	2100.0	0.835	0.607	0.477	0.885	0.611	0.410	0.852	0.570	0.449	0.646	0.303	0.060	0.985	0.970	0.946
44	300.0	0.920	0.655	0.435	0.994	0.703	0.356	0.994	0.937	0.875	0.937	0.615	0.134	0.967	0.745	0.463
	900.0	0.943	0.721	0.460	1.017	0.815	0.449	1.007	0.961	0.895	0.898	0.582	0.103	0.995	0.919	0.519
	2100.0	1.041	0.822	0.486	0.981	0.863	0.542	1.024	0.985	0.881	1.015	0.678	0.100	1.060	0.912	0.595
45	300.0	0.795	0.439	0.310	0.841	0.442	0.207	0.905	0.681	0.577	0.972	0.867	0.460	0.947	0.698	0.503
	900.0	0.847	0.506	0.339	0.888	0.545	0.266	0.937	0.732	0.603	0.984	0.859	0.374	0.976	0.945	0.595
	2100.0	0.850	0.567	0.356	0.904	0.646	0.352	0.918	0.754	0.603	0.879	0.750	0.276	0.991	0.870	0.705
46	300.0	0.732	0.440	0.293	0.858	0.509	0.260	0.961	0.861	0.803	1.096	0.966	0.471	0.867	0.526	0.272
	900.0	0.741	0.486	0.323	0.849	0.592	0.323	0.972	0.882	0.812	1.190	1.036	0.465	0.869	0.684	0.323
	2100.0	0.796	0.535	0.353	0.931	0.681	0.383	1.002	0.920	0.841	1.279	1.168	0.446	0.856	0.613	0.367
47	300.0	0.758	0.437	0.279	0.820	0.456	0.255	0.935	0.808	0.726	0.998	0.885	0.450	0.848	0.520	0.284
	900.0	0.810	0.456	0.284	0.873	0.505	0.274	0.951	0.821	0.731	1.007	0.879	0.450	0.884	0.647	0.302
	2100.0	0.885	0.519	0.312	0.923	0.577	0.315	1.059	0.931	0.814	1.069	0.938	0.462	0.919	0.614	0.339
48	300.0	0.439	0.195	0.183	0.593	0.284	0.278	0.587	0.358	0.348	0.903	0.489	0.510	0.604	0.327	0.326
	900.0	0.471	0.199	0.188	0.639	0.316	0.317	0.635	0.379	0.372	0.947	0.479	0.520	0.614	0.402	0.348
	2100.0	0.534	0.219	0.206	0.697	0.359	0.365	0.737	0.442	0.435	1.111	0.548	0.571	0.654	0.364	0.381
49	300.0	0.699	0.340	0.187	0.699	0.355	0.219	0.816	0.632	0.568	0.966	0.740	0.365	0.917	0.674	0.387
	900.0	0.768	0.389	0.196	0.779	0.434	0.268	0.863	0.678	0.599	0.967	0.700	0.348	0.946	0.820	0.430
	2100.0	0.825	0.451	0.219	0.838	0.525	0.350	0.847	0.675	0.595	0.794	0.555	0.263	0.974	0.825	0.510

50	300.0	0.630	0.216	0.166	0.738	0.249	0.110	0.856	0.588	0.541	0.493	0.487	0.278	0.763	0.304	0.193
	900.0	0.796	0.237	0.167	0.864	0.319	0.128	0.932	0.635	0.557	0.309	0.275	0.164	0.884	0.637	0.218
	2100.0	0.944	0.291	0.176	0.972	0.423	0.165	0.985	0.691	0.576	0.095	0.096	0.049	1.004	0.494	0.288
51	300.0	0.993	0.851	0.699	0.998	0.789	0.470	0.990	0.988	0.983	0.978	0.939	0.781	0.978	0.823	0.511
	900.0	1.008	0.894	0.721	1.036	0.884	0.550	0.990	0.987	0.986	0.980	0.927	0.811	0.983	0.938	0.547
	2100.0	1.041	0.953	0.771	1.161	1.052	0.720	0.994	0.992	0.988	0.996	0.937	0.742	1.013	0.912	0.626
52	300.0	0.639	0.250	0.185	0.822	0.416	0.210	0.973	0.879	0.843	0.658	0.509	0.191	0.742	0.332	0.145
	900.0	0.727	0.299	0.182	0.892	0.524	0.263	0.990	0.907	0.851	0.634	0.459	0.166	0.792	0.481	0.170
	2100.0	0.800	0.400	0.185	0.945	0.676	0.369	1.007	0.954	0.869	0.601	0.387	0.120	0.832	0.473	0.221
53	300.0	0.682	0.324	0.231	0.730	0.290	0.114	0.997	0.948	0.920	0.981	0.813	0.295	0.755	0.353	0.176
	900.0	0.756	0.330	0.230	0.804	0.324	0.119	1.009	0.955	0.925	0.981	0.798	0.291	0.821	0.480	0.181
	2100.0	0.848	0.355	0.234	0.886	0.382	0.131	1.031	0.977	0.943	0.970	0.793	0.276	0.899	0.438	0.195
54	300.0	0.561	0.301	0.193	0.617	0.265	0.148	0.892	0.811	0.761	0.973	0.895	0.647	0.770	0.528	0.278
	900.0	0.609	0.308	0.197	0.673	0.284	0.166	0.913	0.821	0.764	0.971	0.877	0.640	0.810	0.602	0.408
	2100.0	0.655	0.323	0.201	0.723	0.314	0.171	0.927	0.830	0.767	0.961	0.860	0.636	0.845	0.581	0.408
55	300.0	0.518	0.186	0.086	0.707	0.351	0.159	0.952	0.900	0.890	0.893	0.709	0.194	0.670	0.286	0.095
	900.0	0.578	0.190	0.086	0.770	0.392	0.171	0.968	0.913	0.893	0.886	0.677	0.195	0.709	0.332	0.101
	2100.0	0.645	0.205	0.085	0.837	0.460	0.192	0.988	0.939	0.904	0.855	0.640	0.179	0.768	0.331	0.106
56	300.0	0.311	0.168	0.143	0.392	0.150	0.071	0.914	0.839	0.786	0.463	0.073	0.009	0.413	0.202	0.154
	900.0	0.335	0.169	0.143	0.411	0.146	0.072	0.909	0.831	0.785	0.402	0.085	0.008	0.436	0.245	0.156
	2100.0	0.366	0.174	0.144	0.432	0.169	0.074	0.891	0.819	0.769	0.368	0.071	0.008	0.463	0.229	0.162
57	300.0	2.526	1.159	0.794	3.470	1.766	1.090	0.939	0.931	0.959	0.731	0.612	0.387	2.511	1.521	1.092
	900.0	2.968	1.333	0.799	4.097	2.520	1.192	0.975	0.958	0.963	0.728	0.580	0.387	2.838	2.252	1.147
	2100.0	3.782	1.411	0.877	5.067	2.708	1.567	1.009	0.952	0.957	0.707	0.554	0.358	3.352	2.033	1.359
58	300.0	1.005	1.000	1.006	1.056	1.029	1.068	0.991	0.995	0.989	0.777	0.915	0.592	1.017	1.011	1.020
	900.0	1.005	0.997	1.006	1.059	0.994	1.064	0.991	0.999	0.989	0.771	0.930	0.592	1.018	1.011	1.019
	2100.0	1.002	1.000	1.002	1.077	1.063	1.083	0.979	0.980	0.977	0.742	0.910	0.585	1.021	1.016	1.023
59	300.0	0.999	0.997	0.991	0.999	0.997	0.991	0.999	0.999	0.996	0.986	0.915	0.531	0.998	0.996	0.987
	900.0	0.999	0.997	0.991	0.999	0.997	0.991	0.999	0.999	0.996	0.986	0.915	0.531	0.998	0.996	0.987
	2100.0	0.999	0.997	0.991	0.999	0.997	0.991	0.999	0.999	0.996	0.986	0.915	0.531	0.998	0.996	0.987
60	300.0	0.997	0.993	0.983	0.993	0.986	0.965	0.999	0.999	0.996	1.075	0.977	0.486	0.994	0.989	0.973
	900.0	0.997	0.993	0.983	0.993	0.986	0.965	0.999	0.999	0.996	1.075	0.977	0.486	0.994	0.992	0.973
	2100.0	0.997	0.993	0.983	0.993	0.986	0.965	0.999	0.999	0.996	1.075	0.977	0.486	0.994	0.989	0.973
61	300.0	0.994	0.988	0.971	0.987	0.975	0.942	0.999	0.998	0.996	0.978	0.857	0.400	0.991	0.982	0.959
	900.0	0.994	0.988	0.971	0.987	0.975	0.942	0.999	0.998	0.996	0.978	0.857	0.400	0.991	0.988	0.959
	2100.0	0.994	0.988	0.971	0.987	0.975	0.942	0.999	0.998	0.996	0.978	0.857	0.400	0.991	0.982	0.959
62	300.0	0.990	0.981	0.957	0.980	0.963	0.920	0.999	0.997	0.994	0.978	0.828	0.332	0.986	0.975	0.945
	900.0	0.990	0.981	0.957	0.980	0.963	0.920	0.999	0.997	0.994	0.978	0.828	0.332	0.986	0.984	0.945
	2100.0	0.990	0.981	0.957	0.980	0.963	0.920	0.999	0.997	0.994	0.978	0.828	0.332	0.986	0.975	0.945
63	300.0	0.983	0.969	0.941	0.969	0.944	0.896	0.998	0.996	0.993	0.963	0.768	0.279	0.980	0.963	0.931
	900.0	0.983	0.969	0.941	0.969	0.944	0.896	0.998	0.996	0.993	0.963	0.768	0.279	0.980	0.979	0.931
	2100.0	0.983	0.969	0.941	0.969	0.944	0.896	0.998	0.996	0.993	0.963	0.768	0.279	0.980	0.963	0.931
64	300.0	0.974	0.950	0.913	0.955	0.916	0.858	0.996	0.994	0.989	0.945	0.660	0.191	0.971	0.946	0.908
	900.0	0.974	0.950	0.913	0.955	0.916	0.858	0.996	0.994	0.989	0.945	0.660	0.191	0.971	0.971	0.908
	2100.0	0.974	0.950	0.913	0.955	0.916	0.858	0.996	0.994	0.989	0.945	0.660	0.191	0.971	0.946	0.908
65	300.0	0.962	0.925	0.871	0.937	0.883	0.801	0.999	0.995	0.988	0.934	0.587	0.036	0.962	0.928	0.874
	900.0	0.962	0.925	0.871	0.937	0.883	0.801	0.999	0.995	0.988	0.934	0.587	0.036	0.962	0.954	0.874
	2100.0	0.962	0.925	0.871	0.937	0.883	0.801	0.999	0.995	0.988	0.934	0.587	0.036	0.962	0.928	0.874
66	300.0	0.916	0.841	0.799	0.886	0.788	0.750	0.984	0.974	0.967	0.875	0.365	0.193	0.921	0.855	0.815
	900.0	0.916	0.841	0.799	0.886	0.788	0.750	0.984	0.974	0.967	0.875	0.365	0.193	0.921	0.910	0.815
	2100.0	0.916	0.841	0.799	0.886	0.788	0.750	0.984	0.974	0.967	0.875	0.365	0.193	0.921	0.855	0.815
67	300.0	0.840	0.734	0.669	0.811	0.719	0.616	0.980	0.941	0.950	0.766	0.599	0.063	0.856	0.778	0.703
	900.0	0.840	0.734	0.669	0.811	0.719	0.616	0.980	0.941	0.950	0.766	0.599	0.063	0.856	0.787	0.703
	2100.0	0.840	0.734	0.669	0.811	0.719	0.616	0.980	0.941	0.950	0.766	0.599	0.063	0.856	0.778	0.703

A-III-3 Gradient f_x^1 of f_x for Pu-239

		TOTAL			CAPTURE			ELASTIC			REMOVAL			FISSION		
		1000.	100.	10.	1000.	100.	10.	1000.	100.	10.	1000.	100.	10.	1000.	100.	10.
29	300.0	3.7E-04	4.0E-03	2.7E-02	-3.3E-05	2.1E-04	9.8E-03	1.1E-05	3.1E-04	4.4E-03	-9.4E-04	-8.3E-03	-2.0E-02	1.2E-04	8.8E-04	1.3E-02
	900.0	2.6E-04	2.9E-03	1.9E-02	-5.5E-05	1.9E-04	5.2E-03	0.0	1.3E-04	2.8E-03	-1.2E-03	-1.0E-02	-2.6E-02	-5.5E-06	-2.7E-04	7.6E-03
	2100.0	2.2E-04	2.3E-03	1.5E-02	-5.1E-05	-2.4E-04	3.2E-03	-3.7E-06	5.6E-05	1.8E-03	-1.3E-03	-1.1E-02	-2.8E-02	-3.3E-05	-8.3E-05	4.3E-03
30	300.0	4.0E-04	4.5E-03	2.9E-02	-2.1E-05	6.3E-04	1.5E-02	1.7E-05	4.6E-04	6.1E-03	-1.4E-03	-1.2E-02	-3.4E-02	-1.9E-05	4.7E-04	1.1E-02
	900.0	3.1E-04	3.5E-03	2.4E-02	-4.6E-05	1.3E-04	9.2E-03	1.8E-06	2.4E-04	4.2E-03	-1.4E-03	-1.2E-02	-3.5E-02	-7.4E-05	-2.7E-04	8.1E-03
	2100.0	2.9E-04	3.3E-03	2.1E-02	-4.6E-05	-4.2E-05	5.9E-03	0.0	1.7E-04	3.1E-03	-1.4E-03	-1.2E-02	-3.6E-02	-8.0E-06	2.8E-04	6.2E-03
31	300.0	3.1E-04	4.0E-03	3.7E-02	-2.2E-05	8.7E-04	1.9E-02	8.7E-06	5.4E-04	1.0E-02	-1.5E-03	-1.3E-02	-2.3E-02	6.6E-05	1.4E-03	1.9E-02
	900.0	2.4E-04	3.1E-03	2.9E-02	-3.2E-06	6.5E-04	1.3E-02	1.2E-05	4.0E-04	8.6E-03	-1.7E-03	-1.5E-02	-1.4E-02	5.6E-05	-1.1E-03	1.4E-02
	2100.0	2.9E-04	3.3E-03	2.8E-02	1.9E-05	7.1E-04	1.2E-02	3.1E-05	4.9E-04	8.5E-03	-1.8E-03	-1.5E-02	-3.8E-02	7.3E-05	1.0E-03	1.2E-02
32	300.0	2.9E-04	4.2E-03	3.7E-02	-8.8E-05	4.4E-04	2.0E-02	-3.6E-06	5.5E-04	9.1E-03	-5.2E-04	-3.7E-03	-1.1E-02	1.4E-05	1.2E-03	1.9E-02
	900.0	2.5E-04	3.4E-03	3.0E-02	-8.2E-05	1.9E-05	1.4E-02	0.0	3.7E-04	7.2E-03	-5.2E-04	-3.9E-03	-1.1E-02	-1.5E-06	-7.0E-04	1.4E-02
	2100.0	2.2E-04	2.9E-03	2.5E-02	-9.0E-05	-2.8E-04	9.9E-03	-7.1E-06	1.8E-04	5.4E-03	-6.5E-04	-5.1E-03	-1.2E-02	-4.5E-05	7.7E-05	8.9E-03
33	300.0	2.3E-04	3.9E-03	3.4E-02	3.2E-05	2.1E-03	3.2E-02	3.4E-06	8.6E-04	1.3E-02	-1.1E-03	-9.2E-03	-8.4E-02	-2.6E-05	9.5E-04	2.2E-02
	900.0	1.1E-04	2.5E-03	2.8E-02	-3.9E-05	6.9E-04	2.1E-02	-2.2E-05	2.9E-04	9.8E-03	-1.1E-03	-9.2E-03	-9.1E-02	-5.3E-05	-2.5E-04	1.5E-02
	2100.0	9.9E-05	1.9E-03	2.4E-02	-7.0E-05	0.0	1.5E-02	-3.2E-05	-1.7E-05	6.8E-03	-1.1E-03	-8.8E-03	-9.5E-02	-6.5E-05	-1.1E-04	1.0E-02
34	300.0	6.1E-04	7.8E-03	5.3E-02	7.8E-05	3.1E-03	3.5E-02	-2.3E-05	1.0E-03	1.4E-02	-1.1E-03	-8.6E-03	-1.5E-02	6.0E-05	2.3E-03	3.0E-02
	900.0	4.0E-04	5.4E-03	4.2E-02	-3.6E-06	1.5E-03	2.5E-02	-3.6E-05	4.9E-04	1.1E-02	-1.2E-03	-1.0E-02	-1.8E-02	2.4E-05	-1.4E-03	2.1E-02
	2100.0	3.4E-04	4.5E-03	3.7E-02	-4.1E-05	8.2E-04	1.9E-02	-3.1E-05	3.3E-04	9.1E-03	-1.4E-03	-1.1E-02	-1.7E-02	-4.1E-06	7.6E-04	1.4E-02
35	300.0	7.8E-04	8.9E-03	5.8E-02	-1.8E-04	1.0E-03	2.8E-02	-3.5E-05	8.1E-04	1.2E-02	-1.5E-03	-8.2E-03	-1.4E-02	2.5E-04	3.6E-03	2.9E-02
	900.0	6.8E-04	7.7E-03	5.6E-02	-1.6E-04	2.3E-04	2.0E-02	-3.9E-05	3.9E-04	9.9E-03	-1.9E-03	-1.3E-02	-2.2E-02	1.4E-04	1.7E-03	2.1E-02
	2100.0	1.1E-02	7.7E-03	5.4E-02	-9.7E-05	3.8E-04	1.8E-02	-2.4E-05	3.5E-04	8.9E-03	-1.9E-03	-1.4E-02	-2.4E-02	1.1E-04	1.6E-03	1.8E-02
36	300.0	8.0E-04	1.1E-02	6.5E-02	2.8E-04	6.0E-03	5.8E-02	1.6E-04	3.1E-03	2.5E-02	-1.7E-03	-1.1E-02	-1.3E-02	3.1E-04	5.9E-03	4.9E-02
	900.0	4.9E-04	7.4E-03	6.0E-02	1.9E-04	4.0E-03	4.8E-02	1.1E-04	2.1E-03	2.3E-02	-1.8E-03	-1.1E-02	-2.3E-02	2.8E-04	-4.8E-03	4.4E-02
	2100.0	3.6E-04	5.6E-03	5.3E-02	1.2E-04	2.5E-03	3.6E-02	9.8E-05	1.6E-03	2.0E-02	-1.8E-03	-1.1E-02	-2.1E-02	2.8E-04	4.2E-03	4.1E-02
37	300.0	3.1E-04	5.7E-03	4.4E-02	-9.3E-05	1.9E-03	3.6E-02	3.1E-05	1.0E-03	1.1E-02	-2.4E-03	-2.4E-02	-2.9E-02	-1.2E-04	1.7E-03	4.1E-02
	900.0	4.6E-04	6.4E-03	4.6E-02	-8.1E-05	8.6E-04	2.8E-02	2.9E-05	7.5E-04	9.3E-03	-2.6E-03	-2.4E-02	-2.6E-02	-7.5E-05	-1.6E-03	4.1E-02
	2100.0	4.8E-04	6.2E-03	4.6E-02	-1.1E-04	0.0	2.1E-02	-3.7E-06	2.7E-04	6.9E-03	-2.6E-03	-2.4E-02	-2.3E-02	-1.1E-04	8.5E-04	3.8E-02
38	300.0	5.1E-05	5.4E-03	4.1E-02	4.3E-05	4.8E-04	4.0E-02	-1.6E-05	2.1E-03	1.5E-02	-8.0E-04	-5.0E-03	-1.1E-02	-1.8E-04	3.0E-03	4.0E-02
	900.0	-9.7E-05	3.5E-03	4.0E-02	-2.9E-05	2.7E-03	3.4E-02	-1.9E-05	1.5E-03	1.3E-02	-9.2E-04	-6.3E-03	-9.0E-03	-1.2E-04	-2.5E-03	3.9E-02
	2100.0	-2.3E-04	1.5E-03	3.2E-02	-1.3E-04	6.7E-04	2.1E-02	-6.0E-06	1.1E-03	1.1E-02	-1.0E-03	-7.1E-03	-7.4E-03	-5.1E-06	2.8E-03	3.9E-02
39	300.0	6.7E-04	9.6E-03	4.1E-02	1.2E-04	5.9E-03	4.4E-02	3.2E-05	2.4E-03	1.3E-02	-1.1E-03	-9.2E-03	-2.6E-02	1.8E-04	6.5E-03	4.5E-02
	900.0	6.1E-04	8.9E-03	4.4E-02	3.5E-05	3.9E-03	3.8E-02	-3.3E-05	1.6E-03	1.2E-02	-1.3E-03	-9.9E-03	-2.1E-02	1.4E-04	-5.3E-03	4.3E-02
	2100.0	4.5E-04	7.3E-03	4.1E-02	-7.8E-05	2.1E-03	2.9E-02	-9.8E-05	7.5E-04	9.6E-03	-1.6E-03	-1.1E-02	-1.7E-02	7.1E-05	4.1E-03	-4.1E-01
40	300.0	-1.1E-04	4.7E-03	2.1E-02	-5.0E-05	5.1E-03	3.3E-02	-2.5E-05	2.5E-03	1.3E-02	-8.9E-04	-8.2E-03	-2.3E-02	-8.6E-05	4.5E-03	3.4E-02
	900.0	-2.0E-04	3.3E-03	2.3E-02	-1.5E-04	2.7E-03	2.8E-02	-7.3E-05	1.3E-03	1.2E-02	-1.2E-03	-1.3E-02	-2.1E-02	-1.7E-04	-2.2E-03	3.1E-02
	2100.0	-2.3E-04	2.3E-03	2.3E-02	-2.4E-04	7.1E-04	2.1E-02	-9.5E-05	4.9E-04	9.3E-03	-1.5E-03	-1.5E-02	-2.0E-02	-1.9E-04	6.8E-04	2.5E-02
41	300.0	3.1E-04	7.3E-03	4.1E-02	4.0E-04	9.3E-03	8.2E-02	6.9E-05	1.5E-03	1.0E-02	-2.4E-04	4.0E-04	-1.8E-02	2.5E-04	6.6E-03	4.7E-02
	900.0	3.8E-04	7.5E-03	5.1E-02	5.2E-04	9.1E-03	8.7E-02	8.6E-05	1.5E-03	1.1E-02	-3.9E-04	-4.5E-04	-1.5E-02	3.0E-04	-6.3E-03	4.7E-02
	2100.0	5.1E-04	8.1E-03	6.1E-02	6.5E-04	9.1E-03	8.7E-02	1.0E-04	1.6E-03	1.5E-02	-5.3E-04	-1.6E-03	-1.1E-02	3.8E-04	6.2E-03	4.5E-02
42	300.0	3.7E-04	9.2E-03	3.3E-02	3.1E-04	1.0E-02	4.8E-02	1.3E-04	4.2E-03	1.9E-02	-2.5E-04	8.2E-04	-9.0E-03	2.1E-04	7.4E-03	5.4E-02
	900.0	2.2E-04	8.1E-03	4.2E-02	1.9E-04	7.7E-03	4.8E-02	5.9E-05	3.3E-03	2.0E-02	-4.5E-04	-7.1E-04	-7.5E-03	1.5E-04	-5.5E-03	5.3E-02
	2100.0	9.7E-05	5.8E-03	4.2E-02	9.8E-05	5.1E-03	3.6E-02	-2.1E-05	1.9E-03	1.7E-02	-6.3E-04	-2.4E-03	-7.1E-03	1.2E-04	3.7E-03	4.3E-02
43	300.0	6.5E-04	6.3E-03	2.5E-02	5.5E-04	7.6E-03	2.7E-02	5.1E-04	3.9E-03	9.6E-03	-3.7E-04	-3.3E-03	-1.1E-02	4.1E-04	8.1E-03	5.1E-02
	900.0	4.8E-04	5.7E-03	2.5E-02	2.4E-04	5.5E-03	2.5E-02	3.0E-04	3.4E-03	9.2E-03	-5.3E-04	-5.4E-03	-6.4E-03	3.1E-04	-6.6E-03	4.6E-02
	2100.0	3.1E-04	4.4E-03	2.3E-02	-6.4E-05	1.7E-03	1.2E-02	3.8E-05	2.0E-03	8.7E-03	-5.5E-04	-6.9E-03	-2.7E-03	2.2E-04	4.4E-03	2.9E-02
44	300.0	-1.6E-04	8.2E-03	4.9E-02	-2.9E-04	6.6E-03	4.2E-02	-3.5E-06	2.3E-03	1.2E-02	-6.3E-04	-2.5E-03	-3.8E-03	1.9E-04	8.1E-03	3.6E-02
	900.0	-3.0E-04	6.2E-03	4.9E-02	-5.8E-04	1.9E-03	3.7E-02	-5.8E-05	1.5E-03	1.1E-02	-9.0E-04	-3.7E-03	-1.8E-03	1.1E-04	-6.8E-03	3.5E-02
	2100.0	7.7E-05	7.4E-03	3.1E-02	-3.4E-04	5.8E-04	2.5E-02	-2.5E-05	1.3E-03	9.8E-03	-1.1E-03	-5.1E-03	2.1E-03	4.1E-04	8.8E-03	3.8E-02
45	300.0	6.6E-04	8.5E-03	2.6E-02	3.9E-04	9.0E-03	4.0E-02	2.7E-04	4.6E-03	2.0E-02	-5.8E-04	-1.5E-02	-5.9E-02	4.3E-04	1.2E-02	6.3E-02
	900.0	1.7E-04	7.6E-03	2.9E-02	-1.1E-04	6.3E-03	4.6E-02	2.2E-06	3.6E-03	2.4E-02	-6.6E-04	-1.6E-02	-5.9E-02	2.8E-04	-1.1E-02	6.7E-02
	2100.0	-2.0E-04	5.8E-03	3.4E-02	-6.3E-04	1.1E-03	4.7E-02	-3.3E-04	7.6E-04	2.6E-02	-5.4E-04	-1.4E-02	-4.5E-02	1.6E-04	8.5E-03	6.3E-02
46	300.0	-1.3E-04	7.1E-03	2.8E-02	3.5E-04	1.2E-02	4.7E-02	1.0E-04	3.2E-03	8.9E-03	-1.8E-03	-1.5E-02	-6.2E-02	2.5E-04	1.0E-02	4.1E-02
	900.0	-7.1E-04	3.7E-03	2.9E-02	8.3E-05	1.0E-02	4.7E-02	1.7E-05	2.8E-03	9.1E-03	-2.0E-03	-1.7E-02	-6.1E-02	-1.7E-04	-7.0E-03	3.6E-02
	2100.0	-6.1E-04	2.5E-03	2.4E-02	1.6E-04	6.8E-03	3.5E-02	1.6E-04	2.8E-03	9.5E-03	-2.7E-03	-3.4E-02	-5.8E-02	-2.3E-04	2.3E-03	2.2E-02
47	300.0	2.0E-04	1.5E-03	-1.7E-03	7.6E-04	6.9E-03	8.0E-03	1.8E-04	2.2E-03	1.6E-03	-9.4E-04	-7.0E-03	-2.2E-02	5.4E-04	5.5E-03	7.1E-03
	900.0	7.4E-05	2.2E-03	-1.8E-03	7.0E-04	7.8E-03	8.6E-03	1.5E-04	2.6E-03	1.2E-03	-1.1E-03	-6.0E-03	-2.6E-02	4.9E-04	-5.9E-03	7.0E-03
	2100.0	-7.1E-05	2.2E-03	-2.8E-03	6.6E-04	8.0E-03	8.5E-03	1.5E-04	2.4E-03	-1.8E-03	-1.4E-03	-1.1E-02	-3.0E-02	4.7E-04	6.0E-03	6.3E-03
48	300.0	1.3E-03	6.7E-03	9.3E-03	1.0E-03	5.4E-03	5.4E-03	1.5E-03	7.3E-03	5.9E-03	-3.4E-04	2.0E-04	-1.4E-03	7.4E-04	4.1E-03	3.2E-03
	900.0	1.5E-03	7.5E-03	9.8E-03	1.1E-03	5.5E-03	3.1E-03	1.6E-03	7.9E-03	5.1E-03	-3.5E-04	4.4E-03	-7.2E-04	8.4E-04	-4.3E-03	-2.3E-04
	2100.0	1.6E-03	8.7E-03	1.1E-02	1.1E-03	5.8E-03	1.0E-03	1.6E-03	9.6E-03	4.7E-03	-3.4E-04	2.0E-03	1.0E-03	8.8E-04	4.3E-03	-3.9E-03
49	300.0	1.3E-03	9.3E-03	2.4E-02	8.4E-04	8.3E-03	3.2E-02	5.7E-04	5.6E-03	2.8E-02	-3.2E-04	-3.1E-03	-1.8E-02	5.7E-04	6.4E-03	5.0E-02
	900.0	1.2E-03	1.0E-02	2.9E-02	6.4E-04	8.6E-03	3.9E-02	4.5E-04	5.5E-03	3.3E-02	-3.0E-04	9.5E-04	-1.5E-02	4.9E-04	-4.9E-03	5.9E-02
	2100.0	9.8E-04	1.2E-02	3.7E-02	4.4E-04	8.2E-03	4.3E-02	3.4E-04	5.8E-03	3.8E-02	-2.1E-04	-4.2E-04	-8.8E-03	4.1E-04	5.1E-03	6.6E-02

```
50  300.0 3.0E-03 9.6E-03 1.7E-02 2.3E-03 1.5E-02 3.3E-02 1.5E-03 1.2E-02 3.8E-02-2.7E-03-2.6E-02-8.0E-02 2.2E-03 1.5E-02 3.6E-02
    900.0 2.9E-03 1.4E-02 2.0E-02 2.0E-03 1.8E-02 4.1E-02 1.3E-03 1.4E-02 4.5E-02-1.8E-03-1.1E-02-4.9E-02 1.9E-03-1.7E-02 4.4E-02
   2100.0 2.6E-03 1.8E-02 2.6E-02 1.7E-03 1.8E-02 4.9E-02 1.1E-03 1.4E-02 5.0E-02-5.9E-04-5.9E-03-1.6E-02 1.6E-03 1.8E-02 5.2E-02

51  300.0 2.8E-04 5.0E-03 2.4E-02-2.0E-04 4.0E-03 9.7E-02-1.1E-05-8.6E-05-1.2E-02-2.8E-04-2.5E-03-2.1E-01 5.0E-04 6.3E-03 5.3E-02
    900.0 2.2E-04 4.2E-03 3.4E-02-2.3E-04 3.5E-03 1.4E-01-8.9E-06 2.5E-04-1.7E-02-2.6E-04-3.1E-04-3.0E-01 5.0E-04-5.5E-03 6.1E-02
   2100.0 1.2E-05 2.1E-03 3.4E-02-4.0E-04 1.1E-03 2.2E-01-6.3E-06-6.5E-05-2.1E-02-2.4E-04-1.9E-03-3.2E-01 4.8E-04 4.7E-03 6.2E-02

52  300.0 9.2E-04 7.1E-03 1.2E-02 8.9E-04 1.2E-02 3.4E-02 2.8E-04 4.8E-03 2.4E-02-2.6E-03-2.2E-02-4.0E-02 5.6E-05 5.6E-03 9.2E-03
    900.0 7.0E-04 1.0E-02 1.7E-02 6.7E-04 1.3E-02 4.2E-02 2.2E-04 4.4E-03 2.6E-02-2.5E-03-1.9E-02-3.5E-02-1.6E-04-6.1E-03 1.1E-02
   2100.0 4.4E-04 1.1E-02 2.0E-02 4.5E-04 1.0E-02 5.0E-02 1.5E-04 2.7E-03 2.7E-02-2.5E-03-1.7E-02-2.4E-02-3.7E-04 3.5E-03 9.8E-03

53  300.0 1.4E-03 4.5E-03 1.3E-02 1.3E-03 6.1E-03 1.2E-02 3.1E-04 2.8E-03 1.1E-02-2.5E-04-2.5E-03-3.7E-03 1.2E-03 5.5E-03 1.2E-02
    900.0 1.4E-03 5.2E-03 1.2E-02 1.2E-03 6.9E-03 1.3E-02 2.9E-04 3.1E-03 1.1E-02-2.5E-04-4.6E-04-4.9E-03 1.1E-03-6.6E-03 1.3E-02
   2100.0 1.2E-03 5.9E-03 1.1E-02 1.1E-03 7.1E-03 1.5E-02 2.6E-04 2.7E-03 1.1E-02-2.9E-04-3.6E-03-8.3E-03 1.0E-03 6.4E-03 1.5E-02

54  300.0 7.6E-04 3.8E-03 7.0E-03 6.7E-04 2.4E-03-5.9E-03 3.4E-04 2.1E-03 2.9E-03-3.8E-04-3.2E-03-7.6E-03 5.0E-04 3.1E-03-5.6E-03
    900.0 7.7E-04 4.3E-03 6.9E-03 5.8E-04 3.0E-03-9.9E-03 2.9E-04 2.1E-03 2.1E-03-3.9E-04-1.4E-03-8.3E-03 4.3E-04-3.4E-03-8.0E-03
   2100.0 7.4E-04 4.4E-03 6.7E-03 5.0E-04 2.7E-03-7.8E-03 2.5E-04 2.0E-03 1.3E-03-4.1E-04-4.3E-03-1.1E-02 3.7E-04 3.2E-03-7.9E-03

55  300.0 8.2E-04 2.1E-03 2.0E-03 6.9E-04 2.4E-03-1.2E-03 3.6E-04 2.5E-03 3.0E-03-1.4E-03-8.0E-03-8.9E-03 3.5E-04 9.1E-04-2.2E-03
    900.0 7.7E-04 3.4E-03 2.1E-03 5.7E-04 3.4E-03-1.6E-03 3.1E-04 2.3E-03 2.5E-03-1.4E-03-2.0E-03-8.2E-03 2.7E-04-1.9E-03-2.6E-03
   2100.0 6.2E-04 4.6E-03 2.1E-03 4.2E-04 4.0E-03-3.1E-03 2.5E-04 1.9E-03 1.3E-03-1.3E-03 1.8E-03-7.3E-03 1.5E-04 2.6E-03-3.3E-03

56  300.0 4.0E-05 7.0E-04 3.5E-03-2.8E-06 8.5E-04 1.1E-03-9.0E-05-1.9E-04-3.3E-03 2.0E-04 1.2E-03 3.5E-04 6.3E-05 1.1E-03 5.1E-03
    900.0-2.4E-05 9.1E-04 3.4E-03-8.7E-05 3.1E-03 1.1E-03-9.7E-05 6.9E-04-3.3E-03 2.8E-05-2.2E-03 7.2E-05-2.3E-05-2.7E-03 5.0E-03
   2100.0-1.3E-04 9.2E-04 3.6E-03-1.9E-04 7.0E-04 1.1E-03-1.1E-04-2.0E-04-3.5E-03-1.5E-04 3.1E-04-7.1E-05-1.2E-04 1.0E-03 5.4E-03

57  300.0 2.3E-02 7.8E-02 2.3E-01 2.1E-02 1.0E-01 7.3E-01-8.4E-05-3.4E-03-6.8E-03-2.5E-03-2.6E-02-1.2E-01 1.2E-02 6.2E-02 4.3E-01
    900.0 2.5E-02 6.8E-02 2.5E-01 2.2E-02 2.7E-02 7.8E-01 1.3E-04-4.8E-03-5.5E-04-2.5E-03-2.2E-02-1.2E-01 1.3E-02-2.1E-02 4.6E-01
   2100.0 2.5E-02 1.2E-01 3.2E-01 2.3E-02 1.4E-01 9.6E-01 3.5E-04 2.8E-04 1.5E-02-2.4E-03-2.5E-02-1.3E-01 1.3E-02 8.4E-02 5.5E-01

58  300.0 1.6E-05 6.5E-04 3.6E-03-1.5E-04 8.1E-04 3.3E-03 2.1E-05-3.4E-04-3.2E-04 1.1E-03-4.8E-03-1.3E-02-4.9E-05-4.7E-04 1.1E-03
    900.0 1.4E-05 7.0E-04 3.6E-03-1.8E-04 3.1E-03 3.3E-03 2.3E-05-4.4E-04-3.2E-04 1.2E-03-7.1E-03-1.3E-02-5.6E-05-9.5E-04 1.1E-03
   2100.0 1.6E-05-1.5E-04 4.4E-03-2.2E-04-3.1E-03 3.1E-03 2.9E-05 4.3E-04-2.8E-04 1.4E-03-6.0E-03-1.4E-02-7.1E-05-9.5E-04 1.1E-03

59  300.0-7.3E-06 2.4E-05 6.1E-05-9.2E-06 2.7E-05-7.3E-05-3.9E-06 1.5E-05 1.2E-05-5.5E-04-4.4E-03-6.3E-03-1.2E-05 3.8E-05-1.4E-05
    900.0-7.3E-06 2.4E-05 6.1E-05-9.2E-06 2.7E-05-7.3E-05-3.9E-06 1.5E-05 1.2E-05-5.5E-04-4.4E-03-6.3E-03-1.2E-05-3.8E-05-1.4E-05
   2100.0-7.3E-06 2.4E-05 6.1E-05-9.2E-06 2.7E-05-7.3E-05-3.9E-06 1.5E-05 1.2E-05-5.5E-04-4.4E-03-6.3E-03-1.2E-05 3.8E-05-1.4E-05

60  300.0-1.2E-05 1.2E-04-5.5E-04-2.3E-05 2.5E-04-1.3E-03-2.8E-06 2.6E-05-1.6E-04-4.8E-04-3.1E-03 1.6E-03-1.8E-05 2.0E-04-1.1E-03
    900.0-1.2E-05 1.2E-04-5.5E-04-2.3E-05 2.5E-04-1.3E-03-2.8E-06 2.6E-05-1.6E-04-4.8E-04-3.1E-03 1.6E-03-1.8E-05-2.0E-04-1.1E-03
   2100.0-1.2E-05 1.2E-04-5.5E-04-2.3E-05 2.5E-04-1.3E-03-2.8E-06 2.6E-05-1.6E-04-4.8E-04-3.1E-03 1.6E-03-1.8E-05 2.0E-04-1.1E-03

61  300.0-1.6E-05 2.8E-04-9.7E-04-3.0E-05 5.8E-04-2.4E-03-2.5E-06 4.3E-05-2.0E-04-4.3E-04-2.2E-03-6.2E-04-2.1E-05 4.2E-04-1.8E-03
    900.0-1.6E-05 2.8E-04-9.7E-04-3.0E-05 5.8E-04-2.4E-03-2.5E-06 4.3E-05-2.0E-04-4.3E-04-2.2E-03-6.2E-04-2.1E-05-4.2E-04-1.8E-03
   2100.0-1.6E-05 2.8E-04-9.7E-04-3.0E-05 5.8E-04-2.4E-03-2.5E-06 4.3E-05-2.0E-04-4.3E-04-2.2E-03-6.2E-04-2.1E-05 4.2E-04-1.8E-03

62  300.0-1.6E-05 4.5E-04-9.3E-04-3.2E-05 8.6E-04-2.4E-03-2.2E-06 5.9E-05-1.9E-04-3.2E-04-1.6E-03 6.0E-03-2.2E-05 5.8E-04-1.6E-03
    900.0-1.6E-05 4.5E-04-9.3E-04-3.2E-05 8.6E-04-2.4E-03-2.2E-06 5.9E-05-1.9E-04-3.2E-04-1.6E-03 6.0E-03-2.2E-05-5.8E-04-1.6E-03
   2100.0-1.6E-05 4.5E-04-9.3E-04-3.2E-05 8.6E-04-2.4E-03-2.2E-06 5.9E-05-1.9E-04-3.2E-04-1.6E-03 6.0E-03-2.2E-05 5.8E-04-1.6E-03

63  300.0-1.4E-05 8.9E-04-1.5E-03-2.6E-05 1.6E-03-3.4E-03-1.7E-06 1.1E-04-2.7E-04-2.9E-04 5.5E-04 2.8E-03-1.7E-05 1.1E-03-2.4E-03
    900.0-1.4E-05 8.9E-04-1.5E-03-2.6E-05 1.6E-03-3.4E-03-1.7E-06 1.1E-04-2.7E-04-2.9E-04 5.5E-04 2.8E-03-1.7E-05-1.1E-03-2.4E-03
   2100.0-1.4E-05 8.9E-04-1.5E-03-2.6E-05 1.6E-03-3.4E-03-1.7E-06 1.1E-04-2.7E-04-2.9E-04 5.5E-04 2.8E-03-1.7E-05 1.1E-03-2.4E-03

64  300.0-1.6E-05 1.5E-03-2.5E-03-2.8E-05 2.6E-03-5.0E-03-2.0E-06 1.9E-04-4.0E-04-2.8E-04 4.1E-03-9.7E-04-1.8E-05 1.7E-03-3.4E-03
    900.0-1.6E-05 1.5E-03-2.5E-03-2.8E-05 2.6E-03-5.0E-03-2.0E-06 1.9E-04-4.0E-04-2.8E-04 4.1E-03-9.7E-04-1.8E-05-1.7E-03-3.4E-03
   2100.0-1.6E-05 1.5E-03-2.5E-03-2.8E-05 2.6E-03-5.0E-03-2.0E-06 1.9E-04-4.0E-04-2.8E-04 4.1E-03-9.7E-04-1.8E-05 1.7E-03-3.4E-03

65  300.0-2.9E-05 1.8E-03-6.9E-03-4.8E-05 2.8E-03-1.2E-02-3.9E-06 2.2E-04-1.1E-03-3.2E-04-1.5E-03-1.8E-03-3.1E-05 1.7E-03-8.1E-03
    900.0-2.9E-05 1.8E-03-6.9E-03-4.8E-05 2.8E-03-1.2E-02-3.9E-06 2.2E-04-1.1E-03-3.2E-04-1.5E-03-1.8E-03-3.1E-05-1.7E-03-8.1E-03
   2100.0-2.9E-05 1.8E-03-6.9E-03-4.8E-05 2.8E-03-1.2E-02-3.9E-06 2.2E-04-1.1E-03-3.2E-04-1.5E-03-1.8E-03-3.1E-05 1.7E-03-8.1E-03

66  300.0-6.9E-06 3.9E-03-6.9E-03-1.9E-05 5.4E-03-1.8E-02-1.8E-06 5.6E-04 1.7E-03-1.0E-04 6.0E-03-1.4E-02-1.3E-05 3.7E-03-9.2E-03
    900.0-6.9E-06 3.9E-03-6.9E-03-1.9E-05 5.4E-03-1.8E-02-1.8E-06 5.6E-04 1.7E-03-1.0E-04 6.0E-03-1.4E-02-1.3E-05-3.7E-03-9.2E-03
   2100.0-6.9E-06 3.9E-03-6.9E-03-1.9E-05 5.4E-03-1.8E-02-1.8E-06 5.6E-04 1.7E-03-1.0E-04 6.0E-03-1.4E-02-1.3E-05 3.7E-03-9.2E-03

67  300.0 5.2E-05 3.7E-03-6.3E-03 3.6E-05 6.7E-04-8.7E-03 4.9E-06 2.6E-04-1.6E-03 3.1E-04 4.0E-03-9.0E-04 2.8E-05 6.1E-04-7.0E-03
    900.0 5.2E-05 3.7E-03-6.3E-03 3.6E-05 6.7E-04-8.7E-03 4.9E-06 2.6E-04-1.6E-03 3.1E-04 4.0E-03-9.0E-04 2.8E-05-6.1E-04-7.0E-03
   2100.0 5.2E-05 3.7E-03-6.3E-03 3.6E-05 6.7E-04-8.7E-03 4.9E-06 2.6E-04-1.6E-03 3.1E-04 4.0E-03-9.0E-04 2.8E-05 6.1E-04-7.0E-03
```

A-IV-1 Table of infinite dilution cross section for Pu-240

GROUP	UPPER E	LOWER E	LETHERGY	TOTAL	CAPTURE	ELASTIC	REMOVAL	FISSION
26	21500.000	16600.000	0.259	14.7010	0.5961	13.9850	0.3971	0.1347
27	16600.000	12900.000	0.252	14.8940	0.6911	14.0610	0.4576	0.1554
28	12900.000	10000.000	0.255	15.5560	0.7405	14.6350	0.4327	0.1803
29	10000.000	7730.000	0.257	15.6400	0.8127	14.6790	0.4216	0.1666
30	7730.000	5980.000	0.257	16.5420	0.9293	15.4590	0.5302	0.1690
31	5980.000	4650.000	0.252	17.3190	1.0163	16.1950	0.3855	0.1258
32	4650.000	3600.000	0.256	16.2490	1.0053	15.1660	0.3536	0.0780
33	3600.000	2780.000	0.258	15.5890	1.1305	14.3940	0.3583	0.0641
34	2780.000	2150.000	0.257	19.8970	1.5669	18.2710	0.3433	0.0590
35	2150.000	1660.000	0.259	20.7610	2.0090	18.6780	0.6128	0.0741
36	1660.000	1290.000	0.252	23.3020	2.3625	20.8940	1.3134	0.0455
37	1290.000	1000.000	0.255	21.5980	2.8464	18.7090	1.5470	0.0430
38	1000.000	773.000	0.257	29.7760	4.8453	24.6500	0.2962	0.2809
39	773.000	598.000	0.257	16.5140	2.9163	13.4320	0.4653	0.1656
40	598.000	465.000	0.252	20.7480	5.0346	15.7130	0.3758	0.0
41	465.000	360.000	0.256	28.6720	6.0742	22.5980	1.1981	0.0
42	360.000	278.000	0.258	45.0340	9.1950	35.8390	0.3686	0.0
43	278.000	215.000	0.257	19.3340	4.9377	14.3960	0.3444	0.0
44	215.000	166.000	0.259	26.0390	9.3392	16.6960	0.3456	0.0
45	166.000	129.000	0.252	42.4070	19.1640	23.2430	0.3540	0.0
46	129.000	100.000	0.255	93.4710	33.4480	60.0230	0.2002	0.0
47	100.000	77.300	0.257	43.5160	20.4160	23.0990	0.4162	0.0
48	77.300	59.800	0.257	275.7500	91.4810	184.2700	0.1938	0.0
49	59.800	46.500	0.252	9.5447	0.2179	9.3267	0.4325	0.0
50	46.500	36.000	0.256	372.1699	193.6300	178.5400	0.0647	0.0
51	36.000	27.800	0.258	6.4473	0.3995	6.0478	0.2466	0.0
52	27.800	21.500	0.257	9.2601	0.3724	8.8878	0.3345	0.0
53	21.500	16.600	0.259	109.6500	91.1540	18.4990	0.2661	0.0
54	16.600	12.900	0.252	8.9698	0.1949	8.7750	0.3007	0.0000
55	12.900	10.000	0.255	9.6448	0.2105	9.4342	0.3168	0.0000
56	10.000	7.730	0.257	10.3460	0.3306	10.0150	0.3327	0.0000
57	7.730	5.980	0.257	11.2830	0.6042	10.6790	0.3545	0.0001
58	5.980	4.650	0.252	12.7330	1.1962	11.5360	0.3973	0.0002
59	4.650	3.600	0.256	15.3180	2.5439	12.7740	0.4407	0.0004
60	3.600	2.780	0.258	20.8520	6.0170	14.8340	0.5202	0.0010
61	2.780	2.150	0.257	34.4390	15.8470	18.5900	0.6877	0.0025
62	2.150	1.660	0.259	79.0200	51.6990	27.3130	0.9624	0.0083
63	1.660	1.290	0.252	341.1399	279.8799	61.2120	2.8204	0.0451
64	1.290	1.000	0.255	28838.0000	26782.0000	2052.0999	45.7880	4.3197
65	1.000	0.773	0.257	3112.0000	2969.5000	142.0200	0.3934	0.4789
66	0.773	0.598	0.257	421.3398	416.9500	4.3205	0.0345	0.0672
67	0.598	0.465	0.252	226.2700	225.9500	0.2777	0.0008	0.0364
68	0.465	0.360	0.256	172.5500	172.4500	0.0666	0.0022	0.0278
69	0.360	0.278	0.258	148.4100	148.0600	0.3249	0.0106	0.0238
70	0.278	0.215	0.257	137.8300	137.2100	0.6018	0.0197	0.0221

A-IV-2 Shielding factor f_x^0 for Pu-240

		TOTAL			CAPTURE			ELASTIC			REMOVAL			FISSION		
		10000.	1000.	100.	10000.	1000.	100.	10000.	1000.	100.	10000.	1000.	100.	10000.	1000.	100.
24	300.0	1.000	0.996	0.977	0.999	0.998	0.984	0.999	0.997	0.984	1.028	1.007	1.045	0.999	0.998	0.986
	900.0	0.998	0.996	0.985	0.999	0.998	0.990	0.999	0.998	0.989	1.028	1.006	1.052	0.999	0.999	0.993
	2100.0	0.998	0.997	0.990	0.999	0.999	0.995	0.999	0.998	0.992	1.028	1.005	1.055	1.000	1.000	0.997
27	300.0	1.001	0.996	0.973	0.999	0.995	0.976	1.000	0.997	0.981	1.029	0.951	0.946	1.000	0.996	0.981
	900.0	0.998	0.996	0.982	1.000	0.996	0.985	0.999	0.998	0.988	1.022	0.946	0.942	1.001	0.997	0.990
	2100.0	0.999	0.997	0.988	1.001	0.998	0.991	0.999	0.998	0.991	1.027	0.949	0.953	1.001	0.998	0.995
28	300.0	1.000	0.989	0.944	0.996	0.992	0.964	1.000	0.994	0.965	0.982	0.913	0.908	0.992	0.989	0.959
	900.0	1.001	0.993	0.963	0.999	0.996	0.980	1.001	0.996	0.976	1.006	0.936	0.933	0.995	0.993	0.975
	2100.0	0.999	0.994	0.974	0.999	0.997	0.987	1.000	0.997	0.984	0.982	0.914	0.910	0.995	0.994	0.983
29	300.0	1.000	0.986	0.918	0.990	0.984	1.005	0.998	0.991	1.016	0.916	0.923	0.849	0.995	0.990	1.017
	900.0	1.000	0.992	0.952	0.991	0.988	0.961	1.000	0.995	0.970	0.918	0.926	0.858	0.996	0.993	0.976
	2100.0	0.999	0.993	0.973	0.994	0.992	0.997	0.999	0.996	1.020	0.920	0.930	0.825	0.998	0.996	1.005
30	300.0	1.004	0.985	0.925	1.001	0.994	1.042	1.002	0.992	1.018	0.939	0.942	0.883	1.000	0.992	1.037
	900.0	1.009	0.997	0.942	1.004	0.999	0.974	1.004	0.997	0.963	0.942	0.951	0.855	1.003	0.998	0.971
	2100.0	1.011	1.002	0.968	1.004	1.001	1.034	1.005	1.000	1.032	0.932	0.946	0.905	1.004	1.001	1.029
31	300.0	0.978	0.951	0.834	0.990	0.977	1.015	0.989	0.974	0.986	0.861	0.886	0.762	1.007	0.995	1.057
	900.0	0.983	0.966	0.882	0.997	0.990	0.942	0.993	0.983	0.929	0.850	0.877	0.801	1.008	0.998	0.982
	2100.0	0.988	0.976	0.919	1.000	0.996	1.030	0.996	0.989	1.011	0.859	0.888	0.719	1.005	0.997	1.044
32	300.0	1.014	0.985	0.868	1.014	0.995	0.901	1.003	0.989	0.921	0.983	0.988	0.981	1.005	1.005	1.005
	900.0	1.010	0.993	0.918	1.012	1.002	0.948	1.001	0.993	0.948	0.978	0.984	0.989	1.013	1.012	1.023
	2100.0	1.005	0.994	0.947	1.009	1.002	0.969	0.999	0.994	0.963	0.985	0.992	1.001	1.014	1.014	1.031
33	300.0	0.998	0.973	0.870	0.979	0.958	0.835	0.999	0.986	0.926	0.966	0.974	0.948	1.001	0.998	0.987
	900.0	1.000	0.985	0.911	0.985	0.973	0.891	1.000	0.992	0.950	0.963	0.972	0.955	1.004	1.001	0.994
	2100.0	0.999	0.989	0.938	0.989	0.982	0.927	1.000	0.995	0.965	0.962	0.971	0.959	1.002	0.999	0.991
34	300.0	1.017	0.940	0.723	0.999	0.959	0.784	1.006	0.967	0.826	0.951	0.959	0.911	0.993	0.994	0.982
	900.0	1.015	0.966	0.790	1.003	0.979	0.860	1.005	0.980	0.873	0.956	0.965	0.915	0.989	0.991	0.986
	2100.0	1.009	0.978	0.846	1.003	0.989	0.909	1.003	0.987	0.908	0.953	0.963	0.917	0.991	0.993	0.997
35	300.0	0.945	0.863	0.655	0.974	0.927	0.739	0.993	0.943	0.792	0.731	0.728	0.585	1.031	1.017	0.986
	900.0	0.948	0.892	0.712	0.982	0.954	0.816	0.988	0.956	0.835	0.758	0.756	0.597	1.033	1.021	0.988
	2100.0	0.937	0.905	0.769	0.987	0.971	0.878	0.977	0.959	0.870	0.776	0.775	0.606	1.026	1.019	0.993
36	300.0	1.006	0.880	0.635	1.006	0.936	0.694	0.996	0.927	0.741	0.959	0.807	0.402	0.990	0.990	0.966
	900.0	1.016	0.926	0.696	1.008	0.964	0.778	0.999	0.952	0.791	0.962	0.860	0.472	1.068	1.070	1.054
	2100.0	1.028	0.962	0.760	1.009	0.980	0.838	1.004	0.971	0.838	0.965	0.895	0.543	0.977	0.978	0.955
37	300.0	1.015	0.912	0.662	1.019	0.942	0.673	1.008	0.956	0.787	0.939	0.851	0.468	0.903	0.899	0.865
	900.0	1.022	0.955	0.734	1.019	0.972	0.774	1.009	0.977	0.841	0.932	0.876	0.521	0.915	0.911	0.869
	2100.0	1.023	0.977	0.798	1.014	0.984	0.845	1.004	0.982	0.878	0.892	0.854	0.539	0.937	0.933	0.892
38	300.0	0.970	0.783	0.485	0.963	0.836	0.503	0.978	0.879	0.645	1.007	0.959	0.926	0.993	0.780	0.391
	900.0	0.965	0.836	0.548	0.957	0.875	0.595	0.978	0.913	0.708	1.007	0.961	0.923	1.002	0.844	0.474
	2100.0	0.973	0.882	0.617	0.962	0.908	0.679	0.986	0.942	0.770	1.002	0.958	0.915	1.005	0.886	0.555
39	300.0	1.005	0.945	0.781	0.993	0.913	0.617	1.000	0.979	0.909	0.996	0.931	0.892	0.979	0.893	0.471
	900.0	1.019	0.979	0.836	1.005	0.954	0.730	1.007	0.993	0.938	1.117	1.041	0.969	0.992	0.953	0.599
	2100.0	1.032	1.003	0.882	1.022	0.986	0.815	1.015	1.004	0.959	1.374	1.274	1.115	1.003	0.990	0.713
40	300.0	0.983	0.898	0.654	1.001	0.917	0.586	0.998	0.966	0.831	0.991	0.925	0.873			
	900.0	0.973	0.924	0.722	0.986	0.939	0.697	0.985	0.969	0.868	0.966	0.908	0.848			
	2100.0	0.957	0.928	0.781	0.965	0.937	0.770	0.964	0.957	0.888	0.983	0.925	0.851			
41	300.0	0.982	0.723	0.475	0.988	0.792	0.407	0.997	0.844	0.622	0.946	0.815	0.480			
	900.0	1.018	0.804	0.518	1.008	0.867	0.510	1.015	0.900	0.668	0.952	0.865	0.542			
	2100.0	1.039	0.869	0.569	1.020	0.919	0.603	1.026	0.940	0.717	0.956	0.895	0.596			
42	300.0	0.897	0.545	0.333	0.984	0.741	0.391	0.943	0.679	0.437	0.957	0.971	0.993			
	900.0	0.950	0.613	0.360	1.011	0.816	0.479	0.974	0.748	0.468	0.954	0.971	0.994			
	2100.0	0.979	0.676	0.385	1.007	0.856	0.537	0.991	0.808	0.502	0.956	0.974	1.008			
43	300.0	1.001	0.845	0.617	1.007	0.815	0.363	1.003	0.949	0.827	0.939	0.951	0.923			
	900.0	1.017	0.904	0.655	1.022	0.893	0.479	1.007	0.971	0.859	0.930	0.944	0.903			
	2100.0	0.996	0.919	0.690	0.988	0.903	0.555	1.002	0.977	0.882	0.925	0.937	0.891			
44	300.0	1.001	0.756	0.488	0.954	0.731	0.306	0.983	0.898	0.739	1.011	1.012	0.988			
	900.0	1.029	0.847	0.528	0.980	0.827	0.413	0.993	0.935	0.779	0.984	0.985	0.925			
	2100.0	1.122	0.979	0.626	1.111	0.993	0.615	1.048	1.003	0.858	0.949	0.948	0.826			
45	300.0	0.946	0.615	0.325	0.961	0.690	0.261	0.976	0.822	0.589	0.994	0.989	0.967			
	900.0	0.982	0.724	0.366	0.983	0.792	0.360	0.988	0.878	0.639	0.996	0.989	0.962			
	2100.0	1.003	0.807	0.425	0.997	0.862	0.464	0.995	0.916	0.692	0.996	0.988	0.953			
46	300.0	0.676	0.315	0.172	0.865	0.479	0.155	0.852	0.528	0.316	0.938	0.932	1.440			
	900.0	0.741	0.402	0.178	0.910	0.590	0.208	0.909	0.633	0.346	1.452	1.441	1.466			
	2100.0	0.756	0.457	0.183	0.933	0.681	0.266	0.925	0.685	0.374	1.643	1.133	1.332			

47	300.0	0.988	0.497	0.352	0.993	0.639	0.244	0.992	0.665	0.634	1.247	0.852	1.330			
	900.0	0.978	0.669	0.397	0.986	0.754	0.328	0.986	0.852	0.629	1.237	1.237	1.237			
	2100.0	1.015	0.692	0.353	1.004	0.835	0.411	0.995	0.773	0.591	1.241	0.858	1.012			
48	300.0	0.338	0.121	0.061	0.586	0.277	0.101	0.520	0.281	0.138	0.915	1.058	0.847			
	900.0	0.299	0.145	0.062	0.496	0.321	0.120	0.420	0.302	0.151	0.901	0.901	0.890			
	2100.0	0.318	0.175	0.066	0.507	0.375	0.151	0.416	0.333	0.173	0.899	1.055	0.982			
49	300.0	0.999	1.095	0.954	1.003	1.163	0.953	1.001	1.096	0.964	0.966	1.022	0.923			
	900.0	0.993	0.993	0.985	1.002	1.002	1.002	0.995	0.996	0.994	0.959	0.958	0.941			
	2100.0	0.993	1.095	1.047	1.004	1.166	1.101	0.995	1.096	1.055	0.959	1.023	0.977			
50	300.0	0.443	0.170	0.071	0.840	0.341	0.104	0.852	0.378	0.163	1.024	1.024	0.428			
	900.0	0.757	0.227	0.072	0.942	0.460	0.133	0.951	0.493	0.193	0.544	0.544	0.289			
	2100.0	0.840	0.311	0.078	1.019	0.593	0.176	-0.486	0.621	0.236	0.196	0.310	0.142			
51	300.0	0.990	0.988	0.982	1.029	1.036	1.112	0.988	0.986	0.964	0.996	0.993	0.967			
	900.0	0.985	0.984	0.983	1.098	1.110	1.125	0.971	0.968	0.962	0.986	0.982	0.973			
	2100.0	0.994	0.991	0.990	1.109	1.106	1.121	0.968	0.969	0.963	0.987	0.983	0.975			
52	300.0	0.983	0.983	0.969	0.965	0.964	0.860	0.997	0.997	0.986	0.808	0.805	0.679			
	900.0	0.978	0.977	0.971	0.919	0.917	0.871	0.992	0.992	0.987	0.839	0.836	0.649			
	2100.0	0.978	0.981	0.974	0.922	0.948	0.888	0.992	0.994	0.988	0.781	0.706	0.497			
53	300.0	0.693	0.268	0.100	0.980	0.534	0.155	0.945	0.688	0.465	1.009	1.010	1.002			
	900.0	0.700	0.330	0.103	1.040	0.672	0.197	0.963	0.755	0.483	1.005	1.007	1.007			
	2100.0	0.510	0.313	0.108	0.849	0.639	0.220	0.835	0.721	0.493	1.010	1.016	1.016			
54	300.0	1.001	1.001	0.998	0.997	0.997	1.007	1.001	1.001	0.998	0.991	0.990	0.976			
	900.0	0.998	0.998	0.998	1.006	1.006	1.005	0.998	0.998	0.998	0.988	0.987	0.974			
	2100.0	0.998	1.000	1.000	1.007	1.002	1.001	0.998	1.000	1.000	0.984	0.982	0.969			
55	300.0	1.001	1.001	0.997	1.003	1.003	0.987	1.001	1.001	0.998	1.003	1.000	0.918			
	900.0	0.998	0.998	0.998	0.991	0.991	0.990	0.999	0.999	0.998	0.976	0.972	0.931			
	2100.0	0.998	1.000	0.999	0.991	0.998	0.997	0.999	1.000	1.000	0.971	0.970	0.936			
56	300.0	1.000	1.000	0.996	1.006	1.006	0.975	1.001	1.001	0.997	0.983	0.983	0.962			
	900.0	0.997	0.997	0.997	0.983	0.983	0.981	0.998	0.998	0.998	0.989	0.989	0.953			
	2100.0	0.997	0.999	0.999	0.983	0.998	0.995	0.998	1.000	1.000	0.989	0.989	0.948			
57	300.0	1.035	1.034	1.029	0.955	0.955	0.865	0.995	0.995	0.984	0.953	0.953	0.709			
	900.0	1.023	1.023	1.029	0.903	0.903	0.870	0.989	0.989	0.986	0.894	0.894	0.737			
	2100.0	1.029	1.036	1.036	0.887	0.915	0.883	0.987	0.991	0.987	0.883	0.907	0.772			
58	300.0	1.002	1.002	0.989	1.011	1.011	0.930	1.002	1.002	0.992	0.966	0.965	0.907	1.012	1.012	0.926
	900.0	0.991	0.991	0.992	0.954	0.954	0.947	0.995	0.995	0.994	0.953	0.952	0.907	0.951	0.951	0.943
	2100.0	0.990	0.998	0.999	0.952	0.987	0.982	0.994	0.999	0.998	0.947	0.953	0.916	0.949	0.987	0.980
59	300.0	1.004	1.004	0.996	1.013	1.012	0.987	1.002	1.002	0.999	1.000	0.996	0.961	1.013	1.013	0.987
	900.0	1.000	0.999	0.998	0.997	0.997	0.992	1.000	1.000	0.999	0.997	0.993	0.957	0.997	0.997	0.992
	2100.0	1.000	1.002	1.001	0.998	1.007	1.002	1.000	1.001	1.001	0.997	0.995	0.959	0.998	1.007	1.003
60	300.0	1.001	1.000	0.981	1.002	1.001	0.961	1.000	1.000	0.992	1.001	0.991	0.911	1.002	1.001	0.960
	900.0	0.992	0.991	0.985	0.980	0.979	0.968	0.996	0.996	0.994	0.995	0.985	0.908	0.980	0.979	0.968
	2100.0	0.992	0.997	0.991	0.982	0.994	0.983	0.996	0.999	0.997	0.995	0.989	0.911	0.981	0.994	0.982
61	300.0	1.001	0.998	0.949	1.002	0.999	0.927	1.001	1.000	0.980	1.001	0.977	0.792	1.002	0.999	0.926
	900.0	0.982	0.979	0.956	0.970	0.967	0.938	0.992	0.991	0.983	0.989	0.966	0.789	0.970	0.967	0.938
	2100.0	0.983	0.992	0.968	0.973	0.989	0.959	0.993	0.997	0.989	0.990	0.973	0.792	0.973	0.989	0.959
62	300.0	0.998	0.982	0.849	0.999	0.985	0.839	1.000	0.994	0.937	1.002	0.924	0.525	0.999	0.985	0.838
	900.0	0.958	0.944	0.862	0.948	0.935	0.857	0.980	0.975	0.944	0.973	0.902	0.525	0.947	0.935	0.857
	2100.0	0.963	0.973	0.884	0.954	0.973	0.888	0.982	0.989	0.956	0.977	0.919	0.524	0.953	0.973	0.888
63	300.0	0.971	0.832	0.540	0.978	0.875	0.568	0.987	0.927	0.738	0.974	0.619	0.140	0.978	0.875	0.568
	900.0	0.884	0.771	0.558	0.882	0.799	0.593	0.931	0.881	0.753	0.894	0.593	0.137	0.882	0.799	0.592
	2100.0	0.906	0.826	0.584	0.908	0.872	0.632	0.944	0.922	0.777	0.921	0.618	0.132	0.907	0.872	0.631
64	300.0	0.125	0.055	0.033	0.261	0.094	0.033	0.299	0.132	0.065	0.216	0.028	-0.002	0.261	0.094	0.033
	900.0	0.112	0.049	0.036	0.236	0.082	0.040	0.275	0.119	-0.045	0.305	0.032	0.083	0.236	0.082	0.040
	2100.0	0.129	0.057	0.043	0.262	0.104	0.049	0.301	0.142	0.084	0.305	0.031	0.104	0.262	0.104	0.049

A-IV-3 Gradient f_x^1 of f_x for Pu-240

		TOTAL			ELASTIC			REMOVAL			FISSION		
		10000.	1000.	100.	10000.	1000.	100.	10000.	1000.	100.	10000.	1000.	100.
26	300.0	2.4E-05	2.6E-04	2.0E-03	1.0E-06	2.1E-05	5.9E-04	-9.5E-07	4.8E-06	4.9E-04	7.4E-03	2.9E-04	-4.8E-03
	900.0	2.2E-05	2.3E-04	1.7E-03	5.0E-07	9.5E-06	3.5E-04	-1.4E-06	-7.2E-06	2.9E-04	8.9E-05	4.9E-04	-4.0E-03
	2100.0	1.9E-05	2.0E-04	1.5E-03	1.8E-06	1.8E-05	2.9E-04	-1.7E-06	-9.5E-06	1.9E-04	9.8E-05	6.4E-04	-3.2E-03
27	300.0	3.0E-05	3.3E-04	2.3E-03	-9.3E-04	-4.9E-05	3.3E-04	2.1E-06	3.8E-05	7.1E-04	-1.8E-04	-7.6E-04	-7.2E-03
	900.0	3.2E-05	3.4E-04	2.4E-03	-1.0E-03	-6.3E-05	3.0E-05	7.1E-07	1.4E-05	4.5E-04	-2.1E-04	-1.0E-03	-8.0E-03
	2100.0	2.0E-05	2.1E-04	1.5E-03	-8.0E-04	-4.2E-05	-4.5E-05	-7.1E-07	-2.4E-06	2.6E-04	-1.8E-04	-7.0E-04	-6.9E-03
28	300.0	5.4E-05	6.0E-04	4.4E-03	-7.2E-04	-4.8E-05	7.6E-04	2.3E-06	6.8E-05	1.1E-03	-2.5E-04	-1.4E-03	-9.9E-03
	900.0	5.2E-05	5.6E-04	3.9E-03	-3.7E-04	-2.2E-05	4.5E-04	2.1E-06	5.7E-05	8.3E-04	-2.5E-04	-1.4E-03	-9.6E-03
	2100.0	2.2E-05	2.6E-04	2.0E-03	-6.0E-04	-5.0E-05	1.8E-04	-3.4E-06	0.0	3.8E-04	-2.6E-04	-1.4E-03	-9.1E-03
29	300.0	3.3E-05	4.1E-04	3.1E-03	-2.1E-03	-1.8E-04	-1.2E-02	0.0		4.1E-05	-1.1E-02	-1.8E-04	-1.8E-03
	900.0	4.7E-05	5.2E-04	4.0E-03	-2.5E-03	-2.3E-04	-3.0E-05	3.9E-06		6.6E-05	1.3E-03	-2.0E-04	-2.0E-03
	2100.0	4.8E-05	5.1E-04	3.9E-03	-2.1E-03	-2.0E-04	-4.9E-03	4.3E-06		5.9E-05	-7.2E-03	-2.2E-04	-2.2E-03
30	300.0	2.1E-05	3.4E-04	3.4E-03	1.4E-07	5.3E-05	-1.7E-02	-5.6E-06		1.7E-05	-1.4E-02	-2.0E-04	-1.8E-03
	900.0	2.7E-05	3.6E-04	3.7E-03	4.6E-04	1.5E-05	1.1E-03	8.6E-07		5.6E-05	1.2E-03	-2.0E-04	-1.9E-03
	2100.0	3.8E-05	4.4E-04	2.9E-03	8.2E-06	9.8E-05	-8.4E-03	6.7E-06		9.5E-05	-1.0E-02	-2.1E-04	-2.0E-03
31	300.0	1.0E-05	2.4E-04	3.6E-03	-2.0E-05	-1.3E-04	-2.1E-02	-1.8E-03		-9.5E-05	-1.5E-02	-2.7E-04	-2.6E-03
	900.0	2.9E-06	1.4E-04	1.1E-03	-1.7E-05	-1.2E-04	1.1E-03	-1.8E-05		-1.3E-04	1.4E-03	-3.2E-04	-3.1E-03
	2100.0	5.4E-06	1.3E-04	1.0E-03	-1.2E-05	-9.2E-05	-1.2E-02	-1.5E-03		-1.2E-04	-1.1E-02	-3.4E-04	-3.3E-03
32	300.0	1.0E-04	1.1E-03	8.6E-03	5.0E-05	5.9E-04	5.2E-03	2.5E-05		3.2E-04	3.3E-03	-6.5E-05	-6.6E-04
	900.0	6.8E-05	7.6E-04	5.8E-03	3.5E-05	4.1E-04	3.5E-03	1.3E-05		1.8E-04	2.3E-03	-6.6E-05	-6.8E-04
	2100.0	5.8E-05	6.4E-04	4.6E-03	2.5E-05	2.9E-04	2.5E-03	7.5E-06		1.1E-04	1.7E-03	-8.2E-05	-8.5E-04
33	300.0	1.3E-05	2.8E-04	4.0E-03	-3.2E-05	-1.9E-04	2.5E-03	-2.8E-06		4.9E-05	1.8E-03	-1.6E-04	-1.5E-03
	900.0	2.9E-05	3.8E-04	3.9E-03	-2.6E-05	-1.8E-04	1.3E-03	2.3E-07		5.1E-05	1.4E-03	-1.5E-04	-1.5E-03
	2100.0	2.8E-05	3.4E-04	3.1E-03	-2.4E-05	-1.9E-04	2.4E-04	-3.2E-06		-2.3E-06	7.6E-04	-1.6E-04	-1.5E-03
34	300.0	1.6E-04	1.8E-03	1.1E-02	4.1E-05	5.9E-04	6.0E-03	4.5E-05		6.1E-04	5.3E-03	-1.6E-04	-1.5E-03
	900.0	1.1E-04	1.3E-03	9.8E-03	2.1E-05	3.4E-04	4.1E-03	2.7E-05		3.9E-04	4.4E-03	-2.2E-04	-2.1E-03
	2100.0	9.9E-05	1.1E-03	9.1E-03	8.9E-06	1.7E-04	2.7E-03	1.9E-05		2.7E-04	3.6E-03	-2.5E-04	-2.4E-03
35	300.0	5.3E-04	3.6E-03	1.4E-02	3.1E-05	3.7E-04	4.9E-03	1.0E-04		8.7E-04	4.5E-03	-3.2E-04	-3.1E-03
	900.0	3.1E-04	2.7E-03	1.5E-02	8.1E-06	1.7E-04	3.7E-03	3.6E-05		4.2E-04	3.7E-03	-3.7E-04	-3.6E-03
	2100.0	2.1E-04	2.1E-03	1.5E-02	7.8E-06	1.6E-04	3.3E-03	7.1E-07		1.0E-04	2.9E-03	-3.9E-04	-3.9E-03
36	300.0	-2.8E-05	4.5E-04	5.6E-03	-4.1E-06	3.4E-04	5.9E-03	-9.7E-06		2.9E-04	4.1E-03	-1.2E-04	-2.1E-04
	900.0	-2.6E-05	2.9E-04	5.2E-03	-1.9E-05	6.5E-05	4.0E-03	-1.1E-05		1.7E-04	3.7E-03	-1.6E-04	-8.7E-04
	2100.0	-1.2E-05	2.9E-04	4.8E-03	-2.4E-05	-6.8E-05	2.6E-03	-7.8E-06		1.2E-04	3.2E-03	-1.9E-04	-1.3E-03
37	300.0	1.4E-05	6.9E-04	7.5E-03	1.5E-05	5.9E-04	7.9E-03	7.3E-06		3.5E-04	4.5E-03	-2.8E-04	-2.1E-03
	900.0	3.7E-05	7.3E-04	8.2E-03	3.4E-05	6.2E-04	7.5E-03	1.0E-05		2.9E-04	4.1E-03	-3.0E-04	-2.5E-03
	2100.0	4.0E-05	6.7E-04	7.7E-03	5.2E-05	7.1E-04	6.9E-03	9.1E-06		2.2E-04	3.4E-03	-2.9E-04	-2.6E-03
38	300.0	-3.6E-06	6.5E-04	5.0E-03	-4.4E-05	1.8E-04	5.7E-03	-1.1E-05		3.3E-04	4.4E-03	-2.1E-04	-1.1E-03
	900.0	-6.9E-05	6.7E-06	4.4E-03	-1.0E-04	-5.1E-04	3.5E-03	-3.9E-05		-3.7E-05	3.8E-03	-2.2E-04	-1.3E-03
	2100.0	-5.1E-05	-3.0E-05	4.4E-03	-1.1E-04	-7.3E-04	2.2E-03	-3.6E-05		-1.2E-04	3.3E-03	-2.3E-04	-1.4E-03
39	300.0	-9.1E-06	2.5E-04	4.1E-03	-2.9E-06	4.5E-04	8.5E-03	-2.7E-06		1.1E-04	1.9E-03	-3.2E-04	-1.6E-03
	900.0	-2.0E-06	2.1E-04	3.9E-03	9.0E-06	3.7E-04	7.3E-03	-1.2E-06		8.7E-05	1.6E-03	-3.5E-04	-2.0E-03
	2100.0	7.3E-06	2.5E-04	3.9E-03	4.1E-06	2.9E-04	6.0E-03	-3.7E-06		4.7E-05	1.3E-03	-4.5E-04	-3.0E-03
40	300.0	-6.0E-05	-7.6E-05	4.6E-03	-8.9E-06	3.2E-04	8.6E-03	-2.3E-06		5.7E-05	3.5E-03	-2.5E-04	-1.1E-03
	900.0	-2.0E-05	8.2E-05	5.1E-03	-4.3E-06	2.1E-04	7.2E-03	-7.8E-06		-2.8E-05	3.0E-03	-2.2E-04	-1.4E-03
	2100.0	2.5E-05	4.0E-04	5.3E-03	8.7E-06	2.4E-04	5.8E-03	-8.5E-06		-5.3E-05	2.3E-03	-2.3E-04	-1.9E-03
41	300.0	4.8E-05	1.2E-03	4.5E-03	2.4E-05	1.1E-03	8.8E-03	1.7E-05		7.3E-04	4.1E-03	-3.2E-05	3.1E-04
	900.0	5.8E-05	1.3E-03	5.8E-03	2.6E-05	8.9E-04	8.5E-03	1.7E-05		6.4E-04	4.3E-03	-5.5E-05	-1.2E-04
	2100.0	8.1E-05	1.4E-03	6.9E-03	3.3E-05	7.9E-04	7.8E-03	2.2E-05		5.7E-04	4.2E-03	-8.0E-05	-4.9E-04
42	300.0	-8.1E-07	7.9E-04	3.0E-03	-2.6E-05	7.1E-04	7.2E-03	-4.1E-05		9.2E-04	2.5E-03	-4.4E-05	-3.1E-04
	900.0	-4.9E-05	6.8E-04	3.2E-03	-6.3E-05	2.8E-04	6.0E-03	-7.9E-05		2.0E-04	2.3E-03	-5.8E-05	-4.6E-04
	2100.0	-8.3E-05	5.0E-04	3.2E-03	-9.7E-05	-1.7E-04	4.2E-03	-1.1E-04		-1.9E-04	1.5E-03	-7.9E-05	-6.3E-04
43	300.0	2.0E-05	8.2E-04	4.5E-03	3.8E-05	1.2E-03	1.2E-02	1.6E-05		3.8E-04	3.3E-03	-7.7E-05	-6.9E-04
	900.0	6.8E-06	5.7E-04	5.8E-03	3.0E-05	8.9E-04	1.2E-02	1.6E-05		3.2E-04	3.6E-03	-9.7E-05	-8.8E-04
	2100.0	3.4E-07	3.4E-04	6.3E-03	-9.3E-06	2.7E-04	1.1E-02	1.3E-05		2.1E-04	3.6E-03	-1.3E-04	-1.1E-03
44	300.0	4.4E-04	3.4E-03	1.0E-02	3.5E-05	8.6E-04	5.7E-03	1.6E-05		3.3E-04	2.0E-03	-9.9E-05	-1.1E-03
	900.0	5.1E-04	4.3E-03	1.5E-02	8.4E-05	1.2E-03	7.4E-03	3.6E-05		4.6E-04	2.7E-03	-1.8E-04	-1.9E-03
	2100.0	2.2E-05	9.7E-04	6.4E-03	1.2E-04	1.7E-03	8.2E-03	4.8E-05		6.9E-04	3.0E-03	-2.5E-04	-2.6E-03
45	300.0	7.1E-05	1.7E-03	5.4E-03	5.3E-05	1.6E-03	1.0E-02	3.1E-05		9.0E-04	5.4E-03	-6.1E-05	-6.1E-04
	900.0	7.1E-05	1.7E-03	8.2E-03	5.3E-05	1.4E-03	1.2E-02	2.9E-05		7.6E-04	6.4E-03	-7.3E-05	-7.2E-04
	2100.0	7.4E-05	1.5E-03	9.6E-03	5.3E-05	1.1E-03	1.2E-02	2.7E-05		6.0E-04	6.3E-03	-7.4E-05	-7.3E-04
46	300.0	-3.4E-04	5.5E-05	3.9E-04	-9.3E-05	1.4E-03	6.6E-03	-9.3E-05		1.2E-03	2.0E-03	6.8E-04	6.7E-03
	900.0	-4.3E-04	-7.1E-04	1.9E-03	-1.4E-04	8.7E-04	7.0E-03	-1.8E-04		2.7E-04	2.9E-03	-1.3E-04	-1.4E-03
	2100.0	-4.0E-04	-6.4E-04	3.1E-03	-1.6E-04	2.4E-04	6.6E-03	-2.2E-04		-1.8E-05	1.3E-03	-2.1E-04	7.7E-03

47 300.0-2.7E-05 2.7E-03-2.0E-03 4.9E-06 1.5E-03 6.0E-03-9.4E-06 3.3E-03-5.3E-03-1.1E-04 6.7E-03-3.1E-02
900.0 5.5E-05 1.2E-03 3.3E-03 7.9E-05 1.3E-03 7.0E-03 3.4E-05 6.2E-04 2.8E-03-1.0E-04-1.1E-03-1.4E-02
2100.0 7.2E-05 2.7E-03 4.3E-03 7.8E-05 1.2E-03 7.3E-03 2.8E-05 3.0E-03 2.7E-03-1.2E-04 6.4E-03-1.4E-02

48 300.0-1.5E-04 5.3E-05 2.9E-04-1.9E-04 4.5E-04 2.6E-03-2.4E-04 4.0E-05 2.1E-03-6.4E-05-3.6E-03 5.3E-03
900.0-2.8E-05 1.4E-04 6.0E-04-3.7E-05 2.5E-04 3.1E-03-9.4E-05-2.5E-04 2.2E-03-3.9E-05-4.6E-04-3.5E-03
2100.0-3.3E-05 2.0E-04 1.0E-03-3.4E-05 8.6E-05 3.7E-03-9.0E-05-4.5E-04 2.2E-03-3.8E-05-3.6E-03-3.0E-03

49 300.0-3.4E-05-2.3E-03 5.2E-03-1.8E-06-3.2E-03 9.9E-03-1.6E-05-2.1E-03 5.7E-03-4.1E-05-1.7E-03 2.0E-03
900.0-2.2E-05-2.3E-04-9.8E-04 3.5E-06 3.8E-05 2.0E-04-4.5E-06-6.0E-05-3.4E-04-2.6E-05-3.7E-04-1.7E-03
2100.0-2.1E-05-2.3E-03-9.1E-04 4.3E-06-3.2E-03 2.0E-04-4.8E-06-2.1E-03-3.4E-04-2.5E-05-1.6E-03-1.6E-03

50 300.0-8.9E-05 5.3E-04 7.6E-04 7.5E-05 1.8E-03 3.5E-03 7.1E-05 1.9E-03 4.1E-03-1.3E-03-1.3E-02-1.4E-02
900.0-1.9E-04 6.1E-04 1.0E-03-1.1E-05 1.6E-03 4.1E-03-1.5E-05 1.6E-03 4.5E-03-6.3E-04-6.3E-03-1.3E-02
2100.0-2.5E-04 4.7E-04 1.5E-03-8.3E-05 1.0E-03 4.3E-03 2.9E-03 1.0E-03 4.6E-03-2.6E-04-4.0E-03-6.7E-03

51 300.0-1.8E-06-1.1E-05 5.9E-04 6.2E-05 6.3E-04-6.3E-03-2.3E-05-2.2E-04 1.5E-03-5.8E-05-5.1E-04 7.6E-04
900.0 1.0E-05 1.2E-04 5.7E-04-5.1E-05-5.5E-04-4.5E-03 6.0E-06 7.3E-05 9.5E-04-4.1E-05-3.1E-04-7.8E-04
2100.0 7.0E-06 1.1E-04 5.6E-04-8.0E-05-7.7E-04-5.5E-03 1.2E-05 1.3E-04 1.3E-03-3.8E-05-1.9E-04 7.9E-04

52 300.0-2.9E-05-2.9E-04-2.8E-05-2.6E-04-2.6E-03-5.0E-03-2.9E-05-2.9E-04-6.0E-04-4.9E-04-4.8E-03-2.3E- 2
900.0-1.7E-05-1.7E-04-3.9E-04-1.7E-04-1.6E-03-6.9E-03-1.9E-05-1.9E-04-8.6E-04-5.8E-04-5.7E-03-2.0E-02
2100.0-1.7E-05-1.7E-04-3.7E-04-1.8E-04-2.0E-03-7.4E-03-2.0E-05-2.1E-04-8.5E-04-6.0E-04-5.9E-03-1.7E-02

53 300.0-6.4E-04-1.3E-03-4.0E-04-4.3E-04-7.7E-04 6.2E-04-2.8E-04-7.0E-04 1.6E-04-3.2E-05-3.1E-04-1.0E-03
900.0-6.8E-04-2.0E-03-1.7E-04-5.6E-04-2.2E-03 5.2E-04-3.5E-04-1.5E-03 3.1E-04-2.0E-05-1.9E-04-1.2E-03
2100.0-4.6E-04-2.0E-03-2.9E-04-5.5E-04-3.3E-03-1.3E-03-3.2E-04-2.0E-03-7.0E-04-2.3E-05-2.5E-04-1.7E-03

54 300.0-5.3E-06-5.3E-05 9.1E-05 1.7E-05 1.8E-04-4.6E-04-5.2E-06-5.2E-05 1.2E-04-5.6E-05-5.5E-04-3.5E-03
900.0-8.5E-07-8.9E-06-4.1E-05-1.7E-07 1.7E-06 7.2E-05-2.7E-07-3.4E-06-2.8E-05-5.4E-05-5.2E-04-3.6E-03
2100.0-8.5E-07-8.9E-06-4.5E-05-1.7E-07 1.7E-06 7.7E-05-3.0E-07-3.0E-06-3.2E-05-5.6E-05-5.3E-04-3.8E-03

55 300.0-5.7E-06-5.7E-05 9.2E-05-2.9E-05-2.8E-04 2.6E-04-5.3E-06-5.2E-05 5.2E-05-2.5E-04-2.4E-03-9.0E-03
900.0-1.2E-06-1.2E-05-5.2E-05-5.9E-06-5.7E-05-3.8E-04-1.0E-06-1.0E-05-7.0E-05-1.8E-04-1.8E-03-1.1E-02
2100.0-1.4E-06-1.4E-05-6.4E-05-5.9E-06-6.0E-05-4.3E-04-1.1E-06-1.1E-05-7.7E-05-1.7E-04-1.6E-03-1.1E-02

56 300.0-7.7E-06-7.7E-05 1.8E-04-6.1E-05-6.0E-04 2.3E-04-6.7E-06-6.7E-05 2.5E-05-1.9E-04-1.9E-03-1.5E-02
900.0-1.3E-06-1.3E-05-2.9E-05-1.4E-05-1.4E-04-1.0E-03-1.5E-06-1.5E-05-1.2E-04-2.0E-04-2.0E-03-1.4E-02
2100.0-9.7E-07-9.7E-06-9.7E-06-1.4E-05-1.6E-04-1.2E-03-1.6E-06-1.7E-05-1.3E-04-2.1E-04-2.3E-03-1.5E-02

57 300.0-1.8E-06-1.8E-05 7.1E-04-1.9E-04-1.9E-03-1.0E-03-2.1E-05-2.1E-04-4.7E-05-6.1E-04-6.1E-03-1.2E-02
900.0 1.4E-05 1.4E-04-2.7E-05-9.8E-05-9.8E-04-3.2E-03-1.1E-05-1.1E-04-3.7E-04-5.0E-04-5.0E-03-1.8E-02
2100.0-1.8E-06-8.9E-06-2.5E-04-9.3E-05-9.7E-04-3.2E-03-1.0E-05-1.1E-04-3.6E-04-5.1E-04-4.5E-03-1.7E-02

58 300.0-8.9E-06-8.9E-05 1.4E-03-1.1E-04-1.1E-03 5.5E-03-1.3E-05-1.3E-04 6.8E-04 1.9E-05 2.2E-04 1.4E-02-1.1E-04-1.1E-03 5.8E-03
900.0 1.3E-05 1.4E-04 1.0E-03 8.4E-06 8.6E-05 2.3E-03 8.7E-07 8.7E-06 2.9E-04 4.8E-05 5.1E-04 1.4E-02 8.8E-06 9.0E-05 2.4E-03
2100.0 1.6E-05 1.3E-04 9.7E-04 1.1E-05 1.2E-04 2.3E-03 1.2E-06 1.4E-05 2.9E-04 5.8E-05 6.1E-04 1.4E-02 1.2E-05 1.2E-04 2.4E-03

59 300.0-1.2E-05-1.2E-04 9.8E-05-4.0E-05-4.0E-04 3.0E-04-6.0E-06-6.0E-05 3.9E-05-6.7E-05-6.9E-04-5.5E-03-4.1E-05-4.1E-04 3.1E-04
900.0-2.4E-06-2.6E-05-1.8E-04-8.5E-06-8.8E-05-6.6E-04-1.3E-06-1.3E-05-1.0E-04-6.1E-05-6.3E-04-4.8E-03-8.8E-06-9.0E-05-6.8E-04
2100.0-2.6E-06-2.6E-05-1.8E-04-8.8E-06-9.0E-05-6.8E-04-1.3E-06-1.3E-05-1.0E-04-6.2E-05-6.4E-04-4.8E-03-8.9E-06-9.3E-05-7.0E-04

60 300.0-2.3E-05-2.3E-04 4.2E-04-5.2E-05-5.2E-04 9.1E-04-1.0E-05-1.0E-04 1.7E-04-6.4E-05-6.3E-04-3.5E-03-5.3E-05-5.3E-04 9.3E-04
900.0-3.8E-06-3.7E-05-1.8E-04-8.0E-06-8.1E-05-5.0E-04-1.8E-06-1.8E-05-1.0E-04-5.2E-05-5.1E-04-2.9E-03-8.1E-06-8.2E-05-5.0E-04
2100.0-3.8E-06-3.8E-05-1.9E-04-8.1E-06-8.4E-05-5.3E-04-1.8E-06-1.8E-05-1.0E-04-5.2E-05-5.2E-04-3.0E-03-8.2E-06-8.4E-05-5.3E-04

61 300.0-4.6E-05-4.5E-04 1.2E-03-7.4E-05-7.4E-04 1.8E-03-2.1E-05-2.0E-04 4.7E-04-7.8E-05-7.2E-04-1.7E-03-7.4E-05-7.5E-04 1.8E-03
900.0-6.1E-06-5.3E-05-8.7E-06-9.3E-06-8.8E-05-2.7E-04-2.7E-06-2.3E-05-7.5E-05-5.4E-05-4.9E-04-1.2E-03-9.3E-06-8.8E-05-2.8E-04
2100.0-6.3E-06-5.6E-05-2.0E-05-9.3E-06-9.3E-05-3.0E-04-2.7E-06-2.5E-05-8.1E-05-5.4E-05-5.1E-04-1.3E-03-9.4E-06-9.3E-05-3.0E-04

62 300.0-9.2E-05-8.5E-04 2.8E-03-1.2E-04-1.1E-03 3.0E-03-4.5E-05-4.4E-04 1.2E-03-9.6E-05-7.2E-04 4.9E-04-1.2E-04-1.1E-03 3.0E-03
900.0-7.3E-06-3.6E-05 3.9E-04-8.7E-06-7.1E-05-2.4E-04-3.5E-06-2.9E-05-1.1E-04-3.6E-05-2.5E-04 4.9E-04-8.7E-06-7.1E-05-2.4E-04
2100.0-8.0E-06-4.3E-05 3.7E-04-9.4E-06-8.3E-05-3.0E-04-3.8E-06-3.3E-05-1.4E-04-3.8E-05-2.7E-04 4.1E-04-9.5E-06-8.2E-05-3.0E-04

63 300.0-2.0E-04-1.1E-03 4.7E-03-2.2E-04-1.7E-03 5.3E-03-1.3E-04-9.8E-04 3.3E-03-2.1E-04-3.8E-04 2.0E-03-2.3E-04-1.7E-03 5.3E-03
900.0-5.6E-06 2.3E-04 1.8E-03-8.9E-06 5.4E-05 1.3E-03-5.4E-06 3.2E-05 7.8E-04-2.6E-05 2.3E-04 2.4E-03-8.9E-06 5.3E-05 1.3E-03
2100.0-6.0E-06 2.8E-04 1.9E-03-9.4E-06 6.9E-05 1.4E-03-5.7E-06 4.0E-05 8.3E-04-2.8E-05 2.7E-04 2.3E-03-9.5E-06 6.9E-05 1.4E-03

64 300.0-1.3E-05-1.0E-04 7.5E-04-6.4E-05-2.4E-04 2.1E-03-5.9E-05-2.7E-04 2.4E-03 1.8E-04 2.1E-04 3.5E-04-6.4E-05-2.4E-04 2.1E-03
900.0 2.9E-05 4.3E-05 1.8E-04 2.0E-05 7.3E-05 1.1E-03 2.0E-05 7.6E-05 9.0E-03 3.6E-05 1.4E-04-5.2E-03 2.0E-05 7.3E-05 1.1E-03
2100.0 3.4E-05 5.1E-05 2.0E-04 2.0E-05 9.2E-05 1.5E-03 2.0E-05 9.3E-05 1.5E-03 3.8E-05 1.7E-04-6.8E-03 2.0E-05 9.2E-05 1.5E-03

B-I Shielding factor for U-235 (Without interference effect)

		TOTAL			CAPTURE			ELASTIC			REMOVAL			FISSION		
		1000.	100.	10.	1000.	100.	10.	1000.	100.	10.	1000.	100.	10.	1000.	100.	10.
29	300.0	1.000	0.996	0.979	1.000	0.994	0.968	1.000	0.999	0.998	0.978	0.916	0.531	0.999	0.992	0.966
	900.0	1.000	0.998	0.986	1.000	0.996	0.976	1.000	1.000	0.999	0.979	0.920	0.546	0.999	0.994	0.973
	2100.0	1.000	0.999	0.991	1.000	0.997	0.982	1.000	1.000	0.999	0.979	0.919	0.540	0.999	0.996	0.980
30	300.0	1.000	0.993	0.969	0.999	0.990	0.950	1.000	0.999	0.996	0.968	0.892	0.429	0.999	0.991	0.962
	900.0	1.000	0.996	0.978	0.999	0.992	0.961	1.000	0.999	0.997	0.968	0.896	0.442	0.999	0.994	0.972
	2100.0	1.000	0.997	0.984	0.999	0.994	0.969	1.000	1.000	1.000	0.968	0.896	0.437	0.999	0.996	0.980
31	300.0	0.999	0.988	0.951	0.998	0.984	0.927	0.999	0.998	0.992	0.964	0.883	0.486	0.998	0.986	0.937
	900.0	0.999	0.992	0.965	0.998	0.989	0.944	0.999	0.998	0.995	0.965	0.886	0.487	0.998	0.990	0.952
	2100.0	1.000	0.995	0.973	0.999	0.991	0.955	1.000	0.999	0.996	0.964	0.885	0.482	0.999	0.992	0.963
32	300.0	0.998	0.986	0.946	0.999	0.983	0.914	0.999	0.998	0.989	0.982	0.889	0.422	0.999	0.985	0.934
	900.0	0.999	0.991	0.961	1.000	0.988	0.932	0.999	0.998	0.992	0.982	0.890	0.419	0.999	0.989	0.949
	2100.0	0.999	0.993	0.969	1.000	0.993	0.942	0.999	0.999	0.993	0.982	0.888	0.412	1.000	0.992	0.958
33	300.0	0.997	0.980	0.926	0.998	0.980	0.919	0.999	0.997	0.992	0.978	0.877	0.336	0.998	0.978	0.904
	900.0	0.998	0.987	0.945	0.999	0.987	0.942	0.999	0.998	0.995	0.978	0.877	0.330	0.999	0.984	0.924
	2100.0	0.999	0.990	0.957	1.000	0.990	0.955	0.999	0.998	0.997	0.978	0.876	0.321	0.999	0.988	0.936
34	300.0	0.996	0.971	0.895	0.997	0.969	0.880	1.000	0.996	0.985	0.971	0.826	0.313	0.997	0.970	0.878
	900.0	0.997	0.982	0.927	0.998	0.979	0.911	1.000	0.998	0.990	0.971	0.829	0.307	0.998	0.981	0.914
	2100.0	0.998	0.987	0.943	0.999	0.984	0.927	1.000	0.998	0.992	0.971	0.829	0.301	0.999	0.985	0.929
35	300.0	0.996	0.969	0.888	0.998	0.977	0.919	1.000	0.998	0.992	0.980	0.849	0.306	0.997	0.969	0.875
	900.0	0.998	0.983	0.933	0.999	0.988	0.960	1.000	0.999	0.999	0.981	0.851	0.300	0.998	0.981	0.917
	2100.0	0.999	0.990	0.958	0.999	0.994	0.981	1.000	1.000	1.000	0.981	0.854	0.300	0.999	0.990	0.950
36	300.0	0.994	0.954	0.854	0.994	0.954	0.846	0.998	0.992	0.976	0.976	0.823	0.298	0.996	0.964	0.873
	900.0	0.996	0.969	0.891	0.996	0.969	0.887	0.999	0.995	0.983	0.976	0.824	0.287	0.997	0.975	0.907
	2100.0	0.998	0.980	0.924	1.000	0.986	0.916	0.999	0.997	0.988	0.977	0.833	0.289	0.999	0.985	0.937
37	300.0	0.990	0.931	0.814	0.992	0.941	0.823	0.998	0.990	0.975	0.975	0.806	0.282	0.993	0.948	0.844
	900.0	0.993	0.951	0.854	0.995	0.958	0.866	0.998	0.994	0.983	0.975	0.803	0.285	0.996	0.966	0.886
	2100.0	0.996	0.967	0.889	0.996	0.969	0.895	0.999	0.996	0.988	0.975	0.805	0.259	0.998	0.979	0.919
38	300.0	0.987	0.911	0.758	0.987	0.911	0.716	0.998	0.986	0.963	0.953	0.758	0.206	0.991	0.930	0.773
	900.0	0.991	0.937	0.809	0.991	0.934	0.768	0.998	0.990	0.970	0.954	0.759	0.189	0.994	0.951	0.825
	2100.0	0.994	0.954	0.846	0.993	0.947	0.795	0.999	0.992	0.973	0.955	0.765	0.185	0.996	0.966	0.862
39	300.0	0.985	0.907	0.775	0.986	0.918	0.788	0.998	0.988	0.972	0.943	0.746	0.209	0.982	0.921	0.784
	900.0	0.990	0.937	0.839	0.990	0.948	0.860	0.999	0.993	0.985	0.943	0.740	0.192	0.985	0.941	0.834
	2100.0	0.993	0.957	0.887	0.993	0.965	0.901	1.000	0.996	0.992	0.941	0.733	0.177	0.988	0.957	0.882
40	300.0	0.983	0.897	0.753	0.987	0.914	0.765	0.997	0.986	0.968	0.921	0.630	0.193	0.981	0.930	0.835
	900.0	0.989	0.933	0.831	0.993	0.946	0.838	0.998	0.991	0.978	0.923	0.626	0.171	0.985	0.954	0.901
	2100.0	0.993	0.960	0.894	0.995	0.963	0.879	0.999	0.994	0.981	0.924	0.626	0.155	0.988	0.976	0.960
41	300.0	0.979	0.872	0.708	0.980	0.895	0.741	0.995	0.981	0.957	0.936	0.621	0.098	0.980	0.900	0.758
	900.0	0.990	0.917	0.788	0.991	0.940	0.834	0.998	0.988	0.969	0.946	0.621	0.084	0.989	0.930	0.818
	2100.0	1.000	0.947	0.851	1.000	0.970	0.903	1.000	0.993	0.979	0.953	0.624	0.077	1.000	0.954	0.865
42	300.0	0.969	0.830	0.636	0.975	0.851	0.660	0.996	0.982	0.961	0.941	0.646	0.122	0.978	0.873	0.695
	900.0	0.981	0.872	0.703	0.983	0.889	0.733	0.996	0.985	0.967	0.932	0.633	0.108	0.992	0.909	0.758
	2100.0	0.989	0.902	0.754	0.988	0.916	0.787	0.995	0.986	0.968	0.916	0.617	0.099	1.000	0.933	0.800
43	300.0	0.961	0.811	0.583	0.968	0.824	0.585	0.995	0.977	0.952	0.935	0.551	0.152	0.955	0.862	0.650
	900.0	0.980	0.870	0.661	0.982	0.884	0.678	0.996	0.985	0.962	0.913	0.521	0.126	0.973	0.913	0.738
	2100.0	1.000	0.922	0.743	0.992	0.926	0.756	0.998	0.992	0.971	0.909	0.503	0.110	1.000	0.966	0.830
44	300.0	0.959	0.777	0.551	0.976	0.854	0.664	0.997	0.984	0.963	0.942	0.616	0.081	0.972	0.831	0.607
	900.0	0.976	0.836	0.637	0.989	0.912	0.781	0.998	0.990	0.977	0.930	0.603	0.070	0.986	0.875	0.694
	2100.0	0.986	0.879	0.723	0.999	0.954	0.878	1.000	0.996	0.993	0.935	0.603	0.065	0.993	0.904	0.761
45	300.0	0.947	0.751	0.548	0.965	0.800	0.600	0.994	0.971	0.946	0.950	0.634	0.142	0.942	0.814	0.652
	900.0	0.976	0.837	0.680	0.982	0.872	0.730	0.998	0.981	0.958	0.948	0.606	0.104	0.968	0.883	0.781
	2100.0	1.000	0.905	0.798	0.993	0.914	0.813	0.999	0.985	0.960	0.951	0.588	0.079	1.004	0.950	0.893
46	300.0	0.945	0.709	0.447	0.963	0.778	0.484	0.996	0.978	0.960	0.939	0.693	0.151	0.968	0.806	0.555
	900.0	0.965	0.791	0.522	0.977	0.847	0.585	0.995	0.983	0.964	0.939	0.685	0.125	0.981	0.876	0.676
	2100.0	0.979	0.860	0.628	0.987	0.900	0.692	0.995	0.986	0.968	0.963	0.697	0.107	0.991	0.930	0.801
47	300.0	0.935	0.706	0.478	0.950	0.793	0.505	0.993	0.970	0.952	0.958	0.710	0.237	0.970	0.830	0.612
	900.0	0.963	0.802	0.591	0.971	0.842	0.629	0.997	0.983	0.970	0.956	0.718	0.234	0.984	0.901	0.741
	2100.0	0.976	0.867	0.696	0.982	0.899	0.728	0.995	0.989	0.982	0.950	0.726	0.239	0.991	0.941	0.833
48	300.0	0.915	0.637	0.405	0.946	0.717	0.463	0.985	0.965	0.950	0.954	0.680	0.147	0.950	0.744	0.469
	900.0	0.946	0.707	0.451	0.970	0.794	0.552	0.991	0.974	0.957	0.961	0.690	0.122	0.969	0.807	0.543
	2100.0	0.969	0.777	0.524	0.986	0.858	0.652	1.000	0.988	0.969	0.985	0.718	0.104	0.985	0.863	0.633
49	300.0	0.900	0.626	0.405	0.940	0.721	0.473	0.962	0.882	0.834	0.917	0.524	0.135	0.950	0.774	0.566
	900.0	0.934	0.700	0.467	0.963	0.795	0.561	0.982	0.930	0.882	0.936	0.535	0.136	0.968	0.828	0.634
	2100.0	0.955	0.765	0.551	0.975	0.846	0.646	0.992	0.969	0.932	0.915	0.535	0.140	0.981	0.871	0.707

50	300.0	0.920	0.722	0.559	0.942	0.753	0.557	0.991	0.973	0.943	0.986	0.897	0.472	0.952	0.823	0.691
	900.0	0.950	0.771	0.615	0.968	0.813	0.620	0.993	0.974	0.937	0.984	0.892	0.451	0.975	0.867	0.755
	2100.0	0.978	0.824	0.686	0.993	0.870	0.690	0.989	0.972	0.930	0.992	0.889	0.419	1.000	0.918	0.839
51	300.0	0.782	0.422	0.258	0.884	0.611	0.386	0.980	0.942	0.926	0.934	0.604	0.182	0.875	0.601	0.379
	900.0	0.837	0.489	0.294	0.925	0.706	0.473	0.984	0.958	0.945	0.910	0.568	0.160	0.913	0.684	0.455
	2100.0	0.881	0.580	0.379	0.954	0.805	0.603	0.985	0.973	0.960	0.866	0.533	0.145	0.943	0.776	0.575
52	300.0	0.946	0.740	0.544	0.943	0.684	0.528	0.996	0.987	0.980	0.982	0.755	0.597	1.002	0.924	0.797
	900.0	0.966	0.795	0.611	0.962	0.732	0.590	1.008	1.002	0.995	0.980	0.712	0.584	1.008	0.961	0.863
	2100.0	0.982	0.849	0.689	0.980	0.774	0.668	1.005	0.996	0.988	0.996	0.662	0.540	1.018	1.000	0.928
53	300.0	0.648	0.367	0.265	0.779	0.484	0.348	0.939	0.869	0.876	0.939	0.435	0.222	0.775	0.495	0.347
	900.0	0.715	0.408	0.289	0.837	0.556	0.408	0.953	0.881	0.881	0.916	0.418	0.195	0.828	0.557	0.399
	2100.0	0.785	0.478	0.351	0.887	0.652	0.523	0.969	0.904	0.898	0.901	0.421	0.174	0.877	0.640	0.498
54	300.0	0.974	0.777	0.558	0.989	0.878	0.741	0.994	0.985	1.078	0.972	0.774	0.254	1.004	0.873	0.686
	900.0	0.996	0.842	0.668	1.013	0.973	0.892	0.986	0.980	0.966	0.936	0.724	0.230	1.016	0.924	0.784
	2100.0	1.012	0.942	0.823	1.030	1.048	1.049	0.978	0.975	0.965	0.928	0.697	0.215	1.026	0.967	0.879
55	300.0	0.662	0.363	0.260	0.794	0.474	0.293	0.968	0.926	0.896	0.940	0.492	0.176	0.817	0.566	0.416
	900.0	0.746	0.411	0.272	0.862	0.576	0.365	0.980	0.944	0.903	0.949	0.460	0.196	0.874	0.649	0.484
	2100.0	0.824	0.499	0.294	0.919	0.719	0.435	0.962	0.945	0.899	0.930	0.378	0.214	0.924	0.770	0.546
56	300.0	0.673	0.367	0.281	0.788	0.457	0.299	0.984	0.961	0.965	0.965	0.895	0.488	0.808	0.511	0.375
	900.0	0.712	0.383	0.293	0.823	0.489	0.325	0.984	0.981	0.964	0.985	0.893	0.485	0.840	0.540	0.397
	2100.0	0.761	0.411	0.310	0.862	0.535	0.357	0.993	0.964	0.955	1.018	0.915	0.485	0.877	0.581	0.425
57	300.0	0.758	0.378	0.225	0.828	0.438	0.182	0.999	0.990	0.975	0.950	0.642	0.138	0.869	0.558	0.365
	900.0	0.806	0.410	0.230	0.868	0.489	0.200	0.979	0.970	0.954	0.939	0.611	0.129	0.891	0.594	0.325
	2100.0	0.859	0.473	0.256	0.901	0.479	0.236	1.016	1.006	0.986	0.969	0.587	0.118	0.925	0.656	0.382
58	300.0	0.943	0.717	0.619	0.916	0.607	0.319	0.995	0.993	0.984	0.938	0.678	0.088	1.104	1.085	1.182
	900.0	0.974	0.769	0.655	0.918	0.651	0.343	1.027	1.021	1.002	1.016	0.663	0.090	1.152	1.147	1.256
	2100.0	0.989	0.807	0.701	0.897	0.582	0.390	1.028	1.018	1.015	1.005	0.330	0.105	1.221	1.333	1.353
59	300.0	0.846	0.659	0.515	0.815	0.624	0.379	0.996	0.988	0.966	0.895	0.465	0.087	0.793	0.565	0.368
	900.0	0.893	0.709	0.561	0.864	0.678	0.422	1.026	1.021	1.012	0.890	0.484	0.089	0.848	0.645	0.354
	2100.0	0.928	0.751	0.579	0.956	0.784	0.507	0.995	0.991	0.982	0.870	0.505	0.094	0.892	0.699	0.389
60	300.0	1.023	0.903	0.748	1.094	1.060	1.058	1.000	1.001	1.002	0.973	0.778	0.235	1.031	0.953	0.833
	900.0	1.027	0.937	0.807	1.090	1.091	1.123	0.997	0.997	0.999	0.969	0.779	0.239	1.032	0.976	0.887
	2100.0	1.029	0.981	0.953	1.094	1.235	1.225	0.971	0.972	0.970	0.943	0.759	0.231	1.036	1.006	0.951
61	300.0	1.009	1.013	1.017	1.004	1.010	1.024	0.998	0.997	0.994	0.981	0.824	0.431	1.020	1.033	1.063
	900.0	1.019	1.023	1.026	1.036	1.041	1.046	0.994	0.993	0.990	0.977	0.811	0.420	1.037	1.051	1.081
	2100.0	1.034	1.038	1.036	1.144	1.140	1.116	0.968	0.967	0.964	0.951	0.772	0.375	1.068	1.083	1.107
62	300.0	0.987	0.905	0.809	1.001	0.925	0.800	0.999	0.999	0.997	0.984	0.867	0.388	0.993	0.968	0.915
	900.0	0.994	0.937	0.852	1.006	0.966	0.888	0.995	0.995	0.994	0.981	0.863	0.383	1.002	0.988	0.949
	2100.0	0.996	0.964	0.917	1.007	1.001	1.003	0.973	0.972	0.971	0.960	0.842	0.363	1.014	1.010	0.996
63	300.0	0.959	0.938	0.873	0.921	0.888	0.769	0.997	0.996	0.990	0.967	0.748	0.249	0.949	0.927	0.848
	900.0	0.966	0.944	0.877	0.933	0.898	0.776	0.994	0.993	0.987	0.964	0.742	0.244	0.961	0.938	0.857
	2100.0	0.978	0.953	0.886	0.971	0.933	0.811	0.974	0.972	0.967	0.943	0.717	0.226	0.984	0.959	0.878
64	300.0	0.949	0.796	0.592	0.977	0.882	0.702	1.001	1.005	1.007	0.916	0.486	0.110	0.948	0.824	0.627
	900.0	0.947	0.803	0.604	0.972	0.883	0.710	0.998	1.002	1.004	0.913	0.478	0.108	0.945	0.827	0.637
	2100.0	0.940	0.812	0.639	0.963	0.885	0.743	0.979	0.982	0.984	0.894	0.459	0.106	0.937	0.831	0.671
65	300.0	1.028	1.036	1.086	1.067	1.095	1.236	1.000	0.999	0.992	0.945	0.632	0.084	1.028	1.038	1.097
	900.0	1.036	1.044	1.092	1.082	1.112	1.247	0.998	0.996	0.990	0.942	0.629	0.082	1.037	1.048	1.104
	2100.0	1.051	1.060	1.107	1.123	1.156	1.292	0.979	0.977	0.971	0.924	0.615	0.078	1.055	1.067	1.123
66	300.0	0.969	0.953	0.927	0.970	0.956	0.934	0.990	0.988	0.982	0.925	0.467	0.062	0.965	0.947	0.917
	900.0	0.971	0.955	0.930	0.973	0.959	0.939	0.987	0.985	0.980	0.922	0.483	0.049	0.968	0.951	0.923
	2100.0	0.975	0.959	0.936	0.990	0.976	0.957	0.970	0.967	0.963	0.905	0.449	0.059	0.974	0.957	0.930
67	300.0	0.960	0.941	0.864	0.953	0.934	0.917	1.003	1.001	0.996	0.891	0.515	0.137	0.955	0.937	0.921
	900.0	0.962	0.913	0.864	0.955	0.936	0.917	1.000	0.998	0.996	0.888	0.513	0.137	0.958	0.939	0.921
	2100.0	0.965	0.913	0.730	0.969	0.936	0.917	0.983	0.998	0.996	0.872	0.513	0.137	0.963	0.939	0.921

B-II Shielding factor for Pu-239 (Without interference effect)

		TOTAL			CAPTURE			ELASTIC			REMOVAL			FISSION		
		1000.	100.	10.	1000.	100.	10.	1000.	100.	10.	1000.	100.	10.	1000.	100.	10.
29	300.0	0.998	0.981	0.923	0.997	0.978	0.903	1.000	0.993	0.969	0.978	0.921	0.578	0.998	0.983	0.929
	900.0	0.998	0.987	0.945	0.998	0.985	0.931	1.000	0.996	0.979	0.976	0.921	0.576	0.999	0.986	0.948
	2100.0	0.999	0.991	0.959	0.999	0.988	0.945	1.000	0.997	0.984	0.975	0.920	0.574	1.000	0.993	0.964
30	300.0	0.996	0.970	0.895	0.995	0.967	0.865	0.999	0.989	0.955	0.967	0.896	0.517	0.995	0.974	0.898
	900.0	0.997	0.980	0.921	0.996	0.977	0.901	0.999	0.992	0.967	0.963	0.897	0.512	0.995	0.981	0.922
	2100.0	0.999	0.986	0.939	0.997	0.983	0.922	1.000	0.995	0.975	0.960	0.898	0.510	1.000	0.989	0.943
31	300.0	0.995	0.959	0.877	0.996	0.963	0.868	0.998	0.983	0.954	0.962	0.872	0.307	0.994	0.968	0.900
	900.0	0.998	0.975	0.920	0.998	0.979	0.923	0.999	0.991	0.976	0.963	0.882	0.290	0.995	0.979	0.936
	2100.0	1.000	0.985	0.949	1.000	0.988	0.954	1.000	0.995	0.990	0.962	0.884	0.278	1.000	0.989	0.963
32	300.0	0.993	0.947	0.845	0.997	0.952	0.814	0.995	0.977	0.929	0.983	0.901	0.511	0.998	0.965	0.874
	900.0	0.995	0.965	0.886	0.998	0.969	0.869	0.996	0.984	0.950	0.977	0.901	0.504	0.998	0.977	0.911
	2100.0	0.998	0.977	0.915	1.000	0.979	0.899	1.000	0.992	0.967	0.977	0.903	0.502	0.999	0.980	0.928
33	300.0	0.988	0.919	0.788	0.991	0.929	0.777	0.996	0.964	0.895	0.980	0.903	0.493	0.992	0.951	0.839
	900.0	0.993	0.949	0.847	0.996	0.959	0.858	0.998	0.978	0.927	0.981	0.905	0.474	0.995	0.968	0.890
	2100.0	0.997	0.967	0.891	0.999	0.975	0.904	1.000	0.988	0.951	0.986	0.909	0.462	1.000	0.982	0.926
34	300.0	0.985	0.894	0.732	0.986	0.901	0.686	0.994	0.953	0.870	0.974	0.863	0.447	0.989	0.933	0.862
	900.0	0.990	0.929	0.794	0.991	0.935	0.765	0.996	0.970	0.902	0.978	0.876	0.433	0.993	0.950	0.866
	2100.0	0.993	0.949	0.836	0.994	0.952	0.807	0.915	0.978	0.921	0.981	0.885	0.431	1.000	0.974	0.909
35	300.0	0.984	0.893	0.722	0.986	0.900	0.696	0.994	0.959	0.883	0.969	0.800	0.335	0.989	0.926	0.751
	900.0	0.990	0.930	0.782	0.992	0.938	0.781	0.998	0.973	0.910	0.980	0.808	0.329	0.994	0.953	0.814
	2100.0	0.995	0.949	0.819	0.994	0.954	0.823	1.000	0.981	0.925	0.986	0.819	0.315	1.000	0.971	0.853
36	300.0	0.971	0.834	0.652	0.979	0.865	0.656	0.989	0.932	0.855	0.974	0.829	0.302	0.982	0.881	0.692
	900.0	0.984	0.889	0.729	0.988	0.919	0.775	0.995	0.959	0.907	0.977	0.838	0.252	0.994	0.927	0.787
	2100.0	0.991	0.922	0.785	0.991	0.946	0.847	0.998	0.974	0.943	0.977	0.844	0.227	1.000	0.955	0.849
37	300.0	0.974	0.840	0.648	0.977	0.856	0.598	0.994	0.959	0.895	0.971	0.810	0.395	0.982	0.824	0.553
	900.0	0.992	0.894	0.711	0.997	0.919	0.711	0.997	0.973	0.918	0.972	0.813	0.358	0.994	0.867	0.665
	2100.0	0.996	0.923	0.757	1.000	0.947	0.781	0.997	0.980	0.934	0.958	0.806	0.336	1.001	0.917	0.761
38	300.0	0.947	0.736	0.504	0.963	0.782	0.477	0.978	0.886	0.767	0.950	0.763	0.290	0.969	0.807	0.531
	900.0	0.966	0.800	0.561	0.978	0.856	0.589	0.986	0.918	0.803	0.948	0.770	0.260	0.979	0.853	0.591
	2100.0	0.978	0.850	0.622	0.984	0.899	0.676	0.992	0.941	0.857	0.929	0.763	0.236	0.989	0.889	0.653
39	300.0	0.925	0.690	0.479	0.946	0.726	0.428	0.970	0.865	0.753	0.951	0.825	0.402	0.952	0.752	0.477
	900.0	0.955	0.765	0.539	0.970	0.811	0.542	0.982	0.899	0.785	1.007	0.842	0.359	0.974	0.822	0.561
	2100.0	0.976	0.825	0.607	0.987	0.870	0.639	0.991	0.926	0.817	1.062	0.851	0.320	0.993	0.875	0.640
40	300.0	0.908	0.626	0.404	0.930	0.666	0.371	0.966	0.845	0.729	0.935	0.744	0.347	0.949	0.728	0.427
	900.0	0.938	0.698	0.446	0.954	0.752	0.464	0.976	0.881	0.762	0.936	0.724	0.302	0.964	0.790	0.486
	2100.0	0.954	0.754	0.493	0.964	0.804	0.535	0.980	0.905	0.791	0.923	0.703	0.266	0.973	0.835	0.540
41	300.0	0.952	0.773	0.583	0.964	0.785	0.542	0.992	0.959	0.921	0.951	0.754	0.323	0.955	0.798	0.559
	900.0	0.963	0.826	0.631	0.979	0.859	0.664	0.995	0.970	0.936	0.957	0.757	0.279	0.966	0.845	0.622
	2100.0	0.969	0.879	0.730	0.990	0.915	0.788	1.000	0.983	0.960	0.960	0.761	0.245	1.000	0.910	0.722
42	300.0	0.850	0.596	0.412	0.909	0.605	0.324	0.958	0.824	0.714	0.917	0.611	0.190	0.951	0.747	0.512
	900.0	0.935	0.698	0.484	0.946	0.721	0.444	0.975	0.872	0.759	0.952	0.646	0.025	0.974	0.841	0.649
	2100.0	0.966	0.791	0.569	0.965	0.808	0.556	0.993	0.916	0.804	0.977	0.675	0.133	0.992	0.915	0.777
43	300.0	0.708	0.470	0.339	0.748	0.415	0.230	0.730	0.489	0.397	0.912	0.560	0.158	0.941	0.806	0.676
	900.0	0.768	0.528	0.381	0.816	0.508	0.303	0.788	0.528	0.419	0.918	0.539	0.124	0.964	0.876	0.780
	2100.0	0.816	0.594	0.463	0.872	0.607	0.413	0.824	0.564	0.449	0.695	0.387	0.071	0.986	0.951	0.932
44	300.0	0.895	0.608	0.412	0.923	0.630	0.320	0.961	0.918	0.864	0.919	0.589	0.136	0.936	0.701	0.425
	900.0	0.927	0.668	0.434	0.954	0.730	0.399	0.988	0.938	0.880	0.925	0.579	0.105	0.956	0.761	0.470
	2100.0	0.954	0.736	0.458	0.969	0.812	0.502	1.008	0.966	0.883	1.127	0.707	0.107	0.972	0.825	0.534
45	300.0	0.757	0.422	0.302	0.810	0.420	0.202	0.882	0.670	0.576	0.984	0.870	0.527	0.911	0.665	0.472
	900.0	0.833	0.491	0.330	0.877	0.525	0.262	0.921	0.721	0.603	0.998	0.864	0.449	0.947	0.755	0.563
	2100.0	0.884	0.566	0.353	0.925	0.636	0.348	0.928	0.750	0.602	0.893	0.748	0.322	0.978	0.854	0.687
46	300.0	0.767	0.432	0.292	0.832	0.473	0.244	0.949	0.851	0.801	0.952	0.614	0.421	0.844	0.487	0.259
	900.0	0.831	0.490	0.320	0.884	0.553	0.306	0.966	0.871	0.811	0.951	0.522	0.385	0.890	0.556	0.314
	2100.0	0.879	0.553	0.363	0.920	0.628	0.382	0.978	0.898	0.835	0.909	0.386	0.327	0.923	0.619	0.380
47	300.0	0.737	0.440	0.284	0.790	0.447	0.254	0.926	0.806	0.725	0.985	0.874	0.446	0.830	0.518	0.286
	900.0	0.783	0.461	0.289	0.838	0.494	0.273	0.941	0.820	0.731	0.989	0.876	0.445	0.866	0.557	0.304
	2100.0	0.850	0.518	0.317	0.882	0.561	0.313	1.043	0.923	0.814	1.042	0.917	0.456	0.901	0.612	0.342
48	300.0	0.438	0.190	0.188	0.604	0.283	0.278	0.594	0.364	0.355	0.908	0.495	0.511	0.630	0.332	0.330
	900.0	0.488	0.197	0.191	0.671	0.325	0.310	0.651	0.389	0.371	0.951	0.504	0.522	0.685	0.358	0.366
	2100.0	0.555	0.218	0.215	0.735	0.376	0.369	0.743	0.455	0.442	1.115	0.553	0.572	0.745	0.397	0.393
49	300.0	0.668	0.330	0.187	0.685	0.352	0.219	0.808	0.628	0.565	0.981	0.795	0.389	0.903	0.663	0.388
	900.0	0.738	0.373	0.197	0.772	0.431	0.267	0.859	0.674	0.596	0.962	0.773	0.371	0.934	0.728	0.430
	2100.0	0.797	0.435	0.220	0.841	0.524	0.346	0.850	0.675	0.591	0.806	0.604	0.279	0.961	0.812	0.509

50	300.0	0.431	0.177	0.136	0.600	0.218	0.096	0.776	0.566	0.523	0.996	0.987	0.920	0.624	0.266	0.167
	900.0	0.535	0.192	0.137	0.702	0.276	0.110	0.838	0.603	0.537	0.997	0.987	0.920	0.722	0.323	0.187
	2100.0	0.639	0.226	0.143	0.787	0.355	0.139	0.880	0.648	0.552	0.999	0.988	0.913	0.817	0.415	0.241
51	300.0	0.964	0.831	0.692	0.948	0.740	0.459	0.993	0.991	0.984	0.992	0.955	0.723	0.971	0.817	0.506
	900.0	0.974	0.866	0.710	0.967	0.815	0.540	0.994	0.992	0.985	0.997	0.955	0.705	0.978	0.850	0.543
	2100.0	0.991	0.907	0.747	1.000	0.893	0.656	0.999	0.997	0.988	1.010	0.951	0.632	0.994	0.894	0.607
52	300.0	0.621	0.252	0.155	0.789	0.407	0.212	0.953	0.866	0.839	0.966	0.760	0.258	0.731	0.332	0.145
	900.0	0.715	0.299	0.162	0.864	0.514	0.266	0.972	0.892	0.847	0.954	0.717	0.227	0.793	0.393	0.170
	2100.0	0.803	0.390	0.185	0.921	0.656	0.370	0.992	0.930	0.866	0.998	0.648	0.163	0.847	0.475	0.220
53	300.0	0.564	0.285	0.208	0.667	0.269	0.105	0.962	0.918	0.886	0.973	0.861	0.291	0.698	0.334	0.167
	900.0	0.621	0.290	0.208	0.725	0.297	0.109	0.968	0.920	0.885	0.971	0.796	0.286	0.749	0.358	0.170
	2100.0	0.678	0.308	0.212	0.783	0.336	0.118	0.975	0.928	0.890	0.966	0.776	0.270	0.798	0.398	0.183
54	300.0	0.549	0.291	0.214	0.613	0.263	0.125	0.886	0.805	0.799	0.990	0.925	0.391	0.760	0.516	0.413
	900.0	0.594	0.297	0.218	0.670	0.283	0.129	0.906	0.815	0.803	0.990	0.922	0.365	0.801	0.538	0.423
	2100.0	0.639	0.309	0.227	0.726	0.309	0.135	0.927	0.821	0.804	0.989	0.912	0.284	0.792	0.561	0.439
55	300.0	0.508	0.179	0.086	0.704	0.337	0.163	0.944	0.897	0.893	0.948	0.592	0.201	0.673	0.286	0.098
	900.0	0.565	0.185	0.085	0.768	0.377	0.174	0.961	0.908	0.895	0.945	0.564	0.197	0.712	0.306	0.102
	2100.0	0.621	0.199	0.086	0.832	0.439	0.197	0.978	0.933	0.908	0.944	0.504	0.186	0.752	0.335	0.109
56	300.0	0.309	0.167	0.142	0.386	0.150	0.071	0.913	0.839	0.787	0.431	0.074	0.009	0.407	0.202	0.152
	900.0	0.334	0.169	0.142	0.407	0.157	0.072	0.908	0.835	0.785	0.396	0.071	0.008	0.432	0.212	0.155
	2100.0	0.360	0.173	0.143	0.428	0.169	0.074	0.903	0.819	0.771	0.361	0.071	0.078	0.458	0.229	0.161
57	300.0	1.195	0.709	0.563	1.924	1.045	0.727	1.008	1.002	1.019	0.975	0.851	0.533	1.530	1.022	0.816
	900.0	1.292	0.718	0.562	2.138	1.153	0.761	1.029	1.012	1.025	0.976	0.848	0.534	1.632	1.073	0.828
	2100.0	1.390	0.745	0.560	2.320	1.339	0.824	1.049	1.014	1.022	0.977	0.833	0.527	1.734	1.165	0.854
58	300.0	1.002	1.004	1.007	1.030	1.042	1.065	0.994	0.992	0.989	0.967	0.786	0.595	1.008	1.012	1.019
	900.0	1.002	1.004	1.011	1.031	1.044	1.095	0.994	0.992	0.985	0.968	0.777	0.188	1.008	1.012	1.028
	2100.0	1.003	1.000	1.003	1.031	1.058	1.080	0.994	0.981	0.978	0.969	0.751	0.587	1.008	1.015	1.022
59	300.0	0.999	0.998	0.991	0.999	0.998	0.991	0.999	0.999	0.996	0.991	0.918	0.532	0.998	0.996	0.987
	900.0	0.999	0.998	0.991	0.999	0.998	0.991	0.999	0.999	0.996	0.991	0.918	0.532	0.998	0.996	0.987
	2100.0	0.999	0.998	0.991	0.999	0.998	0.991	0.999	0.999	0.996	0.991	0.918	0.532	0.998	0.996	0.987
60	300.0	0.997	0.994	0.980	0.993	0.988	0.960	0.999	0.999	0.996	1.081	0.980	0.484	0.995	0.991	0.969
	900.0	0.997	0.994	0.980	0.993	0.988	0.960	0.999	0.999	0.996	1.081	0.980	0.484	0.995	0.991	0.969
	2100.0	0.997	0.994	0.980	0.993	0.988	0.960	0.999	0.999	0.996	1.081	0.980	0.484	0.995	0.991	0.969
61	300.0	0.994	0.990	0.973	0.987	0.979	0.951	0.999	0.998	0.997	0.984	0.860	0.396	0.991	0.985	0.969
	900.0	0.994	0.990	0.973	0.987	0.979	0.951	0.999	0.998	0.997	0.984	0.860	0.396	0.991	0.985	0.969
	2100.0	0.994	0.990	0.973	0.987	0.979	0.951	0.999	0.998	0.997	0.984	0.860	0.396	0.991	0.985	0.969
62	300.0	0.990	0.984	0.958	0.980	0.969	0.922	0.999	0.998	0.995	0.980	0.828	0.330	0.986	0.979	0.947
	900.0	0.990	0.984	0.958	0.980	0.969	0.922	0.999	0.998	0.995	0.980	0.828	0.330	0.986	0.979	0.947
	2100.0	0.990	0.984	0.958	0.980	0.969	0.922	0.999	0.998	0.995	0.980	0.828	0.330	0.986	0.979	0.947
63	300.0	0.983	0.973	0.935	0.970	0.952	0.885	0.998	0.997	0.992	0.967	0.766	0.188	0.980	0.968	0.924
	900.0	0.983	0.973	0.935	0.970	0.952	0.885	0.998	0.997	0.992	0.967	0.766	0.188	0.980	0.968	0.924
	2100.0	0.983	0.973	0.935	0.970	0.952	0.885	0.998	0.997	0.992	0.967	0.766	0.188	0.980	0.968	0.924
64	300.0	0.974	0.955	0.914	0.955	0.927	0.853	0.996	0.994	0.989	0.951	0.653	0.190	0.971	0.953	0.905
	900.0	0.974	0.955	0.914	0.955	0.927	0.853	0.996	0.994	0.989	0.951	0.653	0.190	0.971	0.953	0.905
	2100.0	0.974	0.955	0.914	0.955	0.927	0.853	0.996	0.994	0.989	0.951	0.653	0.190	0.971	0.953	0.905
65	300.0	0.962	0.935	0.881	0.938	0.900	0.817	0.999	0.996	0.989	0.937	0.588	0.078	0.962	0.938	0.885
	900.0	0.962	0.935	0.881	0.938	0.900	0.817	0.999	0.996	0.989	0.937	0.588	0.078	0.962	0.938	0.885
	2100.0	0.962	0.935	0.881	0.938	0.900	0.817	0.999	0.996	0.989	0.937	0.588	0.078	0.962	0.938	0.885
66	300.0	0.917	0.856	0.795	0.886	0.810	0.735	0.984	0.976	0.968	0.878	0.359	0.246	0.922	0.870	0.819
	900.0	0.917	0.856	0.795	0.886	0.810	0.735	0.984	0.976	0.968	0.878	0.359	0.246	0.922	0.870	0.819
	2100.0	0.917	0.856	0.795	0.886	0.810	0.735	0.984	0.976	0.968	0.878	0.359	0.246	0.922	0.870	0.819
67	300.0	0.840	0.751	0.663	0.811	0.709	0.608	0.980	0.964	0.949	0.765	0.574	0.062	0.856	0.776	0.696
	900.0	0.840	0.751	0.663	0.811	0.709	0.608	0.980	0.964	0.949	0.765	0.574	0.062	0.856	0.776	0.696
	2100.0	0.840	0.751	0.663	0.811	0.709	0.608	0.980	0.964	0.949	0.765	0.574	0.062	0.856	0.776	0.696

B-III Shielding factor for Pu-240 (Without interference effcct)

		TOTAL			CAPTURE			ELASTIC			REMOVAL			FISSION		
		10000.	1000.	100.	10000.	1000.	100.	10000.	1000.	100.	10000.	1000.	100.	10000.	1000.	100.
26	300.0	1.000	0.995	0.964	1.000	0.997	0.979	1.000	0.997	0.980	0.997	0.999	0.986	1.000	0.998	0.983
	900.0	1.000	0.997	0.977	1.000	0.998	0.988	1.000	0.998	0.987	0.997	0.999	0.990	1.000	0.999	0.991
	2100.0	1.000	0.998	0.984	1.000	0.999	0.993	1.000	0.999	0.991	0.997	1.000	0.992	1.000	1.000	0.995
27	300.0	1.000	0.994	0.958	1.000	0.997	0.974	0.999	0.997	0.977	0.995	0.979	0.941	1.000	0.997	0.979
	900.0	1.000	0.997	0.973	1.000	0.998	0.985	1.000	0.998	0.985	0.995	0.980	0.950	1.000	0.998	0.988
	2100.0	1.000	0.998	0.982	1.000	0.999	0.991	1.000	0.999	0.990	0.995	0.981	0.954	1.000	0.999	0.993
28	300.0	0.999	0.988	0.925	1.000	0.996	0.963	1.000	0.994	0.957	0.994	0.968	0.942	0.999	0.995	0.961
	900.0	0.999	0.992	0.945	1.000	0.998	0.978	1.000	0.996	0.970	1.016	0.990	0.972	1.000	0.997	0.977
	2100.0	1.000	0.995	0.962	1.000	0.999	0.987	1.000	0.997	0.979	0.995	0.970	0.959	1.000	0.998	0.987
29	300.0	0.998	0.984	0.904	1.000	0.994	0.951	0.998	0.991	0.944	0.977	0.979	0.940	1.000	0.994	0.958
	900.0	1.000	0.991	0.934	1.000	0.997	0.972	1.000	0.995	0.963	0.980	0.984	0.956	0.999	0.997	0.980
	2100.0	1.000	0.994	0.954	1.000	0.998	0.983	1.000	0.997	0.975	0.984	0.989	0.969	1.000	0.998	0.989
30	300.0	0.998	0.977	0.874	1.000	0.991	0.933	0.999	0.988	0.925	0.961	0.953	0.845	0.999	0.991	0.934
	900.0	0.999	0.985	0.908	1.000	0.995	0.961	0.999	0.992	0.947	0.964	0.963	0.881	0.999	0.994	0.959
	2100.0	1.000	0.990	0.932	1.000	0.997	0.977	1.000	0.995	0.962	0.964	0.968	0.906	0.999	0.996	0.973
31	300.0	0.997	0.965	0.825	0.997	0.983	0.893	0.999	0.981	0.893	0.958	0.972	0.961	0.998	0.986	0.935
	900.0	0.999	0.976	0.870	0.998	0.990	0.933	0.999	0.988	0.924	0.960	0.976	0.976	0.999	0.991	0.957
	2100.0	1.000	0.986	0.905	1.000	0.995	0.958	1.000	0.993	0.947	0.977	0.995	1.001	1.000	0.993	0.969
32	300.0	0.996	0.967	0.838	0.999	0.980	0.863	0.999	0.984	0.906	0.991	0.994	0.994	0.994	0.994	0.993
	900.0	0.998	0.980	0.882	1.000	0.989	0.915	1.000	0.991	0.936	0.986	0.991	1.000	0.999	0.995	0.999
	2100.0	0.998	0.987	0.914	1.000	0.993	0.945	1.000	0.994	0.955	0.995	1.000	1.015	0.995	0.995	1.000
33	300.0	0.996	0.970	0.853	0.996	0.973	0.833	0.999	0.986	0.917	0.985	0.990	0.984	1.000	0.997	0.977
	900.0	0.997	0.981	0.892	0.997	0.984	0.891	0.999	0.991	0.942	0.983	0.989	0.985	0.999	0.997	0.980
	2100.0	0.998	0.988	0.921	0.997	0.989	0.926	1.000	0.995	0.960	0.985	0.990	0.989	0.999	0.996	0.981
34	300.0	0.990	0.917	0.703	0.994	0.953	0.759	0.996	0.957	0.805	0.983	0.986	0.965	0.995	0.995	0.988
	900.0	0.993	0.946	0.758	0.997	0.972	0.833	0.997	0.972	0.851	0.995	1.000	0.988	0.995	0.997	0.997
	2100.0	0.996	0.963	0.808	0.998	0.983	0.885	0.999	0.982	0.887	0.984	0.990	0.987	0.996	0.997	1.000
35	300.0	0.986	0.900	0.686	0.994	0.945	0.728	0.994	0.946	0.791	0.993	0.967	0.813	0.998	0.988	0.957
	900.0	0.992	0.931	0.742	0.996	0.966	0.811	0.997	0.964	0.835	0.997	0.980	0.855	0.997	0.987	0.953
	2100.0	0.993	0.950	0.789	0.996	0.977	0.867	0.997	0.974	0.870	0.979	0.967	0.861	0.996	0.989	0.957
36	300.0	0.977	0.852	0.605	0.990	0.918	0.656	0.989	0.916	0.721	0.969	0.806	0.608	0.998	0.999	0.986
	900.0	0.985	0.894	0.658	0.997	0.951	0.747	0.992	0.942	0.769	0.979	0.865	0.680	1.080	1.082	1.080
	2100.0	0.991	0.925	0.710	0.999	0.968	0.811	0.996	0.961	0.814	0.984	0.903	0.555	0.992	0.993	0.994
37	300.0	0.984	0.882	0.631	0.989	0.910	0.613	0.993	0.940	0.761	0.977	0.868	0.500	1.000	0.997	0.981
	900.0	0.990	0.923	0.689	0.992	0.943	0.708	0.996	0.962	0.813	0.974	0.901	0.563	1.005	1.001	0.985
	2100.0	0.989	0.943	0.738	0.988	0.956	0.774	0.993	0.971	0.850	0.931	0.880	0.585	1.012	1.008	0.991
38	300.0	0.967	0.787	0.479	0.961	0.852	0.494	0.985	0.886	0.641	0.998	0.978	0.958	0.968	0.776	0.388
	900.0	0.980	0.851	0.541	0.990	0.905	0.601	0.991	0.925	0.706	1.000	0.980	0.957	0.980	0.840	0.471
	2100.0	0.991	0.899	0.611	0.998	0.942	0.697	0.996	0.953	0.769	0.998	0.978	0.952	0.987	0.885	0.553
39	300.0	0.992	0.932	0.763	0.989	0.907	0.582	0.998	0.977	0.901	0.996	0.970	0.956	0.982	0.858	0.427
	900.0	1.001	0.962	0.811	1.001	0.949	0.695	1.005	0.991	0.929	1.124	1.088	1.036	0.990	0.917	0.541
	2100.0	1.013	0.985	0.853	1.022	0.987	0.789	1.013	1.003	0.952	1.401	1.341	1.189	0.994	0.953	0.644
40	300.0	0.987	0.886	0.633	0.989	0.897	0.546	0.996	0.956	0.810	0.985	0.956	0.904			
	900.0	0.990	0.927	0.695	0.990	0.936	0.659	0.996	0.973	0.855	0.968	0.940	0.886			
	2100.0	0.983	0.943	0.749	0.980	0.947	0.741	0.988	0.974	0.885	0.987	0.959	0.898			
41	300.0	0.938	0.697	0.461	0.961	0.768	0.374	0.969	0.823	0.608	0.965	0.824	0.482			
	900.0	0.960	0.765	0.494	0.975	0.836	0.468	0.980	0.871	0.647	0.973	0.878	0.547			
	2100.0	0.973	0.820	0.534	0.984	0.886	0.555	0.986	0.906	0.689	0.979	0.912	0.608			
42	300.0	0.852	0.522	0.323	0.934	0.698	0.350	0.915	0.659	0.427	0.979	0.984	0.992			
	900.0	0.895	0.583	0.347	0.956	0.767	0.432	0.940	0.721	0.456	0.979	0.985	0.991			
	2100.0	0.924	0.645	0.375	0.969	0.821	0.504	0.957	0.779	0.491	0.981	0.988	1.002			
43	300.0	0.976	0.824	0.609	0.976	0.785	0.332	0.994	0.940	0.819	0.978	0.980	0.967			
	900.0	0.987	0.875	0.643	0.988	0.862	0.442	0.997	0.962	0.848	0.976	0.979	0.958			
	2100.0	0.992	0.913	0.683	0.995	0.908	0.545	0.999	0.975	0.876	0.976	0.979	0.951			
44	300.0	0.954	0.727	0.479	0.961	0.732	0.292	0.985	0.899	0.733	0.997	0.997	0.987			
	900.0	0.972	0.804	0.511	0.977	0.820	0.386	0.991	0.932	0.767	0.998	0.998	0.985			
	2100.0	0.982	0.858	0.553	0.985	0.876	0.477	0.994	0.953	0.802	1.002	1.002	0.988			
45	300.0	0.921	0.596	0.320	0.948	0.673	0.245	0.969	0.813	0.581	0.995	0.988	0.961			
	900.0	0.952	0.697	0.354	0.969	0.775	0.335	0.982	0.870	0.627	0.995	0.986	0.952			
	2100.0	0.969	0.776	0.401	0.981	0.844	0.431	0.988	0.909	0.677	0.995	0.985	0.942			
46	300.0	0.739	0.308	0.156	0.856	0.455	0.147	0.855	0.512	0.279	0.992	0.979	0.930			
	900.0	0.817	0.381	0.184	0.908	0.562	0.190	0.902	0.597	0.306	0.990	0.974	0.913			
	2100.0	0.871	0.465	0.180	0.940	0.660	0.247	0.931	0.679	0.348	0.988	0.967	0.889			

47	300.0	0.853	0.516	0.285	0.932	0.624	0.228	0.883	0.709	0.516	1.000	0.999	0.990			
	900.0	0.895	0.603	0.309	0.960	0.733	0.308	0.900	0.769	0.550	1.000	0.999	0.990			
	2100.0	0.918	0.683	0.339	0.976	0.812	0.390	0.910	0.814	0.588	1.000	1.000	0.991			
48	300.0	0.564	0.168	0.072	0.760	0.336	0.118	0.748	0.342	0.148	0.999	0.998	0.987			
	900.0	0.674	0.212	0.074	0.841	0.431	0.143	0.829	0.426	0.168	0.999	0.998	0.987			
	2100.0	0.764	0.278	0.080	0.898	0.538	0.183	0.889	0.524	0.203	0.998	0.997	0.985			
49	300.0	1.057	1.056	1.053	1.097	1.097	1.097	1.056	1.056	1.055	0.999	0.997	0.987			
	900.0	1.057	1.056	1.053	1.098	1.098	1.097	1.056	1.056	1.055	1.000	0.997	0.986			
	2100.0	1.057	1.057	1.054	1.099	1.090	1.099	1.056	1.056	1.056	1.000	0.998	0.985			
50	300.0	0.561	0.146	0.061	0.747	0.303	0.095	0.755	0.332	0.139	0.998	0.992	0.970			
	900.0	0.686	0.194	0.062	0.836	0.404	0.117	0.842	0.428	0.161	0.995	0.988	0.965			
	2100.0	0.781	0.267	0.068	0.896	0.513	0.152	1.008	0.533	0.197	0.989	0.981	0.956			
51	300.0	0.997	0.996	0.993	1.000	1.004	1.012	0.996	0.996	0.993	0.998	0.997	0.997			
	900.0	0.996	0.995	0.992	1.003	1.008	1.018	0.996	0.995	0.992	0.998	0.997	0.997			
	2100.0	0.996	0.995	0.991	1.008	1.015	1.030	0.971	0.994	0.991	0.998	0.997	0.997			
52	300.0	0.998	0.998	0.996	0.984	0.983	0.979	0.999	0.999	0.998	0.998	0.995	0.978			
	900.0	0.999	0.998	0.997	0.991	0.990	0.986	0.999	0.999	0.998	0.999	0.996	0.979			
	2100.0	1.000	0.999	0.998	1.007	1.006	1.000	0.988	0.999	0.999	1.003	1.000	0.981			
53	300.0	0.763	0.279	0.118	0.867	0.447	0.133	0.925	0.684	0.506	1.000	1.000	0.998			
	900.0	0.845	0.366	0.123	0.918	0.564	0.173	0.954	0.752	0.530	1.000	1.000	0.999			
	2100.0	0.896	0.467	0.138	0.948	0.668	0.230	0.770	0.811	0.563	0.999	1.000	1.000			
54	300.0	1.000	1.000	1.000	1.001	1.001	1.000	1.000	1.000	1.000	0.999	0.998	0.995			
	900.0	1.000	1.000	1.000	1.001	1.001	1.000	1.000	1.000	1.000	0.999	0.998	0.994			
	2100.0	1.000	1.000	1.000	1.002	1.002	1.000	0.998	1.000	1.000	0.999	0.998	0.992			
55	300.0	1.000	1.000	1.000	0.999	0.999	0.999	1.000	1.000	1.000	0.999	0.997	0.988			
	900.0	1.000	1.000	1.000	0.999	0.999	0.999	1.000	1.000	1.000	0.999	0.996	0.986			
	2100.0	1.000	1.000	1.000	0.999	0.999	0.999	0.998	1.000	1.000	0.999	0.995	0.983			
56	300.0	1.000	1.000	1.000	0.998	0.998	0.997	1.000	1.000	1.000	1.000	0.999	0.996			
	900.0	1.000	1.000	1.000	0.998	0.998	0.998	1.000	1.000	1.000	1.000	0.999	0.996			
	2100.0	1.000	1.000	1.000	0.998	0.998	0.998	1.000	1.000	1.000	1.000	0.999	0.996			
57	300.0	1.000	1.000	0.999	0.996	0.996	0.996	1.000	1.000	1.000	1.000	0.999	0.991			
	900.0	1.000	1.000	0.999	0.997	0.997	0.996	1.000	1.000	1.000	1.000	0.999	0.991			
	2100.0	1.000	1.000	1.000	0.997	0.997	0.996	1.000	1.000	1.000	1.000	0.999	0.991			
58	300.0	0.999	0.999	0.999	0.995	0.995	0.993	1.000	1.000	0.999	1.000	0.998	0.581	0.995	0.994	0.992
	900.0	0.999	0.999	0.999	0.995	0.995	0.993	1.000	1.000	0.999	1.000	0.998	0.981	0.995	0.995	0.993
	2100.0	0.999	0.999	0.999	0.996	0.995	0.993	1.000	1.000	1.000	1.000	0.998	0.981	0.995	0.995	0.993
59	300.0	1.002	1.002	1.002	1.007	1.006	1.007	1.001	1.001	1.001	0.999	0.996	0.964	1.007	1.006	1.007
	900.0	1.002	1.002	1.000	1.007	1.007	1.002	1.001	1.001	1.001	1.000	0.996	0.963	1.007	1.007	1.003
	2100.0	1.003	1.002	1.001	1.008	1.007	1.003	1.002	1.001	1.001	1.000	0.996	0.963	1.008	1.008	1.003
60	300.0	0.997	0.996	0.993	0.993	0.992	0.988	0.999	0.999	0.998	0.999	0.990	0.915	0.993	0.992	0.988
	900.0	0.997	0.997	0.990	0.994	0.993	0.982	0.999	0.999	0.996	0.999	0.990	0.915	0.994	0.992	0.982
	2100.0	0.998	0.997	0.991	0.995	0.994	0.983	0.999	0.999	0.997	0.999	0.990	0.915	0.995	0.994	0.983
61	300.0	0.993	0.990	0.971	0.989	0.986	0.966	0.997	0.996	0.991	0.997	0.974	0.796	0.989	0.986	0.965
	900.0	0.994	0.991	0.966	0.991	0.987	0.957	0.997	0.996	0.988	0.998	0.974	0.795	0.991	0.987	0.957
	2100.0	0.996	0.992	0.968	0.993	0.990	0.960	0.998	0.997	0.989	0.999	0.975	0.795	0.993	0.989	0.960
62	300.0	0.981	0.966	0.887	0.977	0.964	0.894	0.991	0.986	0.959	0.990	0.915	0.524	0.977	0.964	0.894
	900.0	0.984	0.968	0.879	0.980	0.967	0.883	0.992	0.987	0.954	0.992	0.917	0.524	0.980	0.967	0.883
	2100.0	0.989	0.972	0.882	0.987	0.973	0.888	0.994	0.989	0.956	0.996	0.919	0.524	0.987	0.973	0.888
63	300.0	0.932	0.803	0.585	0.935	0.841	0.632	0.963	0.906	0.779	0.938	0.606	0.132	0.935	0.841	0.632
	900.0	0.944	0.810	0.577	0.949	0.851	0.621	0.970	0.912	0.772	0.952	0.610	0.133	0.949	0.851	0.621
	2100.0	0.970	0.825	0.583	0.979	0.872	0.631	0.985	0.922	0.777	0.984	0.618	0.131	0.979	0.872	0.631
64	300.0	0.116	0.052	0.041	0.244	0.087	0.040	0.283	0.125	0.075	0.249	0.029	0.042	0.244	0.087	0.040
	900.0	0.123	0.053	0.040	0.263	0.092	0.040	0.302	0.130	0.074	0.278	0.031	0.045	0.263	0.092	0.040
	2100.0	0.142	0.057	0.042	0.292	0.104	0.043	0.331	0.142	0.078	0.288	0.031	0.049	0.292	0.104	0.043

APPENDIX C 25-Group Constants

Note 1. Shielding factors are given for two different values of R which are tabulated in the following table.

σ_0 (barn)	10	10^2	10^3	10^4
U-235	0.2, 0.6	1, 5	25, 50	——
Pu-239	1, 2	5, 10	50, 100	——
Pu-240	——	5, 10	20, 50	200, 500

Note 2. FT 1, FF 1, FC 1, FE 1, FR 1 appearing at the top of tables of shielding factor represent factors of total, fission, capture, elastic scattering, elastic removal cross sections for smaller value of R and FT 2, FF 2, ... represent the factors for larger R value.

C-I-1 Table of infinite dilution cross section for ^{235}U

MCNP ... 925 URANIUM 235

ATOMIC WEIGHT = 235.11699

GROUP	TOTAL	FISSION	NU	CAPTURE	INELASTIC	ELASTIC	MU-E	ELASTIC-REMOVAL
12	14.062	5.27	2.44	1.4626	0.0	9.33	0.025	0.1043
13	16.445	4.67	2.44	2.1917	0.0	9.59	0.0	0.1067
14	20.237	7.50	2.44	3.3062	0.0	9.43	0.0	0.1000
15	26.035	10.73	2.44	5.6626	0.0	9.64	0.0	0.1114
16	31.820	14.47	2.44	7.8246	0.0	9.52	0.0	0.1135
17	41.174	18.64	2.44	13.0376	0.0	9.50	0.0	0.0962
18	63.354	42.43	2.44	20.2926	0.0	10.63	0.0	0.0888
19	76.200	41.30	2.43	25.2796	0.0	9.82	0.0	0.1066
20	104.591	48.83	2.43	45.6935	0.0	10.47	0.0	0.0977
21	93.685	45.65	2.43	39.1034	0.0	8.73	0.0	0.0847
22	33.020	17.08	2.43	6.7764	0.0	9.46	0.0	0.1062
23	57.904	34.99	2.43	12.8535	0.0	10.07	0.0	0.0850
24	82.406	52.92	2.43	9.2965	0.0	10.79	0.0	0.0786
25	209.630	146.14	2.43	31.8370	0.0	11.96	0.0	0.0

C-I-2 Shielding factor for ^{235}U

FT1

GROUP	TEMP	10.	1.E2	1.E3
12	300	0.9924	0.9904	1.0048
	900	0.9584	0.9914	1.0045
	2100	0.9639	0.9913	1.0022
13	300	0.9029	0.9719	1.0015
	900	0.9178	0.9783	1.0039
	2100	0.9250	0.9805	1.0045
14	300	0.8257	0.9340	0.9856
	900	0.8682	0.9502	0.9919
	2100	0.8891	0.9624	0.9977
15	300	0.6978	0.8748	0.9815
	900	0.7480	0.9031	0.9884
	2100	0.7741	0.9198	0.9947
16	300	0.6951	0.8539	0.9754
	900	0.7706	0.8973	0.9904
	2100	0.8281	0.9263	1.0039
17	300	0.5421	0.7637	0.9596
	900	0.6217	0.8242	0.9718
	2100	0.7047	0.8788	0.9975
18	300	0.3738	0.5852	0.9034
	900	0.4555	0.6561	0.9312
	2100	0.5343	0.7172	0.9553
19	300	0.4421	0.6707	0.9445
	900	0.4897	0.6813	0.9836
	2100	0.5517	0.7348	1.0034
20	300	0.3285	0.4390	0.7215
	900	0.3561	0.4822	0.7816
	2100	0.4233	0.5675	0.8677
21	300	0.4088	0.5039	0.8558
	900	0.4281	0.5318	0.8984
	2100	0.4620	0.5717	0.9305
22	300	0.4433	0.7555	0.9630
	900	0.4791	0.7619	0.9803
	2100	0.4995	0.8727	0.9948
23	300	0.3098	0.6405	0.8687
	900	0.3330	0.6612	0.9005
	2100	0.3650	0.6637	0.8992
24	300	0.9318	0.9184	0.9664
	900	0.9393	0.9131	0.9705
	2100	0.9527	0.9187	0.9705

FT2

GROUP	TEMP	10.	1.E2	1.E3
12	300	0.9688	1.0092	1.0187
	900	0.9730	1.0076	1.0148
	2100	0.9781	1.0050	1.0114
13	300	0.9201	0.9847	1.0064
	900	0.9358	0.9720	1.0097
	2100	0.9410	0.9757	1.0119
14	300	0.8417	0.9414	0.9902
	900	0.8840	0.9717	0.9970
	2100	0.9016	0.9702	1.0032
15	300	0.7164	0.8980	0.9881
	900	0.7655	0.9212	0.9913
	2100	0.7878	0.9311	0.9885
16	300	0.7141	0.8790	0.9781
	900	0.7909	0.9189	0.9929
	2100	0.8434	0.9445	1.0059
17	300	0.5601	0.7752	0.9641
	900	0.6609	0.8440	0.9749
	2100	0.7278	0.9119	1.0084
18	300	0.3827	0.6147	0.9094
	900	0.4636	0.6827	0.9330
	2100	0.5394	0.7441	0.9570
19	300	0.4579	0.6839	0.9782
	900	0.5035	0.7469	1.0115
	2100	0.5687	0.8015	1.0411
20	300	0.3449	0.4780	0.7602
	900	0.3710	0.5166	0.8183
	2100	0.4333	0.5749	0.8771
21	300	0.4150	0.5476	0.9155
	900	0.4350	0.5748	0.9615
	2100	0.4677	0.6160	1.0210
22	300	0.4657	0.7935	0.9640
	900	0.4804	0.7972	0.9810
	2100	0.5018	0.8589	0.9949
23	300	0.3111	0.6488	0.8931
	900	0.3392	0.6803	0.8945
	2100	0.3647	0.6700	0.9068
24	300	0.9334	0.9201	0.9650
	900	0.9336	0.9096	0.9692
	2100	0.9558	0.9414	0.9737

FF1

GROUP	TEMP	10.	1.E2	1.E3
12	300	0.8628	0.9681	0.9839
	900	0.8907	0.9703	0.9826
	2100	0.8959	0.9716	0.9825
13	300	0.8123	0.9420	0.9797
	900	0.8256	0.9478	0.9800
	2100	0.8327	0.9504	0.9802
14	300	0.7689	0.9157	0.9686
	900	0.8031	0.9283	0.9721
	2100	0.8293	0.9387	0.9755
15	300	0.6649	0.8563	0.9599
	900	0.7057	0.8723	0.9597
	2100	0.7291	0.8810	0.9550
16	300	0.7088	0.8612	0.9633
	900	0.7621	0.8864	0.9725
	2100	0.8026	0.9106	0.9847
17	300	0.6772	0.8800	0.9674
	900	0.7600	0.9274	0.9813
	2100	0.8428	0.9560	1.0020
18	300	0.5856	0.8209	0.9476
	900	0.6619	0.8607	0.9184
	2100	0.7179	0.8887	0.9296
19	300	0.5175	0.7035	0.9231
	900	0.5698	0.7363	0.9612
	2100	0.6319	0.8224	1.0199
20	300	0.4710	0.6203	0.8463
	900	0.5317	0.6885	0.8941
	2100	0.6585	0.7754	0.9501
21	300	0.7326	0.8510	1.1445
	900	0.7808	0.9134	1.2546
	2100	0.8463	0.9963	1.3532
22	300	0.2858	0.7687	0.9683
	900	0.3250	0.7253	0.9838
	2100	0.3569	0.8279	1.0010
23	300	0.3925	0.5980	0.8990
	900	0.4050	0.6178	0.8905
	2100	0.4217	0.6103	0.8912
24	300	0.9143	0.9034	0.9604
	900	0.9223	0.9033	0.9652
	2100	0.9401	0.9022	0.9652

FF2

GROUP	TEMP	10.	1.E2	1.E3
12	300	0.8862	0.9621	0.9770
	900	0.8926	0.9618	0.9742
	2100	0.8967	0.9620	0.9733
13	300	0.8222	0.9342	0.9689
	900	0.8345	0.9379	0.9684
	2100	0.8406	0.9391	0.9678
14	300	0.7769	0.9002	0.9589
	900	0.8095	0.9100	0.9616
	2100	0.8322	0.9181	0.9640
15	300	0.6800	0.8670	0.9574
	900	0.7179	0.8766	0.9531
	2100	0.7351	0.8754	0.9430
16	300	0.7235	0.8766	0.9619
	900	0.7726	0.8990	0.9701
	2100	0.8101	0.9148	0.9806
17	300	0.6834	0.8897	0.9718
	900	0.7778	0.9278	0.9838
	2100	0.8404	0.9826	1.0184
18	300	0.5979	0.8335	0.9005
	900	0.6661	0.8683	0.9090
	2100	0.7186	0.8946	0.9145
19	300	0.5365	0.7430	0.9632
	900	0.5866	0.8047	0.9883
	2100	0.6532	0.8514	1.0247
20	300	0.4770	0.6534	0.8741
	900	0.5321	0.7271	0.9196
	2100	0.6575	0.8032	0.9729
21	300	0.7309	0.9264	1.3149
	900	0.7792	0.9930	1.3707
	2100	0.8406	1.0533	1.4459
22	300	0.2878	0.7679	0.9646
	900	0.3322	0.7756	0.9801
	2100	0.3592	0.8758	0.9968
23	300	0.3909	0.6040	0.8786
	900	0.4077	0.6296	0.8798
	2100	0.4224	0.6255	0.8824
24	300	0.9181	0.9046	0.9585
	900	0.9209	0.9002	0.9634
	2100	0.9350	0.9043	0.9703

FE1

GROUP	TEMP	10.	1.E2	1.E3
12	300	0.9933	0.9978	0.9992
	900	0.9944	0.9981	0.9990
	2100	0.9961	1.0000	1.0006
13	300	0.9877	0.9964	0.9989
	900	0.9901	0.9974	0.9993
	2100	0.9911	0.9978	0.9994
14	300	0.9809	0.9911	0.9934
	900	0.9872	0.9936	0.9963
	2100	0.9899	0.9949	0.9972
15	300	0.9549	0.9843	0.9972
	900	0.9630	0.9885	0.9980
	2100	0.9662	0.9910	0.9983
16	300	0.9713	0.9884	0.9990
	900	0.9832	0.9948	1.0010
	2100	0.9925	0.9983	1.0018
17	300	0.9533	0.9770	0.9949
	900	0.9680	0.9845	0.9971
	2100	0.9842	0.9924	1.0010
18	300	0.8738	0.9058	0.9702
	900	0.8891	0.9205	0.9777
	2100	0.9006	0.9307	0.9821
19	300	0.9264	0.9659	0.9898
	900	0.9210	0.9719	0.9937
	2100	0.9192	0.9721	0.9951
20	300	0.9408	0.9194	0.9616
	900	0.9406	0.9248	0.9647
	2100	0.9632	0.9343	0.9675
21	300	1.0273	1.0086	1.0175
	900	1.0251	1.0075	1.0188
	2100	1.0206	1.0187	1.0328
22	300	0.9476	0.9829	0.9962
	900	0.9846	0.9940	1.0043
	2100	0.9557	0.9706	0.9768
23	300	0.9721	0.9885	0.9971
	900	0.9686	0.9858	0.9939
	2100	0.9665	0.9837	0.9931
24	300	0.9622	0.9778	0.9939
	900	0.9591	0.9773	0.9912
	2100	0.9413	0.9576	0.9912

FE2

GROUP	TEMP	10.	1.E2	1.E3
12	300	0.9939	0.9980	0.9991
	900	0.9948	0.9980	0.9988
	2100	0.9963	0.9996	1.0002
13	300	0.9885	0.9963	0.9985
	900	0.9908	0.9972	0.9989
	2100	0.9916	0.9976	0.9990
14	300	0.9820	0.9906	0.9944
	900	0.9880	0.9926	0.9956
	2100	0.9904	0.9941	0.9966
15	300	0.9563	0.9864	0.9955
	900	0.9639	0.9899	0.9980
	2100	0.9667	0.9914	0.9979
16	300	0.9730	0.9934	1.0006
	900	0.9846	0.9965	1.0027
	2100	0.9948	1.0022	1.0036
17	300	0.9561	0.9800	0.9949
	900	0.9721	0.9872	0.9971
	2100	0.9871	0.9944	1.0028
18	300	0.8782	0.9135	0.9710
	900	0.8909	0.9247	0.9771
	2100	0.9015	0.9337	0.9807
19	300	0.9281	0.9670	0.9885
	900	0.9241	0.9743	0.9936
	2100	0.9223	0.9709	0.9922
20	300	0.9326	0.9200	0.9662
	900	0.9310	0.9411	0.9706
	2100	0.9408	0.9332	0.9706
21	300	1.0289	1.0417	1.0307
	900	1.0270	1.0191	1.0289
	2100	1.0210	1.0273	1.0429
22	300	0.9479	0.9824	0.9953
	900	0.9854	0.9984	1.0038
	2100	0.9561	0.9703	0.9763
23	300	0.9719	0.9885	0.9967
	900	0.9691	0.9858	0.9934
	2100	0.9672	0.9836	0.9733
24	300	0.9624	0.9770	0.9934
	900	0.9645	0.9700	0.9907
	2100	0.9421	0.9522	0.9792

FC1

GROUP	TEMP	10.	1.E2	1.E3
12	300	0.8730	0.9658	0.9836
	900	0.8814	0.9682	0.9819
	2100	0.8862	0.9689	0.9806
13	300	0.8261	0.9495	0.9851
	900	0.8430	0.9561	0.9861
	2100	0.8516	0.9597	0.9867
14	300	0.7555	0.9041	0.9662
	900	0.7879	0.9162	0.9745
	2100	0.8046	0.9254	0.9721
15	300	0.5998	0.8474	0.9580
	900	0.6408	0.8712	0.9625
	2100	0.6644	0.8857	0.9623
16	300	0.7321	0.8772	0.9741
	900	0.8194	0.9194	0.9891
	2100	0.8827	0.9447	0.9942
17	300	0.4987	0.7217	0.9518
	900	0.5786	0.7652	0.9308
	2100	0.6424	0.7909	0.9460
18	300	0.4618	0.7144	0.9583
	900	0.5955	0.7928	0.9704
	2100	0.6875	0.8519	0.9911
19	300	0.4214	0.6586	0.9437
	900	0.4720	0.7263	0.9775
	2100	0.5278	0.7497	1.0166
20	300	0.3341	0.4436	0.7945
	900	0.3790	0.4937	0.7938
	2100	0.4480	0.5608	0.8444
21	300	0.3095	0.5031	0.8252
	900	0.3374	0.5380	0.8428
	2100	0.3761	0.5722	0.8408
22	300	0.4985	0.8840	0.9924
	900	0.5548	0.8627	1.0130
	2100	0.6584	1.0267	1.0832
23	300	0.4954	0.7657	0.9536
	900	0.7452	0.7958	0.9441
	2100	0.8529	0.8079	0.9449
24	300	1.1052	0.9896	0.9860
	900	1.1245	0.9687	0.9934
	2100	1.1716	1.0270	0.9934

FC2

GROUP	TEMP	10.	1.E2	1.E3
12	300	0.8770	0.9902	0.9770
	900	0.8834	0.9793	0.9732
	2100	0.8873	0.9780	0.9707
13	300	0.8347	0.9434	0.9758
	900	0.8511	0.9488	0.9764
	2100	0.8581	0.9515	0.9767
14	300	0.7624	0.8534	0.9546
	900	0.7927	0.8713	0.9520
	2100	0.8064	0.8783	0.9575
15	300	0.6035	0.8493	0.9500
	900	0.6422	0.8686	0.9526
	2100	0.6644	0.8769	0.9502
16	300	0.7519	0.9005	0.9831
	900	0.8361	0.9370	0.9926
	2100	0.8942	0.9565	0.9966
17	300	0.5145	0.7326	0.9228
	900	0.6400	0.7691	0.9253
	2100	0.6492	0.7907	0.9347
18	300	0.4913	0.7766	0.9558
	900	0.6010	0.8195	0.9761
	2100	0.6871	0.8782	0.9988
19	300	0.4459	0.7048	0.9592
	900	0.4921	0.7772	0.9885
	2100	0.5553	0.8336	1.0246
20	300	0.3295	0.4709	0.7829
	900	0.3673	0.4766	0.8082
	2100	0.4839	0.5767	0.8544
21	300	0.3070	0.5423	0.8115
	900	0.3344	0.5790	0.8294
	2100	0.3726	0.5933	0.8375
22	300	0.4998	0.8876	0.9982
	900	0.5567	0.9322	1.0187
	2100	0.6643	1.0177	1.0695
23	300	0.6995	0.7719	0.9408
	900	0.7757	0.7939	0.9412
	2100	0.8344	0.8142	0.9489
24	300	1.1116	0.9740	0.9862
	900	1.0876	0.9979	0.9937
	2100	1.1779	1.0336	0.9997

		FR1			FR2		
GROUP	TEMP	10.	1.E2	1.E3	10.	1.E2	1.E3
12	300	0.0941	0.5972	0.7014	0.0832	0.4639	0.5803
	900	0.0961	0.5972	0.6834	0.0839	0.4670	0.5489
	2100	0.0937	0.5932	0.6762	0.0836	0.4573	0.5378
13	300	0.0399	0.5537	0.7932	0.0626	0.4575	0.6840
	900	0.0381	0.5539	0.7824	0.0602	0.4523	0.6569
	2100	0.0365	0.5533	0.7824	0.0589	0.4551	0.6481
14	300	0.0105	0.4489	0.7813	0.0096	0.2347	0.6555
	900	0.0089	0.4394	0.7655	0.0082	0.2123	0.6317
	2100	0.0085	0.4403	0.7541	0.0061	0.1992	0.6138
15	300	0.0024	0.2183	0.6515	0.0022	0.1199	0.5834
	900	0.0017	0.2036	0.6259	0.0016	0.1538	0.5358
	2100	0.0014	0.1962	0.6023	0.0013	0.1332	0.4903
16	300	0.0011	0.1526	0.6936	0.0011	0.1312	0.6367
	900	0.0008	0.1269	0.6438	0.0006	0.0970	0.5722
	2100	0.0005	0.1082	0.6059	0.0005	0.0699	0.5157
17	300	0.0011	0.2464	0.7851	0.0012	0.2063	0.6830
	900	0.0011	0.2341	0.8222	0.0006	0.2011	0.7094
	2100	0.0004	0.2413	0.9081	0.0004	0.2091	0.7824
18	300	0.0064	0.2005	0.7535	0.0062	0.1850	0.7063
	900	0.0061	0.1870	0.7542	0.0060	0.1715	0.7048
	2100	0.0059	0.1712	0.7177	0.0057	0.1542	0.6654
19	300	0.0093	0.1553	0.5511	0.0164	0.0716	0.3812
	900	0.0090	0.1159	0.5343	0.0101	0.1451	0.3668
	2100	0.0086	0.0737	0.4859	0.0098	0.0316	0.3220
20	300	0.0053	0.2484	0.7354	0.0058	0.0795	0.6726
	900	0.0049	0.1020	0.7356	0.0056	0.0162	0.6745
	2100	0.0043	0.2239	0.7075	0.0050	0.2384	0.6490
21	300	0.0033	0.1836	0.4127	0.0027	0.0985	0.2960
	900	0.0027	0.1629	0.4199	0.0025	0.0640	0.3056
	2100	0.0024	0.1405	0.3643	0.0021	0.0542	0.2655
22	300	0.0648	0.4592	0.8903	0.0639	0.4471	0.8465
	900	0.0237	0.4601	0.8858	0.0225	0.4341	0.8423
	2100	0.0228	0.4139	0.8612	0.0221	0.4046	0.8179
23	300	0.0092	0.1990	0.7967	0.0030	0.2174	0.7730
	900	0.0032	0.1921	0.7936	0.0029	0.2131	0.7695
	2100	0.0030	0.1840	0.7760	0.0032	0.2011	0.7557
24	300	0.0057	0.1914	0.7438	0.0003	0.1506	0.7029
	900	0.0039	0.1518	0.7215	0.0027	0.0275	0.7002
	2100	0.0032	0.0317	0.7215	0.0025	0.0349	0.7006

C-II-1 Table of infinite dilution cross section for ^{238}U

MCOUE ... 928 URANIUM 238

ATOMIC WEIGHT = 238.06999

GROUP	TOTAL	FISSION	NU	CAPTURE	INELASTIC	ELASTIC	MU-E	ELASTIC-REMOVAL
11	15.463	0.0	0.0	0.6608	0.0	14.80	0.040	0.1695
12	17.009	0.0	0.0	0.9162	0.0	16.09	0.023	0.3046
13	17.529	0.0	0.0	1.2125	0.0	16.32	0.0	0.2807
14	20.217	0.0	0.0	1.6206	0.0	18.60	0.0	0.1774
15	21.784	0.0	0.0	2.6474	0.0	19.14	0.0	0.1180
16	20.895	0.0	0.0	4.3890	0.0	16.51	0.0	0.1188
17	87.835	0.0	0.0	19.8472	0.0	67.99	0.0	0.0086
18	42.266	0.0	0.0	14.1242	0.0	28.14	0.0	0.1350
19	134.240	0.0	0.0	49.9317	0.0	84.33	0.0	0.2805
20	112.043	0.0	0.0	77.6630	0.0	34.38	0.0	0.0918
21	190.995	0.0	0.0	171.6780	0.0	19.32	0.0	0.0849
22	9.076	0.0	0.0	0.6280	0.0	8.45	0.0	0.0949
23	9.333	0.0	0.0	0.4591	0.0	8.87	0.0	0.0731
24	9.563	0.0	0.0	0.3476	0.0	9.02	0.0	0.0738
25	9.900	0.0	0.0	0.9000	0.0	9.00	0.0	0.0

C-II-2 Shielding factor for ^{238}U

GROUP	TEMP	FT 1.	FT 10.	FT 1.E2	FT 1.E3	FC 1.	FC 10.	FC 1.E2	FC 1.E3	FE 1.	FE 10.	FE 1.E2	FE 1.E3
11	300	0.8099	0.8381	0.9343	0.9889	0.7406	0.8783	0.9636	0.9935	0.8707	0.8952	0.9819	0.9929
	900	0.8369	0.8667	0.9528	0.9920	0.7836	0.9251	0.9775	0.9951	0.8935	0.9175	0.9728	0.9943
	2100	0.8716	0.9090	0.9705	0.9978	0.8081	0.9407	0.9823	0.9962	0.9187	0.9460	0.9891	0.9990
12	300	0.6333	0.6984	0.8496	0.9498	0.6853	0.7799	0.9252	0.9861	0.7388	0.7883	0.9090	0.9838
	900	0.6988	0.7509	0.8905	0.9806	0.7550	0.8433	0.9537	0.9912	0.7879	0.8326	0.9367	0.9898
	2100	0.7479	0.7943	0.9193	0.9858	0.8018	0.8845	0.9697	0.9938	0.8257	0.8666	0.9538	0.9920
13	300	0.5661	0.6414	0.7810	0.9435	0.5338	0.6248	0.8384	0.9695	0.6858	0.7343	0.8601	0.9713
	900	0.6288	0.6825	0.8262	0.9625	0.6159	0.6995	0.8883	0.9806	0.7308	0.7736	0.8951	0.9809
	2100	0.6683	0.7182	0.8635	0.9737	0.6800	0.7574	0.9210	0.9867	0.7654	0.8073	0.9211	0.9868
14	300	0.3501	0.3151	0.6494	0.8709	0.3344	0.4272	0.6784	0.9228	0.5453	0.6194	0.7540	0.9296
	900	0.3994	0.5393	0.6914	0.9087	0.3926	0.4975	0.7520	0.9495	0.5756	0.6489	0.7967	0.9526
	2100	0.4590	0.5669	0.7335	0.9351	0.4485	0.5602	0.8072	0.9651	0.6086	0.6803	0.8345	0.9684
15	300	0.3518	0.4652	0.5667	0.8151	0.1742	0.2316	0.4804	0.8476	0.5217	0.5799	0.6994	0.9052
	900	0.3994	0.4852	0.6095	0.8694	0.2190	0.2963	0.5834	0.9013	0.5563	0.6086	0.7469	0.9383
	2100	0.4613	0.5075	0.6552	0.9071	0.2727	0.3649	0.6712	0.9344	0.5955	0.6407	0.7912	0.9596
16	300	0.5253	0.5328	0.5793	0.7686	0.1083	0.1436	0.3668	0.7515	0.6478	0.6780	0.7386	0.8876
	900	0.5304	0.5393	0.6057	0.8249	0.1507	0.1890	0.4376	0.8271	0.6742	0.6891	0.7875	0.9205
	2100	0.5387	0.5488	0.6477	0.8679	0.1976	0.2378	0.5222	0.8764	0.6820	0.7018	0.7981	0.9436
17	300	0.1666	0.2567	0.3392	0.6085	0.0431	0.0589	0.1469	0.4136	0.1604	0.1848	0.2553	0.4759
	900	0.1636	0.2697	0.3480	0.7141	0.0474	0.0655	0.1782	0.5049	0.1611	0.1887	0.2765	0.5521
	2100	0.2902	0.3010	0.3828	0.8716	0.0478	0.0720	0.2168	0.5994	0.1975	0.2098	0.3129	0.6379
18	300	0.1858	0.2322	0.2661	0.3740	0.0490	0.0657	0.1515	0.4178	0.3170	0.3455	0.4135	0.5805
	900	0.1828	0.2319	0.2727	0.4270	0.0541	0.0743	0.1922	0.5234	0.3128	0.3678	0.4348	0.6528
	2100	0.1904	0.2399	0.2915	0.4982	0.0600	0.0870	0.2411	0.6264	0.3296	0.3824	0.4710	0.7302
19	300	0.0949	0.0935	0.1141	0.1736	0.0246	0.0467	0.0977	0.2544	0.1748	0.1721	0.2032	0.3384
	900	0.0947	0.0935	0.1138	0.1907	0.0247	0.0476	0.1085	0.3228	0.1747	0.1735	0.2139	0.3993
	2100	0.0902	0.0908	0.1053	0.2187	0.0248	0.0500	0.1192	0.4134	0.1674	0.1702	0.2256	0.4744
20	300	0.0754	0.0792	0.0965	0.1669	0.0449	0.0368	0.0865	0.2780	0.2509	0.2422	0.2799	0.4307
	900	0.0748	0.0787	0.0934	0.1966	0.0464	0.0385	0.1020	0.3632	0.2478	0.2427	0.2916	0.4977
	2100	0.0692	0.0761	0.0930	0.2455	0.0529	0.0405	0.1289	0.4622	0.2281	0.2345	0.3085	0.5731
21	300	0.0582	0.0653	0.0862	0.1648	0.0093	0.0248	0.0825	0.2813	0.5230	0.5422	0.5486	0.6313
	900	0.0583	0.0651	0.0854	0.1898	0.0094	0.0252	0.0908	0.3415	0.5293	0.5432	0.5569	0.6681
	2100	0.0557	0.0645	0.0851	0.2290	0.0093	0.0261	0.1048	0.4132	0.4974	0.5417	0.5656	0.7074

GROUP	TEMP	FM 1.	FM 10.	FM 1.E2	FM 1.E3
11	300	0.1310	0.6445	0.8406	0.9273
	900	0.1471	0.7232	0.8981	0.9281
	2100	0.1518	0.6773	0.8621	0.9348
12	300	0.0679	0.3311	0.6689	0.8760
	900	0.0630	0.3423	0.7152	0.8969
	2100	0.0607	0.3482	0.7311	0.8879
13	300	0.0712	0.2295	0.6291	0.9104
	900	0.0635	0.2408	0.7289	0.9352
	2100	0.0589	0.2521	0.7584	0.9214
14	300	0.1992	0.3009	0.8328	0.9758
	900	0.1287	0.4440	0.8463	0.9755
	2100	0.1090	0.4364	0.8260	0.9807
15	300	0.3441	0.6941	0.8788	0.8990
	900	0.2731	0.6300	0.8640	0.9000
	2100	0.2076	0.5649	0.8555	0.9053
16	300	0.4400	0.7179	0.8883	0.9383
	900	0.1997	0.6325	0.8636	0.9362
	2100	0.1073	0.5799	0.8399	0.9348
17	300	0.0691	0.5035	0.9974	0.9950
	900	0.0738	0.6195	1.2414	1.2135
	2100	0.1615	1.4009	3.3881	3.1941
18	300	0.3333	0.8060	0.9631	0.9838
	900	0.2988	0.7813	0.9247	0.9799
	2100	0.2783	0.7641	0.9136	0.9761
19	300	0.0743	0.5012	0.7914	0.9671
	900	0.0744	0.5050	0.7964	0.9979
	2100	0.0660	0.2572	0.7921	1.0662
20	300	0.3849	0.8353	0.9847	1.0017
	900	0.2778	0.8421	0.9893	1.0031
	2100	0.1685	0.7833	0.9944	1.0797
21	300	0.2606	0.3011	0.6326	0.8730
	900	0.2517	0.2909	0.5976	0.9404
	2100	0.2181	0.2696	0.5962	0.8076

C-III-1 Table of infinite dilution cross section for ^{239}Pu

MCODE ... 949 PLUTONIUM 239

ATOMIC WEIGHT = 239.05215

GROUP	TOTAL	FISSION	NU	CAPTURE	INELASTIC	ELASTIC	MU-E	ELASTIC-REMOVAL
12	14.994	2.34	2.89	1.9515	0.02	11.05	0.024	0.1378
13	17.347	2.97	2.88	2.6153	0.0	11.79	0.0	0.1203
14	20.037	4.46	2.87	3.7762	0.0	11.80	0.0	0.1187
15	29.111	8.85	2.87	6.9126	0.0	13.35	0.0	0.0993
16	42.798	14.92	2.87	10.2037	0.0	17.64	0.0	0.1302
17	45.604	18.32	2.87	13.7070	0.0	13.67	0.0	0.0958
18	133.399	73.09	2.87	34.8490	0.0	25.39	0.0	0.1076
19	79.487	25.19	2.87	41.3624	0.0	12.98	0.0	0.0597
20	181.585	104.39	2.87	65.7940	0.0	11.45	0.0	0.0639
21	72.215	35.76	2.87	28.3579	0.0	8.12	0.0	0.0878
22	18.767	9.13	2.87	1.0926	0.0	8.55	0.0	0.0965
23	34.083	22.49	2.87	4.1601	0.0	9.93	0.0	0.0809
24	142.696	92.60	2.87	38.9203	0.0	11.14	0.0	0.1024
25	2665.740	1579.30	2.87	1049.8500	0.0	16.59	0.0	0.0

C-III-2 Shielding factor for ^{239}Pu

GROUP	TEMP	FT1			FT2			FF1			FF2		
		10.	1.E2	1.E3	10.	1.E2	1.E3	10.	1.E2	1.E3	10.	1.E2	1.E3
12	300	0.9332	0.9956	1.0185	0.9597	1.0138	1.0333	0.8470	0.9707	0.9872	0.9078	0.9700	0.9863
	900	0.9478	0.9991	1.0148	0.9671	1.0114	1.0242	0.9083	0.9741	0.9864	0.9163	0.9644	0.9793
	2100	0.9558	1.0021	1.0148	0.9712	1.0124	1.0228	0.9194	0.9775	0.9888	0.9225	0.9732	0.9818
13	300	0.8334	0.9418	0.9983	0.8695	0.9614	1.0090	0.8242	0.9340	0.9746	0.8435	0.9339	0.9661
	900	0.8758	0.9592	0.9975	0.9027	0.9713	1.0020	0.8520	0.9454	0.9720	0.8656	0.9341	0.9611
	2100	0.8993	0.9677	0.9965	0.9234	0.9760	0.9986	0.8693	0.9491	0.9703	0.8719	0.9348	0.9565
14	300	0.7596	0.9194	1.0178	0.8163	0.9665	1.0501	0.6673	0.8660	0.9814	0.6959	0.8761	0.9708
	900	0.8241	0.9583	1.0255	0.8786	0.9948	1.0507	0.7143	0.9008	0.9909	0.7347	0.8849	0.9733
	2100	0.8635	0.9814	1.0314	0.9169	1.0143	1.2932	0.7422	0.9025	0.9901	0.7501	0.9007	0.9686
15	300	0.5368	0.7277	0.9195	0.5735	0.7595	0.9274	0.5560	0.7642	0.9210	0.5744	0.7828	0.9128
	900	0.6086	0.7919	0.9596	0.6471	0.8163	0.9417	0.6212	0.8180	0.9226	0.6589	0.8026	0.9133
	2100	0.6737	0.8400	0.9834	0.7021	0.8557	0.9514	0.7122	0.8319	0.9453	0.7103	0.8039	0.9170
16	300	0.3665	0.5375	0.8050	0.3906	0.5926	0.8125	0.3832	0.6356	0.8872	0.4140	0.6534	0.8799
	900	0.4098	0.5880	0.8393	0.4394	0.6401	0.8275	0.4261	0.6848	0.8829	0.4565	0.6530	0.8681
	2100	0.4623	0.6314	0.8626	0.4975	0.6898	0.8330	0.4828	0.6889	0.8767	0.5117	0.6956	0.8558
17	300	0.4032	0.5809	0.8178	0.4436	0.6404	0.8249	0.5128	0.7532	0.9396	0.5731	0.8059	0.9550
	900	0.4265	0.6153	0.8289	0.4674	0.6940	0.8189	0.5949	0.8438	0.9530	0.6337	0.8312	0.9624
	2100	0.4338	0.6918	0.8822	0.4602	0.7424	0.8760	0.6819	0.9157	0.9886	0.7262	0.9628	1.0068
18	300	0.1573	0.2589	0.5823	0.1363	0.2719	0.6129	0.2418	0.3963	0.7342	0.2416	0.4111	0.7513
	900	0.1590	0.2702	0.6219	0.1378	0.2847	0.6505	0.2518	0.4367	0.7510	0.2502	0.4099	0.7682
	2100	0.1718	0.3002	0.6706	0.1499	0.3151	0.6954	0.2721	0.4456	0.7768	0.2685	0.4603	0.7920
19	300	0.1946	0.2786	0.7151	0.2155	0.3145	0.8211	0.1080	0.2516	0.6341	0.1270	0.2657	0.6256
	900	0.2003	0.3145	0.8211	0.2250	0.3677	0.9263	0.1196	0.3112	0.6722	0.1430	0.2670	0.6571
	2100	0.2155	0.3730	0.9106	0.2463	0.4395	1.0075	0.1427	0.3180	0.7047	0.1690	0.3362	0.6838
20	300	0.1066	0.1907	0.5475	0.1125	0.2115	0.5831	0.0887	0.2691	0.6636	0.0938	0.2798	0.6800
	900	0.1057	0.2040	0.5948	0.1112	0.2377	0.6290	0.0924	0.2959	0.6961	0.0977	0.2817	0.7092
	2100	0.1069	0.2163	0.6443	0.1120	0.2516	0.6730	0.0971	0.3027	0.7275	0.1031	0.3153	0.7356
21	300	0.3194	0.4178	0.9254	0.3265	0.4244	0.9791	0.3580	0.5322	1.0734	0.3697	0.5399	1.1176
	900	0.3194	0.4237	1.0056	0.3263	0.4360	1.0492	0.3616	0.5920	1.1433	0.3731	0.5936	1.1746
	2100	0.3214	0.4400	1.1066	0.3287	0.4542	1.1234	0.3762	0.6082	1.2330	0.3887	0.6429	1.2435
22	300	0.8949	0.9884	0.9876	0.8948	0.9660	0.9826	0.8387	0.9528	0.9808	0.8384	0.9491	0.9729
	900	0.8949	0.9884	0.9876	0.8948	0.9660	0.9826	0.8387	0.9539	0.9808	0.8384	0.9481	0.9729
	2100	0.8949	0.9884	0.9876	0.8948	0.9660	0.9826	0.8387	0.9528	0.9808	0.8384	0.9491	0.9729
23	300	0.7324	0.8783	0.9607	0.7296	0.8817	0.9543	0.6811	0.8654	0.9550	0.6768	0.8698	0.9472
	900	0.7324	0.8783	0.9607	0.7296	0.8817	0.9543	0.6811	0.8700	0.9550	0.6768	0.8651	0.9472
	2100	0.7324	0.8783	0.9607	0.7296	0.8817	0.9543	0.6811	0.8654	0.9550	0.6768	0.8698	0.9472
24	300	0.4325	0.5085	0.7722	0.4290	0.5144	0.7686	0.4573	0.5403	0.8022	0.4530	0.5470	0.7981
	900	0.4325	0.5085	0.7722	0.4290	0.5144	0.7686	0.4573	0.5471	0.8022	0.4530	0.5402	0.7981
	2100	0.4325	0.5085	0.7722	0.4290	0.5144	0.7686	0.4573	0.5403	0.8022	0.4530	0.5470	0.7981

GROUP	TEMP	FC1 10.	FC1 1.E2	FC1 1.E3	FC2 10.	FC2 1.E2	FC2 1.E3	FE1 10.	FE1 1.E2	FE1 1.E3	FE2 10.	FE2 1.E2	FE2 1.E3
12	300	0.8200	0.9412	0.9685	0.8274	0.9348	0.9560	0.9280	0.9876	0.9960	0.9426	0.9883	0.9948
	900	0.8302	0.9474	0.9682	0.8418	0.9379	0.9538	0.9656	0.9900	0.9958	0.9484	0.9895	0.9939
	2100	0.8498	0.9518	0.9687	0.8501	0.9411	0.9548	0.9702	0.9919	0.9965	0.9519	0.9910	0.9944
13	300	0.7137	0.8938	0.9599	0.7333	0.8900	0.9436	0.9066	0.9636	0.9873	0.9162	0.9653	0.9839
	900	0.7555	0.9075	0.9566	0.7686	0.8769	0.9361	0.9262	0.9712	0.9870	0.9336	0.9705	0.9827
	2100	0.7786	0.9134	0.9561	0.7877	0.8993	0.9310	0.9406	0.9763	0.9878	0.9460	0.9745	0.9831
14	300	0.7505	0.9181	0.9681	0.7833	0.9346	0.9877	0.9128	0.9788	1.0032	0.9267	0.9890	1.0091
	900	0.8324	0.9346	0.9705	0.8563	0.9642	0.9928	0.9410	0.9929	1.0040	0.9523	0.9997	1.0090
	2100	0.8751	0.9722	0.9836	0.8946	0.9794	0.9966	0.9575	1.0016	1.0060	0.9671	1.0073	1.0113
15	300	0.4440	0.7317	0.9121	0.4979	0.7534	0.9079	0.7945	0.8942	0.9717	0.8098	0.9063	0.9721
	900	0.5580	0.7883	0.9219	0.5864	0.7985	0.9113	0.8328	0.9222	0.9779	0.8464	0.9304	0.9769
	2100	0.6139	0.8164	0.9435	0.6361	0.8163	0.9054	0.8659	0.9433	0.9857	0.8751	0.9494	0.9823
16	300	0.3363	0.5578	0.8458	0.3796	0.5895	0.8515	0.5500	0.6386	0.8191	0.5586	0.6948	0.8182
	900	0.4079	0.6206	0.8670	0.4530	0.6446	0.8618	0.5608	0.6544	0.8322	0.5695	0.6596	0.8214
	2100	0.4698	0.6604	0.8689	0.5147	0.6763	0.8542	0.5783	0.6678	0.8358	0.5891	0.6692	0.8126
17	300	0.2172	0.4943	0.8450	0.2397	0.5208	0.8390	0.7474	0.8200	0.9559	0.7679	0.8325	0.9411
	900	0.2633	0.5568	0.8588	0.2833	0.5691	0.8308	0.7543	0.8488	0.9666	0.7642	0.8544	0.9627
	2100	0.3077	0.6022	0.8576	0.3216	0.6003	0.8219	0.7617	0.8649	0.9666	0.7504	0.8677	0.9577
18	300	0.1343	0.2338	0.6122	0.1369	0.2434	0.6248	0.4554	0.5212	0.7404	0.4562	0.5393	0.7761
	900	0.1495	0.2556	0.6493	0.1466	0.2663	0.6584	0.4641	0.5381	0.7758	0.4635	0.5564	0.8104
	2100	0.1641	0.2802	0.6807	0.1594	0.2892	0.6836	0.5177	0.6055	0.8672	0.5146	0.6253	0.8799
19	300	0.1864	0.3769	0.8840	0.2410	0.4609	1.0098	0.7574	0.8096	1.0006	0.8037	0.8617	1.0737
	900	0.2226	0.4642	0.9780	0.2915	0.5692	1.0964	0.7821	0.8533	1.0449	0.8392	0.9175	1.1160
	2100	0.2813	0.5758	1.0601	0.3623	0.6833	1.1678	0.8086	0.9025	1.0782	0.8732	0.9714	1.1439
20	300	0.0632	0.2203	0.6561	0.0681	0.2339	0.6871	0.8520	0.8909	0.9612	0.8615	0.9035	0.9778
	900	0.0672	0.2401	0.7067	0.0725	0.2560	0.7329	0.8564	0.8995	0.9756	0.8657	0.9128	0.9903
	2100	0.0730	0.2694	0.7562	0.0791	0.2852	0.7760	0.8721	0.9159	0.9923	0.8815	0.9276	1.0048
21	300	0.2016	0.4504	1.1130	0.2072	0.4643	1.1732	0.9449	0.9785	1.0224	0.9426	0.9949	1.0347
	900	0.2054	0.4817	1.1970	0.2110	0.5114	1.2430	0.9451	0.9802	1.0277	0.9428	0.9894	1.0384
	2100	0.2125	0.5359	1.3044	0.2179	0.5565	1.3235	0.9276	0.9687	1.0218	0.9248	0.9736	1.0295
22	300	0.8020	0.9367	0.9751	0.8015	0.9352	0.9633	0.9733	0.9931	0.9973	0.9733	0.9924	0.9961
	900	0.8020	0.9367	0.9751	0.8015	0.9352	0.9633	0.9733	0.9931	0.9973	0.9733	0.9924	0.9961
	2100	0.8020	0.9367	0.9751	0.8015	0.9352	0.9633	0.9733	0.9931	0.9973	0.9733	0.9924	0.9961
23	300	0.5418	0.7973	0.9303	0.5364	0.8042	0.9186	0.9641	0.9855	0.9951	0.9635	0.9859	0.9943
	900	0.5418	0.7973	0.9303	0.5364	0.8042	0.9186	0.9641	0.9855	0.9951	0.9635	0.9859	0.9943
	2100	0.5418	0.7973	0.9303	0.5364	0.8042	0.9186	0.9641	0.9855	0.9951	0.9635	0.9859	0.9943
24	300	0.2873	0.3795	0.7220	0.2825	0.3873	0.7169	0.9107	0.9277	0.9727	0.9099	0.9291	0.9720
	900	0.2873	0.3795	0.7220	0.2825	0.3873	0.7169	0.9107	0.9277	0.9727	0.9099	0.9291	0.9720
	2100	0.2873	0.3795	0.7220	0.2825	0.3873	0.7169	0.9107	0.9277	0.9727	0.9099	0.9291	0.9720

GROUP	TEMP	FR1 10.	FR1 1.E2	FR1 1.E3	FR2 10.	FR2 1.E2	FR2 1.E3
12	300	0.0403	0.4738	0.5678	0.0309	0.3821	0.4473
	900	0.0359	0.4577	0.5545	0.0281	0.3582	0.4350
	2100	0.0330	0.4516	0.5358	0.0227	0.3483	0.4018
13	300	0.1115	0.5330	0.7294	0.1117	0.4884	0.6047
	900	0.1031	0.5211	0.7100	0.1038	0.4734	0.5712
	2100	0.1009	0.5181	0.7053	0.1011	0.4646	0.5547
14	300	0.0726	0.2912	0.6592	0.0604	0.1879	0.4598
	900	0.0585	0.2660	0.6333	0.0501	0.1705	0.4263
	2100	0.0523	0.2443	0.6031	0.0486	0.1517	0.3891
15	300	0.0173	0.2782	0.5972	0.0140	0.2363	0.5156
	900	0.0098	0.2313	0.5490	0.0080	0.1828	0.4483
	2100	0.0043	0.1912	0.4950	0.0074	0.1401	0.3765
16	300	0.0021	0.1507	0.6087	0.0023	0.1345	0.5499
	900	0.0009	0.1133	0.5631	0.0011	0.0962	0.4898
	2100	0.0003	0.0629	0.5075	0.0004	0.0483	0.3204
17	300	0.0091	0.3339	0.6871	0.0062	0.2866	0.5431
	900	0.0058	0.2779	0.7183	0.0043	0.2759	0.5613
	2100	0.0040	0.3038	0.7304	0.0034	0.2980	0.5608
18	300	0.0221	0.1931	0.6732	0.0186	0.1727	0.6112
	900	0.0176	0.1681	0.6556	0.0148	0.1546	0.5948
	2100	0.0104	0.1143	0.5187	0.0088	0.1036	0.4702
19	300	0.0247	0.1758	0.3707	0.0220	0.1045	0.2442
	900	0.0167	0.1438	0.3410	0.0157	0.0906	0.2357
	2100	0.0090	0.1049	0.3236	0.0052	0.0656	0.2132
20	300	0.0051	0.1818	0.5840	0.0055	0.1703	0.5112
	900	0.0051	0.1670	0.5710	0.0054	0.1642	0.5023
	2100	0.0040	0.1501	0.5383	0.0043	0.1521	0.4727
21	300	0.0202	0.1674	0.2283	0.0140	0.1519	0.1732
	900	0.0187	0.1572	0.2173	0.0132	0.0788	0.1692
	2100	0.0156	0.1256	0.1871	0.0115	0.0586	0.1511
22	300	0.0594	0.6330	0.8767	0.0584	0.6004	0.8139
	900	0.0594	0.6330	0.8767	0.0584	0.6004	0.8139
	2100	0.0594	0.6330	0.8767	0.0584	0.6004	0.8139
23	300	0.0057	0.3682	0.8359	0.0055	0.3811	0.7949
	900	0.0057	0.3682	0.8359	0.0055	0.3811	0.7949
	2100	0.0057	0.3682	0.8359	0.0055	0.3811	0.7949
24	300	0.0019	0.0379	0.5559	0.0019	0.0393	0.5594
	900	0.0019	0.0379	0.5559	0.0019	0.0393	0.5594
	2100	0.0019	0.0379	0.5559	0.0019	0.0393	0.5594

C-IV-1 Tableof infinite dilution cross section for ^{240}Pu

MCUVE ... 940 PLUTONIUM 240

ATOMIC WEIGHT = 240.05400

GROUP	TOTAL	FISSION	NU	CAPTURE	INELASTIC	ELASTIC	MU-E	ELASTIC-REMOVAL
11	15.091	0.10	2.89	0.6757	0.0	14.22	0.040	0.1448
12	16.484	0.15	2.89	0.9177	0.0	15.41	0.029	0.1266
13	17.243	0.07	2.89	1.2343	0.0	15.94	0.018	0.1144
14	21.877	0.05	2.89	2.4040	0.0	19.42	0.008	0.5144
15	22.364	0.15	2.89	4.2608	0.0	17.95	0.003	0.1235
16	31.110	0.0	0.0	6.7413	0.0	24.37	0.003	0.1147
17	53.863	0.0	0.0	20.5959	0.0	33.27	0.003	0.0646
18	110.707	0.0	0.0	37.6035	0.0	72.40	0.002	0.1421
19	128.723	0.0	0.0	64.5000	0.0	64.22	0.003	0.1116
20	63.215	0.00	2.89	30.9353	0.0	12.28	0.003	0.1054
21	11.444	0.00	2.89	0.7067	0.0	10.74	0.003	0.1305
22	23.343	0.00	2.89	8.1395	0.0	15.40	0.003	0.2291
23	9732.560	1.65	2.87	9019.0400	0.0	712.45	0.003	15.2320
24	1262.010	0.20	2.89	1212.5200	0.0	49.30	0.003	0.0005
25	152.893	0.02	2.89	152.5370	0.0	0.33	0.003	0.0

C-IV-2 Shieldirg factor for ^{240}Pu

GROUP	TEMP	FT1 1.E2	FT1 1.E3	FT1 1.E4	FT2 1.E2	FT2 1.E3	FT2 1.E4	FF1 1.E2	FF1 1.E3	FF1 1.E4	FF2 1.E2	FF2 1.E3	FF2 1.E4
11	300	0.9770	0.9993	1.0073	1.0021	1.0100	1.0161	0.9645	0.9823	0.9940	0.9367	0.9775	0.9858
	900	0.9877	1.0008	1.0059	1.0103	1.0102	1.0145	0.9737	0.9848	0.9954	0.9440	0.9805	0.9866
	2100	0.9902	0.9982	1.0025	1.0045	1.0043	1.0078	0.9794	0.9863	0.9944	0.9502	0.9830	0.9883
12	300	0.9088	0.9775	0.9935	0.9439	0.9860	0.9993	0.9814	1.0054	1.0161	0.8966	1.0131	1.0227
	900	0.9423	0.9880	0.9979	0.9795	0.9969	1.0043	1.0014	1.0105	1.0188	1.0473	1.0195	1.0272
	2100	0.9638	0.9941	1.0005	0.9880	1.0033	1.0080	1.0120	1.0133	1.0205	0.9739	1.0255	1.0305
13	300	0.8508	0.9796	1.0200	0.9250	1.0068	1.0212	1.0142	1.0089	1.0210	1.0347	1.0160	1.0180
	900	0.8944	0.9893	1.0134	0.9491	1.0075	1.0269	1.0306	1.0161	1.0181	1.0458	1.0299	1.0322
	2100	0.9249	0.9920	1.0068	0.9658	1.0059	1.0175	1.0412	1.0205	1.0225	1.0911	1.0406	1.0430
14	300	0.6940	0.9149	1.0226	0.7923	0.9644	1.0400	1.0272	1.0001	1.0083	1.0470	1.0188	1.0293
	900	0.7576	0.9465	1.0150	0.8610	0.9839	1.0285	1.0588	1.0256	1.0319	1.1005	1.0423	1.0489
	2100	0.8172	0.9659	1.0096	0.9207	0.9924	1.0338	1.0418	1.0020	1.0052	1.0943	1.0148	1.0168
15	300	0.6379	0.8776	0.9911	0.6908	0.8953	1.0072	0.5361	0.9307	1.0626	0.6579	0.9842	1.1567
	900	0.7020	0.9159	0.9873	0.7538	0.9376	0.9945	0.6652	1.0041	1.0764	0.7758	1.1163	1.1577
	2100	0.7678	0.9506	0.9971	0.8244	0.9660	1.0131	0.7882	1.0588	1.0917	0.9443	1.1206	1.1755
16	300	0.4594	0.6886	0.9647	0.5006	0.7204	0.9784	1.0000	1.0000	1.0000	1.0000	1.0000	1.0000
	900	0.5006	0.7621	1.0072	0.5515	0.7962	1.0146	1.0000	1.0000	1.0000	1.0000	1.0000	1.0000
	2100	0.5433	0.8198	1.0279	0.6026	0.8529	1.0362	1.0000	1.0000	1.0000	1.0000	1.0000	1.0000
17	300	0.2744	0.4769	0.7533	0.3132	0.5078	0.7247	1.0000	1.0000	1.0000	1.0000	1.0000	1.0000
	900	0.3070	0.5381	0.7889	0.3511	0.5835	0.7514	1.0000	1.0000	1.0000	1.0000	1.0000	1.0000
	2100	0.3389	0.6147	0.8065	0.3812	0.6169	0.7385	1.0000	1.0000	1.0000	1.0000	1.0000	1.0000
18	300	0.1272	0.2069	0.4195	0.1478	0.2203	0.3849	1.0000	1.0000	1.0000	1.0000	1.0000	1.0000
	900	0.1347	0.2471	0.4089	0.1567	0.2585	0.4079	1.0000	1.0000	1.0000	1.0000	1.0000	1.0000
	2100	0.1410	0.2822	0.4299	0.1973	0.3014	0.4280	1.0000	1.0000	1.0000	1.0000	1.0000	1.0000
19	300	0.1238	0.2343	0.7208	0.1453	0.2743	0.7697	1.0000	1.0000	1.0000	1.0000	1.0000	1.0000
	900	0.1279	0.2985	0.8276	0.1355	0.3479	0.8520	1.0000	1.0000	1.0000	1.0000	1.0000	1.0000
	2100	0.1393	0.3881	0.9168	0.1126	0.4402	0.9274	1.0000	1.0000	1.0000	1.0000	1.0000	1.0000
20	300	0.2257	0.3431	0.4126	0.2428	0.3124	0.4373	1.0000	1.0000	1.0000	1.0000	1.0000	1.0000
	900	0.2287	0.3804	0.4089	0.2280	0.3346	0.4459	1.0000	1.0000	1.0000	1.0000	1.0000	1.0000
	2100	0.2328	0.3656	0.4858	0.2315	0.3194	0.3754	1.0000	1.0000	1.0000	1.0000	1.0000	1.0000
21	300	0.9535	0.9710	0.9711	0.9407	0.9541	0.9540	0.2102	0.2102	0.3101	0.1556	0.2084	0.2080
	900	0.9509	0.9642	0.9643	0.9369	0.9515	0.9515	0.2005	0.2793	0.2791	0.1917	0.1985	0.1980
	2100	0.9499	0.9638	0.9818	0.9364	0.9503	0.9476	0.1911	0.2626	0.4078	0.1389	0.1883	0.1768
22	300	0.9005	0.9788	0.9880	0.8858	0.9609	0.9698	0.8342	0.9613	0.9756	0.8931	0.9249	0.9381
	900	0.9007	0.9712	0.9804	0.8844	0.9612	0.9702	0.8348	0.9459	0.9596	0.7997	0.9257	0.9390
	2100	0.9063	0.9797	0.9812	0.8891	0.9694	0.9709	0.8482	0.9642	0.9613	0.8112	0.9433	0.9405
23	300	0.0084	0.0197	0.0721	0.0088	0.0197	0.0717	0.0077	0.0301	0.1361	0.0084	0.0308	0.1490
	900	0.0085	0.0194	0.0708	0.0086	0.0196	0.0732	0.0077	0.0746	0.1529	0.0082	0.0303	0.1547
	2100	0.0144	0.0194	0.0743	0.0087	0.0196	0.0768	0.0140	0.0308	0.1607	0.0084	0.0316	0.1624

GROUP	TEMP	FC1 1.E2	FC1 1.E3	FC1 1.E4	FC2 1.E2	FC2 1.E3	FC2 1.E4	FE1 1.E2	FE1 1.E3	FE1 1.E4	FE2 1.E2	FE2 1.E3	FE2 1.E4
	300	0.9680	0.9868	0.9966	0.9837	0.9833	0.9900	0.9795	0.9956	1.0001	0.9853	0.9961	0.9991
11	900	0.9777	0.9891	0.9978	0.9711	0.9860	0.9914	0.9859	0.9966	1.0001	0.9891	0.9966	0.9988
	2100	0.9828	0.9902	0.9982	0.9757	0.9875	0.9921	0.9893	0.9968	0.9995	0.9904	0.9962	0.9977
	300	0.9251	0.9744	0.9791	0.7602	0.9667	0.9692	0.9370	0.9834	0.9915	0.8054	0.9813	0.9873
12	900	0.9484	0.9815	0.9829	0.9413	0.9725	0.9722	0.9575	0.9895	0.9943	0.9644	0.9875	0.9909
	2100	0.9626	0.9860	0.9853	0.8713	0.9774	0.9758	0.9704	0.9931	0.9961	0.8779	0.9919	0.9935
	300	0.8355	0.9604	0.9832	0.8931	0.9598	0.9772	0.8982	0.9801	0.9992	0.9264	0.9853	1.0004
13	900	0.8836	0.9711	0.9829	0.8988	0.9662	0.9726	0.9254	0.9849	0.9960	0.9427	0.9856	0.9939
	2100	0.9106	0.9746	0.9806	0.8983	0.9635	0.9670	0.9426	0.9865	0.9931	0.9505	0.9841	0.9888
	300	0.7056	0.9340	0.9929	0.7504	0.9384	0.9873	0.7947	0.9514	1.0055	0.8381	0.9671	1.0169
14	900	0.7793	0.9576	0.9930	0.8049	0.9552	0.9840	0.8400	0.9665	1.0007	0.8767	0.9749	1.0041
	2100	0.8331	0.9703	0.9926	0.8475	0.9654	0.9831	0.8756	0.9731	0.9947	0.9047	0.9766	0.9938
	300	0.5862	0.8816	0.9745	0.6530	0.8886	0.9644	0.7993	0.9557	1.0037	0.8485	0.9712	1.0267
15	900	0.6765	0.9071	0.9869	0.7428	0.8975	0.9674	0.8527	0.9765	1.0015	0.9022	1.0066	1.0200
	2100	0.7491	0.9262	0.9844	0.7819	0.9174	0.9781	0.9026	0.9941	1.0049	0.9354	1.0088	1.0264
	300	0.4418	0.8007	1.0028	0.5319	0.8313	1.0072	0.5958	0.8079	0.9898	0.6329	0.8297	0.9927
16	900	0.5412	0.8729	1.0262	0.6249	0.8947	1.0239	0.6366	0.8649	1.0132	0.6758	0.8829	1.0122
	2100	0.6133	0.9041	1.0181	0.6853	0.9194	1.0144	0.6779	0.9089	1.0256	0.7152	0.9226	1.0230
	300	0.2279	0.5822	0.8802	0.2738	0.6052	0.8286	0.4367	0.6453	0.8852	0.4944	0.6537	0.8098
17	900	0.2977	0.6695	0.8823	0.3465	0.6799	0.8437	0.4695	0.7019	0.8828	0.4748	0.6927	0.8086
	2100	0.3857	0.7509	0.9136	0.4343	0.7944	0.8766	0.4981	0.7998	0.8719	0.5060	0.7265	0.8149
	300	0.1492	0.3675	0.6332	0.1856	0.3862	0.5919	0.2310	0.3579	0.5457	0.2384	0.3678	0.4855
18	900	0.1861	0.4173	0.5900	0.2296	0.4364	0.5908	0.2655	0.3837	0.4857	0.2634	0.3796	0.4626
	2100	0.2323	0.4744	0.6041	0.2814	0.4894	0.6055	0.2564	0.4019	0.4833	0.2708	0.3995	0.4609
	300	0.1702	0.4468	0.9887	0.2537	0.5702	1.1380	0.2958	0.5217	0.9945	0.3543	0.6382	1.1268
19	900	0.2171	0.5903	1.0954	0.3252	0.7209	1.2196	0.3385	0.6484	1.0869	0.4211	0.7700	1.1974
	2100	0.2858	0.7485	1.1826	0.4012	0.8670	1.2870	0.4021	0.7883	1.1863	0.5179	0.8973	1.2574
	300	0.1581	0.5022	0.8979	0.1754	0.4882	0.7537	0.7265	0.8302	0.9368	0.7259	0.8201	0.8970
20	900	0.1969	0.6025	0.8925	0.2166	0.5494	0.7423	0.7360	0.8538	0.9370	0.7363	0.8358	0.8882
	2100	0.2096	0.5958	0.7046	0.2127	0.4812	0.5587	0.7388	0.8321	0.8750	0.7339	0.8043	0.8297
	300	0.6663	0.7842	0.7641	0.6092	0.6832	0.6649	0.9590	0.9714	0.9714	0.9308	0.9389	0.9389
21	900	0.6572	0.7295	0.7294	0.5720	0.6559	0.6595	0.9578	0.9673	0.9673	0.9485	0.9577	0.9577
	2100	0.6533	0.7211	0.8178	0.5424	0.6515	0.6358	0.9573	0.9661	0.9779	0.9486	0.9571	0.9551
	300	0.8357	0.9617	0.9758	0.8049	0.9256	0.9387	0.9640	0.9920	0.9951	0.9360	0.9841	0.9870
22	900	0.8363	0.9464	0.9600	0.8016	0.9264	0.9396	0.9641	0.9889	0.9919	0.9355	0.9842	0.9871
	2100	0.8497	0.9646	0.9616	0.8130	0.9438	0.9411	0.9668	0.9924	0.9922	0.9379	0.9876	0.9875
	300	0.0077	0.0301	0.1561	0.0084	0.0300	0.1490	0.0419	0.0743	0.2080	0.0430	0.0741	0.2018
23	900	0.0078	0.0296	0.1529	0.0082	0.0303	0.1547	0.0419	0.0734	0.2051	0.0425	0.0742	0.2046
	2100	0.0150	0.0309	0.1608	0.0084	0.0316	0.1624	0.0571	0.0745	0.2116	0.0429	0.0755	0.2129

GROUP	TEMP	FM1 1.E2	FM1 1.E3	FM1 1.E4	FR2 1.E2	FR2 1.E3	FR2 1.E4
	300	0.7281	0.7754	0.9128	0.5342	0.7025	0.7651
11	900	0.7557	0.7983	0.9350	0.5691	0.7295	0.7848
	2100	0.7627	0.7797	0.9107	0.5700	0.7161	0.7721
	300	0.5948	0.7190	0.6394	0.4362	0.5960	0.5371
12	900	0.5673	0.6994	0.6397	0.3572	0.5615	0.5037
	2100	0.5671	0.7029	0.6419	0.4189	0.5364	0.4974
	300	0.6856	0.8072	0.8068	0.4870	0.7176	0.6959
13	900	0.6579	0.8150	0.7932	0.4131	0.6832	0.6601
	2100	0.6377	0.8029	0.7807	0.3633	0.6586	0.6353
	300	0.2799	0.7270	0.7933	0.1894	0.6150	0.6583
14	900	0.2865	0.7319	0.7734	0.1967	0.5989	0.6259
	2100	0.2769	0.7036	0.7318	0.1918	0.5625	0.5813
	300	0.5475	0.7275	0.6463	0.4646	0.6517	0.6316
15	900	0.5299	0.6876	0.7445	0.3770	0.4942	0.6123
	2100	0.4848	0.6745	0.7049	0.3065	0.5500	0.6059
	300	0.6450	0.7866	0.7686	0.5212	0.7195	0.6993
16	900	0.5680	0.7678	0.7292	0.4300	0.6635	0.6433
	2100	0.5017	0.7096	0.6923	0.3961	0.6047	0.5812
	300	0.7333	0.8691	0.9162	0.9045	0.9235	0.9760
17	900	0.6831	1.1107	1.1831	0.3469	0.9537	1.0187
	2100	0.5068	0.9725	1.2890	0.1699	1.0108	1.0918
	300	0.7610	0.9039	0.8922	0.6789	0.8103	0.8369
18	900	0.7364	0.8949	0.8754	0.6280	0.7952	0.8237
	2100	0.7290	0.8891	0.8575	0.6118	0.7723	0.8027
	300	0.4223	0.6116	0.6224	0.2110	0.4353	0.4413
19	900	0.4022	0.6125	0.6282	0.2083	0.4192	0.4276
	2100	0.2933	0.4885	0.5672	0.1967	0.3081	0.3710
	300	0.8405	0.9452	0.9455	0.6884	0.8490	0.8488
20	900	0.8436	0.9357	0.9341	0.6695	0.8370	0.8539
	2100	0.8441	0.9330	0.9328	0.6682	0.8589	0.8543
	300	0.3696	0.5229	0.5229	0.2944	0.3663	0.3654
21	900	0.3536	0.4855	0.4852	0.2798	0.3495	0.3484
	2100	0.3269	0.4409	0.7070	0.2853	0.3210	0.3109
	300	0.6023	0.9146	0.9590	0.5312	0.8640	0.9040
22	900	0.6022	0.9090	0.9522	0.5303	0.8640	0.9044
	2100	0.6008	0.9136	0.9525	0.5266	0.8696	0.9042
	300	0.0007	0.0063	0.1649	0.0	0.0083	0.1856
23	900	0.0007	0.0073	0.1848	0.0001	0.0084	0.1891
	2100	0.0002	0.0057	0.1753	0.0	0.0066	0.1799

APPENDIX D 25-Group Constants without Interfence Effect

D-I Shielding factor for ^{235}U

		FT			FF			FC		
GROUP	TEMP	1.E2	1.E3	1.E4	1.E2	1.E3	1.E4	1.E2	1.E3	1.E4
11	300	0.9482	0.9918	0.9993	0.9648	0.9934	0.9987	0.9648	0.9948	0.9997
	900	0.9659	0.9946	0.9996	0.9780	0.9949	0.9989	0.9788	0.9963	0.9997
	2100	0.9746	0.9963	0.9998	0.9839	0.9958	0.9990	0.9851	0.9972	0.9998
12	300	0.8862	0.9739	0.9957	0.9490	0.9851	1.0054	0.9218	0.9853	0.9988
	900	0.9027	0.9832	0.9969	0.9723	0.9985	1.0056	0.9516	0.9915	0.9993
	2100	0.9289	0.9889	0.9979	0.9843	1.0003	1.0059	0.9685	0.9963	0.9999
13	300	0.7901	0.9479	0.9916	0.9514	0.9974	0.9989	0.8053	0.9631	0.9917
	900	0.8365	0.9657	0.9939	0.9775	0.9979	0.9989	0.8671	0.9770	0.9933
	2100	0.8736	0.9764	0.9952	0.9894	0.9980	0.9989	0.9069	0.9842	0.9938
14	300	0.6406	0.8770	0.9824	0.9881	0.9964	1.0013	0.6555	0.9205	0.9894
	900	0.6958	0.9155	0.9887	1.0150	1.0202	1.0244	0.7433	0.9505	0.9936
	2100	0.7455	0.9388	0.9908	0.9954	0.9982	1.0014	0.8050	0.9641	0.9923
15	300	0.5983	0.8573	0.9801	0.6350	0.8411	0.9806	0.5302	0.8794	0.9852
	900	0.6578	0.9069	0.9894	0.5390	0.9068	0.9909	0.6402	0.9246	0.9917
	2100	0.7177	0.9397	0.9931	0.6417	0.9307	0.9981	0.7300	0.9522	0.9960
16	300	0.4262	0.6403	0.9081	1.0000	1.0000	1.0000	0.3559	0.7420	0.9550
	900	0.4361	0.7026	0.9381	1.0000	1.0000	1.0000	0.4498	0.8133	0.9721
	2100	0.4907	0.7577	0.9573	1.0000	1.0000	1.0000	0.5342	0.8643	0.9826
17	300	0.2489	0.4475	0.8261	1.0000	1.0000	1.0000	0.1929	0.5568	0.8851
	900	0.2667	0.5355	0.8716	1.0000	1.0000	1.0000	0.2534	0.6350	0.9316
	2100	0.2933	0.5991	0.9076	1.0000	1.0000	1.0000	0.3193	0.7335	0.9536
18	300	0.1261	0.2363	0.6120	1.0000	1.0000	1.0000	0.1406	0.3896	0.7910
	900	0.1309	0.2834	0.7072	1.0000	1.0000	1.0000	0.1762	0.4662	0.8818
	2100	0.1400	0.3451	0.7834	1.0000	1.0000	1.0000	0.2240	0.5859	0.9113
19	300	0.0980	0.1798	0.5756	1.0000	1.0000	1.0000	0.1056	0.3136	0.7395
	900	0.0994	0.2453	0.6939	1.0000	1.0000	1.0000	0.1305	0.4199	0.8441
	2100	0.1058	0.2929	0.7830	1.0000	1.0000	1.0000	0.1725	0.5462	0.9040
20	300	0.2427	0.3787	0.7942	1.0000	1.0000	1.0000	0.1361	0.4483	0.8678
	900	0.2472	0.4508	0.8631	1.0000	1.0000	1.0000	0.1743	0.5427	0.9185
	2100	0.2589	0.5322	0.9066	1.0000	1.0000	1.0000	0.2294	0.6651	0.9484
21	300	0.9971	0.9993	0.9995	0.5423	0.5768	0.5779	0.9859	0.9950	0.9957
	900	0.9972	0.9994	0.9996	0.5447	0.5769	0.5780	0.9866	0.9951	0.9959
	2100	0.9973	0.9994	0.9996	0.5450	0.5772	0.5783	0.9870	0.9955	0.9963
22	300	0.9186	0.9861	0.9955	0.8757	0.9770	0.9707	0.8769	0.9772	0.9904
	900	0.9161	0.9865	0.9960	0.8700	0.9780	0.9917	0.8712	0.9782	0.9918
	2100	0.9167	0.9874	0.9969	0.8715	0.9800	0.9938	0.8727	0.9802	0.9939
23	300	0.0086	0.0196	0.0704	0.0077	0.0295	0.1549	0.0077	0.0296	0.1458
	900	0.0085	0.0195	0.0711	0.0077	0.0298	0.1409	0.0077	0.0298	0.1409
	2100	0.0085	0.0193	0.0745	0.0077	0.0303	0.1486	0.0077	0.0303	0.1486

		FE			FR		
GROUP	TEMP	1.E2	1.E3	1.E4	1.E2	1.E3	1.E4
11	300	0.9714	0.9960	1.0001	0.8665	0.9311	0.9838
	900	0.9803	0.9975	1.0002	0.8940	0.9425	1.0049
	2100	0.9865	0.9983	1.0003	0.8808	0.9359	0.9842
12	300	0.9208	0.9868	0.9981	0.8972	0.9240	0.8874
	900	0.9447	0.9918	0.9987	0.9088	0.9286	0.8899
	2100	0.9611	0.9950	0.9994	0.9312	0.9461	0.9055
13	300	0.8695	0.9729	0.9957	0.9119	0.9625	0.9533
	900	0.9034	0.9826	0.9968	0.9304	0.9760	0.9647
	2100	0.9283	0.9882	0.9974	0.9462	0.9663	0.9745
14	300	0.7574	0.9336	0.9917	0.4462	0.8527	0.9439
	900	0.8056	0.9558	0.9947	0.4982	0.8851	0.9610
	2100	0.8447	0.9684	0.9953	0.5145	0.8642	0.9187
15	300	0.7818	0.9374	0.9928	0.7886	0.8954	0.9716
	900	0.8149	0.9449	0.9976	0.7550	0.8688	0.9246
	2100	0.8625	0.9822	1.0008	0.7913	0.8861	0.9424
16	300	0.5635	0.7690	0.9221	0.6027	0.9323	0.9323
	900	0.5969	0.8196	0.9490	0.8179	0.9289	0.9320
	2100	0.6347	0.8622	0.9796	0.7899	0.9267	0.9322
17	300	0.4176	0.6381	0.8977	0.7693	0.9232	0.9755
	900	0.4463	0.7031	0.9289	0.7062	0.9090	0.9737
	2100	0.4788	0.7603	0.9485	0.6360	0.8959	0.9708
18	300	0.2420	0.4082	0.7734	0.8968	0.9723	0.9938
	900	0.2417	0.4432	0.8439	0.8809	0.9657	0.9933
	2100	0.2714	0.5685	0.8956	0.8563	0.9585	0.9934
19	300	0.2117	0.3909	0.7794	0.9343	0.9762	0.9899
	900	0.2355	0.4838	0.8598	0.9270	0.9738	0.9916
	2100	0.2746	0.5872	0.9134	0.9151	0.9723	0.9951
20	300	0.7486	0.8190	0.9618	0.9866	0.9972	0.9982
	900	0.7603	0.8729	0.9767	0.9658	0.9671	0.9983
	2100	0.7767	0.9031	0.9859	0.9648	0.9970	0.9983
21	300	0.9988	0.9998	0.9999	0.9562	0.9964	0.9999
	900	0.9989	0.9998	0.9999	0.9601	0.9964	0.9999
	2100	0.9989	0.9998	0.9999	0.9602	0.9965	1.0000
22	300	0.9733	0.9956	0.9985	0.6367	0.9500	0.9947
	900	0.9721	0.9957	0.9987	0.6371	0.9504	0.9951
	2100	0.9724	0.9961	0.9990	0.6369	0.9511	0.9960
23	300	0.0421	0.0737	0.2071	0.0003	0.0056	0.1659
	900	0.0419	0.0738	0.2123	0.0003	0.0056	0.1571
	2100	0.0420	0.0740	0.2189	0.0003	0.0050	0.1539

D-II Shielding factor for ^{239}Pu

GROUP	TEMP	FT 10.	FT 1.E2	FT 1.E3	FF 10.	FF 1.E2	FF 1.E3	FC 10.	FC 1.E2	FC 1.E3
	300	0.8852	0.9643	0.9944	0.8726	0.9653	0.9920	0.8022	0.9492	0.9891
12	900	0.9066	0.9746	0.9956	0.8922	0.9716	0.9927	0.8301	0.9601	0.9907
	2100	0.9238	0.9810	0.9971	0.9092	0.9800	0.9964	0.8444	0.9659	0.9918
	300	0.7763	0.9102	0.9833	0.7848	0.9312	0.9889	0.6794	0.8962	0.9845
13	900	0.8198	0.9365	0.9901	0.8213	0.9477	0.9914	0.7305	0.9121	0.9886
	2100	0.8502	0.9526	0.9938	0.8415	0.9585	0.9959	0.7582	0.9352	0.9912
	300	0.6902	0.8579	0.9759	0.6229	0.8495	0.9716	0.9907	0.8827	0.9817
14	900	0.7518	0.9047	0.9884	0.6804	0.8910	0.9887	0.7841	0.9325	0.9930
	2100	0.7907	0.9308	0.9936	0.7156	0.9142	0.9953	0.8322	0.9548	0.9957
	300	0.5676	0.6768	0.9194	0.4800	0.7323	0.9420	0.3962	0.6948	0.9324
15	900	0.5222	0.7440	0.9450	0.5405	0.7831	0.9569	0.4886	0.7879	0.9524
	2100	0.5807	0.7961	0.9609	0.6011	0.8221	0.9684	0.5615	0.8139	0.9636
	300	0.3282	0.4950	0.7772	0.3387	0.6132	0.9006	0.2748	0.5009	0.8179
16	900	0.3573	0.5445	0.8194	0.3822	0.6510	0.9190	0.3365	0.5737	0.8619
	2100	0.3961	0.5910	0.8537	0.4141	0.6910	0.9401	0.4001	0.6301	0.8933
	300	0.3449	0.4914	0.7976	0.4312	0.6576	0.8953	0.1771	0.4313	0.8213
17	900	0.3644	0.5523	0.8552	0.5036	0.7315	0.9283	0.2186	0.5189	0.8742
	2100	0.3846	0.6185	0.8969	0.5729	0.8080	0.9534	0.2735	0.5790	0.9102
	300	0.1615	0.2432	0.5419	0.2464	0.3860	0.7301	0.1416	0.2244	0.6051
18	900	0.1690	0.2563	0.5622	0.2106	0.4113	0.7707	0.1005	0.2518	0.6485
	2100	0.1782	0.2926	0.6509	0.2845	0.4475	0.8122	0.1736	0.2827	0.7230
	300	0.1538	0.2762	0.5498	0.0883	0.2491	0.6671	0.1201	0.2784	0.6798
19	900	0.1649	0.2939	0.6233	0.1310	0.2749	0.7215	0.1667	0.3396	0.7641
	2100	0.1615	0.2759	0.7035	0.1141	0.3100	0.7707	0.1764	0.4186	0.8329
	300	0.0909	0.1686	0.4746	0.0787	0.2415	0.6262	0.0516	0.1929	0.6618
20	900	0.0908	0.1699	0.5165	0.0798	0.2500	0.6579	0.0535	0.2065	0.6522
	2100	0.0923	0.1762	0.5625	0.0836	0.2556	0.4101	0.0571	0.2262	0.7082
	300	0.3036	0.3497	0.5499	0.3374	0.4528	0.7213	0.1858	0.3356	0.6570
21	900	0.3061	0.3527	0.5888	0.3447	0.4732	0.7640	0.1914	0.3589	0.7086
	2100	0.3094	0.3623	0.6275	0.3531	0.5085	0.8067	0.1955	0.3989	0.7550
	300	0.8818	0.9722	0.9957	0.8337	0.9591	0.9904	0.7957	0.9474	0.9873
22	900	0.8818	0.9722	0.9957	0.8337	0.9591	0.9904	0.7957	0.9474	0.9873
	2100	0.8818	0.9722	0.9957	0.8337	0.9591	0.9904	0.7957	0.9474	0.9873
	300	0.7320	0.8778	0.9687	0.6804	0.8849	0.9647	0.5405	0.7963	0.9447
23	900	0.7320	0.8778	0.9687	0.6804	0.8849	0.9647	0.5405	0.7963	0.9447
	2100	0.7320	0.8778	0.9687	0.6804	0.8849	0.9647	0.5405	0.7963	0.9447
	300	0.4404	0.5082	0.7775	0.4468	0.5405	0.8084	0.2958	0.3792	0.7298
24	900	0.4404	0.5082	0.7775	0.4468	0.5405	0.8084	0.2958	0.3792	0.7298
	2100	0.4404	0.5082	0.7814	0.4468	0.5405	0.8124	0.2958	0.3797	0.7354

GROUP	TEMP	FE 10.	FE 1.E2	FE 1.E3	FR 10.	FR 1.E2	FR 1.E3
	300	0.9486	0.9852	0.9978	0.0604	0.7150	0.9027
12	900	0.9591	0.9895	0.9983	0.0536	0.7218	0.9044
	2100	0.9655	0.9920	0.9987	0.0491	0.7426	0.9030
	300	0.8902	0.9800	0.9936	0.0885	0.6793	0.9336
13	900	0.9134	0.9722	0.9958	0.0790	0.6855	0.9368
	2100	0.9311	0.9804	0.9709	0.0746	0.6895	0.9401
	300	0.8876	0.9561	0.9941	0.0855	0.5975	0.9323
14	900	0.9179	0.9749	0.9974	0.0662	0.5984	0.9334
	2100	0.9360	0.9851	0.9991	0.0562	0.5779	0.9194
	300	0.7627	0.8710	0.9716	0.0250	0.4115	0.8707
15	900	0.7986	0.9044	0.9815	0.0138	0.3759	0.8202
	2100	0.8329	0.9291	0.9879	0.0086	0.3502	0.8081
	300	0.5408	0.6675	0.8186	0.0036	0.2357	0.7933
16	900	0.5498	0.6678	0.8503	0.0043	0.2027	0.7947
	2100	0.5661	0.6858	0.8726	0.0005	0.1313	0.5999
	300	0.7187	0.7929	0.9287	0.0135	0.2492	0.8340
17	900	0.7325	0.8436	0.9524	0.0071	0.1789	0.8292
	2100	0.7544	0.8697	0.9647	0.0037	0.1108	0.7901
	300	0.4577	0.5645	0.7463	0.0289	0.2500	0.7937
18	900	0.4592	0.5234	0.7908	0.0067	0.2194	0.7427
	2100	0.5251	0.5886	0.8205	0.0134	0.1509	0.6354
	300	0.7041	0.7908	0.8840	0.0498	0.4479	0.8549
19	900	0.7262	0.7766	0.9188	0.1083	0.3830	0.8366
	2100	0.7286	0.8082	0.9457	0.1199	0.3064	0.8684
	300	0.8154	0.8567	0.9253	0.0065	0.1460	0.6952
20	900	0.8148	0.8609	0.9389	0.0047	0.1253	0.6767
	2100	0.8191	0.8684	0.9531	0.0042	0.0973	0.6790
	300	0.9450	0.9565	0.9743	0.0745	0.4497	0.8790
21	900	0.9436	0.9575	0.9779	0.0141	0.4321	0.8780
	2100	0.9283	0.9467	0.9807	0.0700	0.3968	0.8789
	300	0.9725	0.9941	0.9987	0.0449	0.6738	0.9588
22	900	0.9725	0.9941	0.9987	0.0449	0.6738	0.9588
	2100	0.9725	0.9941	0.9987	0.0449	0.6738	0.9588
	300	0.9640	0.9855	0.9962	0.0055	0.3496	0.8909
23	900	0.9640	0.9855	0.9962	0.0055	0.3496	0.8909
	2100	0.9640	0.9855	0.9962	0.0055	0.3496	0.8909
	300	0.9127	0.9283	0.9739	0.0019	0.0361	0.5958
24	900	0.9127	0.9283	0.9739	0.0019	0.0361	0.5958
	2100	0.9127	0.9283	0.9745	0.0019	0.0361	0.5971

D-III Shielding factor for ^{240}Pu

GROUP	TEMP	FT 10.	FT 1.E2	FT 1.E3	FF 10.	FF 1.E2	FF 1.E3	FC 10.	FC 1.E2	FC 1.E3
12	300	0.9428	0.9959	0.9974	0.8798	0.9719	0.9931	0.8698	0.9698	0.9930
	900	0.9509	0.9967	0.9977	0.8889	0.9751	0.9934	0.8796	0.9739	0.9934
	2100	0.9556	0.9971	0.9979	0.8948	0.9768	0.9936	0.8851	0.9751	0.9935
13	300	0.9167	0.9944	0.9947	0.8909	0.9643	0.9923	0.8828	0.9516	0.9933
	900	0.9059	0.9932	0.9957	0.9214	0.9529	0.9931	0.8384	0.9585	0.9942
	2100	0.9135	0.9960	0.9960	0.8292	0.9558	0.9936	0.8479	0.9525	0.9947
14	300	0.8167	0.9308	0.9897	0.7775	0.9218	0.9895	0.7649	0.9108	0.9877
	900	0.8509	0.9457	0.9922	0.7957	0.9363	0.9915	0.7824	0.9235	0.9897
	2100	0.8753	0.9562	0.9939	0.8240	0.9444	0.9930	0.8011	0.9324	0.9916
15	300	0.6806	0.8841	0.9745	0.6505	0.8946	0.9673	0.6029	0.8549	0.9737
	900	0.7263	0.8904	0.9796	0.6928	0.8728	0.9705	0.6449	0.8791	0.9782
	2100	0.7594	0.9089	0.9829	0.7241	0.8873	0.9729	0.6672	0.8923	0.9804
16	300	0.6789	0.8381	0.9675	0.6980	0.8946	0.9655	0.7182	0.8658	0.9738
	900	0.7562	0.8929	0.9812	0.7546	0.8970	0.9785	0.8085	0.9107	0.9842
	2100	0.8164	0.9449	0.9932	0.7978	0.9123	0.9837	0.8749	0.9407	0.9823
17	300	0.5420	0.7596	0.9515	0.6981	0.8963	0.9759	0.6869	0.7184	0.9671
	900	0.6279	0.8480	0.9732	0.7995	0.9569	0.9946	0.2720	0.7670	0.9814
	2100	0.7132	0.8798	0.9895	0.8777	1.0000	1.0125	0.6422	0.8601	0.9709
18	300	0.3640	0.5677	1.0166	0.3785	0.6169	1.1048	0.4723	0.6994	0.9890
	900	0.4456	0.6353	0.9134	0.4566	0.6983	0.9294	0.5882	0.7774	0.9966
	2100	0.5261	0.6883	0.9317	0.5151	0.6685	0.9403	0.6839	0.8311	0.9890
19	300	0.4029	0.5524	0.8518	0.4887	0.6672	0.9158	0.3964	0.6415	0.9812
	900	0.4775	0.6000	0.8483	0.5625	0.7117	0.9390	0.5315	0.6815	0.9914
	2100	0.5020	0.6546	0.9187	0.6044	0.7602	0.9409	0.5050	0.7388	0.9958
20	300	0.3214	0.4490	0.7157	0.4787	0.6965	0.8968	0.3630	0.4919	0.7618
	900	0.3529	0.4997	0.7781	0.5514	0.7193	0.9027	0.4265	0.5626	0.8460
	2100	0.4294	0.5756	0.8379	0.6842	0.8134	0.9443	0.5443	0.6498	0.8816
21	300	0.4035	0.4687	0.7375	0.7237	0.7775	0.9033	0.3120	0.4977	0.8401
	900	0.4238	0.4999	0.8003	0.7736	0.8037	0.9394	0.3406	0.5413	0.8735
	2100	0.4572	0.5604	0.8576	0.8429	0.9162	0.9968	0.3789	0.5728	0.9101
22	300	0.4727	0.7234	0.9614	0.6657	0.7696	0.9706	0.4647	0.8832	0.9677
	900	0.4993	0.7673	0.9797	0.7959	0.7975	0.9863	0.6349	0.9292	1.0083
	2100	0.4812	0.6709	0.9940	0.3072	0.3289	1.0035	0.6243	1.0163	1.0581
23	300	0.5376	0.6381	0.9828	0.3919	0.5965	0.8971	0.6425	0.7437	0.9960
	900	0.5304	0.6505	0.9967	0.4049	0.6023	0.8983	0.7620	0.7456	0.9965
	2100	0.5641	0.6519	0.9938	0.4227	0.6090	0.8993	0.8538	0.8064	0.9973
24	300	0.9152	0.9180	0.9676	0.9173	0.9032	0.9420	1.1202	0.9744	0.9961
	900	0.9460	0.9706	0.9717	0.9274	0.9605	0.9868	1.1588	0.9989	0.9934
	2100	0.9509	0.9781	0.9790	0.9378	0.9617	0.9780	1.1683	1.0053	1.0177

GROUP	TEMP	FE 10.	FE 1.E2	FE 1.E3	FR 10.	FR 1.E2	FR 1.E3
12	300	0.9928	0.9979	0.9994	0.0978	0.6945	0.9021
	900	0.9941	0.9983	0.9995	0.1007	0.7022	0.9029
	2100	0.9952	0.9987	0.9996	0.0967	0.6997	0.9024
13	300	0.9883	0.9963	0.9992	0.0301	0.6018	0.9240
	900	0.9896	0.9973	0.9992	0.0325	0.6062	0.9243
	2100	0.9907	0.9978	0.9993	0.0306	0.6015	0.9247
14	300	0.9799	0.9918	0.9984	0.0748	0.5407	0.9225
	900	0.9865	0.9941	0.9987	0.0090	0.4955	0.9223
	2100	0.9880	0.9954	0.9989	0.0085	0.4998	0.9239
15	300	0.9550	0.9861	0.9974	0.0025	0.2787	0.8014
	900	0.9628	0.9885	0.9982	0.0017	0.2701	0.8027
	2100	0.9662	0.9910	0.9986	0.0013	0.2665	0.8026
16	300	0.9684	0.9849	0.9959	0.0012	0.2016	0.8245
	900	0.9810	0.9913	0.9974	0.0007	0.1789	0.8041
	2100	0.9909	0.9956	0.9983	0.0005	0.1648	0.7996
17	300	0.9553	0.9778	0.9956	0.0010	0.2497	0.8156
	900	0.9692	0.9846	0.9971	0.0005	0.2274	0.8130
	2100	0.9840	0.9894	0.9980	0.0003	0.2471	0.8317
18	300	0.8714	0.9037	1.0205	0.0064	0.2162	1.4780
	900	0.8869	0.9190	0.9790	0.0060	0.2069	0.8647
	2100	0.8990	0.9301	0.9850	0.0057	0.1970	0.8049
19	300	0.9331	0.9658	0.9890	0.0129	0.2661	0.8669
	900	0.9494	0.9716	0.9943	0.0536	0.2105	0.8625
	2100	0.9264	0.9729	0.9926	0.0137	0.1766	0.8537
20	300	0.9572	0.9283	0.9670	0.0049	0.1619	0.7897
	900	0.9550	0.9373	0.9732	0.0045	0.1331	0.7689
	2100	0.9723	0.9527	0.9729	0.0041	0.0926	0.7655
21	300	1.0261	1.0607	0.9976	0.0049	0.3296	0.8336
	900	1.0262	1.0003	0.9997	0.0036	0.3048	0.8991
	2100	1.0204	1.0154	1.0170	0.0032	0.1654	0.8453
22	300	0.9624	0.9831	0.9969	0.0177	0.4648	0.9262
	900	0.9847	0.9986	1.0046	0.0042	0.4495	0.9198
	2100	0.9544	0.9705	0.9772	0.0015	0.4147	0.8943
23	300	0.9719	0.9885	0.9974	0.0034	0.1942	0.8156
	900	0.9684	0.9850	0.9942	0.0033	0.1698	0.8123
	2100	0.9666	0.9837	0.9734	0.0032	0.1796	0.7947
24	300	0.9608	0.9775	0.9943	0.0029	0.1522	0.7632
	900	0.9549	0.9748	0.9916	0.0003	0.1514	0.7607
	2100	0.9409	0.9727	0.9737	0.0035	0.0323	0.7259